

Sustainable Synthesis of Bio-based Recyclable Thermosets

Zur Erlangung des akademischen Grades einer

DOKTORIN DER NATURWISSENSCHAFTEN

(Dr. rer. nat.)

von der KIT-Fakultät für Chemie und Biowissenschaften
des Karlsruher Instituts für Technologie (KIT)

genehmigte

DISSERTATION

von

M.Sc. Pia Simone Löser

1. Referent: Prof. Dr. Michael A. R. Meier

2. Referentin: Dr. Audrey Llevot

Tag der mündlichen Prüfung: 20.07.2020

*„Wie herrlich es ist, dass niemand eine Minute zu warten braucht,
um damit zu beginnen, die Welt zu verändern.“*

- Anne Frank -

Die vorliegende Arbeit wurde von März 2017 bis Juli 2020 unter Anleitung von Prof. Dr. Michael A. R. Meier am Institut für Organische Chemie (IOC) des Karlsruher Instituts für Technologie (KIT) durchgeführt.

Hiermit versichere ich, dass ich die Arbeit selbstständig angefertigt, nur die angegebenen Quellen und Hilfsmittel benutzt und mich keiner unzulässigen Hilfe Dritter bedient habe. Insbesondere habe ich wörtlich oder sinngemäß aus anderen Werken übernommene Inhalte als solche kenntlich gemacht. Die Satzung des Karlsruher Instituts für Technologie (KIT) zur Sicherung wissenschaftlicher Praxis habe ich beachtet. Des Weiteren erkläre ich, dass ich mich derzeit in keinem laufenden Promotionsverfahren befinde, und auch keine vorausgegangenen Promotionsversuche unternommen habe. Die elektronische Version der Arbeit stimmt mit der schriftlichen Version überein und die Primärdaten sind gemäß der Satzung zur Sicherung guter wissenschaftlicher Praxis des KIT beim Institut abgegeben und archiviert.

Karlsruhe, 10.06.2020

Pia Löser

Danksagung

An dieser Stelle möchte ich mich bei all den Personen bedanken, die zu einem Gelingen dieser Arbeit beigetragen haben:

Mein erster Dank geht an Mike. Vielen Dank für dein Vertrauen und deine Unterstützung, deine immer offene Bürotür, viele schöne Aktionen und Konferenzen und den ein oder anderen Gin Tonic. Nicht jeder hat das Glück einen Chef haben, mit dem man nicht nur seine Forschungsergebnisse, sondern auch die neueste Folge der Sendung mit der Maus ausdiskutieren kann.

Another huge thank you goes to Audrey. Thanks so much for all your effort and the great supervision. I really appreciate all the advice and guidance throughout the last years, thanks for always being there for me, in person and in numerous Skype meetings. Merci pour tout!!!

Thank you to all the persons who helped with proof reading: Yasmin, Katharina, Dafni, Roman and Philipp. Thanks for all your comments and corrections.

Ein besonderer Dank geht an die aktuelle und ehemalige Green Hippie Crew in Labor 409. Philip, Julian, Kenny, Eren, Luca und Anja, danke für die tolle Arbeitsatmosphäre und gute Stimmung im Labor. Yasmin, bester Terpen- und Konferenz-Buddy, dir möchte ich danken für eine tolle Zeit, für deine Unterstützung, deine motivierenden Worte bei Terpenproblemen und deine Freundschaft. Danke für all unsere Lauftrainings, Teeпаusen, tollen Gespräche, geteilten Hotelzimmer und Stadterkundungen. Katharina, danke für viele tiefgründige Gespräche, für aktive und weniger aktive Kaffeepausen und deinen Rückhalt bei egal welchen Problemen. Of course a big thank you goes to all former and current group members. Thanks for the great working atmosphere, for all the fun in- and outside of the lab and for making the group so much more than just colleagues. Danke auch an Becci und Pinar für die organisatorische Arbeit im Labor und Büro.

Desweiteren möchte ich mich bei all meinen Studenten bedanken, die mich bei der Arbeit im Labor unterstützt haben: Pascal, Tim, Annika, Bastian und Alina. Danke für euren Einsatz und eure Motivation! Ein weiterer Dank geht an die Analytikabteilung des Instituts für die Messung all meiner Proben. In this regard I would also like to thank Cédric Le Coz and Emmanuel Ibarboure for measuring my samples, as well as the whole team from LCPO Bordeaux for the help in the lab and the warm welcome. Merci beaucoup!

Ein ganz besonderer Dank geht an alle meine Freunde, die immer für mich da sind und mir den Rücken stärken. Danke, dass ihr da seid und mich und meine Welt immer wieder auf den Kopf stellt!

Katha, beste Freundin für immer, danke für deine langjährige Freundschaft, für all unsere tollen Urlaube und Telefonate. Danke für deine Unterstützung egal in welcher Lebenslage, für unzählige Runden Phase 10 und die vielen Kaffee- und Tee-Nachmittage!

Zuletzt geht mein größter Dank an meine Familie, die immer für mich da ist und mich stärkt. Danke für euren Rückhalt und eure Unterstützung!

Abstract

In recent years, the replacement of petroleum-based polymers by more sustainable alternatives has become an important research field in polymer chemistry. Depletion of fossil resources and increasing environmental concerns require a change in production methods and resource provisioning. This also applies for thermosetting polymers. This work therefore focusses on the sustainable synthesis of bio-based monomers for thermosetting polymers.

In the first part of the thesis, vanillyl alcohol was used as renewable substrate and was modified by an allylation and, in some cases, epoxidation procedure. In order to introduce recyclability into the final polymer networks, the modified vanillin building blocks were subsequently coupled to form dimeric structures bearing cleavable linker groups. This way, cleavable bis-allyl ethers and diglycidyl ethers were obtained and subsequently used for thermoset formation. In the second part of this thesis, terpenes were explored as versatile feedstock for the synthesis of bio-based diamines, useful epoxy resin hardeners. The synthesis protocol entailed the epoxidation of the terpene double bonds, followed by a rearrangement to the respective carbonyl structures. These biscarbonyls can finally be converted to diamines *via* reductive amination. Thus, in a first step, different epoxidation procedures were investigated. For the rearrangement of these epoxidized substrates, a reaction procedure was established employing bismuth triflate as efficient catalyst. The reductive amination of the obtained biscarbonyls proved to be difficult. Therefore, as alternative pathway, bio-based diamines were synthesized by aminolysis of bio-based bisepoxides. In the third part of the thesis, the thiol-ene polymerization of the vanillin-based cleavable bis-allyl ether monomers was investigated. Cross-linked polymer films were prepared and their thermomechanical properties were analyzed. Moreover, the coupled diglycidyl ethers of vanillyl alcohol were investigated as monomers in epoxy resins together with the synthesized limonene-based amino alcohol hardener. The material properties of the obtained resins were investigated and the suitability of the monomers for epoxy resin synthesis was assessed. In the last part of this thesis, different degradation conditions were explored to establish a protocol for the controlled degradation of the synthesized cross-linked polymers. In a first step, the cleavable monomers were used as model system to identify suitable degradation conditions. Subsequently, the most promising conditions were transferred to one of the polymer films to prove the degradability of the polymer system.

Zusammenfassung

In den letzten Jahren hat sich die Polymerforschung zunehmend um nachhaltige Alternativen zu den etablierten erdölbasierten Polymeren bemüht, sodass sich dieses Forschungsgebiet zu einem wichtigen Teilbereich der Polymerchemie entwickelt hat. Sowohl die Verknappung von fossilen Rohstoffen, als auch zunehmende ökologische Bedenken erfordern einen Wandel bei den Produktionsmethoden und der Rohstoffbasis. Dies gilt auch für duroplastische Kunststoffe. Der Fokus dieser Arbeit liegt daher auf der nachhaltigen Synthese biobasierter Monomere für die Herstellung von Duroplasten.

Im ersten Teil der Arbeit wurde Vanillylalkohol als nachwachsender Rohstoff für die Monomersynthese untersucht. Zunächst wurde dieser durch Allylierung mit Allyl methyl carbonat und anschließende Epoxidierung der eingeführten Doppelbindung modifiziert. Um eine Rezyklierbarkeit des Materials zu erreichen, wurde der modifizierte Vanillylalkohol im nächsten Schritt zu symmetrischen Dimeren gekuppelt, wobei spaltbare Linkergruppen eingeführt wurden. Dabei wurden säurelabile Bisallylether und Bisepoxide erhalten. Im zweiten Teil der Arbeit wurden Terpene als nachwachsender Rohstoff für die Synthese biobasierter Amine als Härter für Epoxidharze untersucht. Dafür wurde ein Syntheseweg beginnend mit einer Epoxidierung der vorhandenen Doppelbindungen mit anschließender Umlagerung zu Biscarbonylen etabliert. Durch eine anschließende reduktive Aminierung können Diamine synthetisiert werden. Zunächst wurden verschiedene Epoxidierungsmethoden untersucht. Anschließend wurde die Umlagerung zu den entsprechenden Carbonylen optimiert, wobei sich Bismuth triflat als effizienter Katalysator für verschiedene Substrate erwies. Da sich die anschließende reduktive Aminierung der Biscarbonyle als schwierig herausstellte, wurden die Diamine über einen alternativen Syntheseweg durch Ringöffnung von biobasierten Epoxiden mit Ammoniak hergestellt. Im dritten Teil der Arbeit wurden die abbaubaren Bisallylether, die auf Basis von Vanillylalkohol synthetisiert worden waren, für Thiol-en Polymerisationen verwendet. Eine genaue Untersuchung der thermomechanischen Eigenschaften der erhaltenen Polymerfilme ermöglichte die Identifizierung geeigneter Monomere für den potentiellen Ersatz erdölbasierter Produkte. Des Weiteren wurden die gekuppelten bisfunktionellen Epoxide zusammen mit den zuvor hergestellten Amin-Härtern für den Einsatz in Epoxidharzen untersucht. Über die Materialeigenschaften der erhaltenen Harze konnte die Eignung der einzelnen Monomere für die Synthese von Duroplasten beurteilt werden. Schließlich wurden im letzten Teil der Arbeit verschiedene Reaktionsbedingungen für die kontrollierte Zersetzung der hergestellten vernetzten Polymere getestet. Zunächst wurde der Abbau an den Monomeren optimiert. Im

Folgenden wurden die besten Bedingungen dann auf einen der synthetisieren Polymerfilme übertragen, um die Abbaubarkeit der Polymere zu demonstrieren.

Table of Contents

Abstract	I
Zusammenfassung.....	III
1 Introduction.....	1
2 Theoretical Background and State of the Art.....	3
2.1 Green and Sustainable Chemistry	4
2.1.1 Introduction.....	4
2.1.2 The 12 Principles of Green Chemistry	5
2.1.3 Assessment of Sustainability	7
2.2 Renewable Resources as Feedstock in Polymer Chemistry	11
2.2.1 Introduction.....	11
2.2.2 Lignin Valorization for Sustainable (Semi-)Aromatic Polymers.....	14
2.2.3 Terpenes: A Diverse and Valuable Resource.....	26
2.3 Epoxy Resins: High Performance Thermosetting Polymers	48
2.3.1 Introduction.....	48
2.3.2 Bisphenol A in Epoxy Resins	50
2.3.3 Bio-based Epoxy Resins	51
2.4 Strategies for Recyclability in Thermosetting Polymers.....	62
2.4.1 Recyclability and Biodegradability of Polymers	62
2.4.2 Examples for Recyclable Thermosets.....	64
3 Aims.....	77
4 Results and Discussion	79
4.1 Synthesis of Cleavable Bisepoxide Monomers.....	80
4.1.1 Alkylation of Bio-based Phenols.....	80
4.1.2 Coupling of Allyl Vanillyl Alcohol to Diene Monomers.....	82
4.1.3 Synthesis of Diglycidyl Ether Monomers from Allylated Vanillyl Alcohol	87
4.2 Terpenes as Feedstock for Renewable Amine Hardeners.....	94
4.2.1 Epoxidation of Terpenes.....	95
4.2.2 Meinwald Rearrangement of Epoxidized Terpenes	99

4.2.3	Reductive Amination of Terpene-based Biscarbonyl Substrates	110
4.2.4	Aminolysis of Terpene-based Bisepoxides	114
4.3	Polymerization of Bis-allyl Ether Monomers	121
4.3.1	Synthesis of Linear Polymers	121
4.3.2	Synthesis of Cross-linked Thiol-Ene Films	124
4.4	Synthesis of Epoxy Resins from Diglycidyl Ether Monomers	133
4.4.1	Reactivity Test of Carbonate Linker with Amines	133
4.4.2	First Curing Test with Priamine®	135
4.4.3	Epoxy Resin Studies	137
4.5	Degradation Studies	143
4.5.1	Establishment of Degradation Conditions	143
4.5.2	Degradation of Thiol-Ene Film P5	148
5	Conclusion and Outlook	151
6	Experimental Section	157
6.1	Materials	157
6.2	Characterization Methods	159
6.3	Experimental Procedures	163
6.3.1	Experimental Procedures for Chapter 4.1	163
6.3.2	Experimental Procedures for Chapter 4.2	189
6.3.3	Experimental Procedures for Chapter 4.3	230
6.3.4	Experimental Procedures for Chapter 4.4	238
6.3.5	Additional procedures	245
7	Appendix	247
7.1	Abbreviations	247
7.2	List of Figures	250
7.3	List of Tables	255
7.4	Publications	257
7.5	Conference Contributions	257
8	Bibliography	259

1

Introduction

In the last decades, the world population has drastically increased and is expected to reach ten billion people by the end of the century.^[1] This growth will cause problems regarding the supply of resources, for instance food or energy, for all people, but also an increased demand for commodity products for everyday life, many of which are provided by the chemical industry.^[2] Since the industrial revolution, the development of our society, including the chemical industry with its supply chains and production methods, has mainly been based on the use of fossil resources. However, the quantity of available fossil resources is continuously depleting at an increasing pace.^[3] Thus, the need for a more sustainable energy and resource production has been recognized, for instance by the Brundtland Report in 1987^[4] or by the United Nations in their “2030 Agenda for Sustainable Development”, which was released in 2015.^[5] According to the agenda, the protection of our planet has to be achieved *“through sustainable consumption and production, sustainably managing its natural resources and taking urgent action on climate change, so that it can support the needs of the present and future generations”*.^[5] Sustainable development includes the change from fossil-based resources to renewable resources such as lignin, cellulose, starch, natural oils etc. for the production of chemicals and products. Furthermore, it includes the transition from an unsustainable linear economy to a circular economy, where products and processes are designed with the goal of resource economy and waste elimination.^[6] Polymers constitute a major production field of the chemical industry with more than 300 million tons being produced worldwide every year.^[7] To date, most produced polymers are derived from fossil resources, with the polymer production accounting for about

7% of the worldwide consumption of oil and gas.^[8] Of the produced polymers, approximately 50% are used for disposable applications, such as packaging, agricultural films, disposable consumer items or other short-lived products that are discarded within a year after production.^[9] As a result, substantial amounts of polymers end up in landfills or in the environment, for example in the oceans. Already by 2050, the weight of plastics in the oceans is predicted to surpass that of fish.^[10] With the depletion of fossil resources as well as the environmental concerns arising from polymer waste, the development of bio-based and, in certain application fields, (bio-)degradable polymers becomes a necessity.^[10] This implies both the synthesis of already established chemicals, monomers or polymers used in the plastics industry from renewable feedstock as well as the development of novel building blocks for the production of novel materials with comparable or new properties.^[11] A lot of research on the synthesis of bio-based polymers has already been reported and many different renewable resources, including carbohydrates, such as starch or cellulose, vegetable oils, lignin and terpenes, have been explored for the synthesis of sustainable monomers.^{[12][13][14]} This development is stimulated by a change of the public opinion towards polymeric materials in recent years.^[15] With an increasing demand for more sustainable products, the development of renewable and environmentally benign polymers continues to be a great research challenge for the polymer community.^[16] This goal can be achieved by a combination of extensive basic research in order to find solutions to societal challenges on a molecular level. This work aims to contribute to the combined research effort that has been made towards sustainable biomass valorization and polymer production. Vanillin, as lignin-derived platform chemical, is explored as valuable aromatic building block to synthesize materials with good thermomechanical properties. Furthermore, the utilization of terpenes for monomer synthesis is investigated, as terpenes, especially in cross-linked polymers, have not been extensively utilized to date. Besides the transformation of renewable resources into novel monomers, this thesis also addresses the problem of recyclability of thermosetting polymers, as the development of efficient recycling strategies constitutes a valuable benefit towards a more sustainable production of consumer products.

2

Theoretical Background and State of the Art

In the following chapter, recent developments in the field of sustainable chemistry, renewable resources and bio-based polymers are discussed to provide an overview of the topics relevant to this thesis. In chapter 2.1, the basics of green and sustainable chemistry are described, including its development and tools for assessing the sustainability of a reaction or product. Chapter 2.2 covers the use of renewable resources for polymeric materials. A special focus is put on vanillin as lignin-derived platform chemical and limonene as one of the most important terpene structures in the chemical industry. Chapter 2.3 discusses epoxy resins as high performance thermosetting material and problems related to the use of bisphenol A in their syntheses. Bio-based alternatives for traditional epoxy resins are also highlighted. Finally, in chapter 2.4, the problem of recycling thermosetting polymers is addressed. Therefore, different options and strategies for the implementation of recyclability in thermosets are presented. The special focuses on vanillin and terpenes as bioresources and on epoxy resins as thermosets were decided according to the experiments performed in the framework of this PhD work.

2.1 Green and Sustainable Chemistry

2.1.1 Introduction

Nowadays, the term sustainability is used in many different contexts. However, the most common definition of sustainability was stated in 1987 in the Brundtland Report and defined sustainability as a *“development that meets the needs of the present without compromising the ability of future generations to meet their own needs”*.^[4] Since then, the definition has been a driving force of many improvements in our modern society as well as in the chemical industry. Based on this concept of sustainability, Green Chemistry emerged in the 1990s and aims to push sustainability on a molecular level.^[17] Green Chemistry is defined as the *“design of chemical products and processes to reduce or eliminate the use and generation of hazardous substances”*.^[18] An important milestone in the development of Green Chemistry was the postulation of the Twelve Principles of Green Chemistry in 1998 by Anastas and Warner. They have quickly become the most important reference for a sustainable chemical synthesis and will be discussed in chapter 2.1.2.

Since it has been established in the 1990s, Green Chemistry has had an enormous impact not only on research but also on the chemical industry.^[19] It shifted the traditional evaluation of process efficiency from only focusing on the yield towards more benign methods, and the additional economic benefit resulting from not having to dispose of unnecessary waste.^[20] By now, numerous scientific journals covering different aspects of sustainability have been established. Research fields cover the implementation of more sustainable solvents,^[21] novel catalysts^[22] and biocatalysis^[23] as well as the exploitation of renewable feedstock.^[24] One of the first established and most prominent journals is the Green Chemistry journal published by the Royal Society of Chemistry, which was launched in 1999.^{[25][26]}

The research field of Green Chemistry is well defined by the Twelve Principles of Green Chemistry and mainly focuses on the way a chemical reaction or the synthesis of a product should be carried out. This way, it serves as a tool for implementing sustainability in process design.^[17] In addition, the term Sustainable Chemistry represents a broader concept, which does include Green Chemistry, but goes a step further. Sustainable Chemistry also takes into account the whole value chain of a product, the societal and economic aspects of chemical development, as well as the environmental impact and the treatment of a material at the end of its life.^{[27][28]} Thus, Sustainable Chemistry offers solutions to different challenges that need to be addressed by our society in the upcoming future in order to ensure a sustainable development.

2.1.2 The 12 Principles of Green Chemistry

The Twelve Principles of Green Chemistry were introduced in 1998 by Paul Anastas and John Warner.^[28] They serve as a guideline for chemists for designing chemical reactions and new products to improve the overall sustainability of a process.^[18] The Twelve Principles are summarized in Table 2.1.

Table 2.1 The 12 Principles of Green Chemistry.^[28]

Number	Principle	Description
1	Prevention	It is better to prevent waste than to treat or clean up waste after it is formed.
2	Atom Economy	Synthetic methods should be designed to maximize the incorporation of all materials used in the process into the final material.
3	Less Hazardous Chemical Synthesis	Whenever practicable, synthetic methodologies should be designed to use and generate substances that pose little or no toxicity to human health and the environment.
4	Designing Safer Chemicals	Chemical products should be designed to preserve efficacy of the function while reducing toxicity.
5	Safer Solvents and Auxiliaries	The use of auxiliary substances (<i>e.g.</i> solvents, separation agents, etc.) should be made unnecessary whenever possible and, when used, innocuous.
6	Design for Energy Efficiency	Energy requirements of chemical processes should be recognized for their environmental and economic impacts and should be minimized. If possible, synthetic methods should be conducted at ambient temperature and pressure.
7	Use of Renewable Feedstocks	A raw material or feedstock should be renewable rather than depleting whenever technically and economically practicable.
8	Reduce Derivatives	Unnecessary derivatization (use of blocking groups, protection/ deprotection, temporary modification of physical/chemical processes) should be minimized or

		avoided if possible, because such steps require additional reagents and can generate waste.
9	Catalysis	Catalytic reagents (as selective as possible) are superior to stoichiometric reagents.
10	Design for Degradation	Chemical products should be designed so that at the end of their function they break down into innocuous degradation products and do not persist in the environment.
11	Real-Time Analysis for Pollution Prevention	Analytical methodologies need to be further developed to allow for real-time, in-process monitoring and control prior to the formation of hazardous substances.
12	Inherently Safer Chemistry for Accident Prevention	Substances and the form of a substance used in a chemical process should be chosen to minimize the potential for chemical accidents, including releases, explosions, and fires.

The principles include different aspects of reaction design, such as the choice of reactants, catalysis, and avoidance of derivatization steps. One of the most important principles is the prevention of waste. Already in the planning stage, the formation of waste should be avoided whenever possible. Another important point is the utilization of renewable resources, which is especially relevant considering the fast depletion of fossil resources and the problems arising thereof. The Twelve Principles do not only focus on the origin of the chemicals that are used, but also on their safety or toxicity. All reactants used should be innocuous and not pose a threat to humans or the environment.

More than 20 years after being published, the Twelve Principles have become one of the most important guidelines used in the field of Green Chemistry all over the world. In a review article published in 2018, Anastas *et al.* reevaluated the Twelve Principles and reviewed the progress made in the last years.^[29] One of many examples for efficient waste prevention is demonstrated in the synthesis of the pharmaceutical product Sertraline hydrochloride, an inhibitor of serotonin uptake used to treat depressions. A new reaction pathway allowed for an improved yield while reducing reaction steps, toxic waste products and the consumption of energy and water.^[30] For this improvement, Pfizer received the Presidential Green Chemistry Challenge award in 2002.^[29,31] Overall, there has been a huge advancement in the field,^[32] covering all Twelve Principles, where Green Chemistry “*spans the diversity of chemical disciplines and allied*

fields".^[29] However, some challenges remain and need to be addressed in the future, especially regarding the lack of data concerning the assessment of sustainability and the quantification of environmental and social benefits that can be gained from new methodologies.^[29] Therefore, methods for assessing the sustainability of a chemical process or a new product will be discussed in the following chapter.

2.1.3 Assessment of Sustainability

In order to compare chemical syntheses, it is necessary to establish evaluation tools that allow quantifying the 'greenness' of the respective synthesis. For a long time, yield and selectivity were the most important criteria taken into consideration when evaluating the success of a chemical reaction.^[29] Over time, different methods and concepts have been developed to assess the sustainability of a chemical process or product. The first method, which was introduced in 1991 by Barry Trost, is the concept of Atom Economy.^[33] It is an easy tool for quickly assessing the efficiency of a reaction. Written down as the second Principle of Green Chemistry, Atom Economy describes the number of atoms of all reactants that are incorporated into the final product. An ideal Atom Economy is 100% and can for instance be reached with addition reactions, such as Diels-Alder reactions, where all atoms of the starting materials end up in the desired product without the generation of additional by-products. However, with Atom Economy, the obtained number is merely based on the reaction equation. Additional substances, such as auxiliaries or solvents, are not taken into account. Furthermore, a yield of 100% and a stoichiometric use of reactants are assumed in the calculation, which is usually not achieved in chemical syntheses. Therefore, Roger Sheldon proposed the so-called Environmental factor (E factor).^[34] The E factor gives the amount of waste per kg of the final product. For the calculation, all reactants, including auxiliaries and solvents, are taken into consideration. In this regard, waste is defined as everything except for the desired product. An ideal E factor would be zero, meaning that no waste is formed during the reaction. Typical E factors in the chemical industry are listed in Table 2.2. Bulk chemicals, which are produced in high amounts, have comparably low E factors, while fine chemicals and pharmaceuticals produce a much higher amount of waste (up to 100 kg waste per kg product). This can be explained by elaborated synthesis procedures that usually require several reaction steps.

Table 2.2: E factors in the chemical industry.^[34]

Industry segment	Volume / tons per annum	E factor / kg waste per kg product
Bulk chemicals	10^4 - 10^6	<1-5
Fine chemical industry	10^2 - 10^4	5->50
Pharmaceutical industry	10 - 10^3	25->100

By now, the E factor has been widely accepted in chemical research and industry, as it offers a simple tool for measuring the efficiency of a reaction or process and its sustainability. However, the obtained values for E factors strongly depend on the boundary conditions used for the calculations, *e.g.* whether the synthesis of a starting material, which might have to be synthesized before in a multi-step process, is included in the calculation, or not. This can lead to inconsistent values in the assessment of chemical processes and shows the importance of standardized methods in the chemical industry.^[6]

In mass-based calculation procedures like Atom Economy or the E factor, the amount of waste is quantified. However, the nature of the waste and thus its environmental burden is not taken into consideration. To account for this, Sheldon suggested an environmental factor EQ, where Q is an arbitrarily assigned unfriendliness multiplier.^[35] High values of Q denote environmentally problematic reactions and should be avoided. The quantification of Q is carried out considering safety, health and environmental hazards of the raw materials and the produced waste.

The concept of the environmental factor was taken further by Eissen and Metzger in 2002.^[36] They introduced EATOS (Environmental Assessment Tool for Organic Synthesis) as easy calculation tool, especially for the comparison of reactions on a laboratory scale and for the daily use in synthetic chemistry, where they define Environmental Indices (EI) as refined assessment tool compared to the environmental factor EQ. For the calculation, the mass index S^{-1} , *i.e.* the amount of raw materials per kg of product (input of the reaction) and the E factor (amount of waste per kg of product, output of the reaction) are determined. These are then split into different categories such as substrates, catalysts, solvents, auxiliaries etc. In a next step, every compound of the feed and the waste stream is multiplied with a specific Potential Environmental Impact factor Q_{in} or Q_{out} (PEI kg^{-1}). Values for Q range from 1 (for compounds having no environmental impact) to a maximum of 10, taking into account potential risks, environmental impacts and toxicological effects. As a result, environmental indices (EI) of the feed and the waste stream can be calculated using the equations in Figure 2.1.

$$EI_{in} = Q_{input} \cdot S^{-1} = \frac{\sum_m Q_{m\ in} [PEI / kg] \cdot Raw\ material_m [kg]}{Product [kg]}$$

$$EI_{out} = Q_{output} \cdot E = \frac{\sum_n Q_{n\ out} [PEI / kg] \cdot Waste_n [kg]}{Product [kg]}$$

Figure 2.1 Environmental Indices applying EATOS introduced by Eissen and Metzger.^[36]

As an example, four different synthesis routes of 4-methoxyacetophenone *via* Friedel-Crafts acylation were compared. Applying the above described calculations, the obtained values for EI_{input} and EI_{output} ranged from 5.96-76.1 and 7.80-86.4, respectively. Thus, EATOS serves as straightforward tool to identify preferable reaction pathways. However, to date, this evaluation tool suffers from a limited database and can therefore not give a complete picture of the process or the reaction. A more extensive database is needed to broaden the potential scope of applications.^[37]

With the same objectives as the previously described examples, many different metrics for process assessment have been developed.^[38] However, for a complete assessment of the sustainability of a chemical or a product, a full life cycle assessment (LCA) is necessary. LCA is the *“compilation and evaluation of the inputs and outputs and the potential environmental impacts of a product system throughout its life cycle”*.^[39] This includes all the mass- and energy-flows of a product, from raw material acquisition to the distribution, use and the final deposition after its use (*“cradle-to-grave”* model).^[40] LCA has a very broad applicability. Therefore, LCA has become an important tool for decision-making in industry and other organizations. By now, some companies have developed their own LCA databases, such as the FLASC tool from GlaxoSmithKline^[41] or the BASFs eco-efficiency tool.^[42] Similarly as discussed above, setting the boundary conditions has a tremendous impact on the outcome of this exercise.

All the metrics mentioned above have the goal of preventing waste and reducing the overall impact of a process or product. They take up the basic idea of Green Chemistry, which is *“being benign by design”*.^[43] A concept, which takes this idea even further is the *“cradle-to-cradle”* model. In this case, a product life cycle is not only considered from the raw material to its disposal, but the circle is closed by envisaging the full recycling of the product.

One vision of the cradle-to-cradle concept is the idea, that products should not only be designed for recycling (which usually equals downcycling), but for upcycling, so that the resulting products can be used at the same level of application.^[44] Introduced by McDonough and Braungart,^[45] it envisions a full circular economy, where all resources can be divided into either a biological or a technical circle (Figure 2.2).^[46] In addition, all energy used should originate from renewable

energy sources. Thus, cradle-to-cradle strives for a completely sustainable society without resource depletion or waste that needs to be treated.

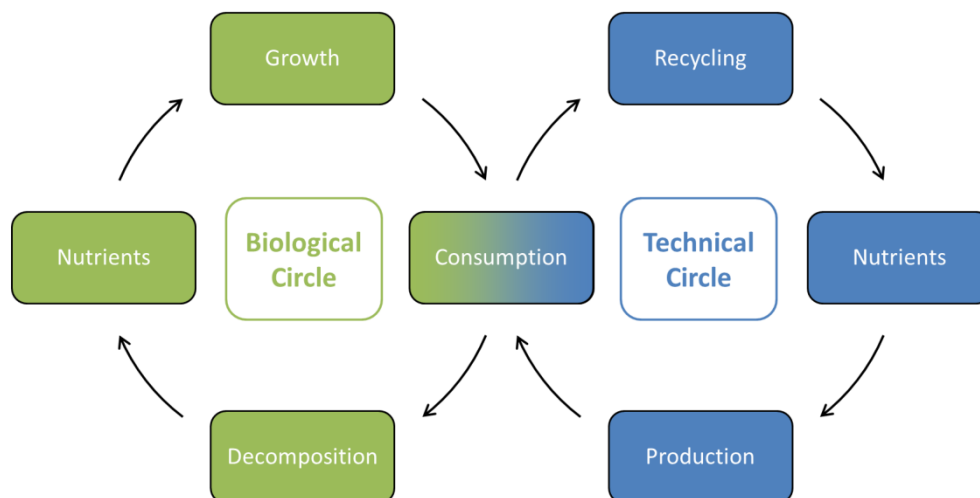


Figure 2.2 Technical and biological circle according to the cradle-to-cradle model.^[46]

To conclude, Green Chemistry is an important research area and has gained more and more attention over the last years. It strives to implement sustainability on a molecular level of chemical or product design. This includes not only the use of renewable resources, but also other reagents and reaction conditions. Different metrics to assess the sustainability of chemical processes have been developed, *e.g.* Atom Economy or the E factor. However, further development towards a full life cycle assessment is necessary to enable a better comparison of different production processes. That way, a lower environmental impact for chemicals and final consumer products can be achieved. As polymers constitute a major part of these consumer products and are to date mainly produced from non-renewable fossil resources, processes for polymer production with a lower environmental impact offer the chance to improve the overall sustainability of the products.

2.2 Renewable Resources as Feedstock in Polymer Chemistry

2.2.1 Introduction

Today, the majority of the resources used in the industry originate from fossil resources. To develop a more sustainable society, the raw materials used in industry have to change towards renewable resources. Figure 2.3 shows the use of renewable resources in the chemical industry in 2018 in Germany.^[47]

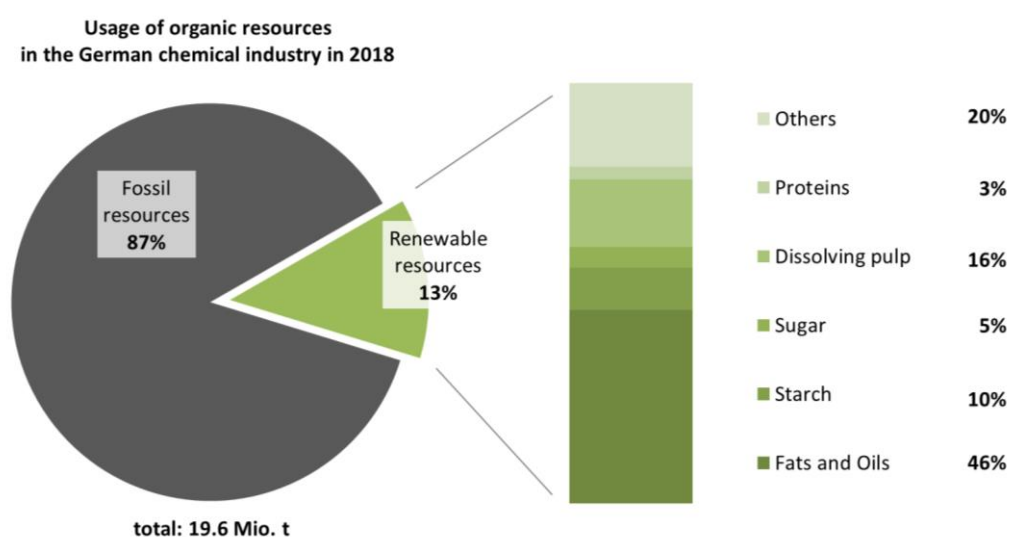


Figure 2.3 Amount and type of renewable resources used in the German chemical industry in 2018.^[47]

Figure 2.3 reveals that 87% of the resources were based on fossil resources such as gas, oil and coal, while only 13% of the used resources are renewable. Among these 13%, fats and oils represent the highest amount with 46%, followed by the carbohydrates such as starch, sugar and dissolving pulp, which corresponds to a combined amount of around 30%. The rest consists of proteins and other materials.

Even if in the last decade academic research on the synthesis of chemicals from renewable resources has greatly enhanced, the chart indicates that industrially, a fully bio-based economy is far from being reached. In 2019, 16.7 million hectares of the in total 35.8 million hectares of surface area in Germany were used for agricultural purposes. Of those 16.7 million hectares, 82% were exploited for food- and feed production and only 2% were used for the production of plants for chemical production. The remaining 16% were plants used for energy generation (14%) and fallow land (2%).^[47] Considering these numbers, an increase of the production volume

of renewable resources for the chemical industry without risking a competition between industry and the food- and feed production can be envisaged.

Polymers represent an important production area of the chemical industry. Polymers offer unique material properties and are used in most areas of our daily life.^[7] Plastics have shaped today's modern society. According to PlasticsEurope, 359 million tons of plastics were produced worldwide (61.8 million tons in Europe) in 2018.^[7] This number includes thermoplastics, polyurethanes, thermosets, elastomers, adhesives, coatings, sealants and polypropylene (PP) fibers. Not included are polyethylene terephthalate (PET) fibers, polyamide (PA) fibers and acrylic fibers. However, polymers also cause several problems, for instance if they end up in the environment and also if they are produced from fossil resources, which is shown in Figure 2.4 (left).^[16] The time scale of crude oil formation by natural processes is significantly slower compared to the rate of polymer production, use and disposal. Additionally, if disposed in landfills or released into the environment, non-biodegradable polymers take several hundred years to degrade, causing severe waste problems. In the ideal case, polymers get fully recycled or incinerated. However, this has not been realized yet in many countries. On the other hand, renewable resources are renewed in a much shorter timeframe, thus closing the loop between production, use and degradation.

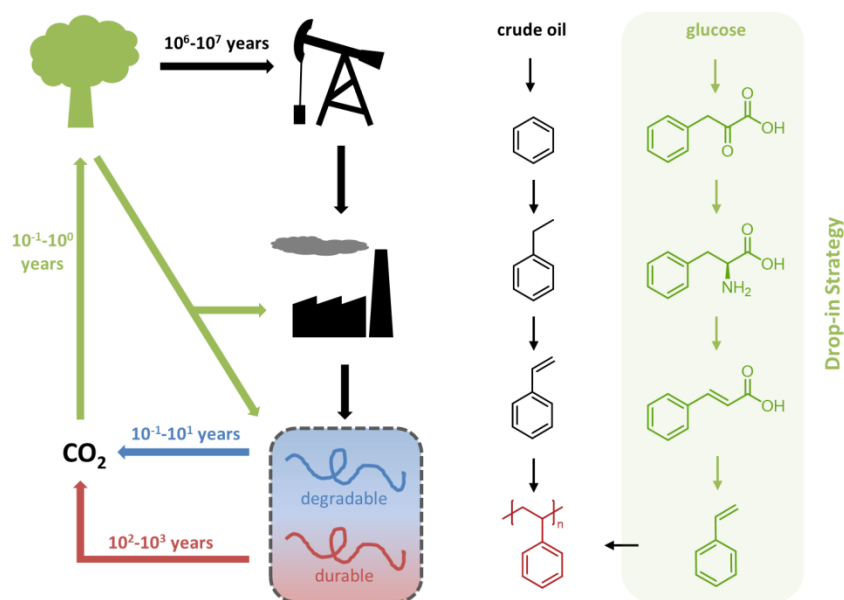


Figure 2.4 Relative time scales for production and degradation of polymers and an example for the drop-in strategy for the replacement of fossil-based polymers (adapted from ^[16]).

For the transition from fossil-based polymers towards renewable alternatives, there are two possible strategies. The first strategy, also known as drop-in strategy, aims to establish synthesis routes for conventional monomers from renewable resources. Exemplarily, the drop-in strategy

for polystyrene is shown in Figure 2.4 (right). Classically, styrene is synthesized in two steps using benzene from crude oil. Starting from glucose as renewable substrate, styrene can also be produced by a biotechnological process in four steps. With the drop-in strategy, the obtained bio-based polymers can directly substitute fossil-based products, as they are compatible with the already existing infrastructure. However, bio-based polymers should compete with petrochemical equivalents economically, while offering the benefit of a lower carbon footprint. Another strategy for the implementation of renewable feedstock is the development of new synthesis routes and products. Renewable resources can either be directly polymerized or used for the production of novel platform chemicals, which can be used for the synthesis of polymers with new structures. Depending on their thermal and mechanical properties, these polymers offer alternatives to existing polymers or even offer new interesting properties.^[12] As a consequence, the sustainable synthesis of renewable polymers has been and continues to be an important research topic.^[13] Figure 2.5 shows the most important classes of renewable resources for the synthesis of bio-based polymers.

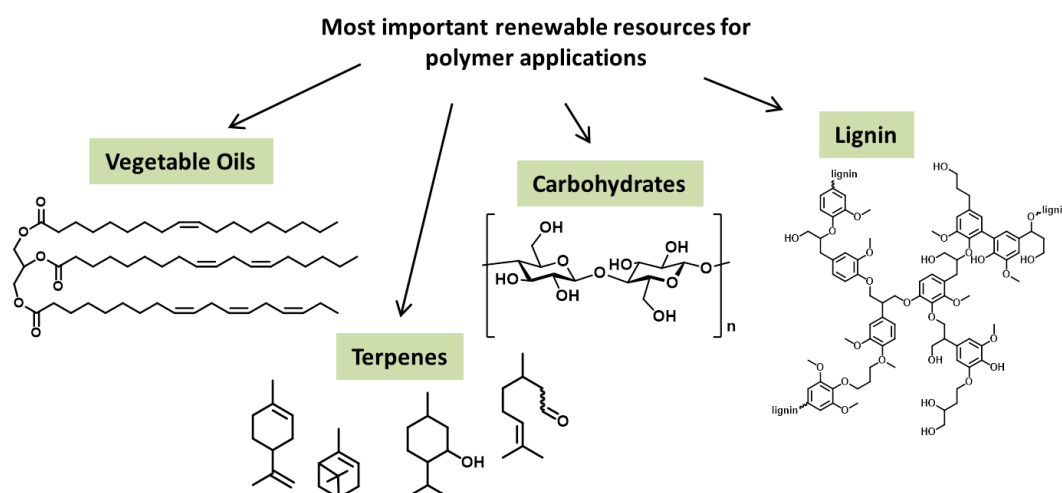


Figure 2.5 Most important renewable resources for polymer applications.

Vegetable oils have been excessively exploited for the synthesis of sustainable polymers. They offer manifold advantages, for example a high availability, biodegradability and low toxicity. Polymeric materials obtained from vegetable oils also display a broad range of thermal and mechanical properties.^[48] Similarly, carbohydrates including cellulose, starch, hemicellulose, chitin and sugars, as well as platform molecules derived thereof are already well established. Carbohydrates are the most abundant class of naturally occurring polymers and, besides their high abundance, offer advantages such as biocompatibility, nontoxicity and biodegradability.^[13] However, also lignin and terpenes have shown a great potential. As lignin and terpenes are used

as starting materials in this work, these resources will be covered in more detail in chapter 2.2.2 and 2.2.3.

Bio-based polymers offer the possibility to reduce the dependency on limited fossil resources, while at the same time reducing the environmental impact of plastics. Therefore, and caused by an increasing consumers demand, the chemical industry has an increasing interest in implementing sustainable alternatives. However, today bioplastics account for only one percent of the total amount of plastics produced annually.^[49] To date, that low number is mainly caused by the high cost of bio-based polymers compared to their petrochemical analogues.^[8] According to European Bioplastics, the European Association of the bioplastic industry, the global production capacity reached 2.11 million tons in 2019 (compared to over 350 million tons of polymers produced in total).^[49] Importantly, according to European Bioplastics, bioplastics are defined as plastics which are bio-based, biodegradable, or both. This way, also fossil-based but biodegradable plastics such as polybutylene adipate terephthalate (PBAT) are included in the statistics. The number can be divided into biodegradable and non-biodegradable polymers. The non-biodegradable plastics contain drop-in products such as bio-based polyethylene (PE, 11.8% of all bioplastics), polypropylene (PP, 0.9%), polyethylene terephthalate (PET, 9.8%), as well as numerous polyamides (PA, 11.6%), and polytrimethylene terephthalate (PTT, 9.2%). The highest amount of biodegradable plastics is made up of starch blends (21.3%), followed by polylactic acid (PLA, 13.9%) and the fossil-based PBAT (13.4%). Other representatives are polybutylene succinate (PBS, 4.3%) and polyhydroxyalkanoates (PHA, 1.2%).

To summarize, the implementation of bio-based polymers continues to be an important challenge. At the moment, production costs of bio-based alternatives are still higher than their petrochemical counterparts, but as bio-based polymers offer great advantages such as a high abundancy, a huge structural variety as well as a lower carbon footprint, their industrial production is promising.^{[49][24]} Because of their relevance to this work, lignin (and especially lignin-derived vanillin) and terpenes as well as their exploitation in polymer synthesis will be discussed in detail in the following chapters.

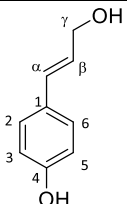
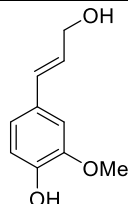
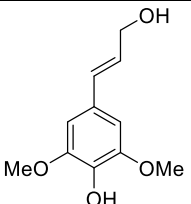
2.2.2 Lignin Valorization for Sustainable (Semi-)Aromatic Polymers

2.2.2.1 Lignin Structure and Isolation

Lignin is a heterogeneous, highly abundant biopolymer. Together with cellulose and hemicellulose, they represent the major components of lignocellulosic biomass.^[50] Lignin

constitutes the third-most abundant biopolymer and the only renewable resource with an aromatic structure that is available in high amounts from renewable resources.^[51] In plant cell walls, lignin is embedded between the cellulose and hemicellulose and acts as a framework holding the lignocellulosic matrix.^[50] Depending on the wood source, lignin can make up 15-35% of the dry lignocellulosic mass. Lignin is biosynthesized from the three main building blocks coumaryl alcohol, coniferyl alcohol and sinapyl alcohol; each of them exhibits a phenylpropane structure featuring a different number of methoxy groups. Table 2.3 shows lignin contents of several lignocellulosic sources as well as the structure and composition of the three phenylpropane units.^[1] Softwood has the highest lignin content with around 27-33 wt% and mainly contains coniferyl alcohol with small amounts of sinapyl alcohol. In contrast, hardwood contains both building units in equal amounts. Grasses have the lowest lignin content and additionally contain low amounts of coumaryl alcohol, which does not bear methoxy groups.

Table 2.3 Lignin content and composition of the main lignocellulosic sources.^[1]

	Lignin / wt%	Phenylpropane unit / %		
Structure		 <p>Coumaryl alcohol</p>	 <p>Coniferyl alcohol</p>	 <p>Sinapyl alcohol</p>
Softwood	27-33	-	90-95	5-10
Hardwood	18-25	-	50	50
Grasses	17-24	5	75	25

In the primary structure of lignin, these three monolignols are connected by carbon-carbon and carbon-oxygen bonds. The polymerization is achieved by radical enzymatic polymerization initiated by the enzymes peroxidase and laccase. The most common linkage is the β -O-4 linkage between the β -carbon of one unit and the phenolic hydroxyl group of another unit (for assignment, see Table 2.3). It accounts for almost 50% of all linkages in softwood.^[52]

Traditionally, lignin is obtained as a by-product in the pulp and paper industry. Despite its high abundance, lignin has only been used scarcely for the manufacture of new materials or products. It is estimated that of the 150 million tons of the global annual production of chemical pulp, a total amount of around 70 million tons of lignin is obtained.^[53] In 2010 for instance, only about

2% of the isolated lignin was used for specialty products. The rest was burned as a cheap fuel for energetic use.^[54]

For isolating lignin from the other wooden components, different pulping processes have been developed. Depending on the pulping process and the lignin source, the structure and properties of the isolated lignin differ.^[55] In industry, four different pulping processes are used. The main pulping process, producing over 90% of all chemical pulps, is the Kraft pulping.^[56] In the Kraft process, lignocellulosic biomass is reacted with an aqueous solution of sodium hydroxide and sodium sulfide, also called white liquor, at temperatures of around 170 °C.^[57] During the cooking, depolymerization takes place by cleavage of the ether linkages of the lignin structure. After cellulose isolation, the remaining pulp liquor, called black liquor, is usually incinerated generating energy for the pulp mill. Alternatively, lignin can be obtained by precipitation. Kraft lignin contains degraded oligomers bearing thiol groups from the incorporation of sulfur.^[56] The second pulping process is the sulfite pulping. In this case, biomass is treated with sodium-, ammonium-, magnesium- or calcium (bi)sulfite. Depending on the counter ion, the pulping proceeds in alkaline, neutral or acidic conditions. During the pulping, sulfonate groups are inserted into the lignin structure, yielding degraded oligomers with a higher sulfur content (4-8 wt%) compared to Kraft lignin.^[56] The third process, the so-called soda pulping, is related to the Kraft process; however, no sodium sulfide is employed.^[56] It was historically applied to non-woody biomass such as straw, grasses, bagasse etc. which contain a lower amount of lignin and a larger amount of alkali-labile ester linkages. Through the absence of sulfur-containing substances, no sulfur is incorporated during the soda pulping process. This is also the case for organosolv pulping, where the biomass is mixed with an organic solvent, *e.g.* alcohols (methanol, ethanol, butanol), polyols (ethylene glycol, glycerol), cyclic ethers, organic acids (formic acid, acetic acid) or ketones.^[56] Organosolv pulping yields oligomeric fragments containing alkoxy groups (if an alcohol is used for pulping) or ester groups (upon employing acids). The organosolv process is considered an eco-friendly alternative to the Kraft process.^[58] Apart from the aforementioned processes, several other pulping processes have been developed, resulting in lignins with different structures and properties.^[56]

2.2.2.2 Application of Lignin for Polymeric Materials

After isolation, despite its heterogeneous structure, lignin can be directly used for the synthesis of polymers. As the lignin fragments contain a high amount of free phenolic and aliphatic hydroxyl groups, they can be used for polyurethane-, polyester-, phenolic- or epoxy resin syntheses (Figure 2.6).^[55] However, these hydroxyl groups exhibit a different reactivity in polymerization reactions. For example, aliphatic hydroxyl groups show a higher reactivity in

polyurethane synthesis compared to aromatic phenol groups.^[59] Together with the steric hindrance of lignin, this can decrease the reactivity of lignin in polymerization reactions.^[60]

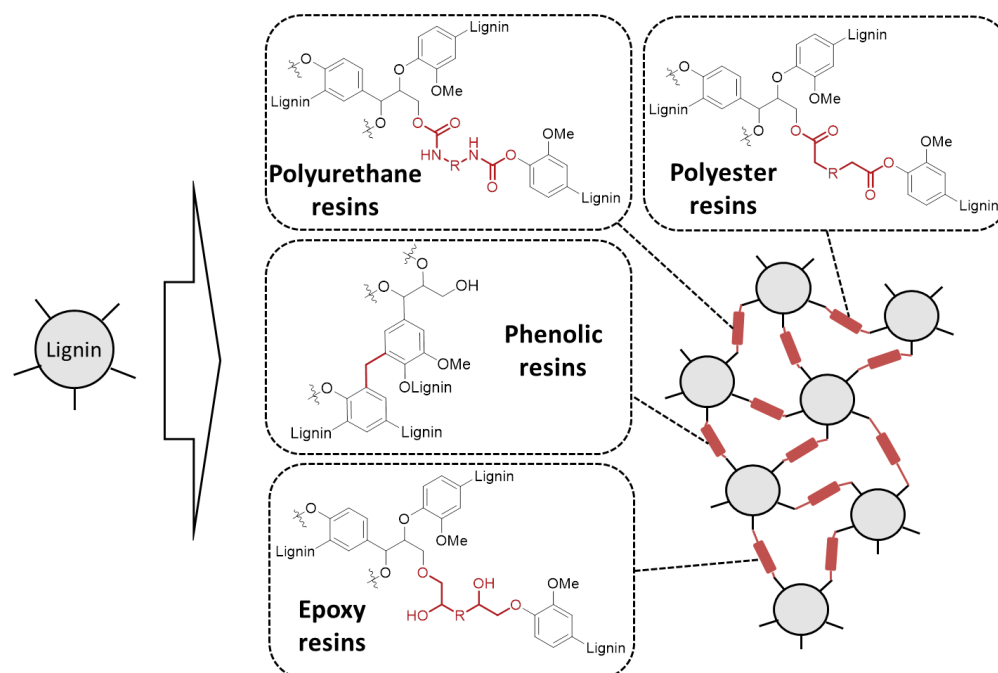


Figure 2.6 Possibilities for the direct polymerization of lignin (adapted from ^[55]).

Polyurethanes are formed by the reaction of di- or poly-isocyanates with polyols. With lignin being used as polymeric polyol, polymers can be formed in a reaction with diisocyanates.^[61] Different diisocyanates have been used, for example 4,4'-methylene bis(phenylisocyanate)^[62] or oligoethyleneoxide diisocyanate.^[63] For the former, Vanderlaan *et al.* showed the film formation with organosolv lignin together with polyethylene glycol (PEG) as co-monomer.^[64] The authors reported samples with a lignin content of up to 35 wt% and were able to vary the cross-linking density depending on the lignin content. Pan and Saddler investigated the replacement of conventional polyols by ethanol organosolv lignin and kraft lignin in rigid polyurethane foams.^[65] Foams providing a good structure and strength were obtained up to a lignin content of 25-30 wt% and 19-23 wt%, respectively. By adding a chain extender such as butanediol, the strength of the foams was enhanced.

For the formation of polyesters, lignin is reacted with dicarboxylic acids or acid chlorides.^[52] For example, Gandini *et al.* reported the polymerization of kraft lignin with aliphatic sebacoyl- or aromatic terephthaloyl diacid chlorides.^[66] In both cases, materials with a thermal stability above 200 °C were obtained. A different linker was used by McDonald *et al.*, who synthesized polymeric networks from lignin and highly branched poly(ester-amines) obtained by melt polycondensation of 1,1,1-triethanolamine and adipic acid.^[67] The tensile strength of the

polymers increased with increasing lignin content. Additionally, the T_g was varied by using different dicarboxylic acids.

In phenolic resins, where phenols are typically reacted with formaldehyde, the partial substitution of phenol through lignin has been investigated, especially for the use as adhesives. For example, Vázquez and co-workers compared the performance of lignin-phenol-formaldehyde resins with lignin-free samples applying them as adhesive for plywood.^[68] The authors found that the gelation time of lignin-containing samples increased. However, traction tests of the glued boards gave satisfactory results for all samples. In a similar way, Adhikari *et al.* found that lignin-modified phenolic resins were thermally more stable than the original unmodified resins. At a lignin content of 50%, the material retained 78% of its adhesive strength for wood-wood systems and 86% for aluminium-aluminium systems.^[69] In 2013, Castellán *et al.* showed the synthesis of a completely bio-based phenolic resin from lignin and glutaraldehyde showing similar or superior properties than the respective phenol-formaldehyde resin.^[70] The reactivity of lignin during polymerization is sometimes limiting but can be increased by modification of lignin, such as hydroxymethylation or phenylation.^[55]

For the synthesis of epoxy resins, which will be further discussed in Chapter 2.3, lignin with its hydroxyl groups can be applied as curing agent or hardener. Delmas *et al.* applied wheat straw lignin as a polyol substitute of bisphenol A using polyethyleneglycol diglycidyl ether as epoxide monomer. Thermomechanical results were similar to a bisphenol A based epoxy-amine system.^[71] For the application as adhesive, Feldman *et al.* reported the use of different lignins in epoxy-lignin polyblends with several amine hardeners. Hardwood lignin gave better adhesion properties compared to softwood lignin and values 178% higher than the control epoxy polymer. Additionally, an insertion of up to 20% of mineral fillers did not affect the adhesive strength of the resins.^[72]

In summary, the direct use of lignin for thermosetting polymers shows promising results. This is advantageous, as lignin is a cheap and abundant resource and an application without further modification is beneficial in terms of sustainability. However, in many cases, chemical modification of the lignin structure is required before the use in formulations or polymerizations. Different modification pathways have been reported,^[13] for example the methylation of the hydroxyl groups present in the lignin structure.^{[73][74]} A common pathway is the oxyalkylation, especially the oxypropylation with propylene oxide^[73] or propylene carbonate as more sustainable alternative.^[75] Another useful method is the transesterification, as shown by Labidi *et al.*, who showed the modification of organosolv lignins with fatty acids to be used as

fillers in poly(lactic acid) (PLA).^[76] In a similar way, Avérous *et al.* used transesterification with oleic acid for the synthesis of polyols that were used for polyurethane formation.^[77] In order to increase the amounts of hydroxyl groups in the lignin structure, demethylation of the methoxy groups is also possible, for example applying Lewis acids.^[78] Another sustainable pathway comprises allylation of the aromatic hydroxyl groups of lignin using allyl methyl carbonate.^[79] Allylated lignin was subsequently polymerized with different plant oils in an olefin metathesis curing reaction.^[80]

The use of lignin in polymer materials shows great potential. However, due to its complex and heterogeneous macromolecular structure, which strongly depends on the origin as well as on the isolation procedure, the development of industrialized procedures remains challenging.^[52] Therefore, further depolymerization of lignin to synthesize aromatic platform chemicals is an attractive alternative and will be discussed in the following chapter.

2.2.2.3 Synthesis of Platform Chemicals from Lignin

Currently, lignin is mostly used for the generation of heat and electricity, but also hydrogen and syngas production.^[1] However, as lignin is the only abundant renewable resource for aromatic structures, an efficient utilization of lignin for the synthesis of aromatic platform chemicals is desirable.

During the pulping and the following depolymerization process, lignin bonds are cleaved and a complex mixture of monolignolic substances is formed.^[81] The composition of this mixture strongly depends on the pulping procedure and the depolymerization method. Generally, the products contain an aromatic core with one or two methoxy groups in *ortho* position and a side chain in *para* position. Depending on the pulping conditions, the side chains for example vary from alkyl and alkenyl chains to alcohols, carbonyl and carboxyl groups. The obtained molecules can either be isolated or used for a subsequent upgrading for the synthesis of specific chemical products. A schematic illustration of the obtained product mixture and the possible upgrading strategies is depicted in Figure 2.7.^[56] The main tool for the modification of the core structure is hydrodeoxygenation, which leads to a defunctionalization. This is important for the synthesis of drop-in chemicals such as toluene or phenol, which have a lower oxygen content than lignin building blocks. Moreover, the side chain could be modified for example by hydrogenation, oxidation or decarboxylation reactions. Figure 2.7 shows the great potential of lignin for the synthesis of diverse chemicals and structures. A proper use of a so far under-exploited resource could help replacing petroleum-based platform chemical by a more sustainable alternative.

Many promising procedures for lignin conversion have been presented in recent years.^[50,56,82] However, efficient processes on industrial scale still remain a challenge.^[50]

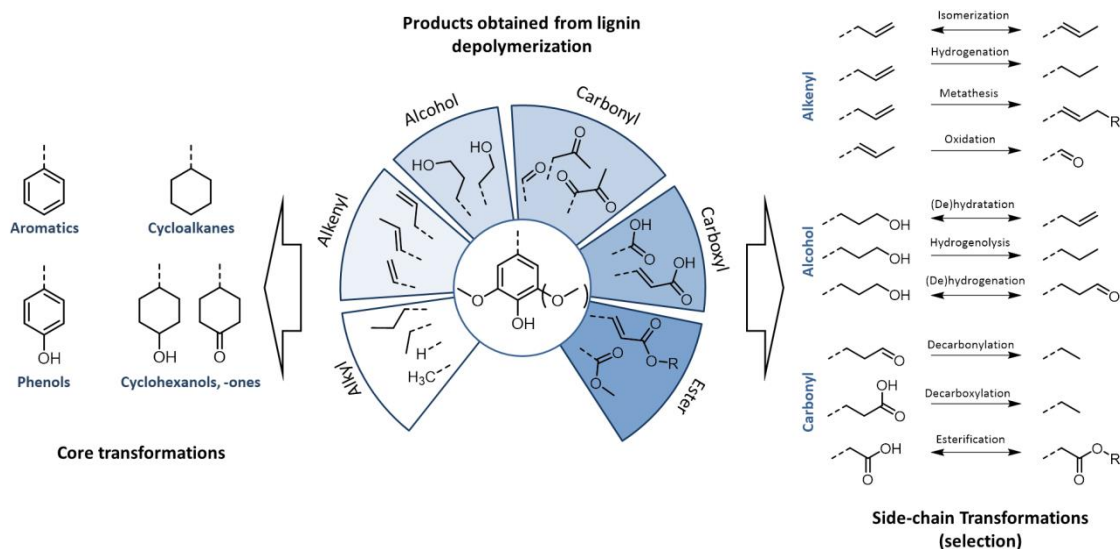


Figure 2.7 Products obtained from lignin depolymerization and following upgrading strategies (adapted from ^[56]).

Currently, vanillin is one of the only substances produced from lignin on an industrial scale. Vanillin (4-hydroxy-3-methoxybenzaldehyde) is the highest volume aroma chemical produced worldwide. Being used in large amounts in the food and cosmetic industry as flavoring and fragrance ingredient, it is currently produced in a scale of 20 000 tons per year.^[83] Initially, vanillin was synthesized from eugenol *via* an isomerization and oxidation process.^[84] However, this process was soon replaced by the production from lignin waste sulfite liquor.^{[85][86]} When synthetic vanillin obtained from petroleum became a cheap alternative, almost all lignin-to-vanillin plants closed at the end of the 1990s. Today, the Norwegian company Borregaard is the only factory which is still producing vanillin from lignin. The main production pathway is currently starting from petroleum (85%), only 15% are still produced from lignocellulosic biomass. The production from the vanilla plants accounts for under 1%.^[83] In the lignin-to-vanillin production nowadays, only lignin from sulfite pulping is used; however, much research is put into making the use of different lignin sources accessible and increasing vanillin yields.^[87] Processes generally involve subjecting an aqueous solution of lignin to an alkaline oxidative depolymerization, followed by the isolation of the formed vanillin. At the moment, production of vanillin from lignin is too expensive to be competitive with its petrol-based analogue, but this could change if oil prices rise.^[83] Additionally, further development of biorefineries with a better valorization of lignin could help establishing bio-based aromatic chemicals as a viable option in the future.

2.2.2.4 Polymers from Vanillin-derived Molecules

As discussed, lignin constitutes a versatile and valuable resource for the chemical industry. Many different compounds can potentially be obtained from lignin and many of these compounds have already been investigated for the use in novel polymeric materials.^{[88][89]} Interesting monomers are for example vanillin and vanillic acid, as well as *p*-coumaric acid, ferulic acid, syringaldehyde or 4-hydroxybenzoic acid. As vanillin constitutes an important chemical in this thesis and also with regards to industrial availability, this chapter highlights advances that have been made in the synthesis of polymers based on vanillin as well as its derivatives, vanillic acid and vanillyl alcohol. The synthesis of epoxy resins is not included in this chapter and will be discussed in detail in chapter 2.3.

Thermoplastic Polymers

For the synthesis of thermoplastic polymers from vanillin, all different classes of polymers have been investigated. A straightforward method of polymerization is the homopolymerization to polyvanillin, which was reported by Amarasekara *et al.* (Figure 2.8). They synthesized dimeric vanillin *via* enzymatic catalysis, followed by electrochemical reductive polymerization in aqueous sodium hydroxide solution. Polymers with average molecular weights of around 10,700 g/mol exhibiting dispersities between 1.42 and 1.58 and a thermal stability up to 300 °C were obtained.^[90] The dimeric vanillin was also polymerized with aliphatic diamines to form Schiff base polymers, which were able to complex metal ions such as copper, iron and cobalt.^[91]

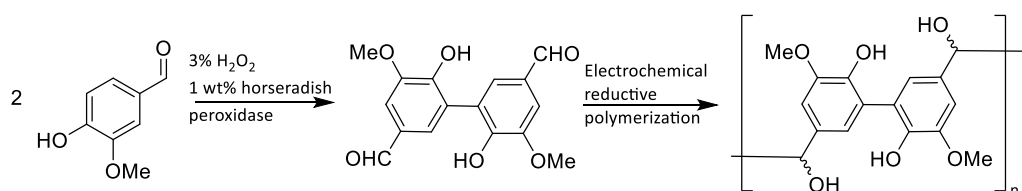


Figure 2.8 Electrochemical polymerization of vanillin to polyvanillin.^[90]

Polyesters are another important polymer class and have been extensively investigated. Indeed, the first report of vanillin polymerization was the synthesis of polyesters reported in 1955 by Bock and Anderson. Vanillic acid was dimerized at the phenol group using aliphatic dibromides and the resulting diacids were then polymerized with ethylene glycol.^[92] A similar approach was reported by Pang *et al.*, who synthesized two different diacids from vanillic acid. The first was obtained by coupling two molecules with 1,4-dibromo butane, the second by a reaction of vanillic acid with chloroacetic acid. Both diacids were subsequently polymerized with a set of α,ω -diols to yield polymers with molecular weights of $M_w = 16.6\text{--}78.7$ kDa, dispersities (\mathcal{D})

between 1.39 and 2.00 and T_g s ranging from 5 to 67 °C.^[93] The same group also reported the polymerization of the respective methyl ester analogues with aliphatic diols obtained from 10-undecen-1-ol, another bio-based compound.^[94] To show the practical use of vanillin-based polymers, Miller and co-workers synthesized an alternative polymer for the commodity plastic PET (Figure 2.9). Vanillin was transformed to acetylferulic acid, followed by hydrogenation and polymerization catalyzed by zinc acetate. With a T_g of 73 °C, the obtained polymer showed similar thermal properties as PET ($T_g = 67$ °C). Thus, it could be a renewable alternative for this high-volume commodity polymer.

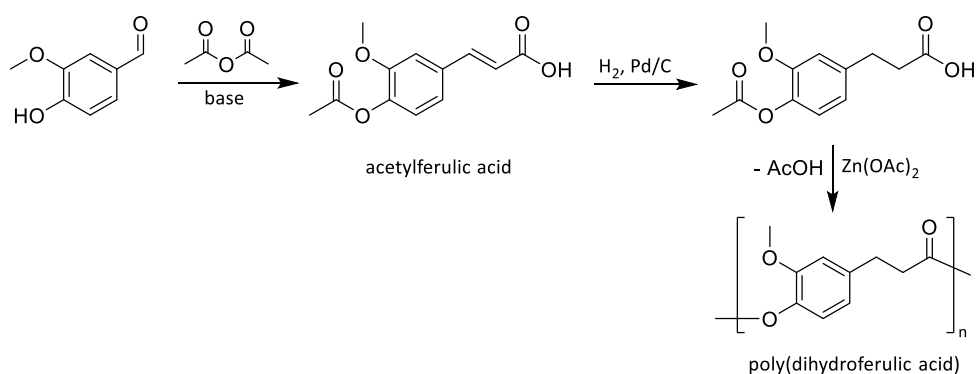


Figure 2.9 Poly(dihydroferulic acid) as PET alternative published by Miller *et al.*^[95]

Miller and co-workers also investigated the influence of methoxy groups in the substrates on the properties of the resulting polymers. They synthesized aromatic/aliphatic polyesters from 4-hydroxybenzaldehyde, vanillin and syringaldehyde and found that an increase in methoxy groups led to a decrease in the glass transition temperature. Furthermore, they observed that polyalkylene vanillates generally showed higher melting temperatures than the other samples.^[96] The synthesis of (semi-)aromatic polyesters was also reported by Cramail *et al.* They used enzymatic coupling of vanillin and methyl vanillate to form symmetric biphenyl monomers, which were subsequently polymerized with a series of bio-based diesters, leading to polyesters with glass transition temperatures between -5 and 139 °C and a thermal stability of up to 350 °C.^[97] A similar series of biphenyl monomers was converted to α,ω -dienes, which were subsequently polymerized *via* acyclic diene metathesis polymerization (ADMET). For the vanillin-based polymer, molecular weights of $M_n = 29$ kDa and a dispersity of $\mathcal{D} = 1.7$ were obtained. Furthermore, a T_g of 156 °C and a thermal stability up to 380 °C were reported.^[98]

ADMET polymerization was also used by Firdaus and Meier, who used vanillin and fatty acid derivatives for the synthesis of two different diene monomers (Figure 2.10).^[99] Both monomers were subsequently polymerized by ADMET and thiol-ene polymerization. For the ADMET polymers of the monoester and the diester, molecular weights of 49.6 kDa ($\mathcal{D} = 1.96$) and

25.6 kDa ($\bar{M}_n = 1.88$) were obtained, respectively. When subjected to thiol-ene, the molecular weights were lower and ranged between 9.60 and 16.1 kDa. All polymers showed low T_g s between -37.1 and -17.9 °C, which can be attributed to the long aliphatic chains in the polymer backbone. Additionally, melting points between 36.1 and 68.8 °C were reported for the thiol-ene polymers.

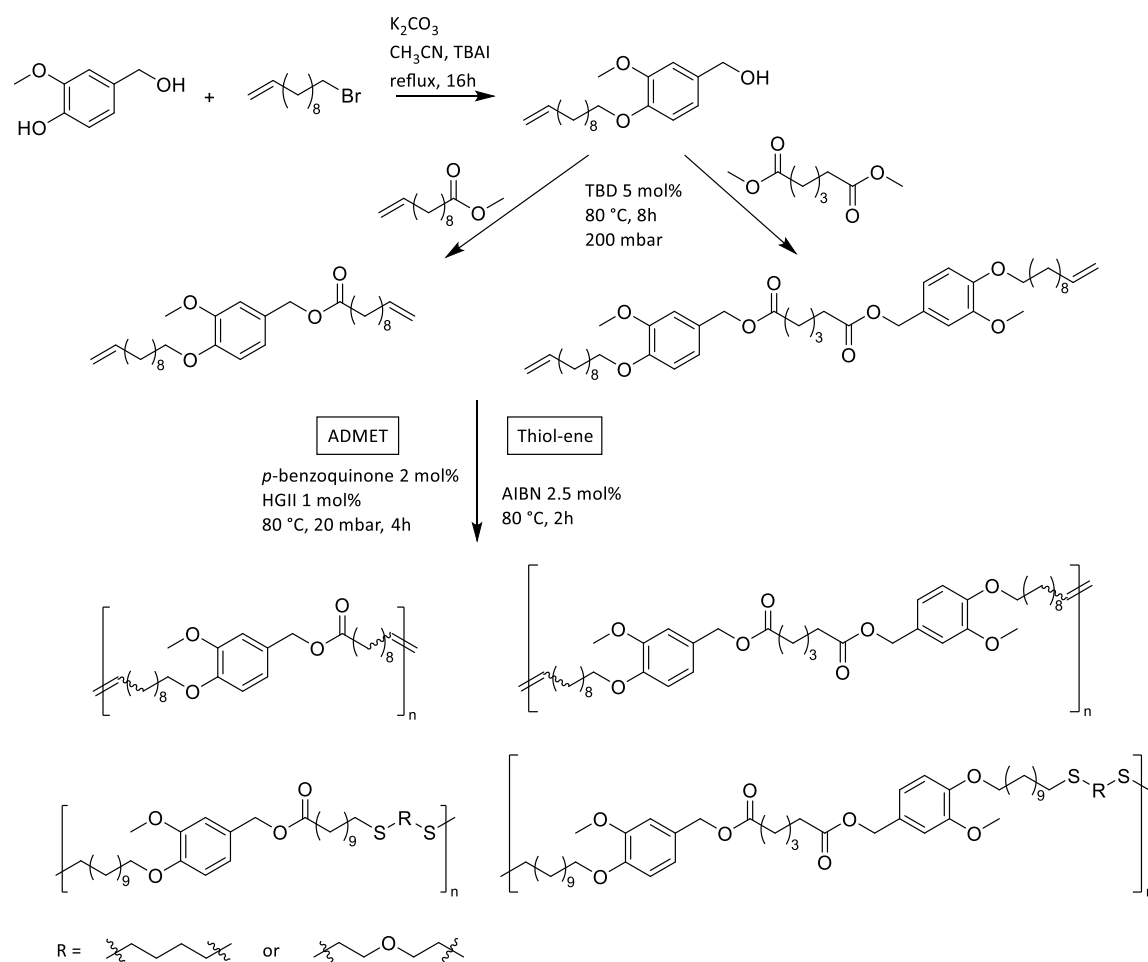


Figure 2.10 Synthesis of renewable copolymers derived from vanillin and fatty acid derivatives.^[99]

Another possibility to increase the amount of renewable content in a conventional polymer consists of introducing vanillin or syringaldehyde into the backbone of poly(acrylate)s or poly(meth acrylate)s (Figure 2.11). This was shown by Zhou and co-workers in 2016.^[100] They obtained polymers with high glass transition temperatures between 95 and 180 °C and a good thermal stability.

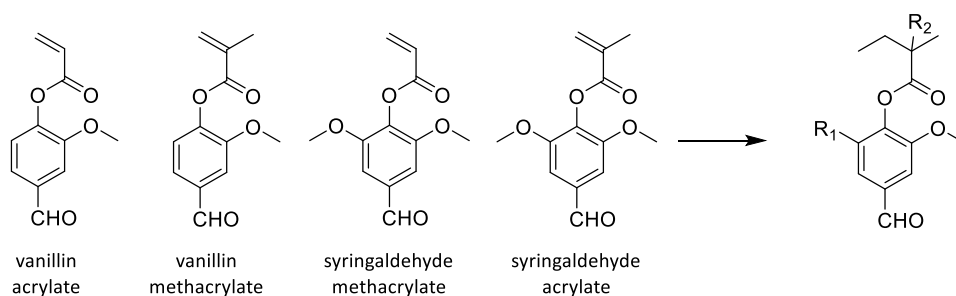


Figure 2.11 (Meth)acrylates functionalized with vanillin or syringaldehyde for the synthesis of partially bio-based poly acrylate and poly(meth) acrylate polymers.^[100]

In addition to the aforementioned polymerization strategies, many other routes have been reported, for example the synthesis of polycarbonates,^[101] polyamides,^[102] formaldehyde polymers^[103] or polyacetals.^[104]

Thermosetting Polymers

Vanillin has also been investigated for the use in thermosetting polymers. Apart from the use in epoxy resins, a common strategy is the modification with acryl- or (meth)acryl moieties to prepare vinyl ester resins. Using this strategy, a completely vanillin-based thermoset was synthesized by Zhang and Kessler. They used vanillyl alcohol and inserted a methacryl group at both hydroxyl groups applying methacrylic anhydride. The formed tetrafunctional monomer was then polymerized *via* free-radical polymerization, yielding a material with a T_g of 99 °C, a storage modulus of 4.7 GPa and a thermal stability ($T_{d10\%}$) up to 341 °C.^[105] The same group also reported the polymerization of methacrylated vanillin with acrylated epoxidized soybean oil in different molar ratios. Increasing the amount of methacrylated vanillin from zero to 80 wt%, T_g s between -4 and 103 °C were obtained.^[106] A similar strategy was used by Stanzone and co-workers, who synthesized methacrylated vanillin and the cross-linker glycerol dimethacrylate in a two-step, one-pot reaction (Figure 2.12). After curing, the resin showed a glass transition temperature of 155 °C and a storage modulus of 3.6 GPa.^[107] Furthermore, the same polymer system was compatible with stereolithography, which allows for photopolymerization with rapid production times.^[108]

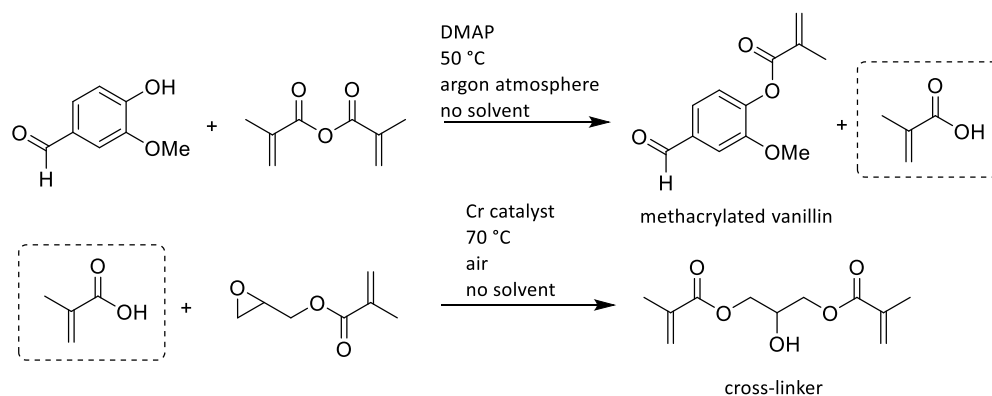


Figure 2.12 Vinyl ester resin based on vanillin and glycerol dimethacrylate.^[107]

Another combination of two renewable resources was shown by Saimoto *et al.* They functionalized vanillin and similar compounds with methacrylate moieties. The aldehyde group was then used for coupling the monomer with the amine groups of chitosan in an imine condensation. Thus, it was possible to cure the modified chitosan under UV irradiation for the use as bio-based coating.^[109]

For the synthesis of benzoxazine resins, a high performance thermoset class, Sini and Varma synthesized bis-benzoxazine monomers using vanillin, different diamines and formaldehyde.^[110] Polymerization occurs *via* ring-opening polymerization of the benzoxazine ring. For the partially bio-based polymers, high T_g s (202-255 °C) were reported. They also showed good adhesive strength and can find application in high temperature adhesives.

High glass transition temperatures were also reached using vanillin-based polycyanurates reported from Harvey *et al.*^[101] They coupled two vanillin molecules to form stilbene-type bisphenols. These were subsequently transformed to cyanate esters using cyanogen bromide followed by polymerization *via* thermal cyclotrimerization. A resin with a T_g of 202 °C and a thermal stability up to 335 °C was formed. The presented polymer shows interesting thermal properties; however, the use of toxic CNBr is not favorable in terms of sustainability.

A very recent example for thiol-ene polymerization was given by Alabi and co-workers. They synthesized defined, vanillin-based polyurethane macro-monomers with different chain lengths *via* sequential reductive amination and carbamation. The monomers were cross-linked with dithiols *via* thiol-ene through vinyl moieties in the monomer backbone. Interestingly, the sequence of the macro-monomer had influence on the network topology and its thermal and mechanical properties, allowing a selective tuning of the polymer properties.^[111]

Apart from the work described above, additional interesting vanillin-based polymers have been reported,^{[112][113]} further demonstrating the great potential of lignin-based structures, especially of vanillin, for the application in polymer science. With a further development of bio-refineries and a broader production of new platform chemicals from lignin, an even more extended portfolio of viable polymers will hopefully be accessible in the future.

2.2.3 Terpenes: A Diverse and Valuable Resource

2.2.3.1 Chemical Structure and Utilization of Terpenes

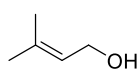
Terpenes are a class of natural compounds produced by many plants and fungi and represent the largest and most diverse class of secondary metabolites.^[114] To date, around 55,000 different terpenes are known.^[114]

Terpenes are formally derived from isoprene units (2-methyl-1,3-butadiene). Depending on the number of isoprene units, terpenes are categorized as hemi- (C₅), mono- (C₁₀), sesqui- (C₁₅), di- (C₂₀), sester- (C₂₅), tri- (C₃₀), tetra- (C₄₀) or polyterpenes. The isopropyl group of isoprene is usually referred to as '*head*', the ethyl group as '*tail*'. Terpenes with 10-25 carbon atoms exhibit isoprene units connected in a '*head-to-tail*' connection (so-called '*isoprene rule*'). Longer terpenes contain one '*tail-to-tail*' connection. Through cation formation, cyclization can take place (also shown in Figure 2.15). Selected terpenes sorted by the amount of carbon atoms are depicted in Figure 2.13.^[115] Well-known terpenes are monoterpenes such as limonene, menthol or pinene as well as the diterpene retinol (vitamin A) or the polyterpene *cis*-polyisoprene, which is used for the production of natural rubber. Due to their high structural variety, terpenes constitute a valuable class of natural compounds, which can be transformed into numerous products with applications in fragrances, perfumes, flavors, and pharmaceuticals as well as useful synthetic intermediates.^[116]

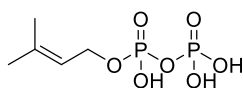
Number of carbon atoms

C₅

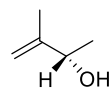
Hemiterpenes



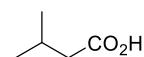
Prenol



Isopentenyl pyrophosphate



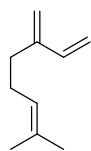
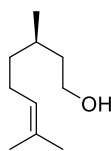
(S)-3-Methyl-3-butene-2-ol



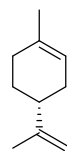
Isovaleric acid

C₁₀

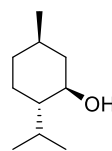
Monoterpenes

 β -Myrcene

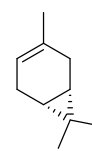
(R)-(+)-Citronellol



(R)-(+)-Limonene



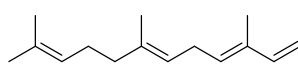
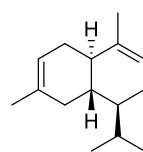
(-)-Menthol

 α -Pinene

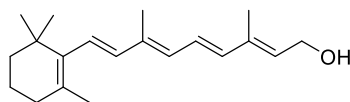
(+)3-Cyrene

C₁₅

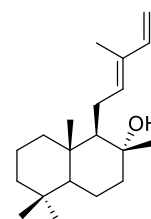
Sesquiterpenes

 α -Farnesene β -CadineneC₂₀

Diterpenes



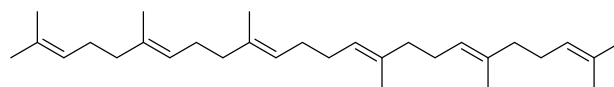
Retinol (vitamin A-alcohol)



Abienol

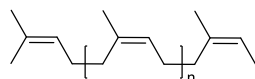
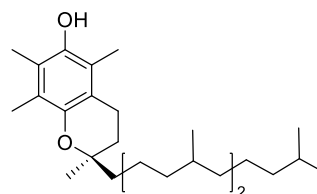
C₃₀

Diterpenes



Squalene

Polyterpenes

*cis*-Polyisoprene(+) α -Tocopherol (vitamin E)**Figure 2.13** Examples for terpenes sorted by the amount of isoprene units.^[115]

In the plant, terpenes are synthesized in an enzymatic process, starting from the activated acetic acid derivative acetyl coenzyme A (acetyl-CoA). This biosynthetic pathway for the precursor geranyl pyrophosphate is shown in Figure 2.14.^[115] The reaction starts with the condensation of two acetyl-CoA molecules to form acetoacetyl-CoA. Through a cascade of enzymatic conversions, acetoacetyl-CoA is transformed to isopentenyl pyrophosphate. Two molecules of isopentenyl pyrophosphate are then coupled to form geranyl pyrophosphate. Repeating of this coupling enables the formation of higher terpenes such as sesquiterpenes.

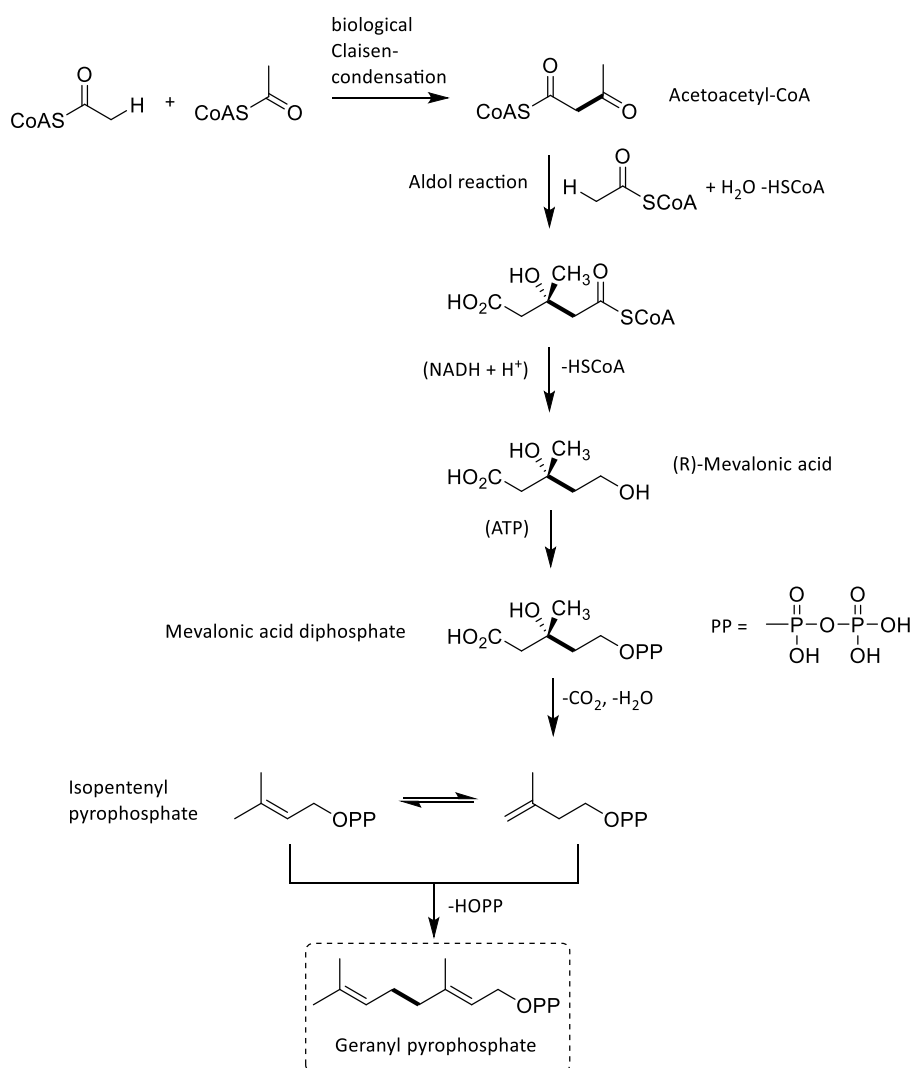


Figure 2.14 Biosynthetic pathway for the intermediate geranyl pyrophosphate starting from acetyl-CoA.^[115]

Starting from the intermediate geranyl pyrophosphate, different monoterpene structures can be formed. Figure 2.15 shows some possible reaction pathways. In a first step, a *p*-menthane cation is formed, which can isomerize to structures like α - or β -pinene, limonene, 3-carene, borneol or camphene.^[14] This way, plants are able to biosynthesize a high amount of different structures with various roles, *e.g.* as attractant or as protection against enemies.^[115]

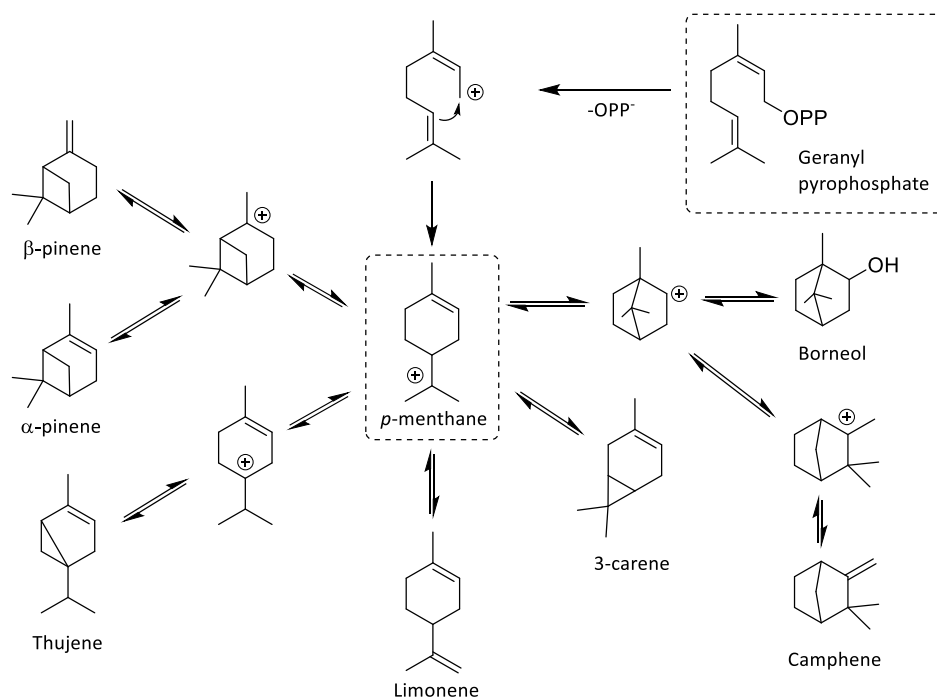


Figure 2.15 Transformation of geranyl pyrophosphate into different monoterpene structures.^[14]

The nature of the plant influences the nature and amount of produced terpenes. For example, pinenes can be found in turpentine of coniferous trees, limonene is mostly found in citric fruits, such as lemons or oranges, menthol causes the smell of peppermint and eugenol can be extracted from cloves. For the extraction of the valuable essential oils, treatments such as cold expression (juice oils), steam distillation (peppermint oil, lemon grass oil), infusion (coffee, tobacco, rum), solvent extraction (lilac flower, thyme), vacuum distillation (orange oil terpenes, pine oil) or a combination of several techniques, are used.^[116] More than 300,000 tons per year are produced globally. Turpentine is the major resource for terpenes regarding the total production volume. It is primarily composed of α -pinene (45-97%), then β -pinene accounts for 0.5-28% and also low amounts of other terpenes are found. Another high-volume substance is (*R*)-limonene, which is produced as a by-product in the citrus industry in an amount of 70,000 tons per year.^[14] Considering this production volume, especially α -pinene and limonene are interesting substrates for the chemical industry to produce fine chemicals, but also for the synthesis of novel polymeric materials.

2.2.3.2 Chemical Modification of Terpenes

Due to their large structural diversity, terpenes constitute a useful resource for the chemical industry. For many purposes, such as flavors and fragrances, terpenes can directly be used without further modification. However, through chemical modifications, terpenes produced in higher volume can be transformed into other terpene structures, or new structural motifs can be

synthesized for example for polymer production. Numerous modification pathways have been explored. Figure 2.16 exemplarily shows possible chemical modifications of pinene.

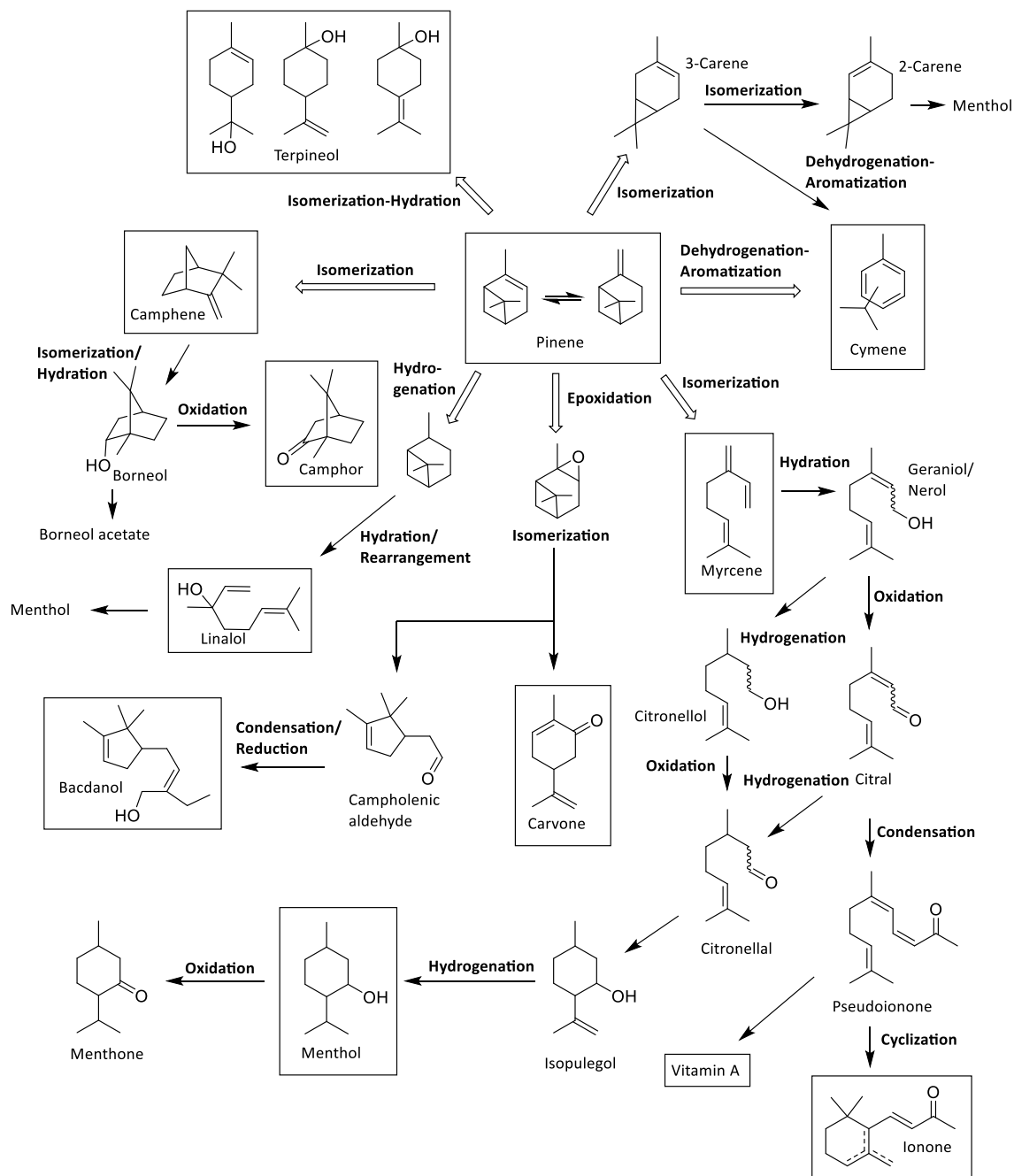


Figure 2.16 Chemical modification pathways for pinene (adopted from reference ^[24]).

Important transformations include isomerization reactions, hydrogenation reactions to obtain saturated hydrocarbons, and also oxidation and reduction reactions. Moreover, one of the most important transformations of terpenes is the epoxidation of the existing double bonds. Epoxides are a valuable class of compounds, which can be used for many different purposes. Especially in polymer chemistry, epoxides are important intermediates for direct polymerization or for the

synthesis of other functional monomers. Therefore, the epoxidation of terpenes and their rearrangement into carbonyl groups as a useful follow-up reaction are discussed in the following section.

Terpene Epoxidation

The epoxidation of terpenes has been extensively investigated and many different catalytic systems have been presented.^{[117][118]} Therefore, in the following section, only selected examples are shown to give an overview over available catalytic options and catalysts. These examples have been selected for their relevancy to the sustainability of epoxidation conditions. A general challenge in the transformation of terpenes is finding selective and efficient reactions, as terpenes are prone to isomerization and other side reactions.

A well-known method for the epoxidation of olefinic substrates is the use of peracids, especially *m*-chloroperbenzoic acid (*m*CPBA) (Figure 2.17).^[119] Reactions proceed *via* a nucleophilic attack of the double bond on the peroxy O-O bond in a concerted reaction process.

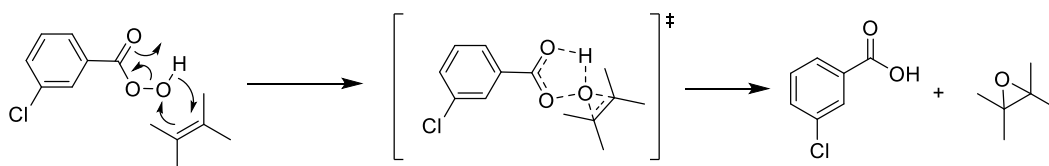


Figure 2.17 Mechanism for the epoxidation of double bonds applying *m*CPBA.^[119]

*m*CPBA offers the advantage of easy handling and usually results in good yields.^[119] However, procedures employing *m*CPBA show a low atom economy and are not considered as sustainable. As an alternative, catalyst-free procedures have been reported, for example using the oxidation agent Oxone[®], a potassium peroxydisulfate salt. Kaliaguine *et al.* used this procedure for the double epoxidation of limonene (Figure 2.18).^[120] Acetone acts as solvent and oxidation agent by reacting with Oxone[®] to form dimethyl dioxirane (DMDO). The influence of the Oxone[®]/limonene ratio as well as the Oxone[®] addition rate was studied. Using 1.30 eq of Oxone[®] per double bond and a reaction time of 45 min, limonene dioxide was formed quantitatively without the formation of side products. Compared to *m*CPBA, Oxone[®] is considered as a more sustainable alternative, having the same benefits of being easy to handle, stable, non-toxic and cheap.^[121] However, stoichiometric amounts are required, which can be considered as a drawback. Up to date, a selective and high-yield-synthesis of limonene dioxide is difficult and not easy to achieve with other methods.

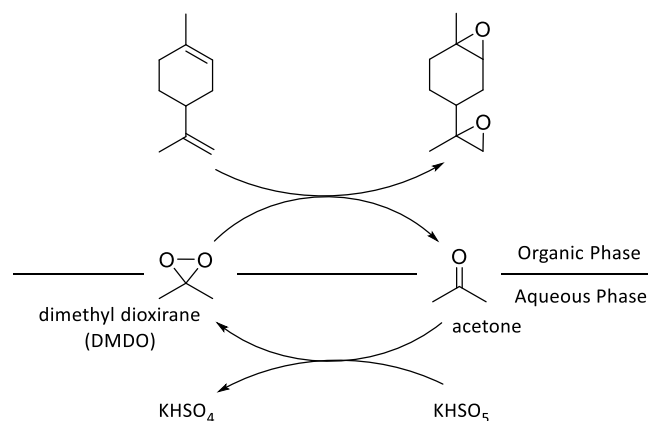


Figure 2.18 Catalyst-free epoxidation of limonene with Oxone[®] and acetone.^[120]

Regarding the epoxidation of α,β -unsaturated ketones, *e.g.* carvone, a selective oxidation of the internal double bond can be reached by using hydrogen peroxide in an alkaline sodium hydroxide medium.^[119] This concept was selected by Fioroni and co-workers, who reported 90% yield of carvone-1,2-oxide in a aqueous reaction mixture applying 2.00 eq H_2O_2 and 0.50 eq of cetyltrimethylammonium hydroxide, which additionally facilitated the solubilization of the substrate.^[122]

In the last years, enzyme catalysis has gained increased interest as sustainable alternative to conventional procedures in the chemical community, as it usually entails mild reaction conditions. In most cases, the enzyme *Candida Antarctica* lipase B (CALB) is used. An example for sustainable enzyme catalysis was given by Olivo *et al.*^[123] They used CALB in combination with urea-hydrogen peroxide as oxidation agent in ethyl acetate. The oxidant is slowly released from a solid urea-hydrogen peroxide, thus circumventing a slow addition of aqueous hydrogen peroxide. Using this reaction procedure, α -pinene was oxidized in a yield of 95% in 5.5 h. In contrast, 85% yield of α -pinene oxide was reported by Rüschen, Klaas and Warwel, who used CALB with aqueous H_2O_2 and dimethyl carbonate as co-oxidant.^[124] The authors proposed the perhydrolysis of dimethyl carbonate to carbonic peracid monomethyl ester as oxygen transfer agent as a possible reaction mechanism (Figure 2.19). Efforts were also devoted to improve the recyclability of the lipase. For example, Stamatis *et al.* proposed the immobilization of CALB on organic-modified clays, which enabled a reusability of the lipase for up to four cycles.^[125]

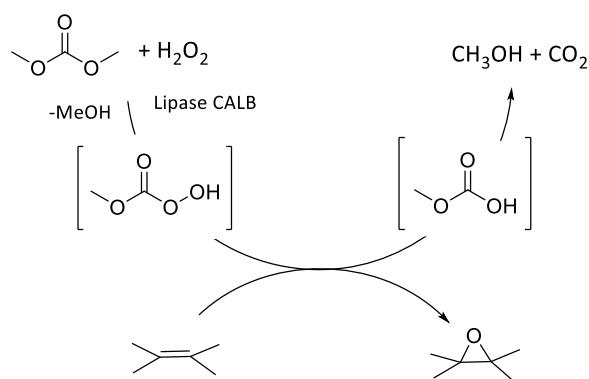


Figure 2.19 Proposed reaction mechanism for the epoxidation employing CALB in dimethyl carbonate.^[124]

Besides catalyst-free or chemo-enzymatic procedures, most epoxidation protocols entail the usage of metal catalysts. Up to date, different protocols with metal catalysts have been reported.^[117] For example, tungsten-based polyoxometalate catalysts have been proposed. In 1996, Ishii *et al.* reported the epoxidation of various terpenes in biphasic conditions with chloroform as solvent, 0.5 mol% peroxotungstophosphate as catalyst and hydrogen peroxide as oxidant.^[126] Limonene was oxidized to limonene-1,2-oxide in a yield of 91%. γ -Terpinene was also epoxidized to the respective bisepoxide in a yield of 79%. To replace halogenated solvents in polyoxometalate-catalyzed reactions, Nardello-Rataj *et al.* screened eighteen eco-friendly solvents in a system with amphiphilic dodecyltrimethylammonium polyoxotungstate nanoparticles.^[127] Using 2-MeTHF and 1.5 eq H_2O_2 , limonene was oxidized to limonene-1,2-oxide in a yield of 73% after 3 h. Similarly, the more demanding substrate α -pinene oxide was obtained in a yield of 51% with 2.0 eq H_2O_2 in 4 h. In contrast, Bull *et al.* very recently developed a reaction procedure for the solvent-free epoxidation of terpenes.^[128] They prepared a phase transfer polyoxotungstate catalyst and reached very good yields for various terpene substrates with H_2O_2 as oxidant, *e.g.* for the epoxidation of limonene (94% limonene-1,2-oxide yield), 3-carene (92%) or α -pinene (85% yield).

Not only polyoxotungstate catalysts have been used, also the direct use of sodium tungstate (Na_2WO_4) has been investigated. Wang *et al.* showed the epoxidation of natural rubber applying a Na_2WO_4 /acetic acid/hydrogen peroxide system.^[129] They reached an epoxidation of 52% after 24 h reaction time. At the same time, hydrolytic degradation took place, leading to telechelic epoxidized liquid natural rubber, which could be used for the preparation of solid polymer electrolytes. Sodium tungstate was also applied to monoterpenes, as shown by Grigoropoulou and Clark.^[130] Using a phosphate-buffered hydrogen peroxide solution with catalytic amounts of Na_2WO_4 , several terpenes were oxidized with yields varying between 47 and 88%.

The most popular metal catalyst for terpene epoxidation is methyltrioxorhenium (MTO). In 1998, Jacobs *et al.* used a catalytic system consisting of 0.5 mol% MTO and 0.4 eq pyridine in dichloromethane and with hydrogen peroxide as oxidant.^[131] They obtained 80% yield for the epoxidation of α -pinene and 90% yield of limonene dioxide in the epoxidation of limonene. Similarly, Rudler and co-workers used the same biphasic system of dichloromethane and aqueous H₂O₂ with 1 mol% MTO per double bond for the oxidation of several terpene substrates, reaching yields between 35% (α -pinene) and 98% (citronellal).^[132] The benefit of adding a mono- or bidentate Lewis basic additive was also confirmed by Kühn *et al.* They found that *t*-butylpyridine was the most efficient additive for the epoxidation of α -pinene and limonene, yielding 95% of α -pinene oxide and 77% of limonene-1,2-oxide, respectively, while using 0.5 mol% MTO.^{[133][134]} In 2010, Yamazaki also reported good results in the presence of 3-methylpyrazole and 1-methylimidazole. Several terpenes were oxidized employing a low catalyst loading of 0.2-0.3 mol% MTO with either 10 mol% 3-methylpyrazole together with 1 mol% 1-methylimidazole, or solely 10 mol% of 3-methylpyrazole and aqueous H₂O₂. For α -pinene, yields up to 95% were obtained and limonene was transformed to limonene dioxide in an excellent yield of 98%.^[135] Furthermore, an interesting procedure was published by Saladino and co-workers.^[136] They used the benefits of Lewis-base adducts and increased the stability of these adducts by microencapsulation in a polymeric polystyrene support (Figure 2.20). The different encapsulated catalysts were then used for the epoxidation of substrates, such as cyclooctene or styrene, but also for the monoterpenes 3-carene, limonene and α -pinene. For all three terpene substrates, excellent yields of 98% or higher were achieved in a dichloromethane/acetonitrile solvent mixture with hydrogen peroxide as oxidant. Additionally, the catalyst choice allowed for the complete suppression of diol formation, which is a common side reaction during epoxidation, especially for sterically demanding substrates. The encapsulation also enabled the removal and recycling of the catalyst and all catalysts proved to be stable for at least five recycling experiments.

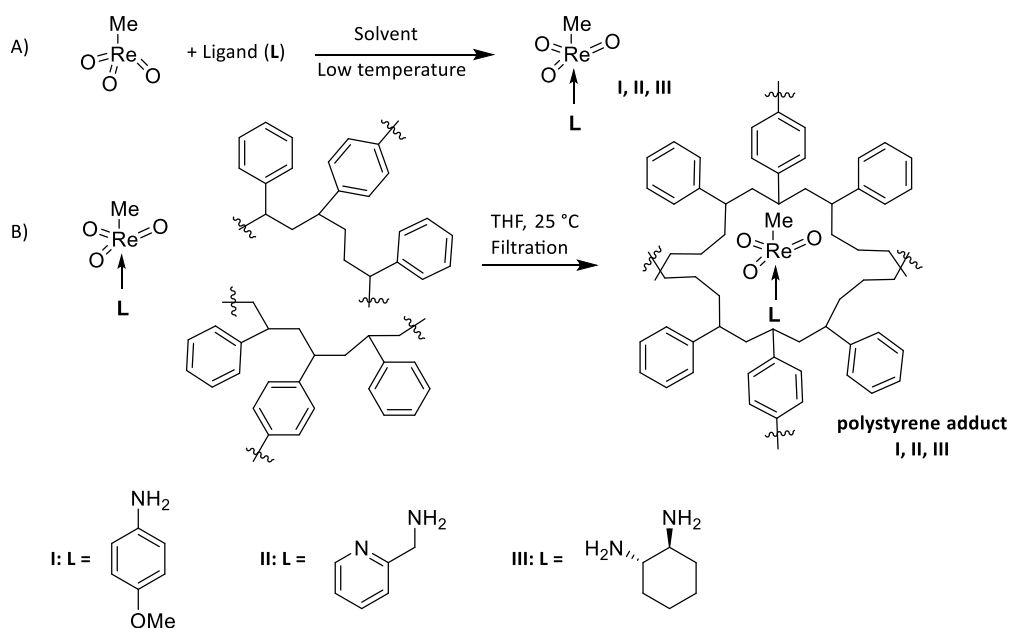


Figure 2.20 Preparation of microencapsulated Lewis base adducts of MTO according to Saladino *et al.*^[136]

Besides rhenium, manganese has been investigated as catalyst in epoxidation reactions. For example, Meier *et al.* studied the epoxidation of α -pinene, first with the model substance Mn(III) acetate.^[137] Compressed air was used as sustainable and abundant oxidant in a toluene/dimethyl formamide solvent mixture. With these conditions, 35% yield of α -pinene oxide was achieved. In a second step, the replacement of Mn(III) acetate by a manganese-based metal-organic framework (MOF) gave comparable results while being recyclable. The heterogeneous catalyst preserved its activity for at least five reaction cycles. This example shows the high potential of using air as oxidation agent, which is even more desirable than oxidants such as hydrogen peroxide, as air is abundant and does not have to be pre-synthesized. Another interesting concept for catalyst recycling was developed by Pereira and co-workers, who reported the synthesis of a hybrid Mn(III)-porphyrin magnetic nanocomposite.^[138] For the epoxidation, molecular oxygen was used, giving high yields of epoxide. For example, limonene was oxidized to limonene-1,2-oxide and obtained in an isolated yield of 95% and α -pinene oxide was synthesized in an isolated yield of 96%. Due to the magnetic properties of the employed nanoparticles, the catalyst was easily recovered and reused in five consecutive runs without loss of activity. As an alternative to conventional catalysts, Grison *et al.* recently reported on the synthesis of Eco-CaMnO_x catalysts directly obtained by a controlled thermal treatment of Mn-rich biomass.^[139] After a detailed analysis, the catalysts were used for the epoxidation of several terpenes in a system with sodium bicarbonate and hydrogen peroxide as oxidant. The authors observed high conversions, with yield and selectivity varying between medium and high, depending on the substrate and the catalyst employed.

A cheap and abundant catalyst for olefin epoxidation is alumina, Al_2O_3 . Various examples have already shown a successful application with different substrates.^{[140][141][142]} Generally, hydrogen peroxide is used as oxidant. The epoxidation strategy was also used for sterically demanding terpene substrates, such as α -pinene or limonene with good results.

Several other metal catalysts have also been used for the epoxidation reaction of terpenes and should also be mentioned. For example, copper was investigated and proved to be a good catalyst for terpene oxidation. Different strategies were followed to develop greener procedures using copper catalysts, such as immobilization in an ionic liquid,^[143] or utilization of a Cu-MOF in combination with molecular oxygen as sustainable oxidation system.^[144] Titanium,^[145] chromium,^[146] gallium,^[147] or iron^[148] also showed a good catalytic activity for terpene epoxidation.

In summary, great progress has been made in the last years and research on this topic remains intensive. Only with the development of sustainable, selective and cheap catalytic systems, a broader usage of terpenes in the chemical industry can be reached.

Terpene Epoxide Rearrangements*

As mentioned before, epoxides are valuable synthetic building blocks, benefiting from their high reactivity to undergo different organic transformations.^[149] A very useful method for converting epoxides into another valuable functional group is the rearrangement into carbonyl compounds (Meinwald rearrangement),^[150] traditionally catalyzed by a Lewis acid (Figure 2.21).^[151]

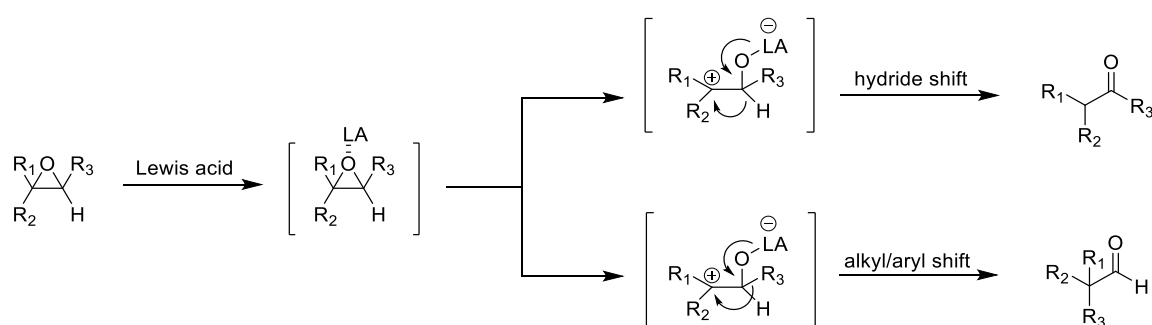


Figure 2.21 Mechanism of the Meinwald rearrangement.^[151]

Depending on the substrate, solvent and the chosen catalyst, the reaction can proceed *via* two different pathways. In the case of a hydride shift, a ketone is formed whereas a shift of the alkyl

* This section was previously published in the introduction of: Löser P.S., Rauthe P., Meier M.A.R., Llevot A. 2020 Sustainable catalytic rearrangement of terpene-derived epoxides: towards bio-based biscarbonyl monomers. *Phil. Trans. R. Soc. A* **378**: 20190267.

or aryl group leads to the formation of an aldehyde. While typically Lewis acids such as boron trifluoride (BF_3), zinc bromide (ZnBr_2) or magnesium bromide (MgBr_2) have been used for rearranging epoxides,^[152] heterogeneous catalysts have also shown to be active towards various substrates, e.g. active alumina,^[153,154] alumino- and borosilicates^[155,156] and acidic resins such as Amberlyst 15.^[157] The reaction efficiency and product distribution are not only influenced by the catalyst, but also by the chemical structure of the substrate. High yields are easily achieved with aromatic substances,^[158] whereas the rearrangement of aliphatic substrates is more challenging regarding reactivity and selectivity.^[151]

During the rearrangement reaction, the hydride shift is usually favored over the migration of alkyl groups. In order to obtain a selective alkyl shift, Takanami *et al.* reported the use of the porphyrin complex $\text{Cr}(\text{TPP})\text{OTf}$.^[159] With a catalyst loading between 1 and 20 mol%, they showed the regio- and stereoselective rearrangement of epoxides to aldehydes *via* alkyl migration for different aliphatic and aromatic substrates with yields between 56-99%. In a similar fashion, Kunz *et al.* used a pincer-type rhodium catalyst to rearrange terminal epoxides into methyl alkyl and aryl ketones with generally good product yields.^[160]

The Meinwald rearrangement of renewable resources has also been investigated. For example, Alsalme *et al.* recently showed the complete and selective rearrangement of epoxidized methyl oleate to the corresponding ketone (100% yield) using 3 wt% of YCl_3 as catalyst.^[161] Not only fatty acids, but also epoxidized vegetable oils were rearranged successfully.^[157] However, the most prominent examples for the rearrangement of bio-based epoxides encompass α -pinene oxide and limonene oxide. Classical Lewis acids, such as ZnBr_2 ^[162] or $\text{Cu}(\text{BF}_4)_2 \cdot n\text{H}_2\text{O}$ ^[163] as well as some of the heterogeneous catalysts mentioned above, have been applied to α -pinene oxide substrates.^[152,155] During this rearrangement, the five-membered cyclic campholenic aldehyde was obtained, in most cases, as the main reaction product. This was also confirmed by Salakhutdinov *et al.*, who used supercritical solvents for the thermal transformation of α -pinene oxide. Thermolysis in isopropyl alcohol yielded campholenic aldehyde as main product together with pinocamphone formed by hydride shift with a combined yield of 80% (Figure 2.22).^[164]

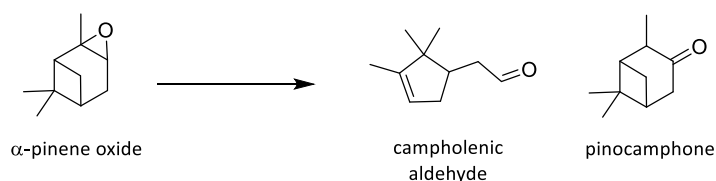


Figure 2.22 Main products obtained in the thermal transformation of α -pinene oxide in supercritical solvents.^[164]

Jana *et al.* reported a yield of 85% for the rearrangement of α -pinene oxide to campholenic aldehyde using a high amount (6 eq) of InCl_3 catalyst. A better result of 88% was obtained using bismuth(III) oxide perchlorate, $\text{BiOClO}_4 \cdot \text{H}_2\text{O}$, with a lower catalyst loading of 20 mol%.^[165]

The rearrangement of limonene oxide has been extensively studied employing different catalysts.^[152] Figure 2.23 shows possible reaction products of this transformation. Dihydrocarvone **C** is formed by hydride shift, whereas products **A** and **B** are formed by alkyl migration with simultaneous ring contraction.

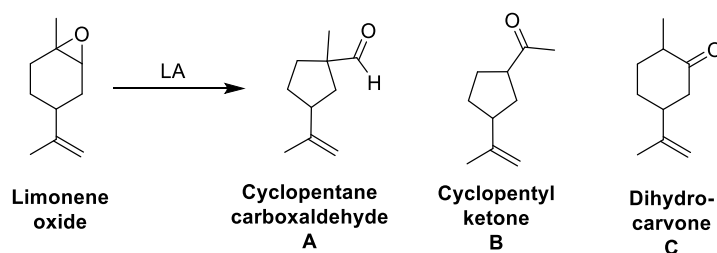


Figure 2.23 Possible reaction products for the rearrangement of limonene oxide.

A yield of 59% of dihydrocarvone **C**, 30% of cyclopentane carboxaldehyde product **A** and 10% of a cyclopentyl ketone derivative **B**, were achieved using 1.7 mol% ZnBr_2 as catalyst.^[166] A similar product mixture of cyclopentane carboxaldehyde **A** and dihydrocarvone **C** in a ratio of 14:86 (82% combined yield) was obtained for *trans*-limonene oxide with 1 mol% of erbium triflate, $\text{Er}(\text{OTf})_3$.^[167] Using the *cis*-isomer, the two products were formed in a ratio of 20:80 (87% overall yield). This difference in reactivity and selectivity between the two isomers was reported by Psaro *et al.* Indeed, using heterogeneous silica alumina catalysts, *cis*-limonene oxide reacted to cyclopentane carboxaldehyde **A** (77% yield), whereas *trans*-limonene oxide yielded dihydrocarvone **C** (70% yield).^[154] A slightly higher dihydrocarvone yield of 76% starting from a *cis*- and *trans*-limonene oxide mixture was reported by Tanabe *et al.*, using LiClO_4 as catalyst.^[152] However, the combination of a relatively high catalyst loading of 0.66 eq and toluene as solvent affected the sustainability of the procedure. In a similar fashion, Sankararaman *et al.* employed a stoichiometric amount of LiClO_4 in diethyl ether to synthesize dihydrocarvone **C** in a high yield of 90%.^[168] In 2013, Costa and Gusevskaya reported dihydrocarvone yields of up to 82% employing heteropolyacids for the rearrangement of limonene oxide with a low catalyst loading of 0.1 mol% in 1,4-dioxane as solvent.^[169] However, it is recommended to substitute 1,4-dioxane according to solvent selection guides for greener procedures.^[170]

Overall, these reports show the increasing interest in epoxide rearrangements, which constitute a powerful tool for the transformation of epoxides into carbonyls, another valuable functional

group. With this transformation, the scope of application of the terpene feedstock can be further enhanced.

2.2.3.3 Terpene-based Polymers

Terpenes have been intensively investigated in polymer chemistry. Besides polyisoprene, which has been used long before the synthetic polymers were invented, nowadays also other terpene structures have gained attention as attractive monomers. Indeed, a large number of terpene-based polymers have been reported to date.^{[171][172][173]} Especially pinene and limonene, which are produced on a large scale, are interesting starting materials for direct polymerization or for the synthesis of new monomers. Due to the vast amount of literature, the following section is limited to polymers obtained from limonene and highlights some possible valorization pathways of this versatile monoterpene.

Thermoplastic Polymers from Limonene

Probably the first homopolymerization of limonene was reported by Roberts and Day in 1950. They investigated the cationic polymerization of limonene as well as α - and β -pinene applying Lewis acid catalysts.^[174] Later, in 1965, the polymerization of limonene with Ziegler-type catalysts was studied, but resulted in low molecular weight polymers.^[175] Brum and Forte attempted cationic polymerization using AlCl_3 as catalyst and obtained an oligomeric product with a molecular weight of ~ 500 Da. This low molecular weight was attributed to the role of limonene as good chain transfer agent.^[176] Thus, homopolymerization of limonene remains challenging. Therefore, copolymerization with other olefin substrates was attempted. For example, the copolymerizations with methyl methacrylate,^[177] styrene,^[178] *N*-vinyl pyrrolidone^[179] or maleimide^{[180][181]} have been reported.

The polymerization of functionalized limonene is a good alternative to the direct polymerization, circumventing the challenges of chain transfer and enabling a broader scope of polymerization techniques and chemical structures. A straight-forward method for the polymerization of modified limonene was shown by Howdle *et al.*, who functionalized terpenes with acrylic acid applying a hydroboration and esterification protocol (Figure 2.24).^[182] For limonene acrylate, polymers with a molecular weight of 17 kDa, a dispersity of $\bar{D} = 2.23$ and a T_g of -5 °C were obtained.

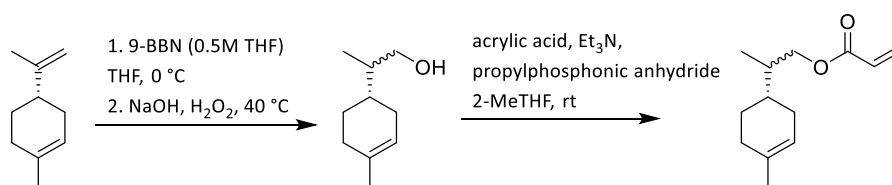


Figure 2.24 Functionalization of limonene with acrylic acid applying a hydroboration and esterification protocol.^[164]

Limonene oxide has been intensively investigated for the synthesis of sustainable polymers. It is easily obtained from limonene by the epoxidation of the *endo*-cyclic double bond and shows an interesting reactivity, for example for the copolymerization with carbon dioxide to form polycarbonates. The first report of a polycarbonate from limonene oxide was published in 2004 by Coates *et al.*^[183] They investigated different β -diiminate zinc acetate complexes and reaction conditions in order to optimize the synthesis procedure (Figure 2.25).

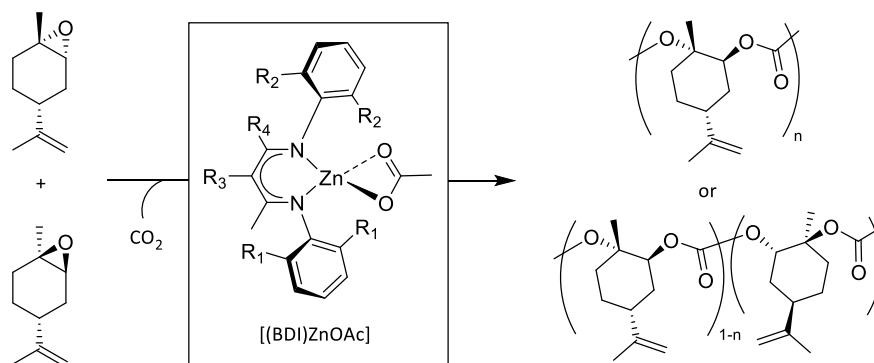


Figure 2.25 Alternating copolymerization of limonene oxide using a β -diiminate zinc acetate complex as catalyst.^[183]

The authors discovered that only *trans*-limonene oxide was reactive in the polymerization, yielding polymers with molecular weights up to 10.8 kDa. Applying lower temperatures, regioregular polycarbonates were achieved. More recently, Rieger *et al.* also reported the synthesis of poly(limonene carbonate) polymers using the same class of catalyst, a β -diimido zinc(SiMe_3)₂ complex.^[184] Using this catalyst, the authors were able to synthesize polymers with a molecular weight up to 145 kDa and a dispersity of $\mathcal{D} = 1.3$. However, only one isomer of the limonene oxide mixture was reactive during the polymerization. Therefore, Greiner *et al.* performed a stereoselective epoxidation of limonene to obtain a high amount of the *trans*-isomer.^[185] The polymerization of this monomer mixture containing more than 85% *trans*-limonene oxide yielded high-molecular weight polymers (>100 kDa) with good thermal properties ($T_g = 130$ °C). However, the stereoselective synthesis of *trans*-limonene oxide included the use of halogen-containing chemicals and stoichiometric amounts of base. Hydroxylic

impurities were furthermore masked by O-methylation with methyl iodide. These substances highly diminish the sustainability of the process. Instead of using pure *trans*-limonene oxide, Kleij *et al.* established a different catalyst, which enabled the conversion of both stereoisomers. With the novel amino-triphenolate Al(III) complex, conversions up to 71% and polymers with $M_n = 6.7$ kDa ($\mathcal{D} = 1.55$) were reached.^[186] The same group also reported the successful side group modification of poly(limonene carbonate). In a first step, applying the same Al(III)-type catalyst, limonene oxide was polymerized ($M_n = 1.3$ -15.1 kDa). In a second step, the unreacted *exo*-cyclic double bond in the limonene repeating unit was epoxidized and subsequently transformed into a cyclic carbonate applying CO₂ to yield polymers with a T_g of up to 180 °C.^[187] The functionalization of poly(limonene carbonate) to modulate the polymer properties was also exploited by Hauenstein and Greiner. They showed different modifications, for example complete hydrogenation to improve extrusion and injection molding, the addition of an alkyl ester to obtain a rubbery material or the addition of an anti-bacterial agent.^[188] Thus, poly(limonene carbonate) represents a versatile platform for a variety of applications.

Not only polycarbonates, also polyesters from limonene have been investigated. An attractive way for polyester synthesis is the ring-opening copolymerization of epoxides with cyclic anhydrides. In 2007, Coates *et al.* showed that the β -diiminate zinc complex, which was active for the synthesis of limonene oxide-based polycarbonates (see section above), was also efficient for polyester synthesis.^[189] Diglycolic anhydride and maleic anhydride were used as anhydride sources. Polymerizations were carried out in toluene and yielded polymers with 36 kDa ($\mathcal{D} = 1.2$) and 12 kDa ($\mathcal{D} = 1.1$) and glass transition temperatures of $T_g = 51$ °C and 62 °C, respectively. Moreover, Duchateau *et al.*^[190] and Kleij and co-workers^[191] showed that aromatic anhydrides can be used, for example phthalic anhydride. In the latter case, different renewable epoxides were copolymerized with phthalic anhydride employing a binary iron(III) aminotriphenolate catalyst and PPNCl (bis(triphenylphosphine)iminium chloride) as co-catalyst. With limonene oxide, good molecular weights ($M_n = 10.5$ kDa, $\mathcal{D} = 1.24$) and a high glass transition temperature of $T_g = 131$ °C were reached. A fully bio-based polyester based on limonene oxide was published by Robert *et al.* in 2011.^[192] The authors developed a tandem procedure for the cyclization of several renewable diacids to form cyclic anhydrides. These were subsequently polymerized with different epoxides. In the case of limonene oxide, camphoric acid was converted to camphoric anhydride using dimethyl dicarbonate and an aluminium Salen complex. Then, limonene oxide was added to form the corresponding polyester (Figure 2.26). Polymers up to a M_n of 27 kDa with a dispersity of $\mathcal{D} = 1.2$ were obtained. By using a tandem catalytic pathway, the sustainability of the overall process is enhanced compared to traditional procedures.

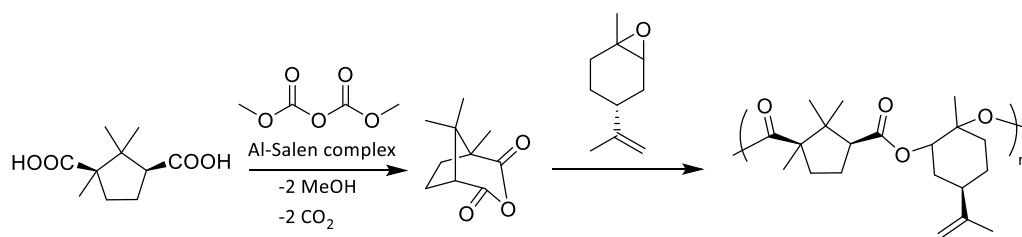


Figure 2.26 Tandem copolymerization of limonene oxide with camphoric acid resulting in alternating, bio-based polyesters.^[192]

A different approach for the synthesis of limonene-based polyesters was developed by Howdle *et al.*^[193] The authors used a hydroboration procedure to convert limonene into its corresponding 1,5-syn and 1,5-anti diol. They also explored and compared three different synthetic routes regarding their sustainability for the preparation of a limonene-based hydroxy acid. The most sustainable option, shown in Figure 2.27, consists of a two-step oxidation procedure and employing catalytic protocols and benign oxidants, such as air and hydrogen peroxide.

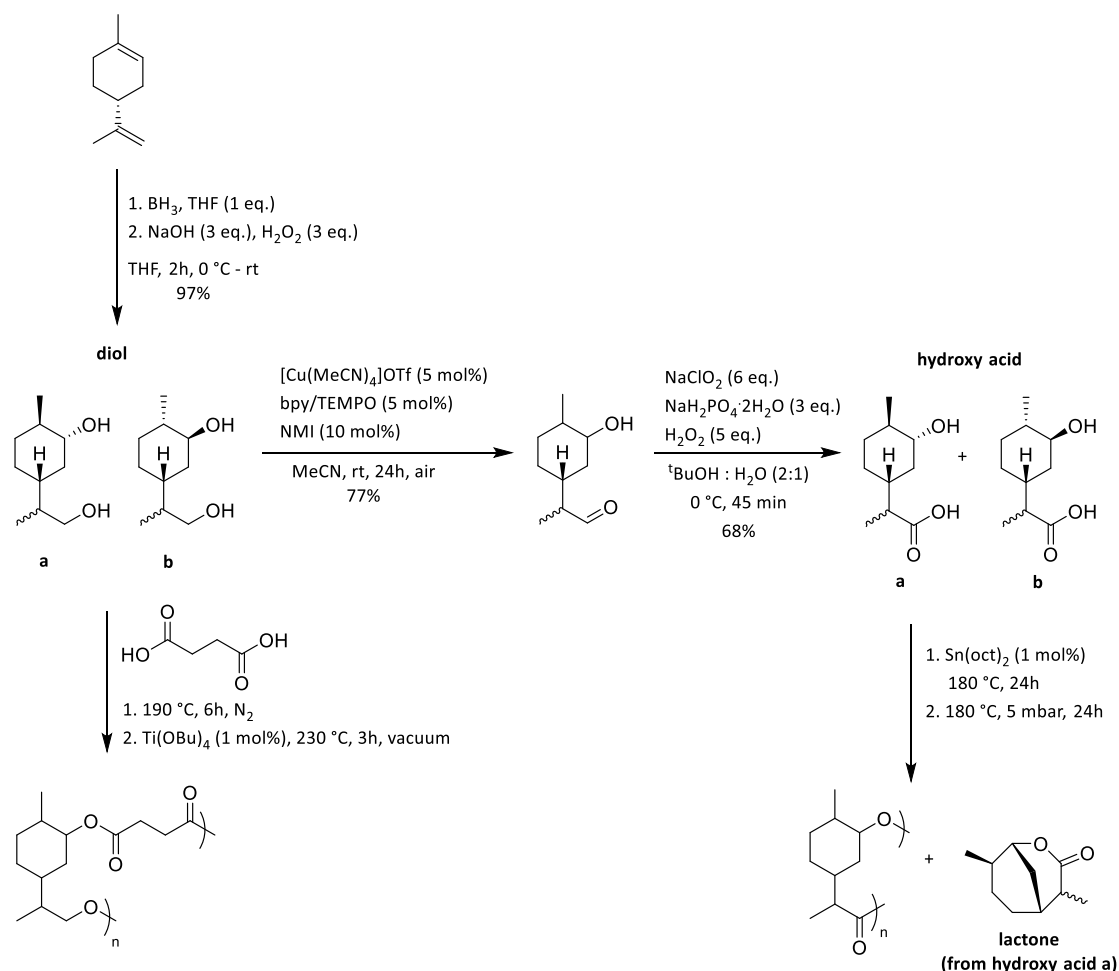


Figure 2.27 Limonene-based synthesis of AB-type hydroxy acids and subsequent polymerization; and alternative polyester synthesis *via* copolymerization of the diol intermediate with succinic acid.^[193]

In a first attempt, to reach fully limonene-based polyesters, the synthesized hydroxy acid was homopolymerized applying $\text{Sn}(\text{oct})_2$ as catalyst. However, only a low molecular weight polymer ($M_n = 2.6$ kDa, $D = 1.4$) was obtained. This can be explained by the sterical hindrance of the secondary alcohol, which is slow to react in polyester synthesis. Furthermore, the formation of a lactone structure was observed, further impeding a good polymerization. Therefore, the diol intermediates were copolymerized with succinic acid, yielding fully bio-based polyesters with molecular weights up to 30.4 kDa and glass transition temperatures of up to 23 °C.

As most terpenes are unsaturated compounds, efficient reactions to convert double bonds are beneficial for their valorization. A powerful reaction to exploit the double bonds of limonene is the thiol-ene reaction, as shown in an extensive study by Firdaus and Meier.^{[194][195][196]} Thiol-ene reactions were used to couple thiols with different functionalities to the double bonds, thus creating bisfunctional monomers which were further polymerized. Figure 2.28 shows all reaction pathways and polymerizations. For example, limonene was converted to a diamine using cysteamine hydrochloride or to a diester with methyl thioglycolate. The diamines were polymerized with fatty acid-based dimethyl esters to yield polyamides (route **A**). To get a more rigid and fully limonene-based polymer, the diamine was also copolymerized with the limonene diesters (route **B**). The limonene diesters were polymerized with fatty acid-based diols to form polyesters (route **C**). Moreover, an AB-type monomer can be prepared by successive modification of the two double bonds, applying methyl thioglycolate and 2-mercaptoethanol. These heterodifunctional monomers were homopolymerized to polyesters (route **D+E**). When only 2-mercaptoethanol was used, a renewable diol was formed. This was either copolymerized with fatty acid-based dimethyl esters to form polyesters (route **F**) or with limonene dicarbamates, which were obtained in a two-step procedure by first forming the corresponding diamine and subsequent functionalization with dimethyl carbonate (route **G**). Alternatively, the dicarbamates were also polymerized with linear diols to increase the structural diversity of the system (route **H**). Finally, limonene was transformed into a dithiol to use the thiol-ene reaction for polymerization with diene co-substrates (route **I**). All the obtained polymers were investigated in regard of their material properties, as summarized in Table 2.4.

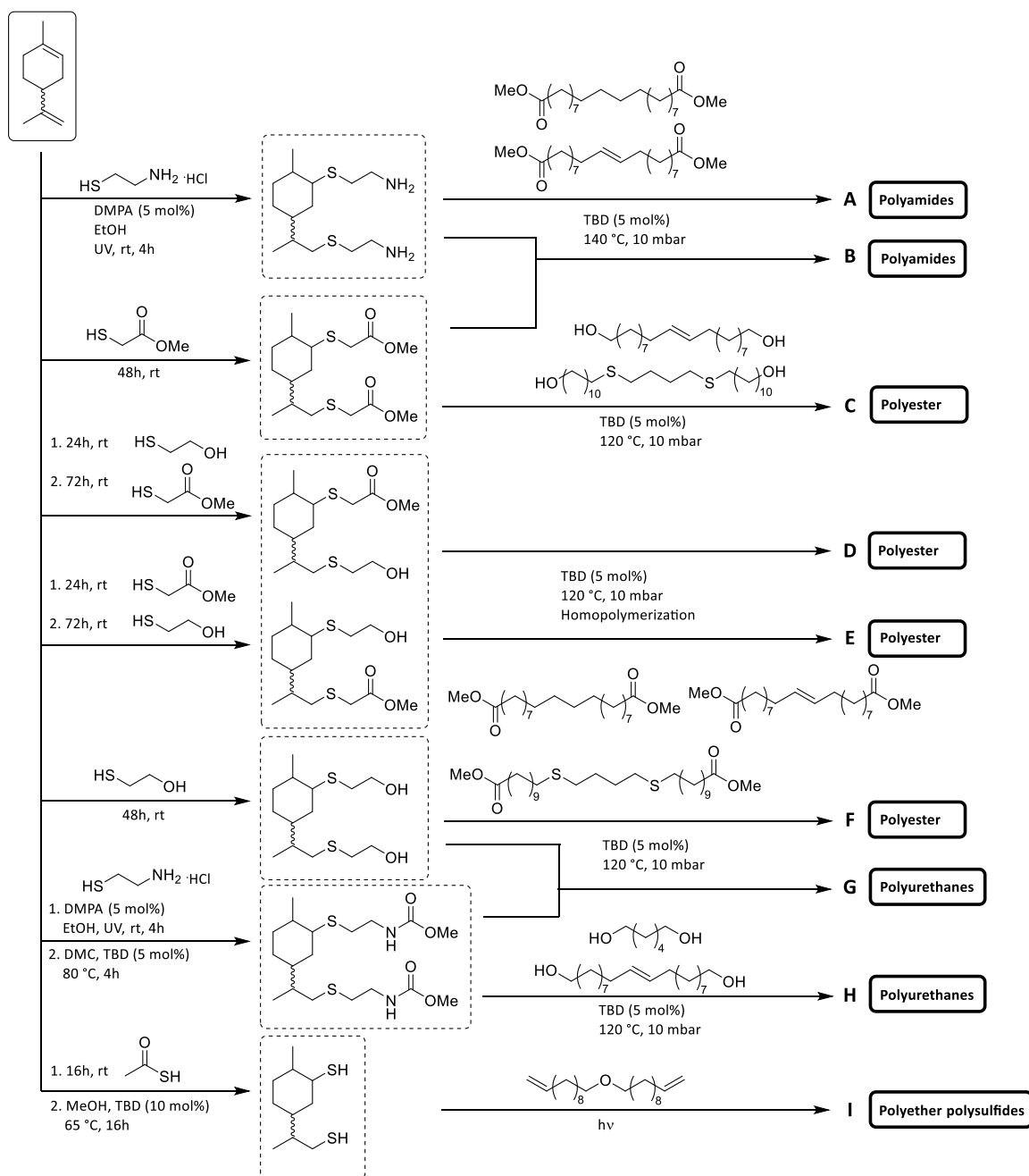


Figure 2.28 Monomers obtained from limonene by thiol-ene coupling reactions and subsequent polymerization to polyesters, polyamides, polyurethanes and polyether polysulfides.^{[194][195][196]}

Table 2.4 Material properties obtained by the polymerization of limonene-based monomers shown in Figure 2.28.

Pathway	Molecular Weight M_n / kDa	Dispersity \mathcal{D}	T_g / °C
A	5.5-10.6	1.86-1.97	n.a.
B	6.4-7.9	1.97-2.28	41.4-41.5
C	18.9-24.7	1.97-2.47	-47.8 - -45.4
D+E	7.7-10.5	1.65-1.89	-10.4 - -9.2
F	9.2-15.3	1.75-2.40	-46.6 - -41.9
G	6.2-7.9	1.79-1.87	18.3 + 18.5
H	8.7-12.6	1.81-2.15	14.6-15.9
I	31.8	2.20	24.1

The comparison of the polyester synthetic pathways, *e.g.* route **C**, route **D+E** and route **F**, showed that the longer the chain of the co-monomer, the higher the molecular weights that were achieved. This can be attributed to the higher steric hindrance of the cyclic terpene structure. Moreover, by incorporating a long aliphatic chain, lower T_g values were obtained. The same trend was observed when comparing the polyurethane polymers, *i.e.* route **G** and route **H**. When comparing polyamide (route **B**) vs. polyurethane (route **G**) synthesis, it is noticeable that very similar molecular weights of around 6-8 kDa were reached. However, polyamides showed higher T_g values, 41 °C vs 18 °C, respectively.

Comparing the molecular weights listed in Table 2.4, it shows that in all approaches, medium to relatively high molecular weights were reached. This can partly be attributed to the steric hindrance of the limonene backbone. Another reason might be the polymerization pathway itself, as all polymers were synthesized *via* polycondensation reactions. One exception to this is route **I**, which is based on a polyaddition reaction. This way, high molecular weights of $M_n = 31.8$ kDa were achieved, which shows the high potential of thiol-ene reactions for polymer chemistry.

Thermosetting Polymers from Limonene

Although the majority of polymers synthesized from limonene are thermoplastic polymers, thermosetting polymers have also been reported. For example, Versace *et al.* combined two different reaction types for the formation of a renewable coating material.^[197] Limonene oxide and limonene dioxide were copolymerized with eugenol and a trithiol *via* thiol-ene and cationic

photopolymerization. Additionally, β -carotene was used as a natural photosensitizer. Due to the use of eugenol, the coatings showed anti-bacterial properties and could therefore be used to reduce bacterial adhesion on the surface.

Thiol-ene reactions were also implemented for the synthesis of thermosets. Johansson *et al.* reported a polymer system where the monomer synthesis as well as the final polymer formation is based on thiol-ene reactions.^[198] By reacting limonene with tri- and tetrathiols *via* selective thiol-ene reaction at the *exo*-cyclic double bond, a branched tri- and tetraene was formed. In a subsequent step, these polyalkenes were polymerized with the same tri- and tetrathiols to obtain highly cross-linked thiol-ene resins (Figure 2.29). The thiol-ene films showed T_g s between -8 and 12.4 °C and storage moduli $E' = 0.4$ -8.9 MPa. As expected, polymers with higher cross-linking density, *i.e.* polymers from tetra-enes and tetra-thiols, reached the highest values for glass transition temperatures and mechanical properties.

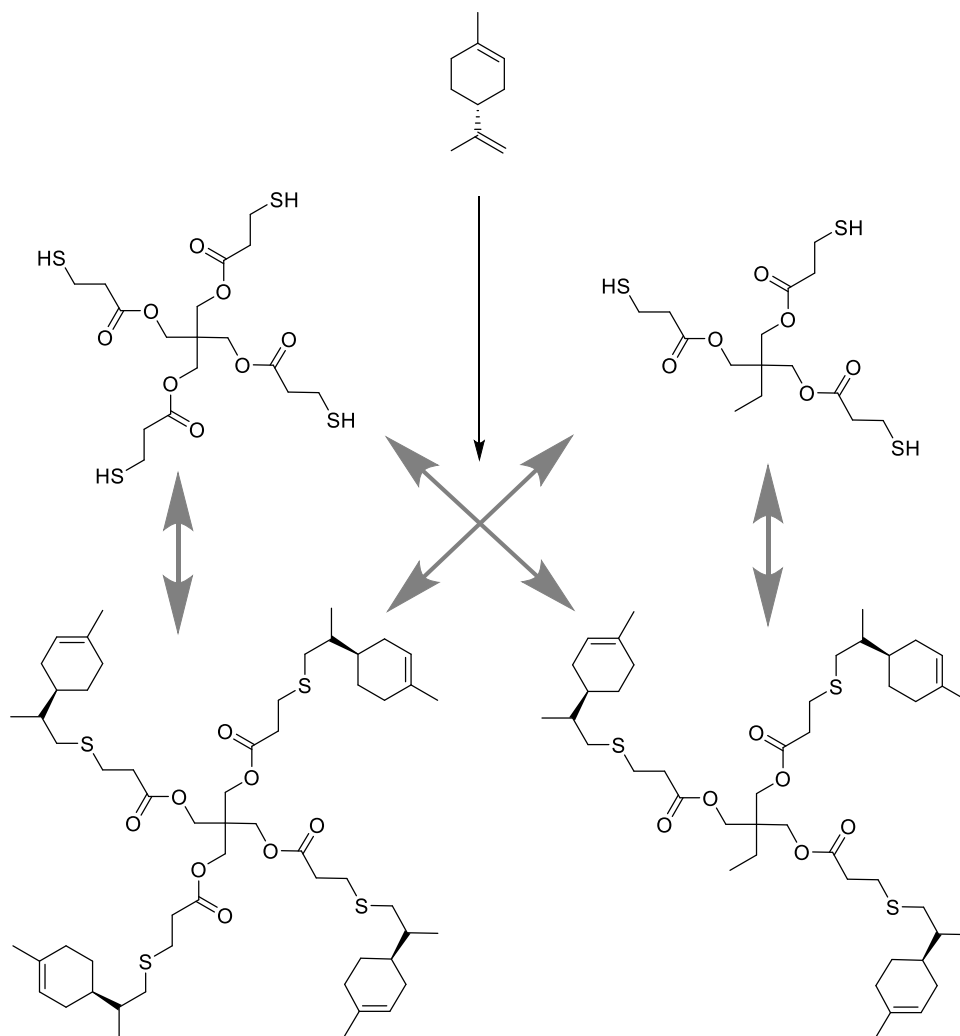


Figure 2.29 Synthesis of branched tri- and tetraenes obtained by thiol-ene reaction between limonene and tri- and tetrathiols. Polymers were obtained by subsequent thiol-ene reaction combining the formed monomers (gray arrows).^[198]

The same polymer system (trimethylolpropane tris(3-mercaptopropionate) and limonene) was also used for the recycling of commercial polystyrene by Heaton and co-workers.^[199] In a first step, polystyrene was dissolved in limonene and impurities were filtered off. Then, the trithiol and a photoinitiator were added and a homogeneous mixture was obtained by heating to 140 °C. The polymer blend was then cured in a hot mold using UV irradiation, yielding flexible network polymer films with a polystyrene content of up to 30 wt%.

Another approach for the synthesis of limonene resins is the cross-linking of pre-formed thermoplastic polymers. This approach was used by Li *et al.*, who showed the cross-linking of poly(limonene carbonate) *via* thiol-ene reaction of the pending *exo*-cyclic limonene double bond. As thiol compound, either a commercial trithiol or a bio-based polythiol (mercaptanized soybean oil) was used. All resins showed high T_g s above 100 °C, good acetone resistance and high hardness, making them suitable for coating applications.^[200] A similar procedure was reported by Kleij *et al.*, who synthesized terpolymers from limonene, cyclohexene oxide and CO₂. In a subsequent step, these polycarbonates were cross-linked with 1,2-ethanedithiol in a thermal thiol-ene reaction, yielding polymers with T_g s up to 150 °C.

A class of thermosets which has gained increased interest in the last years is the class of non-isocyanate-based polyurethanes (NIPUs). They can serve as sustainable alternative for conventional, isocyanate-based polyurethanes and are synthesized by a reaction of cyclic carbonates with amine hardeners. Limonene has been exploited for NIPU synthesis, for example by transforming limonene into a *bis*-cyclic carbonate, as shown by Mülhaupt *et al.*^[201] Starting from limonene dioxide, CO₂ was incorporated to form cyclic carbonates using tetrabutyl ammonium bromide (TBAB) as catalyst. The limonene biscarbonate was then reacted with either diamines for the synthesis of linear poly(hydroxy urethanes) and prepolymers, or with polyfunctional amines (hyperbranched polyethylenimine and citric acid aminoamides) to form poly(hydroxyl urethane) resins. NIPU thermosets were rigid and brittle materials, showing T_g s of up to 70 °C and high Young's moduli up to 4100 MPa. The same group also reported the synthesis of 100% bio-based NIPU thermosets from limonene biscarbonate and carbonated pentaerythritol glycidyl ether cured with 1,5-diaminopentane.^[202] Different mixing ratios were tested, yielding resins with T_g s up to 62 °C and Young's moduli up to 4040 MPa. In order to use limonene as bio-based hardener for NIPU synthesis, Mülhaupt and Blattmann also used the aminolysis of epoxides to form β -amino alcohols, as shown in Figure 2.30. By reacting limonene dioxide with ammonia solution, the epoxide is ring-opened and a diamine is formed. NIPU thermosets from the limonene amino alcohol and a trimethylolpropane-based tris-cyclic carbonate exhibited T_g s of 49 and 55 °C, depending on the amine content.

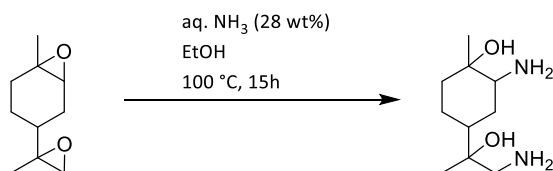


Figure 2.30 Aminolysis of limonene dioxide for the preparation of bio-based curing agents as reported by Mülhaupt *et al.*^[203]

Overall, renewable resources are a valuable feedstock for polymer chemistry. Besides their high abundance and high structural variety, they offer a sustainable alternative to conventional, petrol-based polymers with unique material properties. For the replacement of aromatic substances, especially vanillin has proven to be a suitable feedstock. It can be produced sustainably from lignin and has shown to provide good thermomechanical properties in different reported polymers. Limonene has also a great potential for the synthesis of sustainable plastics; not only for thermoplastics, but also in thermosetting polymers. The double bonds of limonene can be chemically modified with a variety of reactions, offering a toolbox for polymers with different thermal and mechanical properties. Especially the cyclic structure can be exploited to induce rigidity in the polymer backbone, which is beneficial for many applications.

2.3 Epoxy Resins: High Performance Thermosetting Polymers

2.3.1 Introduction

Thermosets are a class of polymers consisting of interconnected molecules, which form a three-dimensional network. For network formation, depending on the polymerization technique applied, the average monomer functionality must be above two. After mixing of the monomers, a curing step by heat or UV initiation leads to network formation.^[204] Their cross-linked nature prevents thermosetting polymers from being soluble or reprocessable after the curing/polymerization step, contrary to thermoplastic materials. However, due to the high cross-linking density, thermosets exhibit outstanding thermomechanical properties, such as high moduli, strength, durability as well as thermal and chemical resistance.^[205] There are several types of thermosetting polymers involving different linker functionalities and curing mechanisms. Common examples are polyurethanes, epoxy resins, melamine resins, phenolic resins etc.^[7] Although thermosetting polymers constitute less than 20% of the overall polymer production, they are an important material class due to their unique properties. Within the thermoset

family, epoxy resins account for approximately 70% of the thermoset market (excluding polyurethanes). Since their first commercial production in the 1940s, epoxy resins have found broad applications, for example in coatings, electrical laminates, adhesives and high performance composites.^[204]

Epoxy resins are composed of monomers or prepolymers containing at least two epoxide functional groups. These epoxides can be cured with different hardeners, which induce the network formation. Common curing systems include aliphatic, aromatic and cycloaliphatic amines, as well as carboxylic anhydride systems or catalytic curing with tertiary amines.^[206] The curing mechanisms of the most commonly used epoxy resins are shown in Figure 2.31.^[207]

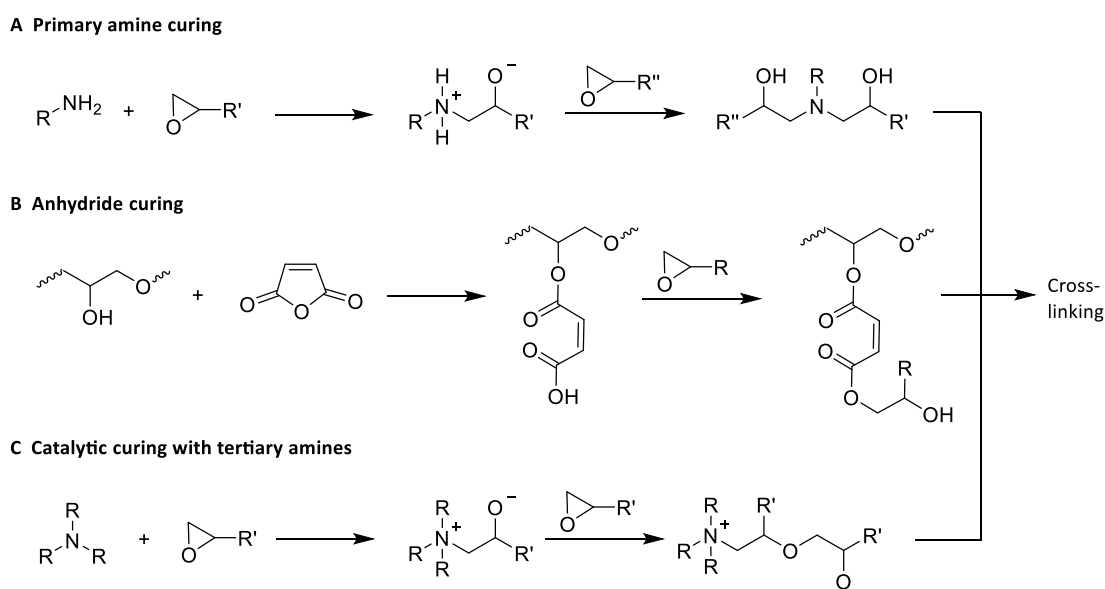


Figure 2.31 Most common mechanisms for cross-linking of epoxy resins: primary amine curing (A), anhydride curing (B) and catalytic curing with tertiary amines (C).^[207]

Curing with primary amines proceeds *via* ring-opening of the oxirane ring with the primary amine. In a second step, the resulting secondary amine reacts with another epoxide moiety. In anhydride curing, the first step consists of an esterification of a free hydroxyl group, for instance from an added accelerator, with the acid anhydride. The formed carboxylic acid reacts with another epoxide, connecting two epoxy monomers with an ester moiety. In contrast, in curing processes catalyzed by tertiary amines, ether linkages are formed. The curing is initiated by the reaction of the amine with the epoxide group. Without other curing partners, as in routes A and B, the resulting hydroxyl group reacts with another epoxide, resulting in a cross-linking of the material.

2.3.2 Bisphenol A in Epoxy Resins

The most commonly applied monomer in epoxy resin synthesis is the diglycidyl ether of bisphenol A (DGEBA). It is formed by the condensation of bisphenol A (bis(4-hydroxyphenylene)-2,2-propane) with epichlorohydrin (Figure 2.32).^[207]

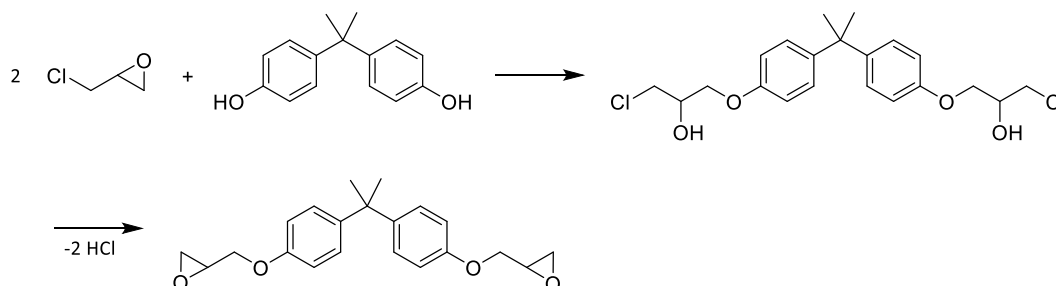


Figure 2.32 Synthesis of DGEBA from bisphenol A and epichlorohydrin.^[207]

Due to the rigid aromatic structure, DGEBA-based resins exhibit good thermal resistance and attractive mechanical properties. These properties led to manifold applications for DGEBA, accounting for around 90% of epoxy thermosetting polymers.^[204] For example, BPA is used to line metal cans, in toys, water pipes, drinking containers, sports equipment and consumer electronics. However, BPA has been found in human serum, urine and even in placental tissue and the umbilical cord blood, due to leaching from consumer products. This is problematic, as BPA has been shown to act as endocrine disruptor that can cause adverse effects to the human health.^[208] Phenols linked to a carbon atom bearing methyl groups, as is the case for BPA, are able to mimic the natural estrogen 17 β -estradiol (Figure 2.33) and are thus able to bind to estrogen receptors. Additionally, those harmful effects can even be caused at low doses of BPA.^[209]

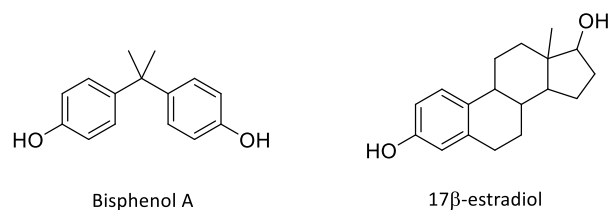


Figure 2.33 Chemical structures of bisphenol A and the natural estrogen 17 β -estradiol.^[209]

Due to the concerns related to the use of BPA in consumer plastics, many regulatory bodies have restricted the use of BPA, for example in baby bottles, food containers and medical supplies. The BPA-analogues 4,4'-methylenediphenol (BPF) and bis(4-hydroxyphenyl) sulfone (BPS) have been established as substitutes.^[209] However, studies have shown that these substitutes exhibit

toxicities similar or even higher than that of BPA and should also be replaced. This toxicity issue has led to an increased research effort for more suitable alternatives.^[209] Renewable resources are an attractive option for the development of epoxy resins with novel structures. However, to find structures that are comparable to DGEBA regarding thermal and mechanical properties, especially aromatic motifs need to be considered. Therefore, in the next chapter, progress in the synthesis of bio-based epoxy resins with a focus on aromatic structures, such as vanillin, as starting material is discussed.

2.3.3 Bio-based Epoxy Resins

Various renewable resources have been investigated as sources for epoxy monomers. These include vegetable oils^{[210][211]} and carbohydrates, *e.g.* cellulose or starch, as well as monomers derived thereof.^[212] In recent years, epoxy resins based on many different bio-based substrates have been reported and extensively reviewed.^{[204][213][212]} Unfortunately, only very few examples have so far reached an industrial production. These mainly consist of epoxidized natural oils and modified cardanol.^[209] In terms of thermomechanical properties, especially aromatic building blocks are crucial in thermoset synthesis. There are different sources for aromatic building blocks suitable for epoxy resin synthesis; for example lignin, vanillin, ferulic acid and tannins are obtained from lignocellulosic biomass, cardanol is obtained from cashew nutshell liquid, and furan-derived molecules, such as 1,5-furandicarboxylic acid, can be synthesized from carbohydrates. The transformation of terpenes into aromatic molecules has also been shown.^[209] Among the investigated bio-based aromatic monomers, vanillin constitutes one of the most important substrates. Therefore, also in regard of this work, this section will focus on vanillin-based epoxy resins reported in literature. Furthermore, the use of terpenes in thermosets both as epoxy precursor and hardener will be discussed.

2.3.3.1 Epoxy Resins from Vanillin

The synthesis of epoxy resins from vanillin can be performed following two strategies. The first pathway consists of a direct transformation of vanillin (or one of its derivatives) into a monoaromatic monomer containing two or more epoxide moieties. The second possible route is coupling two vanillin molecules to form a dimeric structure, which is structurally more similar to BPA. This route offers the opportunity to vary the type of coupling, *e.g.* ester or acetal linker groups, as well as the chain length of the linker moiety and will be discussed in the section below.

An interesting example for the conversion of vanillin into different monoaromatic glycidyl ether monomers was reported by Caillol and co-workers.^{[214][215]} Starting from vanillin, several derivatives were synthesized, such as the reduced form vanillyl alcohol or the oxidized vanillic acid. A diphenol was obtained by subjecting vanillin to an oxidative decarboxylation reaction, leading to methoxy hydroquinone. Furthermore, vanillyl amine was formed in an amination reaction. All vanillin derivatives were subsequently reacted with epichlorohydrin to form the corresponding glycidyl ether monomers (Figure 2.34).

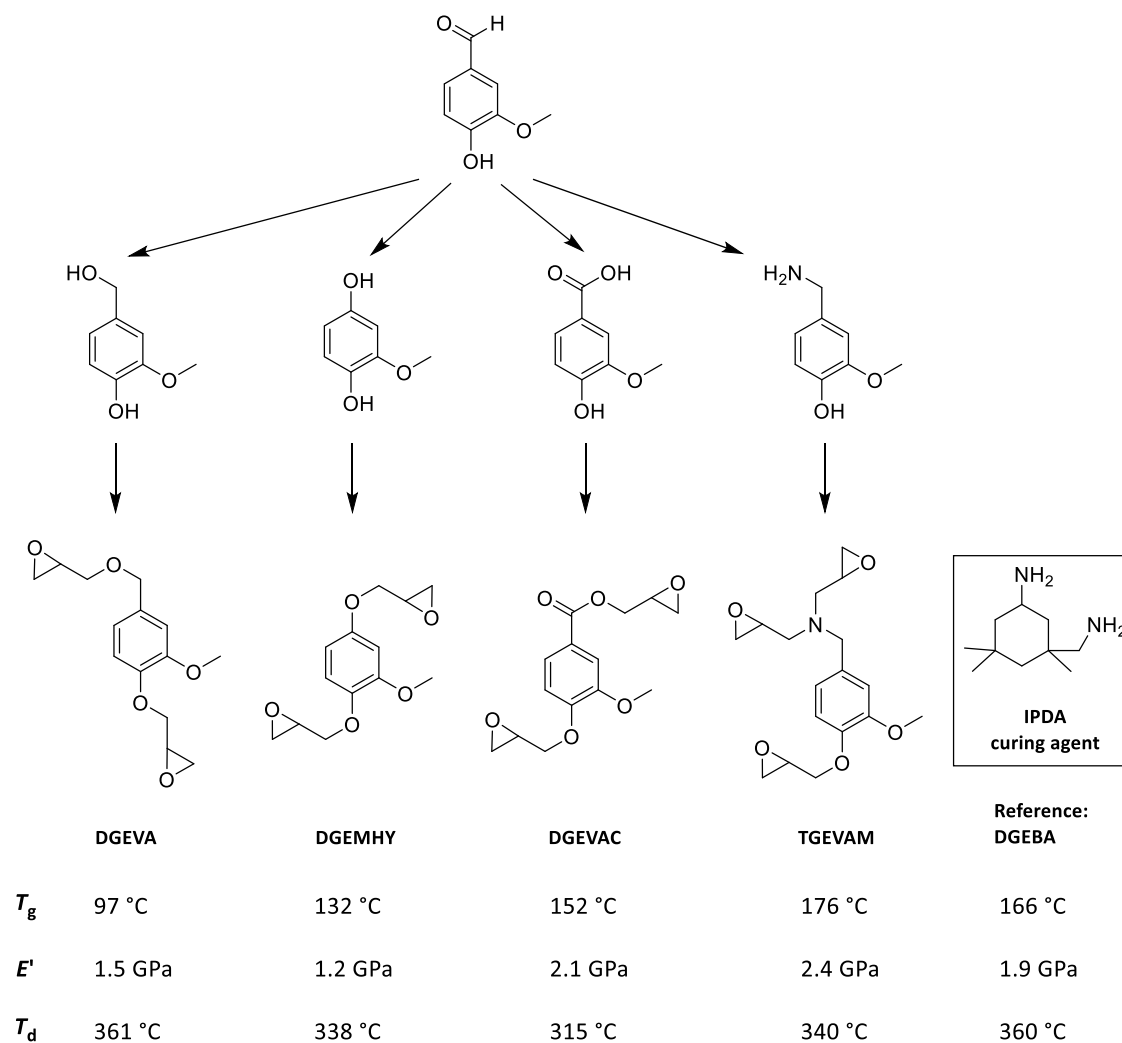


Figure 2.34 Bio-based glycidyl ethers synthesized from vanillin and its derivatives. All monomers were polymerized with IPDA and the resulting polymer properties (T_g , E' and T_d) were compared to the DGEBA reference.^{[214][215]}

All epoxy monomers were cured with the common industrial hardener isophorone diamine (IPDA) and compared to DGEBA as reference. Reported thermomechanical properties are included in Figure 2.34. For the bisepoxide-based resins, glass transition temperatures between 97 and 152 °C were obtained, being lower than for the DGEBA resin (166 °C). However, with

152 °C, the polymer obtained from diglycidyl ether of vanillic acid showed the highest T_g while the storage modulus E' (2.1 GPa) was comparable to that of DGEBA (1.9 GPa). The trifunctional TGEVAM exhibited higher T_g and E' values, which was attributed to higher cross-linking through the third glycidyl ether group. All resins showed good thermal resistance with high degradation temperatures, T_d , between 315 °C and 361 °C.

Renewable vanillin can be obtained by the depolymerization of lignin. However, during lignin depolymerization, a broad mixture of phenolic substances is formed from which vanillin has to be isolated.^[83] To circumvent this isolation step and further increase the sustainability of epoxy resin synthesis from vanillin, Caillol and co-workers aimed for the direct synthesis of epoxy resins from the mixture obtained after lignin depolymerization.^[216] They prepared a model mixture of substances found in the product stream of lignin depolymerization, such as vanillin, syringaldehyde, *p*-hydroxy benzaldehyde and their oxidized analogues. In order to increase the phenol content of the mixture, oxidative decarboxylation was performed first, followed by glycidylation with epichlorohydrin to form epoxide monomers (Figure 2.35). After analyzing the product mixture composition, it was polymerized with IPDA. Depending on the initial substrate mixture (with compositions simulating hard- or softwood lignin), T_g s of 99 °C and 113 °C, respectively, were reported. Storage moduli, E' , around 3.3 GPa were reported, which are high compared to the value obtained for the resin of pure vanillin-derived monomer DGEMHY discussed above ($E' = 1.2$ GPa). Transferring this procedure to real biorefinery downstream mixtures would thus offer the possibility for an easy resin synthesis, omitting vanillin separation and purification.

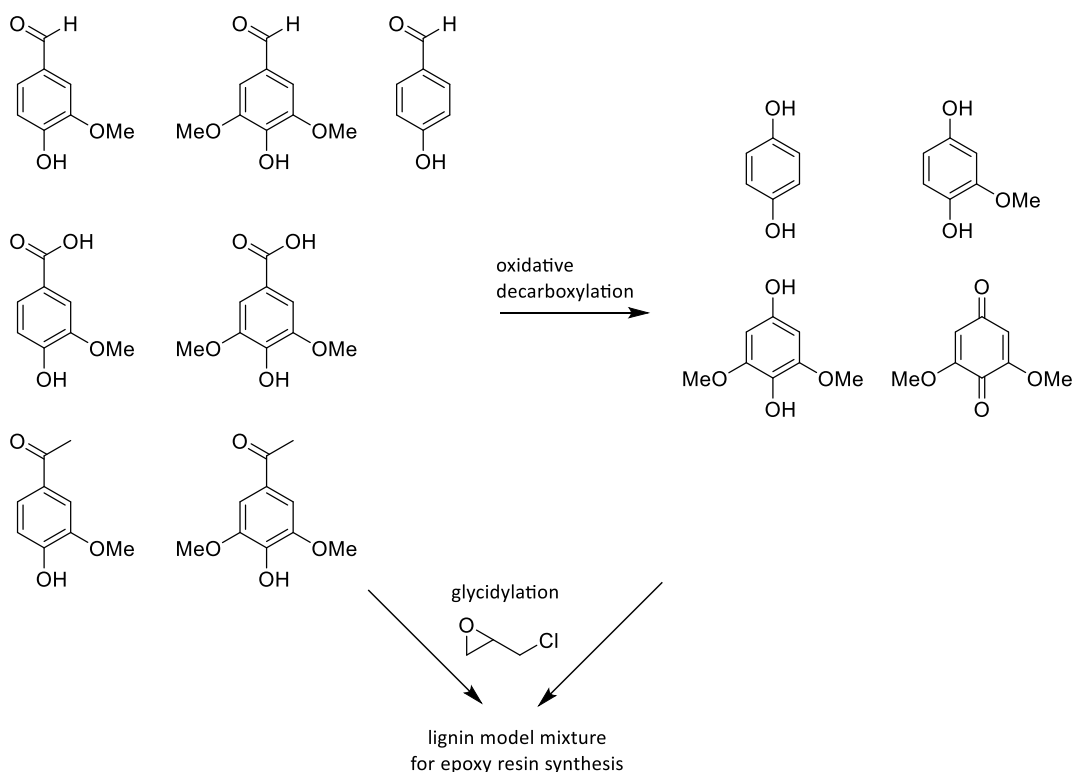


Figure 2.35 Substrates used in the oxidative decarboxylation and subsequent glycidylation for the preparation of a lignin model mixture for epoxy resin synthesis.^[216]

The coupling of vanillin to form dimeric epoxy monomers has been achieved through different approaches. For example, a direct enzymatic C-C coupling of two vanillin molecules was shown by Cramail *et al.*^[217] After reduction of the aldehydes of the divanillin, the hydroxyl groups were treated with epichlorohydrin to form monomers with two, three or four epoxide moieties (Figure 2.36). The monomers were cured with IPDA, leading to resins with T_g s between 138-198 °C, which are comparable or higher than that of the DGEBA reference (152 °C). Furthermore, the storage moduli $E' = 1.9$ -2.4 GPa surpassed the reference ($E' = 1.7$ GPa). A modulation of the degree of glycidylation thus allowed for the tuning of material properties, which were promising for the use in high-performance epoxy resin applications.

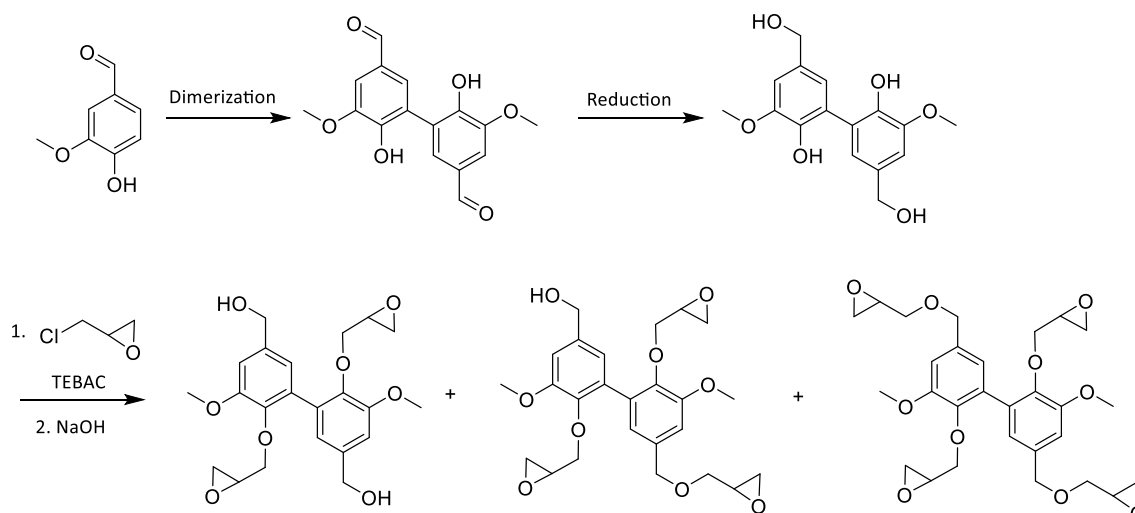


Figure 2.36 Structures of bio-based epoxy monomers obtained from divanillyl alcohol, reported by Cramail *et al.*^[217]

In order to produce coupled monomers with a spacer of one carbon atom, Stanzione and co-workers coupled vanillyl alcohol and guaiacol in an electrophilic condensation reaction (Figure 2.37). The resulting bisphenol was subsequently reacted with epichlorohydrin to form a diglycidylether prepolymer, which was compared to other bis-epoxide alternatives upon curing with 4,4'-diaminodicyclohexyl methane.^[218] Compared to DGEBA, the bisguaiacol resin showed a lower T_g (104 °C compared to 149 °C), but a superior storage modulus (3.35 GPa compared to 2.37 GPa).

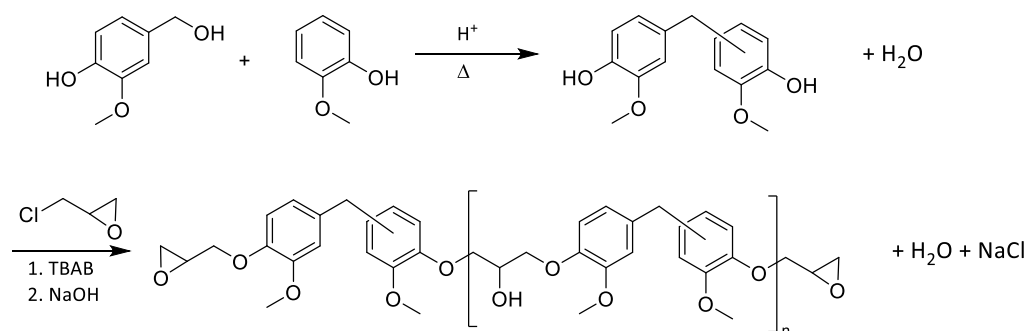


Figure 2.37 Synthesis of bisguaiacol bisepoxide from vanillyl alcohol and guaiacol reported by Stanzione and co-workers.^[218]

The same group also reported the polymerization of the same bisguaiacol monomer with a renewable furan-based diamine, resulting in materials with a high bio-derived carbon content of >97%.^[219] Using this system, a slightly lower T_g of 87 °C and a storage modulus of $E' = 3.29$ GPa was reported. The synthetic procedure of electrophilic condensation was also used by Epps *et al.*, who reacted vanillyl alcohol with different potentially lignin-derived phenols, such as phenol or syringol to form glycidylether prepolymers.^[220] These prepolymers were cured with the

aromatic 4,4'-methylenedianiline yielding resins with T_g s between 113 °C and 151 °C, which is slightly lower than the value reported for DGEBA (167 °C). When comparing monomers without methoxy groups (phenol) with monomers bearing two methoxy groups (syringol), the additional methoxy groups led to lower T_g s and lower thermal stability of the resulting resin. A similar study was reported by the group of Abu-Omar who coupled vanillin and other lignin-derived aldehydes with lignin-derived phenols bearing different numbers of methoxy groups to form triphenolic structures (Figure 2.38). After glycidylation, these monomers were cured with diethylenetriamine (DETA). Also in this case, an increase in methoxy groups resulted in a decrease in thermomechanical properties as well as in the onset degradation temperature.^[221]

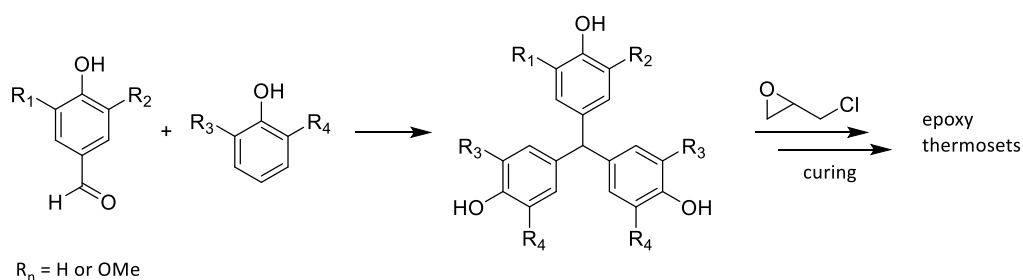


Figure 2.38 Synthesis of lignin-derived triphenolic structures with different numbers of methoxy groups for the synthesis of epoxy resins.^[221]

An interesting possibility for vanillin coupling is the reaction with pentaerythritol, which leads to the formation of a spirodiacetal ring structure.^[222] Ma and co-workers used this acid-catalyzed coupling for the synthesis of a diglycidyl ether monomer, as shown in Figure 2.39 (A). Upon curing with IPDA, an epoxy resin with a T_g of 164 °C and thermal stability up to 278 °C was obtained. The resin remained stable under neutral and basic conditions. Composites with carbon fibers were also produced from this resin. Upon immersion in 1M HCl solution (acetone/H₂O = 9:1 (v/v)), the composite completely dissolved and allowed for recycling of the carbon fibers, which maintained their morphology and mechanical properties.

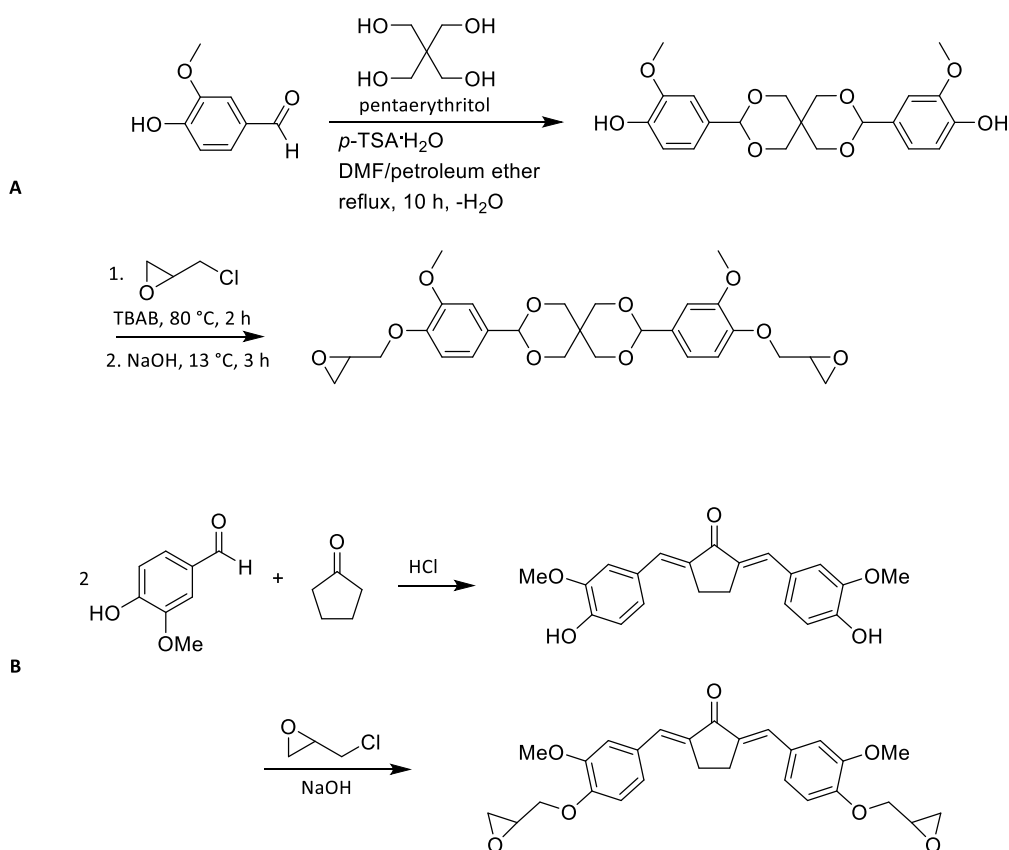


Figure 2.39 Synthesis of a spiroacetal diglycidyl ether monomer from the reaction of vanillin with pentaerythritol and epichlorohydrin^[223] (A) and vanillin coupled by aldol condensation^[224] (B).

Other coupling reactions have also been described, including aldol reactions, as shown by Shibata and Ohkita. They performed a double aldol condensation between vanillin and cyclopentanone followed by glycidylation with epichlorohydrin (Figure 2.39 (B)). After curing with phenolic hardeners, resins with properties comparable to those of DGEBA-based resins were obtained.^[224]

Most of the monomers reported so far were synthesized using epichlorohydrin as glycidylation agent. However, although epichlorohydrin can be synthesized from renewable glycerol,^[225] it remains a toxic compound and more sustainable routes towards glycidyl ether formation are desirable. Therefore, Aouf *et al.* reported an alternative synthesis for the diglycidyl ether of vanillic acid (DGEVAC).^[226] Vanillic acid was first allylated using allyl bromide and potassium carbonate. In a second step, the allyl group was epoxidized employing the lipase CALB and the benign oxidant hydrogen peroxide (Figure 2.40 (A)). In a similar fashion, vanillic acid was coupled with 1,5-dibromobutane to form a dimeric structure. Allylation with allyl bromide and the same epoxidation procedure yielded the respective bisepoxide (Figure 2.40 (B)). Although this route uses the halogenated compound allyl bromide and a high amount of base, it constitutes a good

alternative to epichlorohydrin, especially considering the sustainable oxidation procedure. Furthermore, more sustainable allylation procedures have been reported, for instance applying diallyl carbonate.^[80]

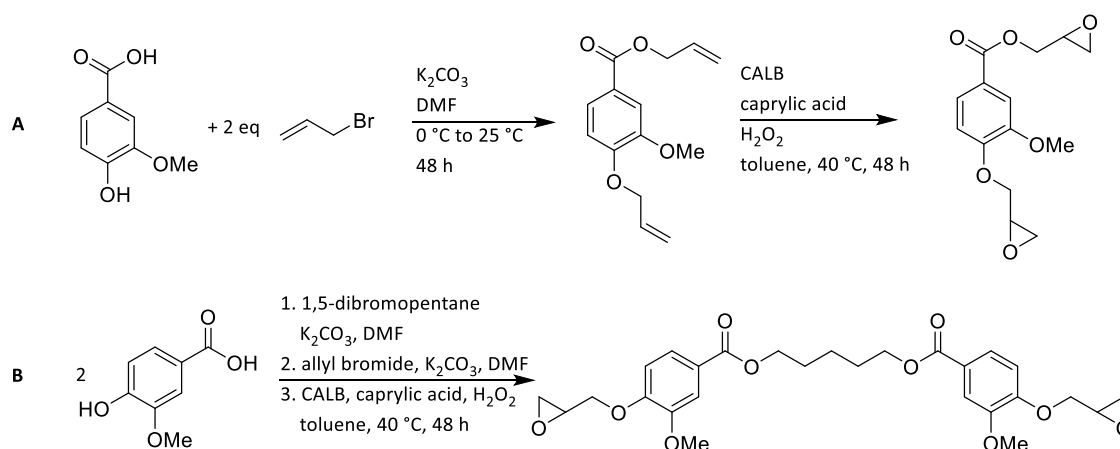


Figure 2.40 Synthesis of bisepoxide monomers by allylation and subsequent epoxidation reported by Aouf *et al.*^[226]

Finally, an interesting property of vanillin is its performance as flame retardant. Vanillin was used for the synthesis of a flame retardant agent by a coupling with 4,4'-oxydianiline or 4,4'-diaminodiphenylsulfone and a subsequent reaction with a phosphorous-containing phenanthrene structure. The product was mixed with a traditional DGEBA-based epoxy resin to increase the fire resistance of the polymer.^[227] Alternatively, vanillin was used for the synthesis of diglycidyl ether monomers bearing phosphorus side groups that were subsequently cured to high-performance epoxy resins showing good flame-retardance properties.^{[228][229]}

Overall, vanillin and its derivatives have shown great potential as substitute for DGEBA in epoxy resins. The synthesis of monoaromatic as well as coupled vanillin monomers has been shown. The obtained epoxy resins often exhibited properties comparable to the DGEBA-based references, making them suitable for a sustainable replacement. However, the toxicity of all these novel molecules and their precursors, reactants and degradation products has to be investigated in the future.

2.3.3.2 Epoxy resins from Terpenes

Terpenes have been used to a great extent in the synthesis of polymers, as already discussed in chapter 2.2.3.3. However, most of these polymers are thermoplastic polymers and only a small number of the reported polymers are thermosets. Regarding epoxy resins, only few examples encompassing terpene feedstock can be found.

One early example for the incorporation of terpenes into epoxy resins was published in a US patent in 1968.^[230] Phenols were reacted with terpenes, such as limonene (Figure 2.41), to form diphenolic addition products. The hydroxyl groups were subsequently reacted with epichlorohydrin to introduce epoxy functionalities.

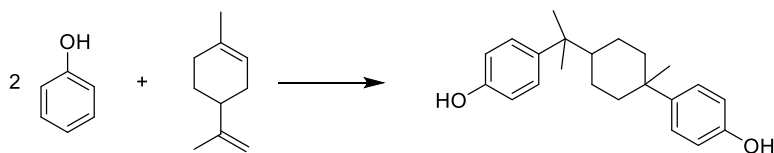


Figure 2.41 Phenol-limonene addition product for epoxy resin synthesis reported in 1964.^[230]

In a similar fashion, Xu and co-workers coupled limonene with 1-naphthol to form a bisphenolic structure.^[231] The pendant aromatic moieties were then polymerized with formaldehyde to form a polymer bearing free hydroxyl groups. By glycidylation of the phenols with epichlorohydrin, a polymeric epoxy precursor was obtained. The curing was carried out with a polymer obtained by the polymerization of BPA and formaldehyde, as well as with the amine hardener dicyanodiamide. Resins with glass transition temperatures of $T_g = 182\text{ }^\circ\text{C}$ and $171\text{ }^\circ\text{C}$ and a thermal stability up to $343\text{ }^\circ\text{C}$ and $332\text{ }^\circ\text{C}$, respectively, were synthesized.

Wu *et al.* reported the synthesis of terpinene-based epoxy monomers. In a first step, the authors prepared terpene-maleic ester type epoxy resins, as shown in Figure 2.42. At first, this epoxy monomer was ring-opened with amines bearing hydroxyl groups to obtain polyols, which were subsequently reacted with isocyanates to form polyurethane/ epoxy resin composites.^{[232][233]} Furthermore, by reacting the terpene-maleic ester monomer with a hydrophilic amine (Figure 2.42), a waterborne epoxy resin was obtained.^[234] To improve the material properties, cellulose nanowhiskers were embedded into the resin. Samples with a cellulose content of 0-8 wt% were prepared, reaching T_g s between $43.1\text{ }^\circ\text{C}$ (8 wt% cellulose) and $47.8\text{ }^\circ\text{C}$ (0 wt% cellulose). Although the incorporation of cellulose had little impact on the glass transition temperature, it greatly enhanced the mechanical properties of the resins, increasing the Young's modulus from 295.6 MPa without cellulose to 800.1 MPa with 8 wt% cellulose.

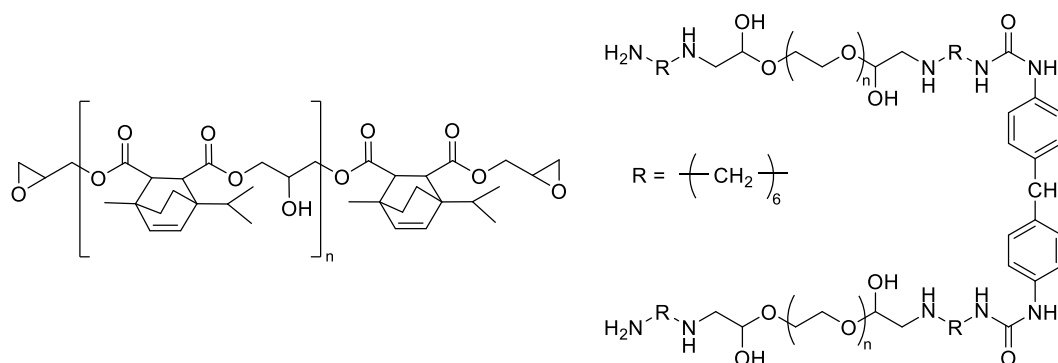


Figure 2.42 Structure of a terpene-maleic ester type epoxy monomer and a hydrophilic amine for the synthesis of waterborne thermoset nanocomposites with cellulose nanowhiskers.^[234]

As already discussed in chapter 2.2.3.3, thiol-ene reactions represent a powerful tool for the functionalization of terpene double bonds. This strategy was pursued for the synthesis of epoxy resin monomers, for example with limonene oxide as depicted in Figure 2.43.^[235] By coupling the external double bond of limonene oxide with di-, tri- or tetrafunctional thiols, multi-functional epoxy resin precursors were formed. Curing was carried out with branched polyethyleneimines of different molecular weights ($M_n = 600, 1,800$ and $10,000$ g/mol). The obtained resins showed good thermal stabilities of up to 243 °C; however, no glass transition temperature data was reported.

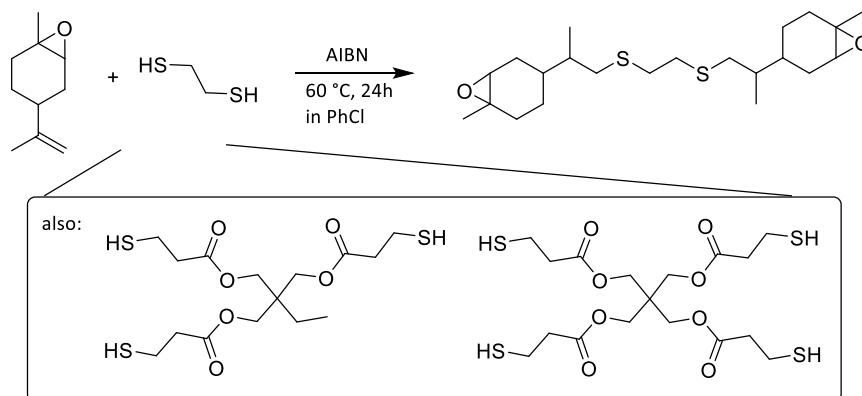


Figure 2.43 Synthesis of multi-functional epoxide monomers from limonene oxide *via* thiol-ene reaction (adapted from^[235]).

A similar approach was also used by Caillol *et al.*^[236] The authors coupled limonene oxide with a linear dithiol to form a bisepoxide, which was cured with hexahydro-4-methylphthalic anhydride and 2-ethyl-4-methylimidazole as initiator. After optimization of stoichiometry and amount of initiator, a material with a T_g of 75 °C and decomposition at $T_{d\ 10\%} = 261$ °C was obtained.

Besides using terpenes as epoxy component, their use as epoxy resin hardener has been reported. An early report described the synthesis of 1,8-diamino-*p*-menthane (Figure 2.44 A).^[237]

The synthesis was carried out by reacting limonene with aqueous HCN and a sulfuric acid solution, followed by hydrolysis of the formed formamide. When this menthane diamine was reacted with DGEBA, a resin with a glass transition temperature of $T_g = 155\text{ }^\circ\text{C}$ was formed.^[238] A similar diamine from limonene was synthesized by Meier *et al.* via thiol-ene reaction of limonene with cysteamine hydrochloride (Figure 2.44 B).^[194] However, the monomer was only used for the synthesis of linear polymers. As these are not thermosetting polymers, the results are outside the scope of this section.

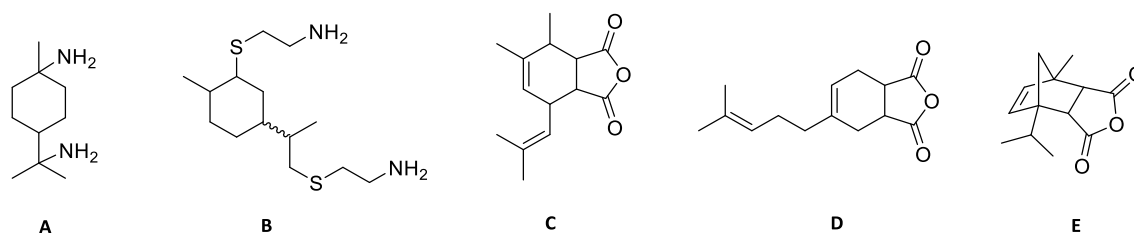


Figure 2.44 Terpene-based curing agents: 1,8-diamino-*p*-menthane (A), limonene dithioether of cysteamine (B), cyclic anhydride from alloocimene and maleic anhydride (C), cyclic anhydride from myrcene and maleic anhydride (D) and cyclic anhydride from α -terpinene and maleic anhydride (E).

Cyclic anhydrides are another attractive curing agent for epoxy resins. The introduction of anhydride groups into terpene structures was carried out by a Diels-Alder reaction between the terpenes inherent double bonds and maleic anhydride. An example for this was already reported in 1965 when Milks and Lancaster reacted alloocimene (2,6-dimethyl-2,4,6-octatriene), which can be produced by thermal isomerization of α -pinene, with maleic anhydride to yield a bicyclic anhydride structure (Figure 2.44 C).^[239] Later, this product was used for the curing of epoxidized soybean oil, yielding resins with a T_g of $48.4\text{ }^\circ\text{C}$.^[240] Additionally, composites with up to 75 wt% lyocell fibers were prepared. The incorporation of fibers drastically improved the mechanical properties, leading to a tensile strength of 65 MPa and a tensile modulus of 2.3 GPa, which are values that are three times higher than those of the original non-reinforced sample.

Analogous to alloocimene, myrcene was also used for the Diels-Alder reaction with maleic anhydride.^[241] The product shown in Figure 2.44 D was used for the curing of DGEBA, yielding resins with a T_g of $61.6\text{ }^\circ\text{C}$. Materials with pure myrcene-based curing agents were brittle with a tensile strength of 48.7 MPa. By mixing with a co-curing agent based on the reaction of the myrcene anhydride with ricinoleic acid, the elongation at break increased (259.43% vs. 7.54%), while T_g and the tensile strength ($45.1\text{ }^\circ\text{C}$ and 11.1 MPa) decreased for the 25:75 mixture.

Finally, a reaction with maleic anhydride was also reported for α -terpinene, a cyclic terpene containing two conjugated double bonds, which can be obtained from α -pinene and which

contains two conjugated double bonds.^[242] The product (structure E in Figure 2.44) was used for the curing of glycidylated isosorbide, a renewable epoxide. Due to the rigid structure of isosorbide as well as the cyclic structure of the curing agent, a high glass transition temperature of $T_g = 136.6$ °C and a storage modulus of 2.17 GPa was achieved. Thus, the system represents a good alternative for established epoxy resins, combining good thermomechanical properties with a renewable feedstock.

In summary, terpenes represent an interesting feedstock for epoxy resin synthesis. The cyclic structure for example of pinene- or limonene-derived terpenes offers the possibility to induce rigidity in the polymer, resulting *e.g.* in relatively high glass transition temperatures. At the same time, due to the sterically demanding structure, selective terpene conversion remains challenging. Even if many promising examples have been reported, compared to other renewable substrates, terpenes are still scarcely used and more research is needed to establish an efficient terpene valorization in polymer chemistry. Compared to terpenes, vanillin has been extensively researched. Many promising examples have been published and the obtained polymers have shown comparable properties to the commonly used DGEBA-based resins. However, for a more sustainable transformation, some challenges remain, for example the introduction of epoxy groups into the monomers. To date, mostly glycidylation using epichlorohydrin is performed. To replace this toxic compound, sustainable alternatives are desirable.

2.4 Strategies for Recyclability in Thermosetting Polymers

2.4.1 Recyclability and Biodegradability of Polymers

Globally, more than 300 million tons of polymers are produced every year.^[7] The uses of polymeric materials are manifold and they have found applications in almost every field of daily life. As a result, some polymers are being used for many years, while products such as packaging are often only used for a short time period. At their end of life, different waste treatment options exist, *e.g.* landfills, energy recovery or recycling.^[243] When disposing polymer waste in landfills, no material is recovered. Additionally, as conventional polymers, such as polyethylene or polystyrene, need a long time to degrade, landfills are an unfavorable choice and can also lead to contamination of the environment through leaching of chemicals and polymers. With energy recovery, the incineration of the waste leads to an energetic benefit. However, besides

energy, no valuable resource material is regained. This benefit can only be reached with a good recycling strategy that involves sorting, washing and drying the postconsumer polymer products before melt processing to produce new materials.^[243] However, in many cases, mechanical recycling proves difficult due to inseparable composite materials, plastic contamination or residual catalysts. Figure 2.45 shows the plastic post-consumer waste treatment for the year 2016 in Europe (including EU28 as well as Norway and Switzerland) and Germany.^[244] In Europe, a total amount of 27.1 million tons (Mt) of post-consumer plastic waste was collected. Around 27.3% was discarded into landfills and 41.6% was used for incineration; the remaining 31.1% was used for mechanical recycling. Germany belongs to the countries with landfill restrictions, which has a positive impact on recycling and energy recovery quota. Only 0.8% of consumer plastics end up in landfills, while a large amount is burned (60.6%) or recycled (38.6%).

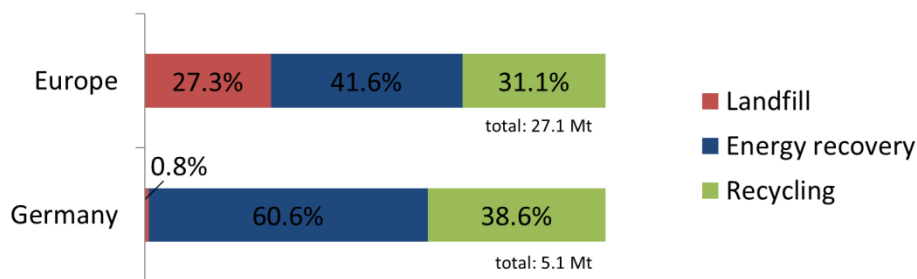


Figure 2.45 Plastic post-consumer waste treatment in 2016 in Europe (EU28+NO/CH) and Germany.^[244]

One alternative to solve the plastic waste managing problem is the use of biodegradable polymers. Different classifications of degradable polymers exist. Although the terms are sometimes used interchangeably, they do have a different meaning. For example, a biodegradable polymer is “a degradable plastic in which the degradation results from the action of naturally-occurring micro-organisms such as bacteria, fungi, and algae”.^[245] In contrast, a compostable polymer is “a plastic that undergoes biological degradation during composting to yield carbon dioxide, water, inorganic compounds, and biomass at a rate consistent with other known compostable materials and leaves no visually distinguishable or toxic residues”.^[245] This procedure usually requires elevated temperatures, which is normally only possible in industrial composting sites. Therefore, not all materials that are labelled as compostable will undergo biological decomposition under ambient temperatures in the environment or in household composting piles. This also applies to a degradable polymer, which is “designed to undergo a significant change in its chemical structure under specific environmental conditions resulting in a loss of some properties that may vary as measured by standard test methods appropriate to the plastic and the application in a period of time that determines its classification”.^[245] For example,

this can encompass photodegradable or hydrodegradable polymers, which do not necessarily biodegrade under ambient conditions, but might be suitable for chemical recycling.

In contrast to thermoplastic polymers, which melt at elevated temperatures, thermosetting polymers cannot be reprocessed, mechanical recycling is limited to grinding and further use as additive in another matrix. Their highly cross-linked structure makes them high-performance polymers with outstanding properties, but impedes a recycling by melting and reprocessing.^[246] Therefore, besides degradable thermosets, the focus is shifted on developing reprocessable thermosets, which mainly involves chemical recycling, but also dynamic materials such as self-healing polymers. The following section will discuss different strategies and examples reported in literature for recyclable thermosetting polymers with a focus on examples encompassing renewable feedstock. It is important to note that many reports only show a successful degradation of the polymer (depolymerization), but the remaining fragments are not used for the synthesis of new materials. The following chapter therefore focusses on the reports including the successful synthesis of new polymers.

2.4.2 Examples for Recyclable Thermosets

Different options have been established to improve thermoset recyclability. In general, the network needs sufficient functional groups that are either cleavable or dynamic to provide exchange reactions. An overview of the available options is shown in Figure 2.46.^[247] The first option results in the depolymerization of the polymer, thus recovering monomers or small fragments, which can be reused in another polymerization cycle. Depolymerization can for example be reached by thermal depolymerization or solvent-assisted depolymerization. In contrast, covalent adaptable networks (CANs) use exchangeable covalent bonds. Through the flexible exchange of linkages, macroscopic flow can be achieved without a loss of material properties.^[248]

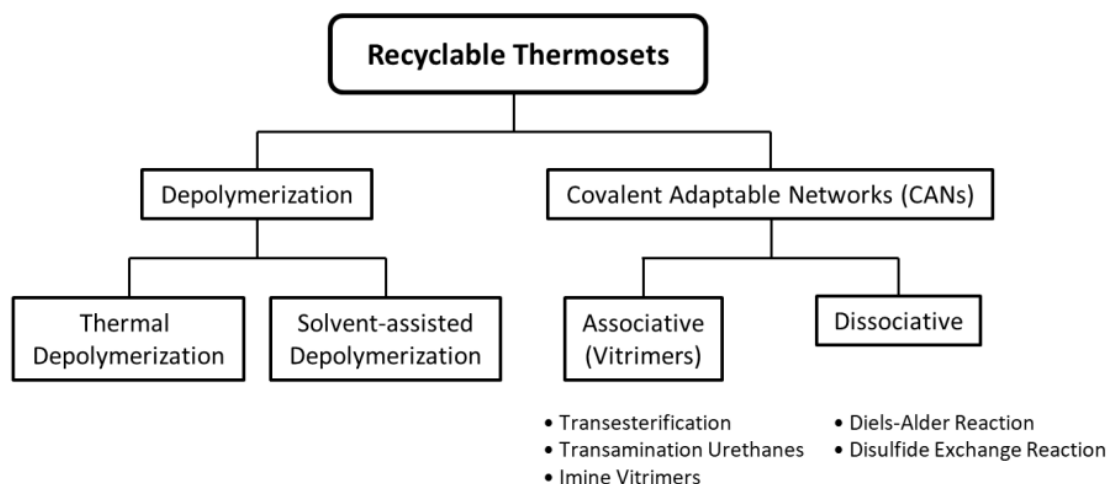


Figure 2.46 Strategies for the implementation of recyclability in thermosetting polymers (adapted from [247]).

Regarding depolymerizations, Hillmyer *et al.* reported the thermal depolymerization of a bio-based elastomer. They synthesized a bio-based β -methyl- δ -valerolactone (MVL), which was used for the synthesis of elastomers using two different pathways, a tandem copolymerization/cross-linking with a bis(six-membered cyclic carbonate) and cross-linking of linear poly(MVL) with a free-radical generator (Figure 2.47).^[249] In both cases, the obtained networks were depolymerized by applying stannous octanoate ($\text{Sn}(\text{oct})_2$) and pentaerythritol ethoxylate as high-boiling tetraol and heating to 150 °C. This way, 91% and 93%, respectively, of the pure reformed monomeric lactone was obtained. In a similar way, the same group also synthesized polyurethane foams from the same monomer.^[250] Also in this case, 97% of lactone was recovered after heating to 250 °C through the thermal depolymerization and reformation of the cyclic monomer. It has to be noted that this depolymerization method was employed to elastomers, which do have a lower cross-linking density compared to thermosets. Therefore, the method also has to be extended to thermosetting polymers.

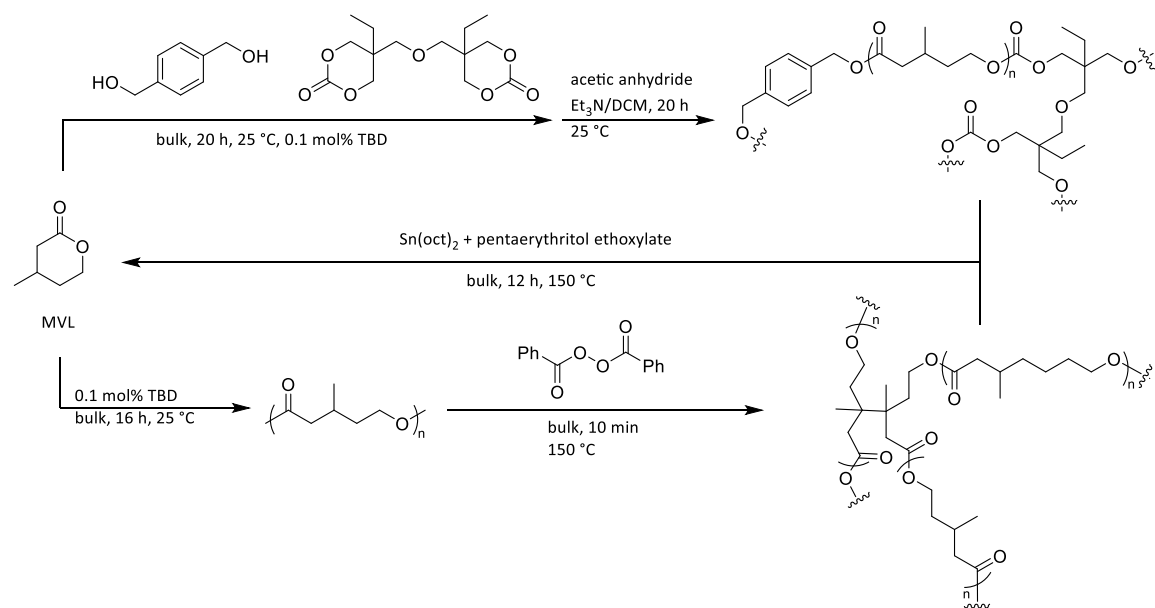


Figure 2.47 Cross-linking of bio-based β -methyl- δ -valerolactone (MVL) by tandem copolymerization/cross-linking with a bis(six-membered cyclic carbonate) and cross-linking of linear poly(MVL) with a free-radical generator. Thermal depolymerization was carried out using $\text{Sn}(\text{oct})_2$ and pentaerythritol ethoxylate at $150\text{ }^\circ\text{C}$.^[249]

Another option for depolymerization is the solvent-assisted depolymerization, *e.g.* hydrolysis or similar network degradation through a solvent. One class of materials that can be hydrolyzed are poly(hexahydrotriazine)s. They are formed by the condensation of primary amines with paraformaldehyde. An example for the successful recycling of such a network was given by García and co-workers.^[251] The authors synthesized the non-bio-based aromatic diamine 4,4'-oxydianiline and reacted it with paraformaldehyde (Figure 2.48). The formed cyclic poly(hexahydrotriazine) covalent network showed good thermal properties (T_g s up to $193\text{ }^\circ\text{C}$) and were stable under neutral conditions. However, in strongly acidic solutions ($\text{pH} < 2$), the resin completely depolymerized and allowed for the recovery of the *bis*-aniline monomer.

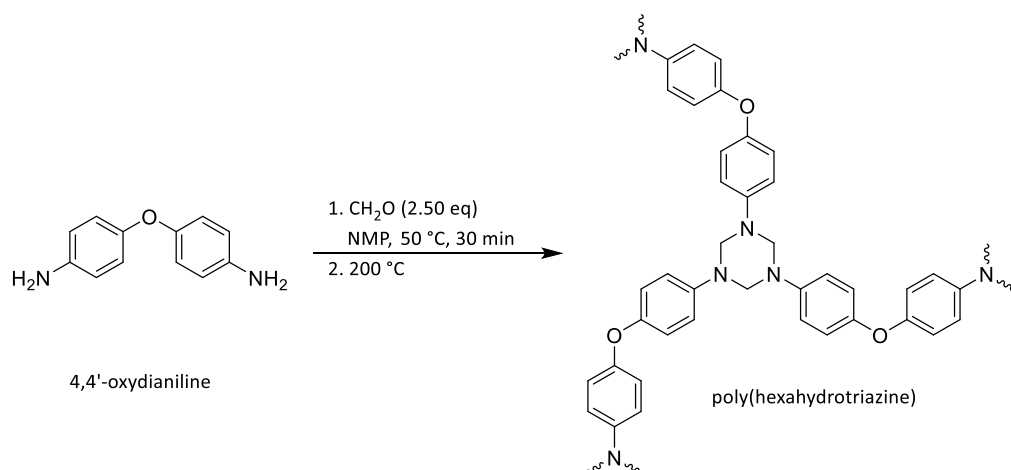


Figure 2.48 Synthesis of a poly(hexahydrotriazine) network from 4,4'-oxydianiline and paraformaldehyde.^[251]

Degradation of the ester group of polyester thermosets, such as anhydride-cured epoxy resins, has also been demonstrated. An example for a bio-based recyclable polyester resin was reported by Hillmyer *et al.* (Figure 2.49).^[252] By reacting isosorbide with succinic anhydride, a diester monomer was formed. This monomer was subsequently polymerized with glycerol to produce cross-linked polyesters with a T_g of 55 °C. The resin showed degradability in acidic and basic solutions and was used for the synthesis of a new polyester resin. However, upon recycling, a loss in tensile properties was observed. This was explained by the poor reactivity of the isosorbide in esterification reactions, which allowed for the isosorbide to degrade before being reincorporated into the network.

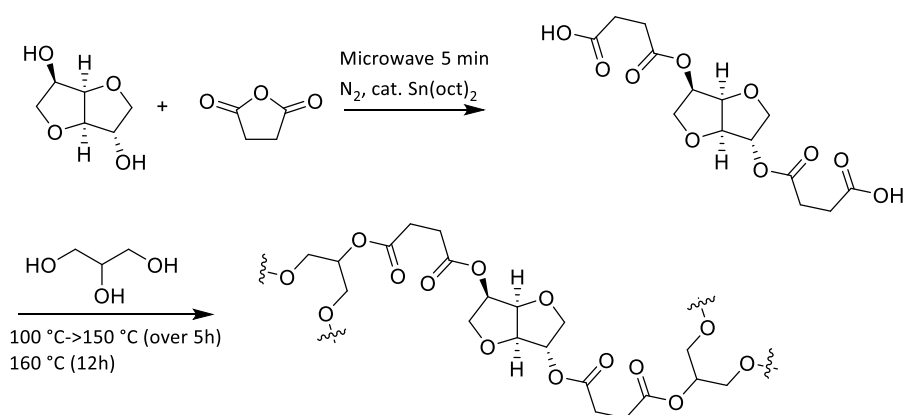


Figure 2.49 Synthesis of recyclable, bio-based polyester from isosorbide, succinic anhydride and glycerol.^[252]

A different possibility for the recycling of polyesters was reported by Xu and co-workers.^[253] They used a traditional anhydride-cured BPA-based epoxy resin and showed degradation by microwave-assisted catalysis using diethylenetriamine (DETA). At a temperature of 130 °C, 99%

of the resin was degraded within 50 minutes. Through the use of DETA, ester bonds were cleaved and free acid groups were converted to amines. The obtained degradation products were directly mixed, up to an amount of 40 wt%, with uncured epoxy precursors for re-curing without any separation process. Up to an amount of 30 wt% of recycled oligomers, the newly formed polymers exhibited T_g s higher than the pristine sample through the incorporation of amine groups. Furthermore, thermal and mechanical properties were similar or superior to neat epoxy resins. Thus, amination with DETA was shown to be an effective way to recycle epoxy resins, which were initially cured with anhydrides. Moreover, all materials and solvents applied during the process were completely incorporated into the new material, avoiding additional waste formation. However, the system only allows for one recycling cycle, which can be considered as a drawback.

As shown in Figure 2.46, covalent adaptable networks are a good option for achieving recyclability in thermosetting polymers. As already mentioned, CANs exhibit exchangeable covalent bonds, which allow for reshaping of the material. CANs can be divided into two categories, *i.e.* dissociative and associative CANs. A schematic illustration of both mechanisms is depicted in Figure 2.50.^[248] In dissociative networks, bond exchange is achieved by previous cleavage of linkages that are then reformed in a separate step. This cleavage leads to a loss of the network integrity, usually observed by a sudden drop of viscosity, which is characteristic for thermoplastic materials. Typical examples for dissociative CANs are Diels-Alder reactions or disulfide exchange reactions. In contrast, in associative networks, cross-links are only broken when a new bond has been formed. Thus, associative CANs exhibit a fixed cross-linking density, making them permanent as well as dynamic networks. Associative CANs are also called 'vitrimers', as they behave like typical inorganic silica materials. Examples for associative CAN mechanisms are transesterification, transamination or imine metathesis of imine-Schiff base networks.

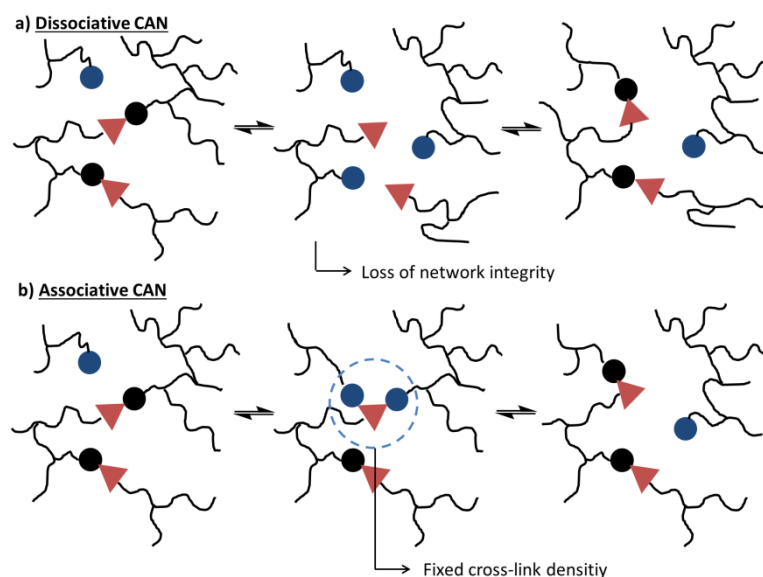


Figure 2.50 Schematic illustration of covalent adaptable networks (CANs): a) dissociative and b) associative CANs (black: binding, blue: non-binding).^[248]

The synthesis of dissociative CANs by Diels-Alder reaction of furan-based dienes and maleimide has been extensively studied.^[254] In general, two strategies have been used for the formation of the networks: (i) the synthesis of functional polymers that were cross-linked with a bifunctional linker or (ii) the synthesis of functional monomers that were either directly cross-linked using a reversible reaction, or in case of an irreversible cross-linking reaction, with monomers that bear a reversibly cleavable functional group that enables reshaping after a non-reversible curing step. For example, Broekhuis *et al.* showed the functionalization of polyketones with furan groups. In a second step, cross-linking was achieved using an aromatic bismaleimide linker, creating networks with T_g s up to 100 °C.^[255] The authors were able to show the loss and recovery of material properties upon heating and subsequent cooling, respectively, by dynamic mechanical analysis (DMA) measurements. The properties were largely retained for at least six cycles, showing the usefulness of Diels-Alder reactions in reversible network formation.

Renewable resources have also been used for Diels-Alder-based CANs. For example, Shibata *et al.* reported the direct polymerization of tung oil, which contains a high amount of conjugated double bonds, with 1,1'-(methylenedi-4,1-phenylene)bismaleimide (BMI) as shown in Figure 2.51.^[256] Resins with a T_g up to 150 °C were obtained. The same group also synthesized diene monomers *via* aldol condensation of cyclopentanone with furfural and cinnamaldehyde that were cross-linked with the same bismaleimide, leading to resins with high T_g s >370 °C and good thermal stabilities of $T_{d 5\%}$ >450 °C.^[257] In both cases, no recycling of the resins was reported. In a report of Avérous and co-workers, bio-based tannins were used as natural polyphenols and

functionalized with furan moieties.^[258] In this case, cross-linking was achieved with an oligo(propylene oxide)-based bismaleimide. Upon heating to 120 °C, the polymer returned to the liquid state, allowing for reshaping of the material.

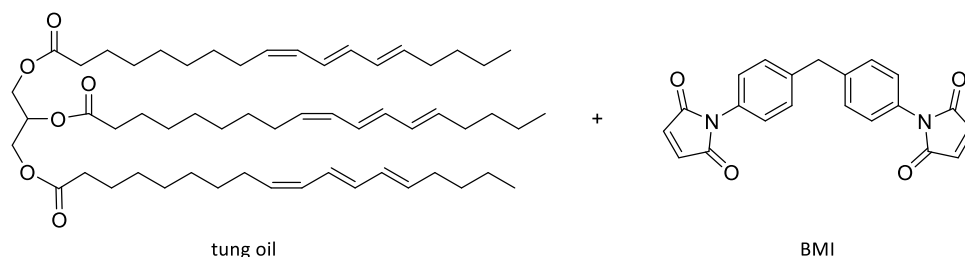


Figure 2.51 Structures of tung oil and 1,1'-(methylenedi-4,1-phenylene)bismaleimide (BMI) used for the synthesis of Diels-Alder-based CANs as reported by Shibata *et al.*^[256]

Another example for a dissociative CAN was shown by Wang *et al.*^[259] The authors reacted bio-based isosorbide with epichlorohydrin to form epoxy prepolymers (Figure 2.52). The prepolymers were cross-linked with a disulfide-bearing diamine to yield an epoxy resin with a T_g of 41 °C. The disulfide-containing resin showed crack healing upon thermal treatment, being fully repaired after one hour at 100 °C. Additionally, it was possible to recycle the material through hot-pressing. After three cycles, the material showed a slight decrease in T_g (34 °C) and storage modulus (1.77 GPa vs. 1.99 GPa for the pristine sample). This was explained by the decrease in cross-linking density through the recycling process, for example due to oxidation of the sulfur at higher temperatures. Nevertheless, it shows the potential of disulfide exchange in the synthesis of reprocessable resins.

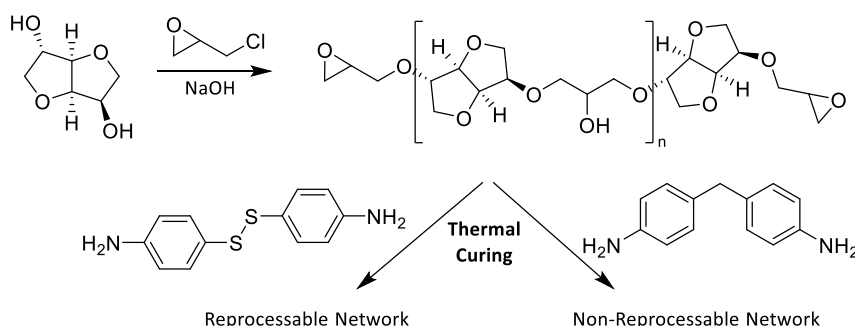


Figure 2.52 Synthesis of isosorbide-based epoxy resin bearing disulfide bonds for thermal reprocessability through disulfide exchange reaction.^[259]

Associative CANs are also called vitrimers because they show a gradual viscosity decrease upon heating, which is a property of vitreous silica.^[248] Transesterification is a well-explored reaction for vitrimers, which was established by Leibler *et al.* in 2011.^[260] The authors polymerized DGEBA with different long chain dicarboxylic and tricarboxylic acids to form polyester resins. By

incorporating zinc acetate ($\text{Zn}(\text{OAc})_2$), the material was able to relax stress in 58 h at high temperatures (100 °C) through transesterification reactions. Ground samples were reprocessed by injection molding. After this report, the use of zinc catalysts in polyester resins was widely investigated.^[261] To date, several bio-based examples have been reported, for example by the group of Zhang. They synthesized a bio-based bisepoxide by coupling eugenol with 1,4-dibromobutane followed by epoxidation.^[262] Polymerization with succinic anhydride and zinc acetylacetonate ($\text{Zn}(\text{acac})_2$) yielded a polyester with a T_g of up to 47 °C and a stress relaxation time of 35 min at 200 °C, depending on the anhydride/epoxy ratio. The materials showed crack healing upon heating as well as shape memory properties. Samples with free hydroxyl groups underwent transesterification reactions at temperatures above 150 °C, while the other samples were recycled by alcoholysis in ethanol and subsequent heating to 190 °C for 3 h to form new materials.

The same group also reported the synthesis of a vanillin-based epoxy resin as shown in Figure 2.53.^[263] Vanillin was reacted with guaiacol to form a triphenol, which was subsequently glycidylated using epichlorohydrin and cross-linked with a cyclic anhydride in the presence of $\text{Zn}(\text{acac})_2$ as catalyst. Due to the high aromatic content, resins with T_g s up to 187 °C were prepared. The materials showed crack healing in a hot press at 220 °C. During the healing, crack widths were reduced by 90% within just five minutes. As the material exhibited comparable thermomechanical properties to traditional DGEBA-based resins, the system constitutes a suitable replacement.

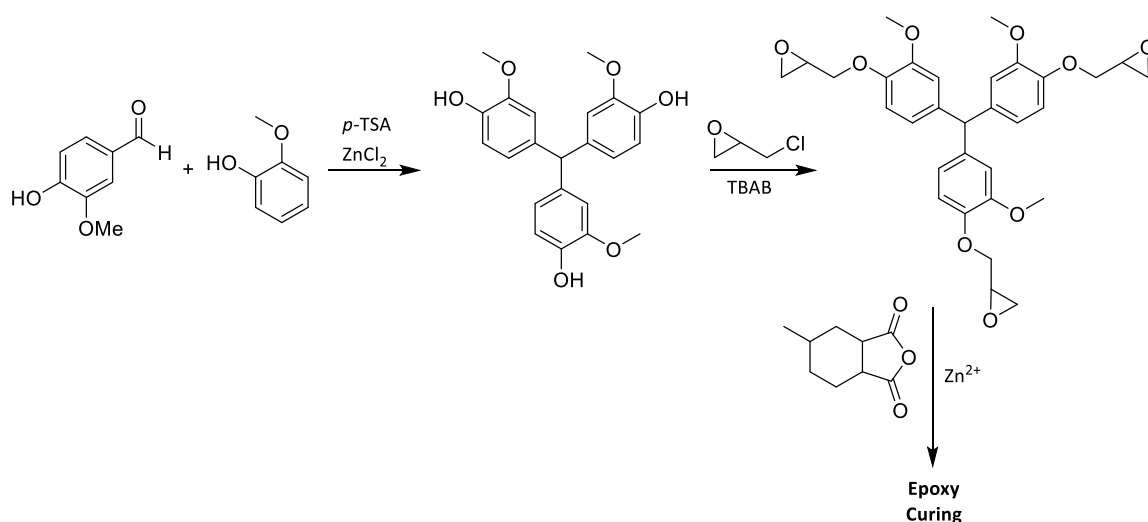


Figure 2.53 Synthesis of a vanillin-based triepoxy monomer. Curing was performed using a cyclic anhydride and $\text{Zn}(\text{acac})_2$ as catalyst to yield high T_g vitrimers.^[263]

Apart from vanillin, lignin has also been used for the preparation of bio-based vitrimers. Zhang and co-workers reported two different lignin-based systems, in which lignin was functionalized with carboxylic acid groups. In the first case, the introduction of the carboxylic acid groups was achieved by reacting lignin hydroxyl groups with anhydrides.^[264] The resulting polyacid was then reacted with a poly(ethylene glycol) (PEG)-epoxy, again applying $\text{Zn}(\text{acac})_2$ as catalyst. The resins exhibited T_g s up to 76 °C, stress relaxation at 200 °C up to 720 s and complete crack healing, depending on the COOH/OH-ratio. In the second system, carboxylic acid groups were introduced by ozonolysis of lignin. The resins were formed by curing with a sebacic acid-based bisepoxide and the same zinc catalyst.^[265] Using this system, a higher T_g of 133 °C was reported. Above 160 °C, the resins showed fast stress relaxation (up to 81 s at 200 °C) and a good shape memory as well as self-healing behavior. For example, by hot pressing at 190 °C, the scratch width in all samples was reduced by over 70% within five minutes and the samples were reshaped into uniform films.

A renewable vitrimer based on lactic acid was presented by Hillmyer *et al.*^[266] In a first step, pentaerythritol and lactide were polymerized using $\text{Sn}(\text{oct})_2$ as catalyst, yielding hydroxyl-terminated star-shaped poly(lactic acid) prepolymers. These prepolymers were subsequently reacted with methylenediphenyl diisocyanate in different ratios that led to materials with T_g s up to 57 °C. The vitrimer behavior of the material was attributed to transesterification between the PLA backbone and the unreacted terminal hydroxyl groups. All samples containing catalyst were fully mendable *via* hot compression molding and showed stress relaxation times below 50 s at 140 °C. Furthermore, most samples showed full recovery of tensile properties.

Finally, a bio-based and catalyst-free vitrimer was reported by Altuna and co-workers.^[267] The authors reacted epoxidized soybean oil with citric acid, obtaining materials exhibiting good self-healing properties. After heating samples to 160 °C for 2 h, the same stress and strain levels as those of the original samples were obtained.

Imine formation between a carbonyl and a primary amine has also been widely investigated in vitrimer synthesis. Figure 2.54 shows possible reactions in imine vitrimers. After imine formation (pathway a), the reversibility of the reaction can be used in a dissociative manner to hydrolyze the formed network. However, also associative pathways are possible, such as transamination between an imine group and a free primary amine (pathway b) or imine metathesis between two imines (pathway c).^[248] Pathway b and c are particularly relevant to vitrimer chemistry.

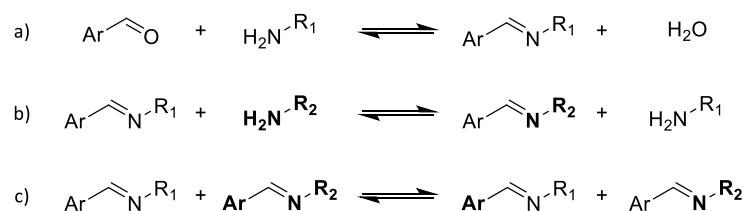


Figure 2.54 Possible reactions in imine vitrimers: a) Imine formation and hydrolysis, b) transamination between an imine and a free amine group, c) imine metathesis between two imine groups.^[248]

Traditional aromatic aldehydes, such as terephthalaldehyde, and amines, such as diethylene triamine or triethylene tetramine, are commonly used for imine-based vitrimer synthesis.^[268] To facilitate malleability, the presence of a small number of unreacted amine groups proved to be beneficial as it enables transamination reactions.^[269] Several different approaches have been reported for the preparation of bio-based imine vitrimers. For example, Avérous *et al.* used fructose-derived 2,5-hydroxymethylfurfural for the synthesis of 2,5-furandicarboxaldehyde as shown in Figure 2.55.^[270] The conversion to a polyimine vitrimer was achieved by mixing with a commercial fatty acid-based mixture of di- and triamines, called Priamine®, followed by solvent-casting and hot pressing at 120 °C. This way, a resin with a low T_g of -10 °C, attributed to the long aliphatic chains of the polyamines, was obtained. The authors reported full stress relaxation at room temperatures in less than one hour as well as reprocessability (compression molding at 120 °C for ten minutes) for at least three cycles without loss of mechanical properties (4.9 MPa Young's modulus after three cycles compared to 4.4 MPa of the original sample).

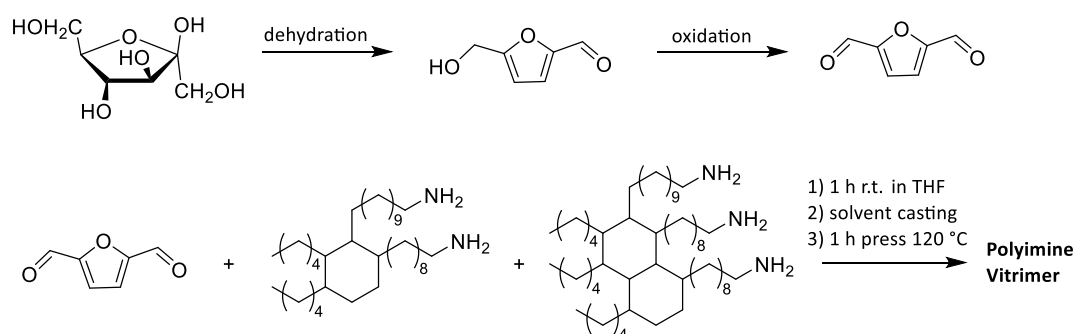


Figure 2.55 Fully bio-based polyimine vitrimer from 2,5-furandicarboxaldehyde and fatty acid-based di- and triamines.^[270]

As aromatic moieties provide good thermomechanical properties to thermosets, vanillin has been investigated for the preparation of sustainable imine vitrimers. Ye and co-workers synthesized a dialdehyde by coupling vanillin with 1,4-dibromobutane, followed by curing with diethylene triamine and triethylene tetramine (Figure 2.56 (A)).^[271] The material showed T_g s up to 64 °C and proved to be recyclable by hot-pressing and acid hydrolysis. A different approach

was reported by Lee and Kang, who incorporated the imine moiety into the monomer structure.^[272] They coupled vanillin with 1,6-hexanediamine to form an imine-containing bisphenol (Figure 2.56 (B)). The bisphenol was then used for the curing of DGEBA, yielding resins with a T_g of 87 °C. The material showed fast stress relaxation above the T_g (10 s at 150 °C), enabling reshaping and thermal healing. Additionally, the material was fully recycled by dissolution in mild acidic solutions through imine hydrolysis. The recycled polymers showed a slightly lower cross-linking density, but retained their reshaping and thermal healing ability.

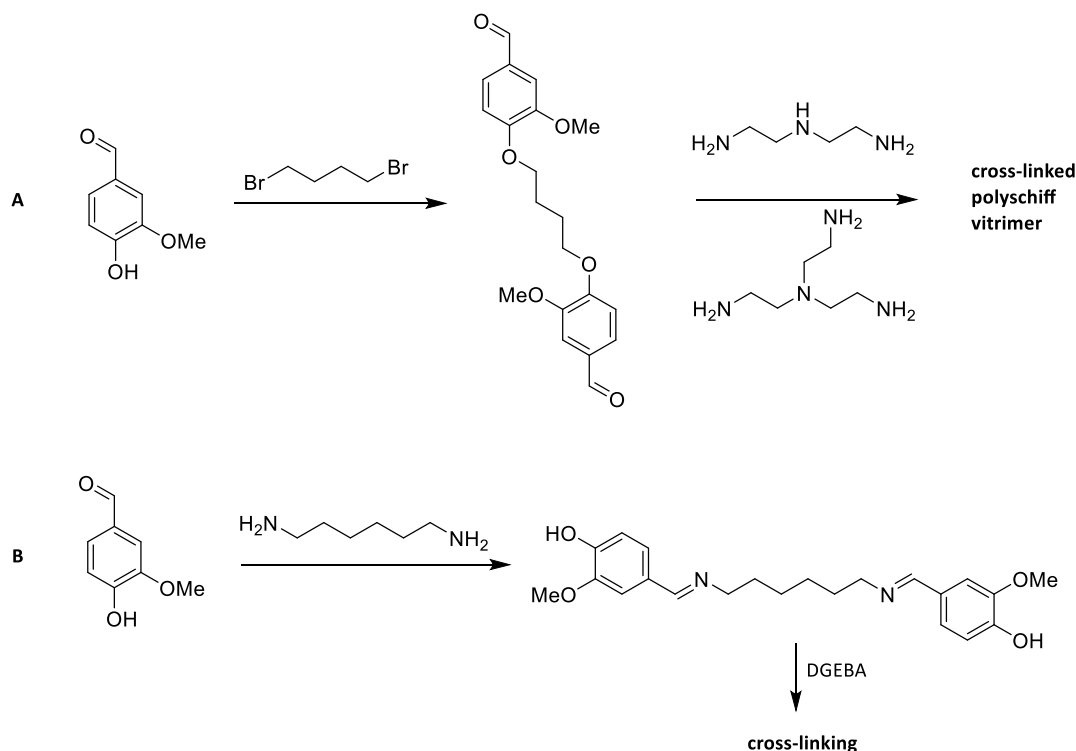


Figure 2.56 Vanillin-based polyimine vitrimers: synthesis of a dialdehyde through coupling at the phenol group and subsequent cross-linking with polyamines (A),^[271] synthesis of imine-containing bisphenol for cross-linking with DGEBA (B).^[272]

In order to obtain two functional groups in one vanillin-based molecule, namely an epoxide and an aldehyde, glycidylation at the phenolic group has been reported. After curing, for example with IPDA^[273] or a mixture of IPDA and a polypropylene-based diamine,^[274] materials containing two different groups were obtained. Through ring-opening of the epoxide groups, permanent linkages were formed, whereas the amine formed dynamic imine moieties with the aldehyde group. The materials exhibited high T_g s (up to 139 °C with pure IPDA), stress relaxation times of 50 s at 150 °C and good reprocessability for at least three cycles. Materials were reported to quickly dissolve in acidic solutions that allowed recycling. Similar results were also reported by Zhu *et al.*^[275] who used glycidylated vanillin together with 4,4'-methylenebis(cyclohexane)amine as cross-linker. The resin exhibited a high T_g of 172 °C, which slightly surpassed the result of the

DGEBA reference sample (170 °C). Furthermore, stress relaxation times up to 15.3 s at 220 °C were reported. Chopped films were reprocessed into new films within 20 minutes at 180 °C under 15 MPa pressure. Recycled samples showed an increased cross-linking density, which decreased the elongation at break. However, no loss of other mechanical properties was observed. The same group also reported the synthesis of a vitrimer exhibiting flame retardancy by reacting vanillin with phosphorous oxychloride, thus introducing phosphorous into the final resin.^[276]

In summary, covalent adaptable networks combine the favorable properties of thermosetting polymers with the thermal processability of thermoplastic polymers. This opens up many new possibilities and applications for thermosets, also in terms of sustainability, as it allows for recycling of thermosets, which is not possible in current systems.

3

Aims

The depleting fossil resources as well as environmental concerns drive research towards the development of sustainable alternatives to commercially available polymeric materials. Renewable resources represent an abundant and versatile feedstock that can be exploited for polymer synthesis. This thesis aims to exploit biomass using sustainable procedures and apprehend recyclability to provide more benign alternatives to polymers available to date. In the course of this work, sustainable functionalization methods are implemented to transform terpenes and vanillin using benign reaction protocols. Sustainable transformations are important, as the sustainability of a product does not only depend on the origin of the raw material, but also on its production method including processes and reagents. Therefore, in this work, the Twelve Principles of Green Chemistry are taken as guidelines. As many principles as possible are implemented in each synthetic route, for example the use of renewable resources, catalytic reaction procedures and the use of benign reagents and solvents.

Thermosets represent an important class of polymers with outstanding thermomechanical properties. The production of the widely applied epoxy resins is commonly based on diglycidyl ether of bisphenol A (DGEBA) and isophorone diamine (IPDA). Therefore, the goal of this work is the development of bio-based and sustainable alternatives to these monomers. Vanillin constitutes an aromatic building block that can currently be produced in large amounts from lignin, a by-product of the pulp and paper industry. For this reason, vanillin is investigated as a promising substrate to establish new routes for the synthesis of monomers that can replace DGEBA in thermosetting polymers. Terpenes also constitute a valuable resource, as many

terpenes bear a cyclic structure, making them suitable candidates for the replacement of the epoxy curing agent IPDA. Consequently, the sustainable modification of terpene structures, such as (*R*)-(+)-limonene, (*R*)-carvone or γ -terpinene into diamines is explored, including epoxidation, rearrangement and amination reactions. After the synthesis of these new monomers, polymeric networks will be formed and compared to commercial resins to identify suitable alternatives that offer comparable thermomechanical properties.

A major problem regarding the sustainability of thermosetting polymers is their recycling. As a consequence of their highly cross-linked structure, thermosets cannot be recycled applying conventional melt-processing. In this work, the implementation of recyclability into renewably-sourced thermosets is explored. This entails the formation of cleavable monomers from vanillin that can not only replace DGEBA, but also enable controlled degradation of the polymer network after its usage. Finally, the degradability and recyclability of the cross-linked networks prepared in this work is also investigated.

In summary, this thesis strives for the sustainable synthesis of thermosetting materials that are degradable under certain conditions and thus enable the recycling of materials that are conventionally incinerated after a single application. Besides the use of renewable resources for polymer production and the implementation of recyclability, the sustainability is also considered on a molecular level by implementing benign reaction pathways, following the guidelines of the Twelve Principles of Green Chemistry.

4

Results and Discussion

The following chapter discusses the results obtained in the course of this PhD work. Chapter 4.1 describes the synthesis of a platform of cleavable renewable monomers (bis-allyl and bisepoxide). In a first part, the sustainable allylation of bio-based phenols and their subsequent epoxidation is reported, before investigating different coupling procedures to introduce carbonate or acetal linker moieties. Chapter 4.2 discusses the use of terpenes for the synthesis of bio-based diamine hardeners. A reaction protocol entailing epoxidation of the terpene double bonds and rearrangement to the respective carbonyl groups is developed. Furthermore, different strategies to reach diamine structures are explored. Chapter 4.3 is dedicated to the polymerization of the cleavable bis-allyl ether monomers with terpene-based di- and trithiols. Then, the synthesis of epoxy resins from the cleavable bisepoxides and the terpene-based diamines is discussed in chapter 4.4. Finally, in chapter 4.5, the degradation of the cleavable monomers is investigated. Using the monomers as model substrates, a degradation procedure is established that is subsequently transferred to one of the thiol-ene polymer films synthesized in chapter 4.3.

4.1 Synthesis of Cleavable Bisepoxide Monomers

As already discussed in chapter 2, the synthesis of bifunctional monomers from vanillin or its derivatives can be achieved by two different pathways. The first strategy consists of the direct modification of vanillin, *e.g.* by glycidylation. The other strategy consists of coupling two vanillin molecules to obtain a symmetric monomer. In the latter approach, material properties can be tuned by varying the linker chemistry. This second approach was followed in this work, where cleavable linkers are introduced in order to prepare degradable thermosetting polymers. Thus, bis-allyl and derived bisepoxides consisting of coupled vanillin derivatives are synthesized.

A common strategy for the synthesis of epoxy monomers is the glycidylation with epichlorohydrin. Although epichlorohydrin can be synthesized from renewable glycerol, it remains a toxic and carcinogenic substance. Furthermore, during glycidylation, a stoichiometric amount of chloride species is formed as waste. Therefore, in this work, an alternative pathway *via* allylation and subsequent epoxidation was implemented.

4.1.1 Allylation of Bio-based Phenols

For the synthesis of cleavable bisepoxide monomers from renewable resources, the reduced vanillin-derivate, vanillyl alcohol, was chosen. This molecule features two hydroxyl groups (phenolic and benzylic) that exhibit different reactivity. This difference was exploited to selectively introduce two functionalities, *i.e.* the linker and the allyl group. This first part describes the allylation, while the coupling will be discussed in chapter 4.1.2. Traditionally, the incorporation of allyl ether moieties into phenolic compounds is reached by reacting the phenolic substrate with reactants such as allyl chloride or allyl bromide in a nucleophilic substitution reaction.^[277] However, this strategy requires the stoichiometric amount of base, at the same time creating at least stoichiometric amounts of halogen-containing waste, which is undesirable according to the Twelve Principles of Green Chemistry.^[18] Moreover, the use of halogenated and often toxic substances should be avoided in terms of sustainability. Therefore, as a more sustainable alternative, allylation was carried out *via* Tsuji-Trost reaction employing very low amounts of palladium nanoparticles stabilized on poly(vinyl pyrrolidone) (PVP).^[79] Allyl methyl carbonate was used as allylating agent and was synthesized in a first step from dimethyl carbonate (DMC) **1** and allyl alcohol **2**, which can both be prepared from renewable resources, as shown in Figure 4.1 (top). Using 1,5,7-triazabicyclo(4.4.0)dec-5-ene (TBD) as catalyst, allyl methyl

carbonate **3** was obtained in a transesterification reaction in an isolated yield of 28% after vacuum distillation. The obtained yield is lower than literature yields, where yields of 50% were reported.^[79] Nevertheless, unreacted DMC as well as the by-product diallyl carbonate (22% yield), which could also be used in the Tsuji-Trost reaction, can be recovered. Allyl methyl carbonate was subsequently used for the Tsuji-Trost allylation of vanillyl alcohol **4** (Figure 4.1). The procedure was previously established in the group and uses a very low catalyst loading of 0.1 mol% palladium nanoparticles with catalytic amounts of triphenyl phosphine as ligand (5 mol%).^[79] The reaction is heterogeneously catalyzed in water and proved to be selective for the allylation of phenolic hydroxyl groups. Thus, the allyl group was selectively incorporated at the phenolic position of vanillyl alcohol **4**, leaving the benzylic hydroxyl group free for the coupling reactions. After isolation by extraction, followed by column chromatography, allyl vanillyl alcohol (AVA) **5** was obtained in an isolated yield of 75%.

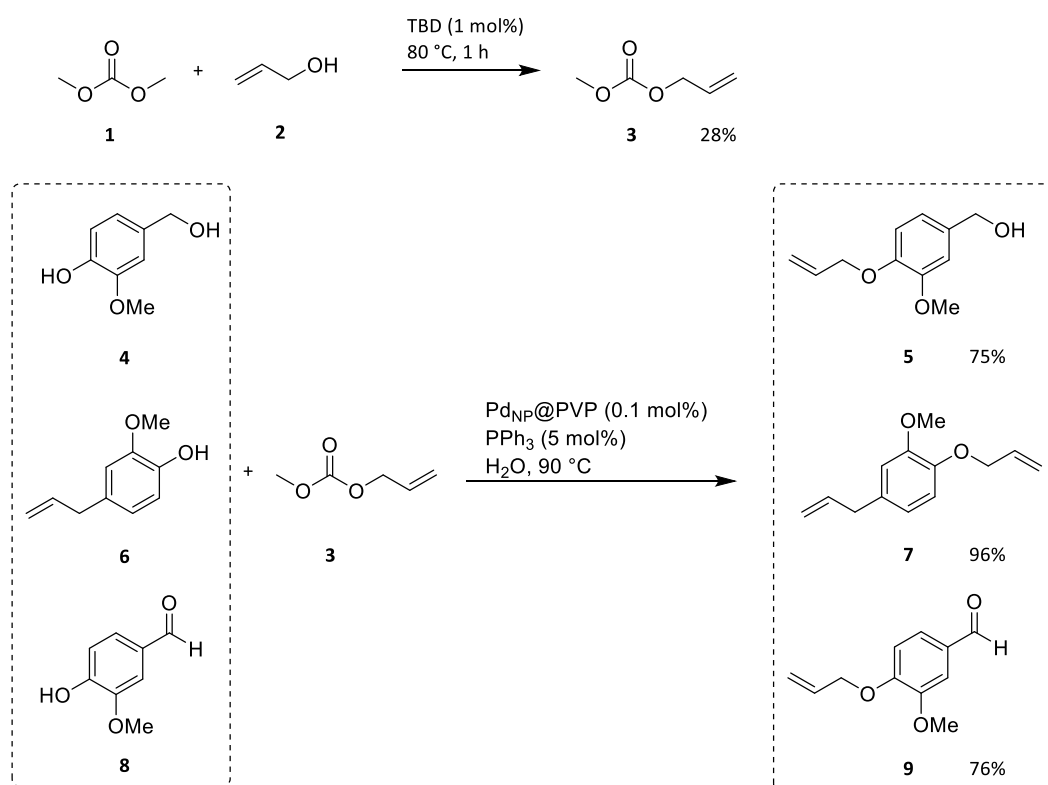


Figure 4.1 Synthesis of allyl methyl carbonate **3** and subsequent allylation of vanillyl alcohol, eugenol and vanillin catalyzed by palladium nanoparticles.

Using the same procedure, the allylation was also carried out for eugenol **6** and vanillin **8**.^[79] Full conversion of eugenol was reached after four hours at 90 °C. After column chromatography, allyl

eugenol **7** was obtained in an excellent isolated yield of 96%. * Allyl vanillin **9** was obtained in an isolated yield of 76% after 22 h reaction time. Figure 4.2 shows the $^1\text{H-NMR}$ spectra of allylated vanillyl alcohol **5** (a), allyl eugenol **7** (b) and allyl vanillin **9** (c). All the characteristic peaks were attributed. Notably, in spectrum (a), the free benzylic hydroxyl group (signal 12 at 5.08 ppm) of AVA **5** can be clearly distinguished. Spectrum (b) shows signals for the two different double bonds (signals 9 + 10 and signals 12 + 13 at 5.99, 5.30 and 5.00 ppm) of allyl eugenol, while for allyl vanillin, the aldehyde peak (signal 11 at 9.84 ppm) is visible.

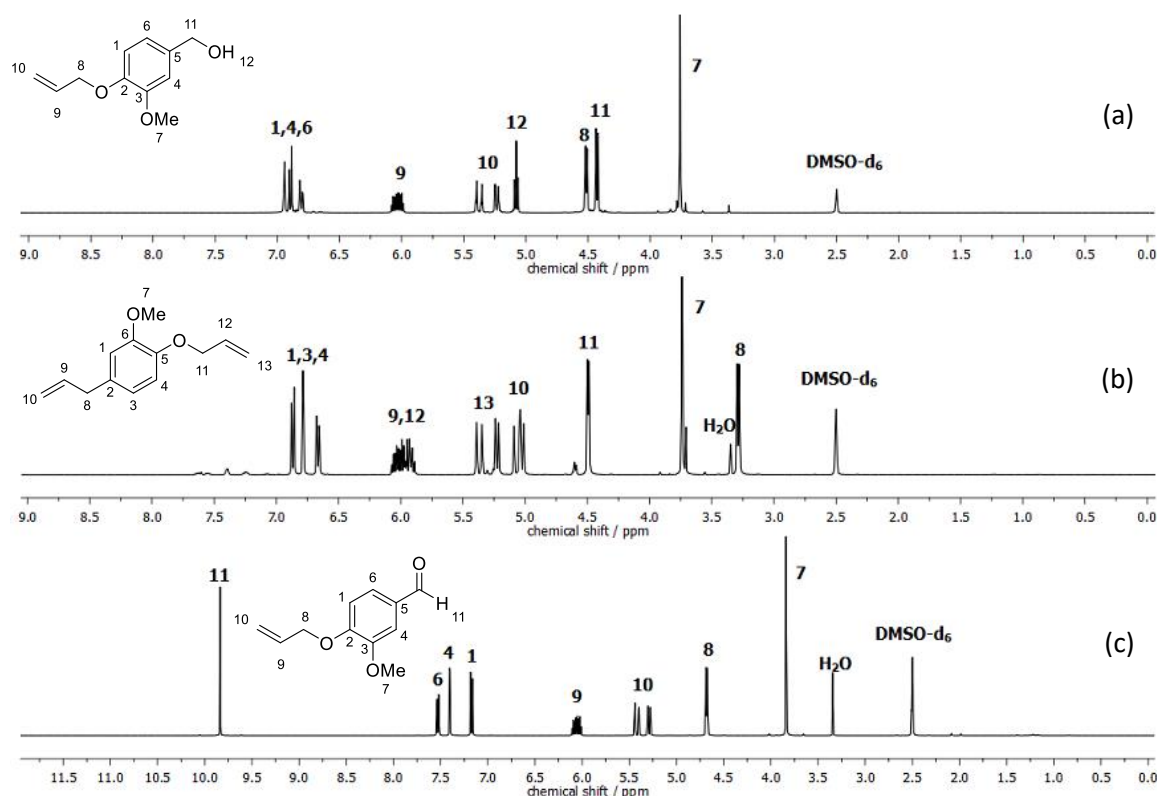


Figure 4.2 $^1\text{H-NMR}$ spectra of allyl vanillyl alcohol **5** (a), allyl eugenol **7** (b) and allyl vanillin **9** (c) in DMSO-d_6 .

4.1.2 Coupling of Allyl Vanillyl Alcohol to Diene Monomers

After the synthesis of AVA **5**, the next step was the introduction of a linker for the formation of symmetric monomers. One option is the coupling of AVA **5** to produce a diene structure, followed by epoxidation. Therefore, in a first step, AVA **5** was used to investigate different coupling conditions and suitable reaction pathways to prepare bis-allyl ether monomers as shown in Figure 4.3.

* This reaction was performed by Annika Nutz in the scope of an internship under my co-supervision.

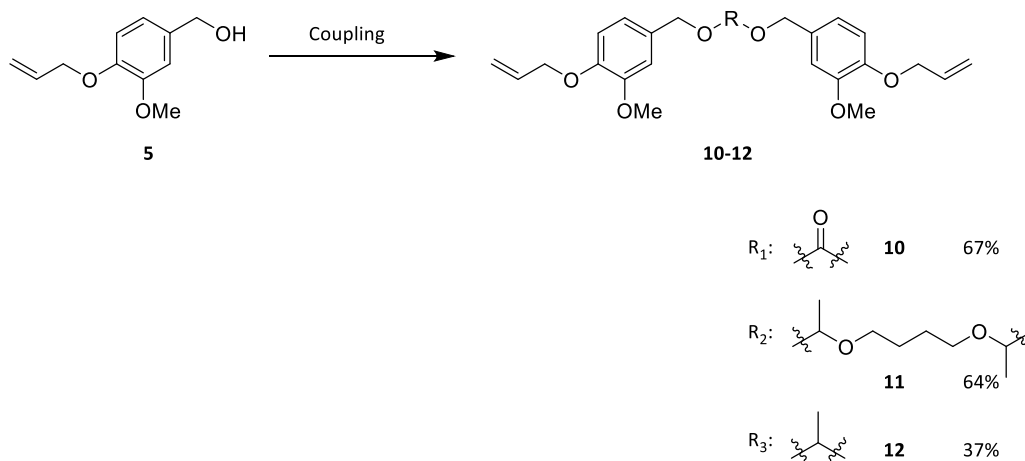


Figure 4.3 Coupling of AVA **5** to symmetric bis-allyl ether monomers **10-12**.

As first acid-cleavable linker unit, a carbonate moiety was selected. To introduce the carbonate functionality, DMC was used as sustainable reagent using TBD as catalyst. In a first attempt, 100 mg AVA **5** were mixed with a slight excess of 2.00 eq DMC and 5.00 mol% TBD in 0.4 mL tetrahydrofuran (THF). The mixture was heated to 80 °C for 47 hours. Despite an incomplete conversion, the product was extracted by adding 10 mL ethyl acetate and the obtained solution was washed with water. After column chromatography, the carbonate-coupled diene **10** was obtained in a yield of 30%. In a next attempt, in order to increase the conversion, the amount of DMC was increased to 5.00 eq. However, this mainly led to the formation of the mono-coupled product (a carbonate bearing one allyl vanillyl alcohol rest and one methyl group). The formation of this side product was expected; however, an increase of DMC could also have resulted in a higher product yield. Therefore, in a next step, a two-step procedure was established. AVA **5** was reacted with an excess of 10.0 eq DMC **1** and 5.00 mol% TBD as catalyst. After 6 h reaction time at 80 °C, AVA **5** was almost completely transformed to the mono-coupled product according to TLC analyses. Subsequently, the excess of DMC was removed under reduced pressure and another 1.05 eq AVA **5** were added. The mixture was heated to 100 °C for 24 h without an additional solvent, as the higher temperature enabled the reaction to proceed in a molten state. After washing and column chromatography, product **10** was obtained in a higher yield of 67%. Through the two-step one-pot procedure, higher conversions were obtained, which significantly improved product yields.

Another interesting target linker is the dimethylketal moiety, as it shows degradability in acidic solutions^[278] and exhibits a high structural similarity to BPA, which is beneficial for reaching materials with similar thermomechanical properties. In the literature, such ketal units have been synthesized by reacting alcohols with reagents such as 2-methoxypropene^{[279][280]} or

2,2-dimethoxypropane,^[281] using acids such as *p*-toluenesulfonic acid (*p*-TSA) or pyridinium *p*-toluenesulfonate (PPTS) as catalyst. The formation of a ketal linker was also attempted with AVA **5**. 2-Methoxypropene, 2,2-dimethoxypropane as well as both acid catalysts (*p*-TSA and PPTS) were tested. However, reactions generally showed low conversions and no product formation was achieved. Additionally, especially using *p*-TSA, the formation of an ether side product, formed *via* ether formation between two benzylic hydroxyl groups of AVA **5**, as shown in Figure 4.4, was observed.

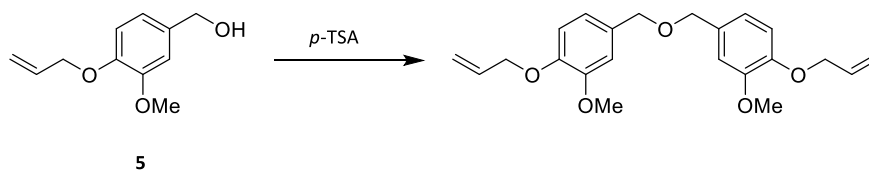


Figure 4.4 Formation of an ether side product from AVA **5** catalyzed by *p*-TSA.

The formation of acetal linkages *via* addition reaction of alcohol groups and vinyl ether moieties was for example shown by Pu and co-workers, who synthesized poly(*L*-lactic acid) (PLLA) polymers exhibiting cleavable acetal groups.^[282] Acetal coupling was achieved by reacting low molecular weight PLLA segments with diethylene glycol divinyl ether, using *p*-TSA as catalyst. As *p*-TSA was shown to be too acidic for the conversion of AVA **5**, leading to increased ether formation, PPTS was investigated as milder alternative. PPTS proved to be a suitable catalyst for the formation of the bisacetal structure **11**. Employing 1,4-butanediol divinyl ether as linker, the double addition was achieved by reacting AVA **5** with 0.50 eq 1,4-butanediol divinyl ether and 5 mol% PPTS. After optimization,* the best results were obtained at 0 °C, after a reaction time of 5 h and using dichloromethane as solvent. A mixture of starting material, the desired product **11** and small amounts of the mono-acetal structure **12** was obtained. After column chromatography, bisacetal **11** bearing two allyl ether groups was isolated in a yield of 64%.

During the bisacetal synthesis, the mono-acetal structure **12** without a C4-linker unit was identified and isolated as by-product, presumably formed *via* an addition reaction between AVA **5** and the vinyl ether, followed by a substitution reaction with a second equivalent of AVA **5** (Figure 4.5).

* The optimization of the reaction conditions was carried out by Bastian Pfeuffer in the bachelor thesis "Synthesis of cleavable monomers for bio-based, recyclable polymers" under my co-supervision

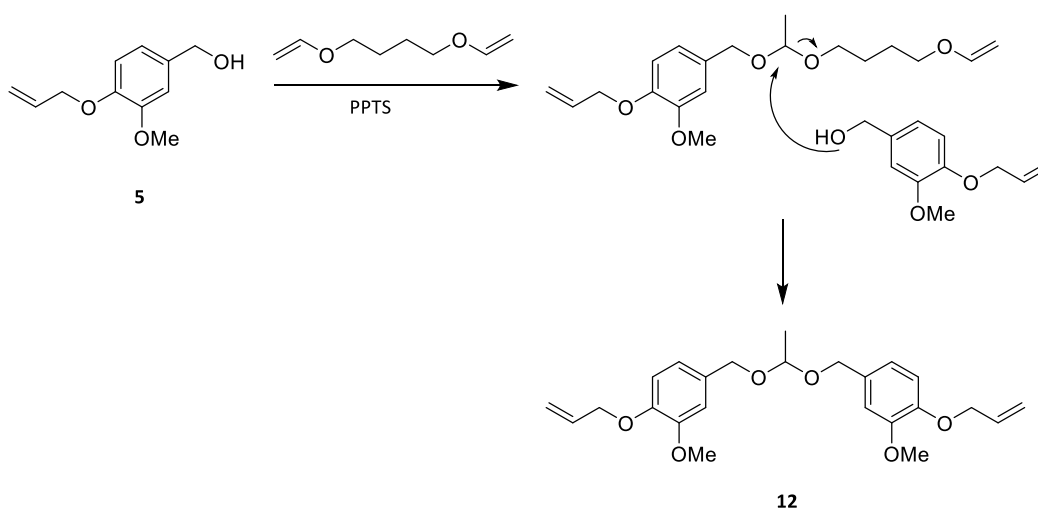


Figure 4.5 Proposed reaction sequence for the formation of mono-acetal **12** from AVA **5** and 1,4-butanediol divinyl ether.

As the mono-acetal **12** also represents an interesting linker moiety, a more selective synthetic procedure towards **12** was investigated. 1,4-butanediol divinyl ether was replaced by ethyl vinyl ether, as it bears the vinyl ether group for the addition reaction and an ethyl group as smaller leaving group. Similar to the carbonate coupling, a two-step procedure proved to give the best results. * 1.00 g AVA **5** was dissolved in 20.0 eq ethyl vinyl ether and 0.2 eq of PPTS were added. After stirring at room temperature for one hour, full conversion of AVA **5** to the mono-coupled ethyl acetal was indicated by thin layer chromatography (TLC). The excess of ethyl vinyl ether was subsequently removed under reduced pressure and an additional 1.00 g of AVA **5** was added with 10 mL 2-MeTHF as sustainable solvent. The reaction mixture was stirred at room temperature for 40 h, followed by purification *via* column chromatography. Finally, product **12** was obtained in an isolated yield of 37%. Increasing the product yield proved to be difficult, as higher temperatures led to a higher ether side product formation. An increased reaction time did not lead to a higher yield. In all cases, a mixture of starting material, mono-coupled ethyl acetal and the desired product was obtained with a maximum amount of 50% product according to crude $^1\text{H-NMR}$ spectroscopy analyses.

Figure 4.6 shows the $^1\text{H-NMR}$ spectra of the three synthesized bis-allyl ether monomers. All characteristic peaks were observed. For the carbonate monomer (Figure 4.6 (a)), a shift of signal 11 towards higher ppm values (from 4.43 ppm in AVA **5** to 5.06 ppm in the carbonate monomer **10**) can be observed, which is induced by the incorporation of the adjacent electron

* The optimization of the reaction conditions was carried out by Bastian Pfeuffer in the bachelor thesis "Synthesis of cleavable monomers for bio-based, recyclable polymers" under my co-supervision

withdrawing carbonate group. For the bisacetal **11** (Figure 4.6 (b)), peaks characteristic of the acetal bridges (signal 12 at 4.73 ppm and signal 13 at 1.24 ppm) and of the C4 carbon linker (signals 14 at 3.48 ppm and signal 15 at 1.55 ppm) are visible. Those signals are clearly missing in the spectrum of monoacetal **12** (Figure 4.6 (c)). Here, only the signals for the acetal bridge can be observed. Furthermore, all monomers were characterized by mass spectrometry and IR spectroscopy.

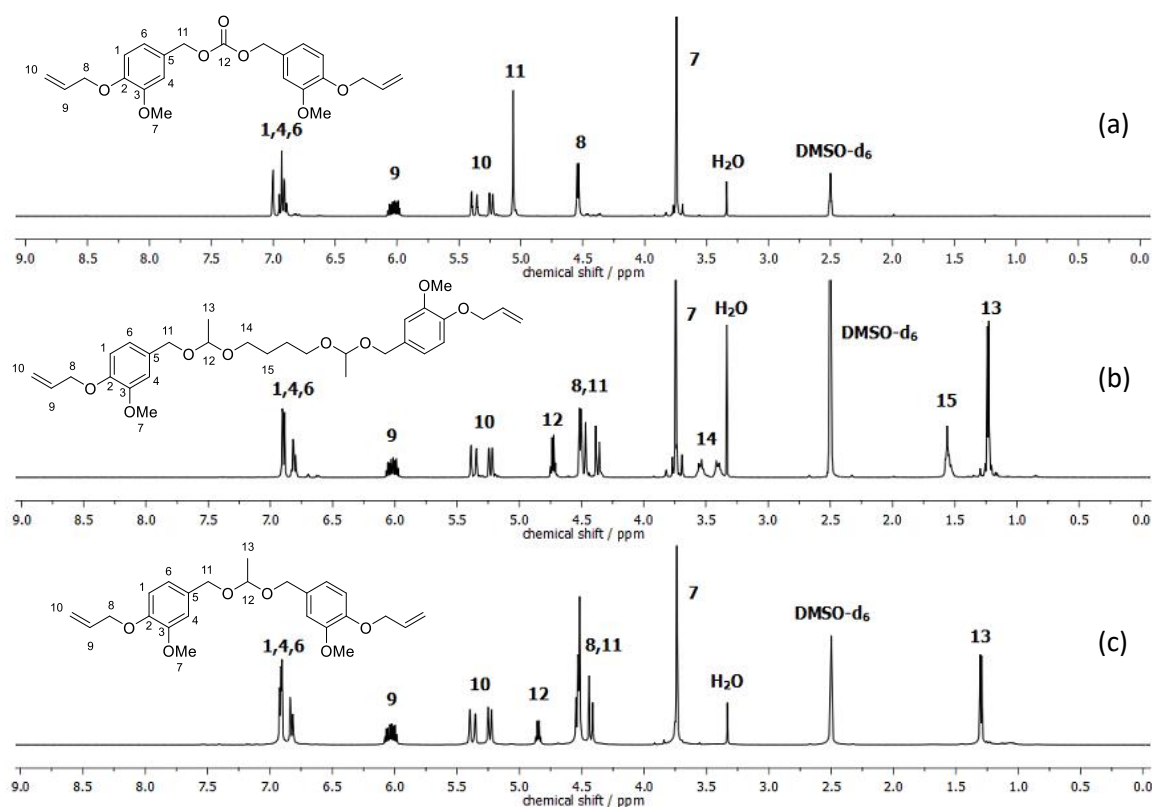


Figure 4.6 $^1\text{H-NMR}$ spectra of coupled bis-allyl ether monomers: carbonate **10** (a), bisacetal **11** (b) and monoacetal **12** (c) in DMSO-d_6 .

Finally, allylated vanillin was used in a Biginelli reaction together with AVA acetoacetate **13**, which was previously synthesized from AVA **5**, *tert*-butyl acetoacetate, and urea (Figure 4.7). Biginelli product **14** was obtained in a yield of 38% after column chromatography. As the Biginelli structure contains an ester functionality, polymers synthesized thereof have the potential to be degraded in acidic and basic conditions. Figure 4.7 also shows the $^1\text{H-NMR}$ spectrum of the diallyl ether **14**. Besides the allylic protons, the signals of the 3,4-dihydropyrimidin-2(1H)one ring structure are observed (signals 14, 16 and 17 at 9.22, 7.70 and 2.27 ppm).

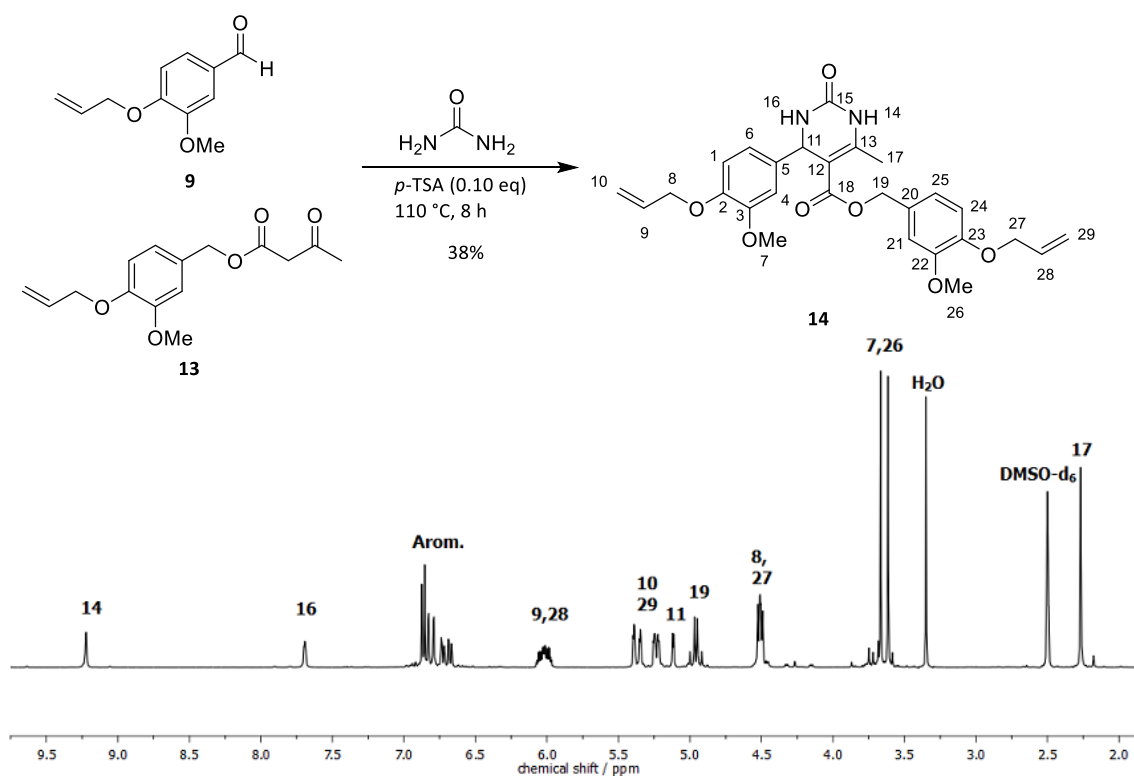


Figure 4.7 Synthesis of bis-allyl ether **14** via Biginelli reaction between allyl vanillin **9**, AVA acetoacetate **13** and urea in DMSO- d_6 .

4.1.3 Synthesis of Diglycidyl Ether Monomers from Allylated Vanillyl Alcohol

For the synthesis of diglycidyl ether monomers, two possible strategies were investigated. The first strategy consisted of epoxidizing the synthesized coupled bis-allyl ether monomers. The other pathway consisted of first epoxidizing AVA **5** to glycidyl vanillyl alcohol (GVA) **15** and a subsequent coupling step. Both strategies and the commercial reference monomer DGEBA are depicted in Figure 4.8.

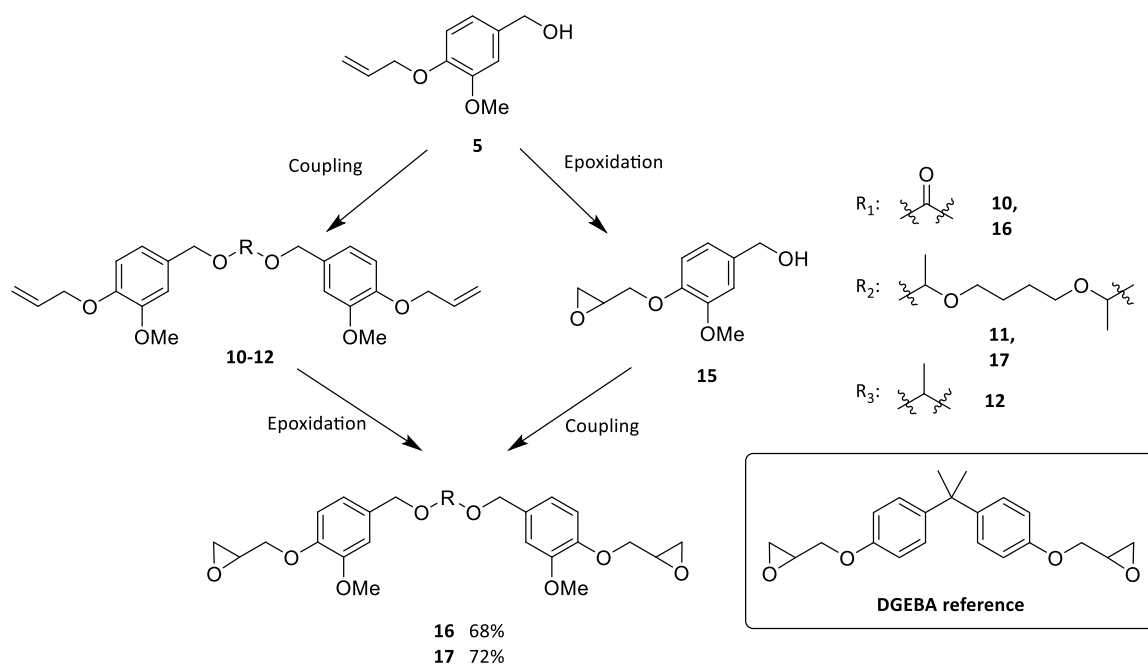


Figure 4.8 Coupling strategy for the formation of diglycidyl ether of vanillyl alcohol **16** and **17** as sustainable alternative to DGEBA.

In a first step, the epoxidation of AVA carbonate **10** was investigated. As shown in Figure 4.9, peracetic acid was used as oxidation agent. Prior to the reaction, peracetic acid and the solvent DMC were dried over 3Å-molecular sieve under argon atmosphere for 2 h. Subsequently, the solution was added to the carbonate **10** and the mixture was stirred at 70 °C under argon atmosphere for 5 h. After the reaction, ethyl acetate was added and the solution was washed with sodium sulfite solution, water and brine. Then, the solution was dried over sodium sulfate and the solvent was removed under reduced pressure.

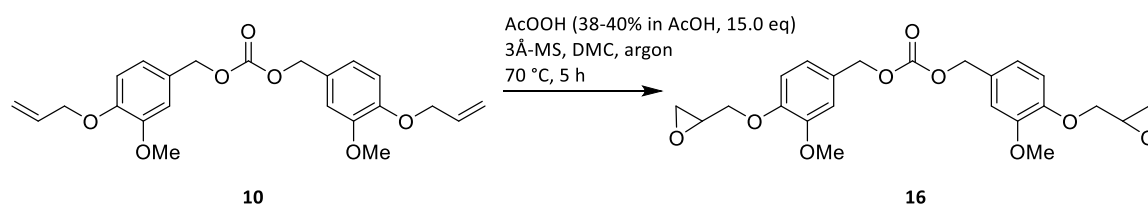


Figure 4.9 Epoxidation of AVA Carbonate **10** to bisepoxide **14** using peracetic acid solution.

According to TLC analysis of the crude product mixture, a mixture of starting material, mono- and bisepoxidized products was obtained. In the next step, two different procedures were tested for the isolation of glycidyl vanillyl alcohol (GVA) carbonate **16**. An isolation of the product by precipitation in ethyl acetate was attempted first. A product precipitated in a yield of 25%, but the $^1\text{H-NMR}$ spectrum showed signals of remaining double bonds and thus the unsuccessful isolation of product **16**. Indeed, as the mono-epoxidized side product has a similar structure as

product **16**, both molecules precipitated. In a second attempt, column chromatography was tested for the isolation of carbonate **16**. Unfortunately, the product tended to strongly adhere to the silica gel, which resulted in low yields of 7%. The problem of an incomplete conversion and a difficult isolation of the desired product led to the investigation of another synthetic pathway. The strategy of coupling AVA **5** prior to epoxidation was abandoned, as it did not show promising results.

As an alternative, the epoxidation of AVA **5** to GVA **15** was investigated. As a reaction with peracetic acid did not lead to a significant conversion of the starting material, another reaction protocol was established, as shown in Figure 4.10. Ammonium bicarbonate (NH_4HCO_3) and hydrogen peroxide (H_2O_2) were employed analogous to a procedure reported by Yao and Richardson,^[283] who showed the epoxidation of different deactivated olefinic substrates using these reagents. As active oxidizing species, the peroxy monocarbonate ion HCO_4^- was proposed.

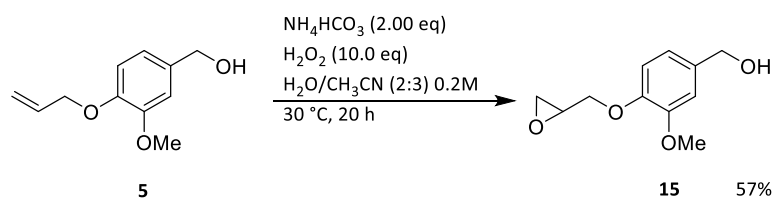


Figure 4.10 Epoxidation of AVA **5** to GVA **15** applying ammonium bicarbonate and hydrogen peroxide.

For the epoxidation, AVA **5** and 2.00 eq ammonium bicarbonate were dissolved in a water/acetonitrile mixture (2:3, 0.2M). Subsequently, 10.0 eq H_2O_2 were added and the solution was stirred at 30 °C for 20 h. To monitor the reaction progress, gas chromatography-mass spectrometry (GC-MS) was performed after 17 h reaction time. The chromatogram (Figure 4.11 (a)) showed complete conversion of AVA **5** (dashed line) and a high selectivity towards the desired product. After a washing step and column chromatography, product **15** was obtained in a yield of 57% due to the affinity of the epoxide structure to the silica gel during column chromatography. This issue could not be circumvented by different tested solvent mixtures.

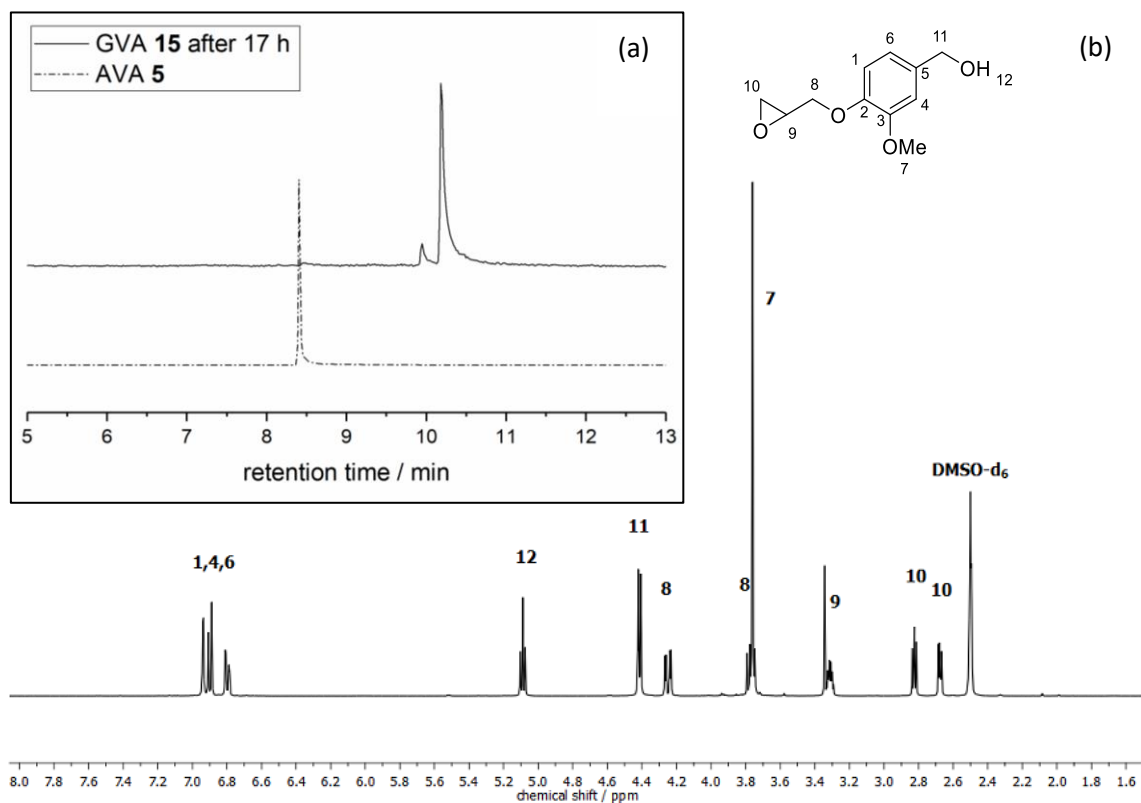


Figure 4.11 (a) GC-MS chromatogram after the epoxidation of AVA **5** (dashed line) applying hydrogen peroxide and ammonium bicarbonate after 17 h reaction time, (b) ¹H-NMR spectrum of isolated GVA **15** in DMSO-d₆.

Figure 4.11 (b) shows the ¹H-NMR spectrum of the isolated product **15**. Besides the unreacted hydroxyl group (signal 12 at 5.09 ppm), the signals of the newly formed epoxide group (signals 9 and 10 at 3.31, 2.82 and 2.68 ppm) and the adjacent CH₂ group (signal 8 at 4.25 and 3.78 ppm) can be distinguished.

After the successful epoxidation of AVA **5**, the previously established coupling procedures of AVA **5** were transferred to its epoxidized counterpart **15** (Figure 4.12).

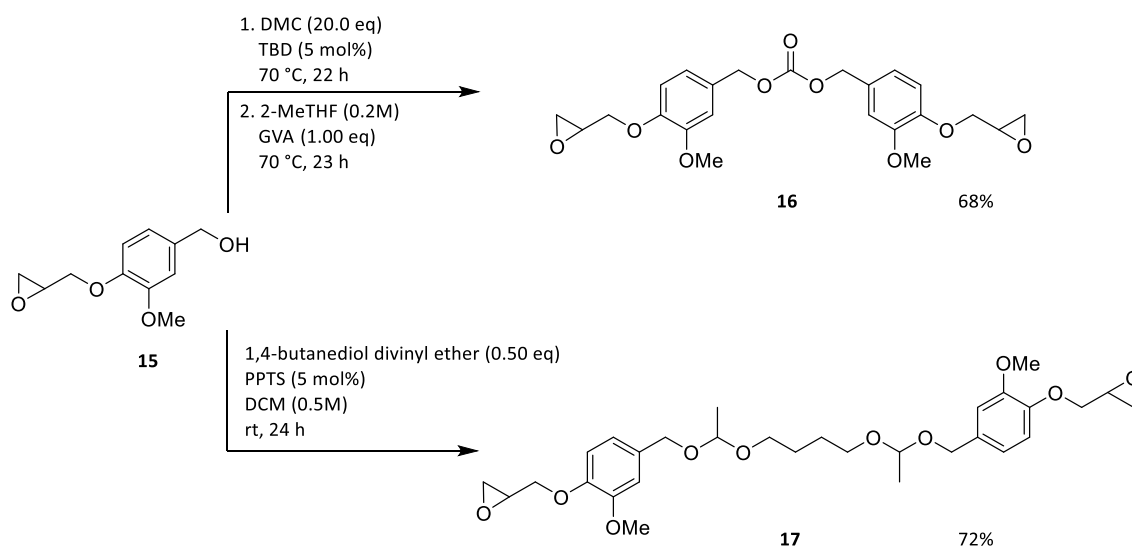


Figure 4.12 Coupling of GVA **15** to GVA carbonate **16** and GVA bisacetal **17**.

The coupling of GVA **15** to GVA carbonate **16** was attempted in a two-step procedure. However, in the second step, 2-MeTHF was added as an additional solvent to ensure a good mixing and thus a good reaction progress. As described previously, the isolation *via* column chromatography proved to be difficult and resulted in low yields. However, in this case the desired product could be isolated by precipitation in cold ethyl acetate, resulting in a yield of 68%. The bisacetal coupling procedure was also transferred to GVA **15** (Figure 4.12, bottom). In contrast to the allylic substrate, higher yields were obtained at room temperature (rt) instead of 0 °C. Furthermore, the reaction time had to be increased to 7 h in order to obtain high conversions (a maximum yield of 88% was observed in the crude $^1\text{H-NMR}$ spectra). However, a higher conversion might be achieved by further adjusting the reaction protocol, for instance by increasing the reaction time or temperature. After column chromatography, product **17** was obtained in a yield of 72%. As the yield for the monoacetal coupling was moderate during the bis-allyl ether synthesis (**12**, 37%), the synthesis of the GVA monoacetal was not attempted.

Figure 4.13 shows the $^1\text{H-NMR}$ spectra of both isolated monomers. In the spectrum of GVA carbonate **16** (Figure 4.13 (a)), besides the disappearance of the hydroxyl group, again a shift of the CH_2 group adjacent to the carbonyl group (signal 11 at 5.07 ppm) can be observed. The spectrum of bisacetal **17** (Figure 4.13 (b)) exhibits signals of the acetal bridge (signals 12 and 13 at 4.74 and 1.25 ppm) and the aliphatic spacer (signals 14 and 15 at 3.48 and 1.57 ppm). Both products also show the signals of the glycidyl ether moiety (signals 8, 9 and 10). Furthermore, all products were analyzed by mass spectrometry and IR spectroscopy, confirming their structures.

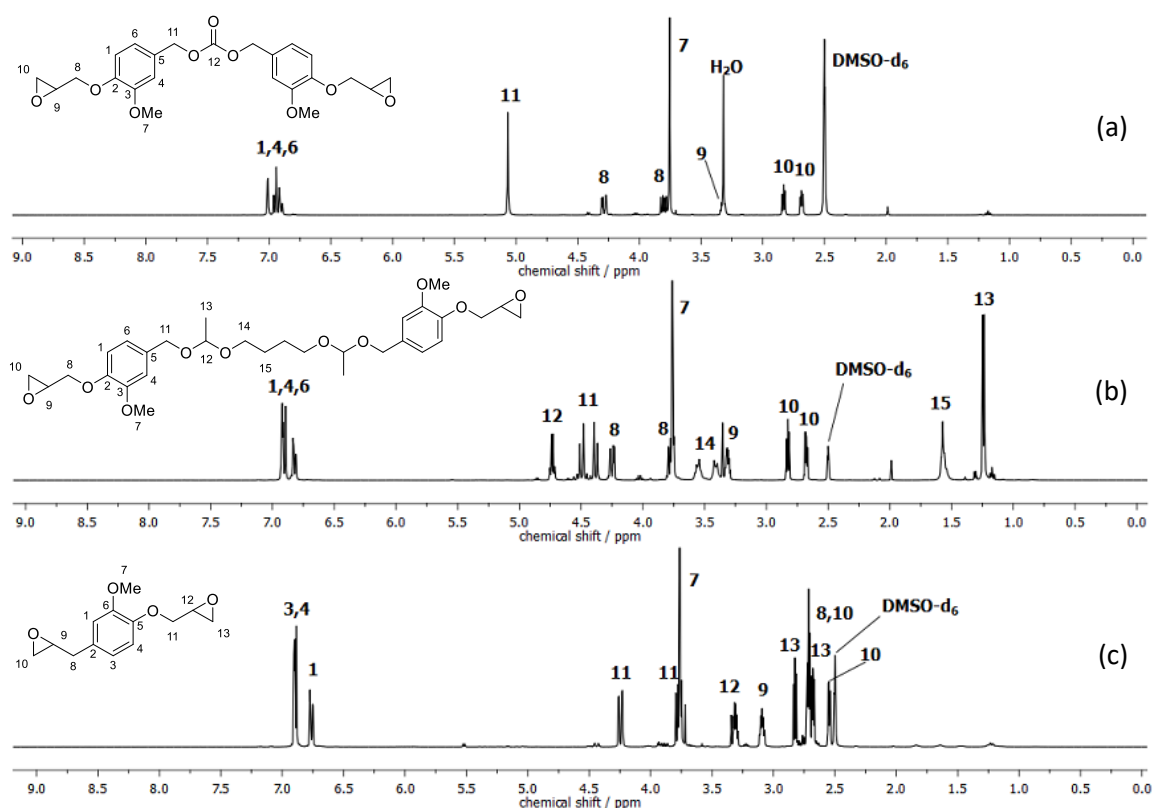


Figure 4.13 $^1\text{H-NMR}$ spectra of glycidyl ether monomers: carbonate **16** (a), bisacetal **17** (b) and epoxidized allyl eugenol **18** (c) in DMSO-d_6 .

In addition to the cleavable monomers **16** and **17**, also allylated eugenol **7** was epoxidized applying the conditions established for the epoxidation of AVA **5** (Figure 4.14). The formed product can also be used in epoxy resin synthesis and acts as a non-cleavable alternative and reference to the cleavable monomers and the commercial reagent DGEBA.

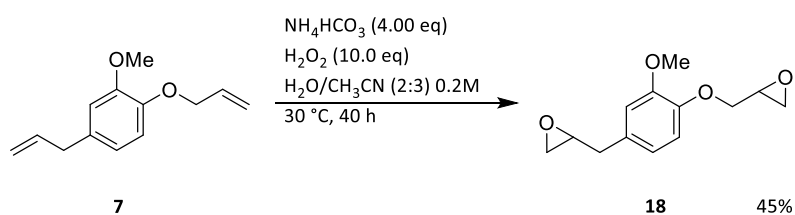


Figure 4.14 Epoxidation of allylated eugenol **7** applying ammonium bicarbonate and hydrogen peroxide to form epoxidized allyl eugenol **18**.

As allyl eugenol bears two terminal double bonds, the amount of ammonium bicarbonate and the reaction time were increased. However, a mixture of starting material, mono-epoxidized products and bisepoxide **18** were obtained after 40 h reaction time. After isolation *via* column chromatography, the bisepoxide was obtained in a yield of 45%. This result can likely be improved by further increasing the reaction time, the excess of hydrogen peroxide or the

reaction temperature. The $^1\text{H-NMR}$ spectrum of the eugenol-based bisepoxide is shown in Figure 4.13 (c). In comparison to the symmetric linkers synthesized before, the spectrum clearly shows signals for two different epoxide functionalities (signals 8, 9 and 10 at 2.71, 3.09, 2.71 and 2.55 ppm and signals 11, 12 and 13 at 4.25, 3.77, 3.31, 2.82 and 2.68 ppm).

The synthesis of bisepoxide **18** from eugenol has already been reported in literature by Zhang *et al.*^[284] The authors used a three-step synthesis procedure starting with an acetylation of the phenol group of eugenol employing acetic anhydride, followed by an epoxidation using *m*CPBA. Finally, a deacetylation and glycidylation step (using epichlorohydrin) led to the formation of bisepoxide **18**. Although the overall reaction yield was higher than the yield obtained in this work (53% vs 43%), during the synthesis, unsustainable (*m*CPBA) and toxic (epichlorohydrin) reagents were employed. Furthermore, the use of protecting groups should be avoided according to the Twelve Principles of Green Chemistry. These reagents greatly diminish the sustainability of the procedure. Therefore, the procedure of allylation and epoxidation described in this work represents a good alternative.

In conclusion, the allylation of vanillyl alcohol and eugenol was performed as reported in literature, applying palladium nanoparticles in water. The procedure was also transferred to the sustainable allylation of vanillin. In a first step, coupling conditions were established for allyl vanillyl alcohol, to form carbonate, mono-acetal and bisacetal diene monomers. Additionally, a Biginelli-based diene was synthesized as a monomer potentially cleavable under basic conditions. As a direct epoxidation of the coupled dienes proved to be difficult, the epoxidation of AVA **5** was carried out first. A reaction procedure applying hydrogen peroxide and ammonium bicarbonate as oxidation system was established. Subsequently, the optimized coupling conditions were transferred to the epoxidized glycidyl vanillyl alcohol. Bisepoxide monomers with a carbonate and a bisacetal linker group were synthesized and isolated. Furthermore, the bisepoxide from allyl eugenol was synthesized as non-cleavable reference in the epoxy resin synthesis.

4.2 Terpenes as Feedstock for Renewable Amine Hardeners

One of the commonly used amine hardeners for epoxy resin synthesis is isophorone diamine (IPDA).^[285] IPDA possesses two amine functionalities and a cyclic structure. It is commonly synthesized from isophorone in a hydrocyanation reaction applying unfavorable HCN as reagent, followed by amination and reduction steps.^[286] In order to find a suitable alternative for IPDA, a similar structural motif is targeted to achieve similar thermomechanical properties of the final material. Terpenes comprise a great variety of cyclic structures, which can potentially be used for the synthesis of sustainable alternatives for IPDA. In this work, a first strategy for the synthesis of terpene-based diamines consisted of the four-step reaction pathway shown in Figure 4.15 (a). Starting from dihydrocarvone, the diamine is synthesized *via* a reaction series established before in the group for the transformation of limonene,^[287] *i.e.* acetoxylation of the double bond, a saponification and isomerization step followed by the reductive amination of the formed bis-carbonyl.

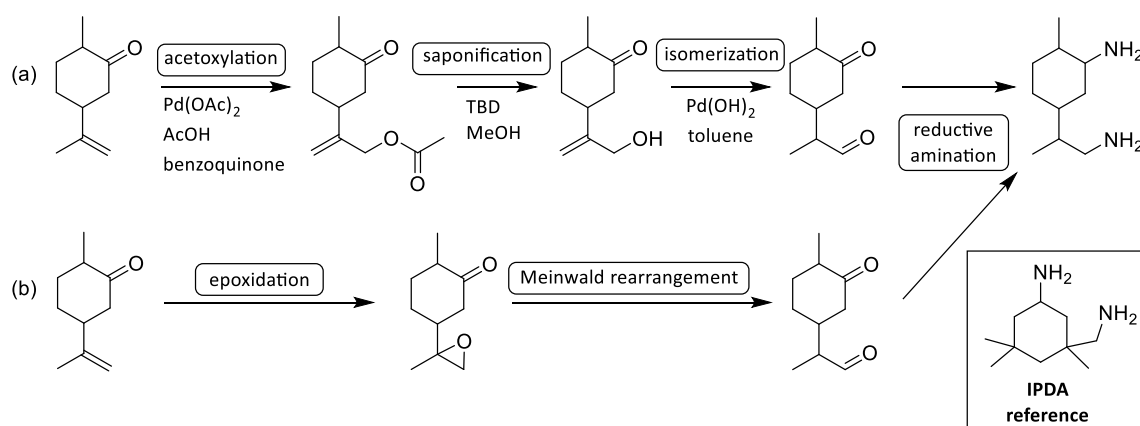


Figure 4.15 Two strategies for the synthesis of a dihydrocarvone-derived diamine: (a) Four-step synthesis *via* acetoxylation, saponification, isomerization and reductive amination, (b) Three-step synthesis *via* epoxidation, rearrangement and reductive amination.

The first three reaction steps were transferred to dihydrocarvone applying literature conditions.^[287] However, only low product yields were achieved with dihydrocarvone as starting material (acetoxylation: 11%, saponification: 53%, isomerization: 37%). Therefore, a different strategy was developed (Figure 4.15 (b)). In a first step, the double bond of dihydrocarvone is epoxidized and the epoxide is subsequently rearranged to a carbonyl group *via* a Meinwald rearrangement. A reductive amination can then be performed on the formed bis-carbonyl. In the following chapters, the results of this strategy on different terpenes are discussed.

4.2.1 Epoxidation of Terpenes

4.2.1.1 Epoxidation of Dihydrocarvone

(+)-Dihydrocarvone **19** was chosen as first substrate to start the investigations. Indeed, as it already contains one carbonyl group, only the transformation of one double bond to the respective epoxide and carbonyl group is required. In order to find the best reaction protocol, different epoxidation procedures reported before in the literature for other substrates were tested in order to find conditions for the highest yield of epoxidized dihydrocarvone **20**. Thus, procedures using classical oxidants such as peracetic acid, but also lipase-catalyzed reactions and metal catalyst, *e.g.* MTO or Na_2WO_4 were investigated. Screenings were performed using gas chromatography (GC) and the products were isolated for structural identification. Depending on the oxidation conditions, epoxidation of **19** led to the formation of the epoxidized dihydrocarvone **20** or the respective epoxy lactone **21** formed by epoxidation and Baeyer-Villinger oxidation of the cyclic ketone (Figure 4.16). All tested reaction protocols and the best yields obtained with the respective methods are summarized in Table 4.1. NMR spectra of the products can be found in chapter 6.3.2.

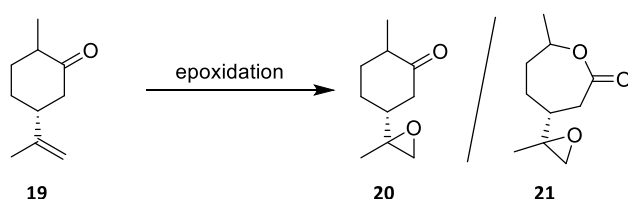


Figure 4.16 Epoxidation of (+)-dihydrocarvone **19** to epoxide **20** and epoxy lactone **21** using several epoxidation procedures.

When dihydrocarvone **19** was reacted with 5.00 eq of peracetic acid, epoxy lactone **21** was obtained in an isolated yield of 58.4% (Table 4.1, entry 1). As the reaction was not screened by GC, no yield of dihydrocarvone oxide **20** was determined. The formation of the epoxy lactone from dihydrocarvone was already reported in literature by Hillmyer *et al.*, who showed the synthesis of **21** (24.5% yield) by oxidation using *m*CPBA as oxidant.^[288] The authors polymerized the lactone by ring-opening polymerizations.

The use of peracetic acid in a smaller amount of 1.10 eq resulted in the formation of epoxide **20** in a yield of 36.2% according to GC analysis (entry 2). At the same time, epoxy lactone **21** was formed in a lower yield of 8.24%. Thus, the selectivity towards the formation of **20** or **21** can be tuned by the amount of peracetic acid used in the reaction mixture.

Table 4.1 Summarized results for the epoxidation of (+)-dihydrocarvone **19** to dihydrocarvone oxide **20** or epoxy lactone **21**.*

Entry	Oxidant	Reaction Conditions	Time / h	Max. Yield 20 / %	Yield 21 / %	Lit.
1	Peracetic acid (38-40% in AcOH, 5.00 eq)	3Å-MS, DMC (0.3M), 70 °C	6	n.a.	58.4 ^a	[289]
2	Peracetic acid (38-40% in AcOH, 1.10 eq)	3Å-MS, DMC (0.3M), 70 °C	16	36.2 ^b	8.24 ^b	[289]
3	H ₂ O ₂ (5.00 eq)	Lipase CALB (200 mg/mmol), DMC (0.1M), 40 °C	28	50.0 ^b	2.75 ^b	[124]
4	UHP ^c (1.10 eq),	Lipase CALB (50 mg/mmol), ethyl acetate (0.5M), 40 °C	21	24.7 ^b	38.6 ^b	[123]
5	H ₂ O ₂ (4.00 eq)	Na ₂ WO ₄ (0.2 eq), Aliquat 336 (3 mol%), H ₃ PO ₄ (0.400 eq), CHCl ₃ (0.2M), 40 °C	5	43.1 ^b	2.77 ^b	[290]
6	H ₂ O ₂ (1.50 eq)	MTO (0.01 eq), DCM (1.0M), rt	4	58.6 ^b	0	[133]
7	Oxone [®] (2.60 eq, 0.52M in H ₂ O)	NaHCO ₃ (4.80 eq), acetone (0.33M), rt	1.5	64.8 ^b	35.2 ^b	[120]

^a Isolated yield, ^b GC yield, ^c Urea-hydrogen peroxide.

Lipases constitute a sustainable alternative to conventional oxidation agents, enabling epoxidation reactions at mild reaction conditions and using benign oxidants such as hydrogen peroxide. In this study, epoxide **20** was formed in a yield of 50.0% (entry 3) in the presence of the lipase CALB and hydrogen peroxide with a low lactone formation of 2.75%. The combination of this enzyme with urea-hydrogen peroxide, which allows for a slower release of the oxidant (entry 4), resulted in a lower yield (24.7%). The use of ethyl acetate as solvent presumably led to the formation of peracetic acid, which causes the formation of lactone **21**. Indeed, **21** was detected in a comparably high yield of 38.6%. Thus, the chosen procedure is not suitable for a selective product formation.

Amongst the metal catalysts studied for this reaction (entry 5 and 6), MTO showed a better performance (58.6% yield) compared to sodium tungstate (43.1% yield), which was used under

* The optimization study was carried out by Pascal Rauthe in the scope of his Vertieferarbeit "Synthesis and optimization of terpene-based epoxides and their subsequent rearrangements" (entry 2-6) and by Tim Trumler in the scope of his Bachelor thesis "Synthesis of bio-based epoxides and diamines" (entry 7) under my co-supervision.

phase-transfer catalysis with Aliquat 336. Advantageously, MTO required less additional reagents and showed good results with only 1.50 eq H₂O₂. The best yields were obtained following a procedure reported by Kaliaguine *et al.*, who used the commercial oxidant Oxone[®] (potassium peroxymonosulfate) in combination with acetone and sodium bicarbonate in the epoxidation of limonene.^[120] Although the epoxidation with Oxone[®] is not a catalytic procedure, it is considered more sustainable than the use of *m*CPBA, offering attractive properties such as being easy to handle, stable and non-toxic.^[121] When applied to dihydrocarvone, epoxide **20** was obtained in a good yield of 64.8% together with 35.2% lactone **21**.

4.2.1.2 Epoxidation of Carvone

For the synthesis of bio-based diamines, (*R*)-(-)-carvone **22** was also investigated as substrate. As carvone features two double bonds, the epoxidation of the *endo*- and the *exo*-cyclic double bond is possible (shown in Figure 4.17). The applied reaction conditions are summarized in Table 4.2.

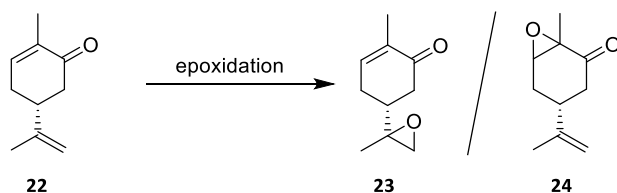


Figure 4.17 Epoxidation of (*R*)-(-)-carvone **22** to carvone-8,9-oxide **23** or carvone-1,2-oxide **24**.

Table 4.2 Summarized results for the epoxidation of (*R*)-(-)-carvone **22** to carvone-8,9-oxide **23** or carvone-1,2-oxide **24**.*

Entry	Oxidant	Reaction Conditions	Product	Time / h	GC Yield / %	Lit.
1	H ₂ O ₂ (5.00 eq)	NaOH (1.25 eq), MeOH (0.6M), 40 °C	24	4	91.2	[119]
2	H ₂ O ₂ (5.00 eq)	Lipase CALB (200 mg/mmol), DMC (0.1M), 40 °C	23	51	61.9	[124]
3	UHP (2.00 eq) ^a	Lipase CALB (50 mg/mmol), ethyl acetate (0.5M), 40 °C	23	29	79.9	[123]
4	Oxone [®] (1.50 eq, 0.52M in H ₂ O)	NaHCO ₃ (4.70 eq), acetone (0.33M), rt	23	0.5	97.5	[120]

^a Urea-hydrogen peroxide, the second equivalent of UHP was added after 24 h reaction time.

* The optimization study was carried out by Pascal Rauthe in the scope of his Vertieferarbeit "Synthesis and optimization of terpene-based epoxides and their subsequent rearrangements" (entry 1-3) and by Tim Trumler in the scope of his bachelor thesis "Synthesis of bio-based epoxides and diamines" (entry 4) under my co-supervision.

The synthesis of carvone-1,2-oxide **24** was performed following a previously reported procedure employing sodium hydroxide and hydrogen peroxide (Table 4.2, entry 1). A high selectivity towards the electron deficient Michael system was achieved, leading to high yields of 91.2% according to GC analysis. Thus, this procedure resulted in the selective epoxidation of the *endo*-cyclic double bond (without reaction on the *exo*-cyclic double bond). When lipase CALB was used, the *exo*-cyclic double bond was converted, yielding epoxide **23** in good yields. In the case of carvone, urea-hydrogen peroxide showed superior results (79.9% yield, entry 3) compared to hydrogen peroxide (61.9% yield, entry 2), even with a lower catalyst loading and less oxidant. This result exemplifies the difficulties arising from terpene conversion, as all terpenes, although being structurally similar, behave differently and reaction conditions need to be optimized individually for every substrate. As Oxone[®] proved to be an efficient oxidizing agent for the epoxidation of dihydrocarvone **19**, it was also tested with (*R*)-(-)-carvone. Applying 1.50 eq Oxone[®], carvone-8,9-oxide **23** was formed in high yields of 97.5%, proving the high potential of Oxone[®] for selective terpene epoxidation.

4.2.1.3 Epoxidation of γ -Terpinene

Although, in contrast to dihydrocarvone **19** and carvone **22**, γ -terpinene does not possess a carbonyl group, biscarbonyl structures can be obtained *via* double epoxidation and rearrangement procedures (the rearrangement will be discussed in chapter 4.2.2). Therefore, the epoxidation of γ -terpinene **25** to γ -terpinene dioxide **26** was investigated (Figure 4.18). Two reaction procedures were applied, which had shown good results with carvone-based substrates, *i.e.* the epoxidation using peracetic acid and Oxone[®]. The obtained results are listed in Table 4.3.

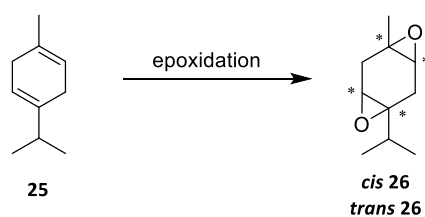


Figure 4.18 Epoxidation of γ -terpinene **25** to γ -terpinene dioxide **26**.

Table 4.3 Summarized results for the epoxidation of γ -terpinene **25** to γ -terpinene dioxide **26**.

Entry	Oxidant	Reaction Conditions	Product	Time / h	Yield ^a / %	Lit.
1	Peracetic acid (38-40% in AcOH, 6.00 eq)	3Å-MS, DMC (0.5M), 70 °C	<i>cis</i> 26	19	27.8	[289]
2	Oxone [®] (2.60 eq, 0.52M in H ₂ O)	NaHCO ₃ (4.70 eq), acetone (0.33M), rt	<i>cis</i> 26 <i>trans</i> 26	3	48.8 26.8	[120]

^a Isolated yield

During the epoxidation of γ -terpinene **25**, four stereoisomers can be formed, *i.e.* two *cis*- and two *trans*-isomers. Interestingly, only *cis* **26** was detected and isolated in a yield of 27.8% when peracetic acid was used. As a high selectivity towards the product was observed in GC-MS measurements, the low yield was presumably caused by an insufficient cooling during the reaction and product losses during column chromatography. In the reaction with peracetic acid, the first formed epoxy group seems to induce the stereoselective formation of the *cis* isomer. In contrast, when using Oxone[®], both *cis*- and *trans*-diastereoisomers were formed and isolated in yields of 48.8% and 26.8%, respectively. Thus, Oxone[®] enables the efficient epoxidation of structurally demanding terpenes, which is often difficult to achieve with other epoxidation systems.

4.2.2 Meinwald Rearrangement of Epoxidized Terpenes^{*}

4.2.2.1 Optimization of the Catalytic Reaction Conditions

With the aim to synthesize biscarbonyl compounds based on renewable feedstock in a sustainable fashion, the rearrangement of the different terpene-based epoxides was investigated. With the objective to implement a maximum of the Twelve Principles of Green Chemistry,^[18] a catalyst, solvent and temperature screening was performed to develop a procedure that operates under mild reaction conditions, with a low catalyst loading and without the need for an inert atmosphere.

First, (+)-limonene oxide **27** was selected as model substrate, as its rearrangement has already been investigated in the literature and both starting material and product, *i.e.* dihydrocarvone

^{*} The results of this chapter were previously published in: Löser P.S., Rauthe P., Meier M.A.R., Llevot A. 2020 Sustainable catalytic rearrangement of terpene-derived epoxides: towards bio-based biscarbonyl monomers. *Phil. Trans. R. Soc. A* **378**: 20190267.

19, are commercially available, which facilitated the reaction monitoring by GC. For determining suitable and synthetically useful reaction conditions, also in terms of sustainability, a deconvolution approach reported by Moran *et.al.*^[291] was applied. A general scheme for the deconvolution of limonene oxide **27** rearrangement is depicted in Figure 4.19. The strategy consists of adding a mixture of catalysts to the reaction medium and of screening different reaction parameters such as solvent, temperature etc. in the presence of this mixture. If any of the catalysts shows activity towards the substrate, the product will be detected by gas chromatography and the best solvent and temperature will be identified (Step 1). Then, a deconvolution is performed to identify the best catalyst of the mixture by separating the different catalysts into individual smaller batches (which can still contain more than one catalyst) to perform several independent reactions (Step 2). This procedure is repeated until the catalyst leading to the highest product yield is identified. By using such a deconvolution approach, the number of screening reactions is drastically reduced. As a possible competition between the different catalysts decreases during the deconvolution procedure and the system is continuously improved, the yields should increase in every step. However, an interaction between different catalysts should be avoided, as this might lead to false negative results. This issue was minimized by screening the complete catalyst mixture under two different reaction conditions (see Figure 4.19) and additionally by still considering all catalysts in the first round of deconvolution. Overall, this kind of deconvolution approach was chosen for this investigation, as the aim was the establishment of a robust and synthetically useful procedure that is applicable to a range of terpene substrates, and not for the development of quantitative models, which would result from, for instance, design of experiment approaches.

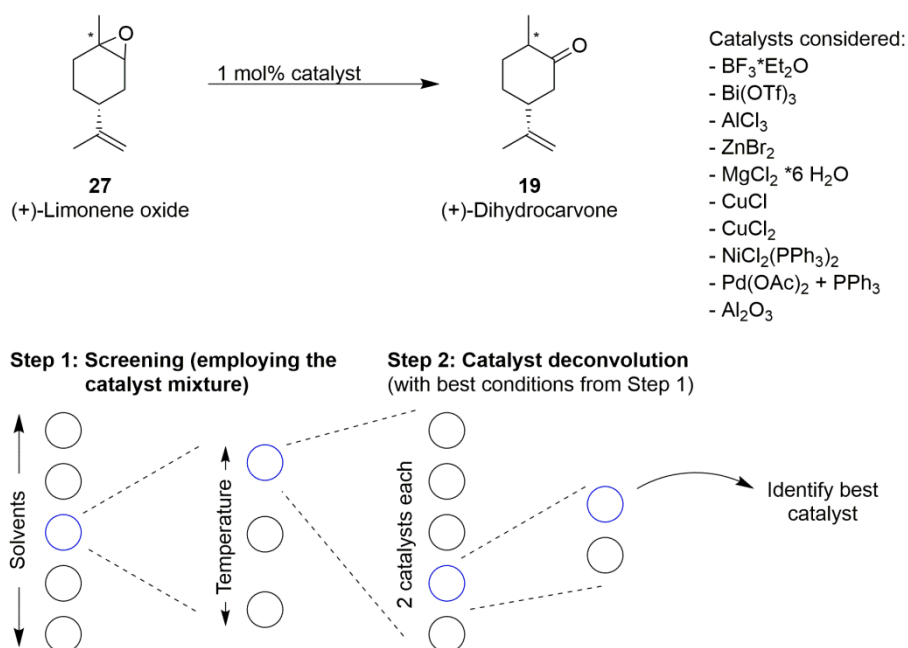


Figure 4.19 Rearrangement of (+)-limonene oxide **27** to dihydrocarvone **19** as model reaction to determine the best catalytic conditions applying a deconvolution approach.

In the study, the conversion of the starting material, the non-isolated yield and the selectivity towards the desired product were determined by GC. For the rearrangement of (+)-limonene oxide **27**, ten different catalysts that have already shown activity towards epoxide rearrangements in the literature were selected (Figure 4.19). In a first step, five different and typically applied solvents (dichloromethane, tetrahydrofuran, toluene, *tert*-butanol and diethyl ether) were screened with all ten catalysts present at a loading of 1 mol% each (Figure 4.20 (a) provides an overview of the obtained result). After 3 h, *tert*-butanol showed the highest limonene oxide **27** conversion (79.5%), but a low selectivity (26.9%) and therefore yield (21.4%) towards dihydrocarvone **19**. With a moderate conversion (57.6%), but a high dihydrocarvone **19** selectivity (68.2%), resulting in the highest yield (39.3%), tetrahydrofuran proved to be the best solvent and was used for the next reactions.

In the next step, the temperature was varied between 20, 40 and 60 °C (Figure 4.20 (b)). Only a small effect was observed on the product selectivity, which remained high in all cases (between 63.5% and 68.2%). However, a temperature of 20 °C was not sufficient to obtain a high limonene oxide **27** conversion. While similar conversions and yields were reached at 40 and 60 °C after 3 h of reaction time, a higher temperature seemed to favor the formation of side products at longer reaction times. Thus, also considering energy savings, a temperature of 40 °C was chosen as best temperature for further reactions.

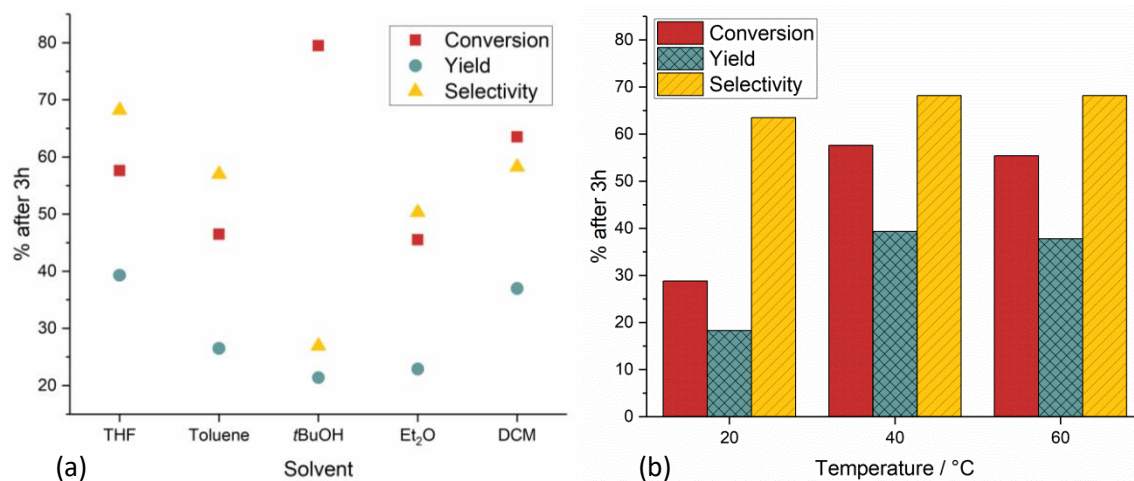


Figure 4.20 Effect of different solvents (at 40 °C) (a) and temperatures (in THF) (b) on the rearrangement of (+)-limonene oxide **27** to dihydrocarvone **19** in the presence of the catalyst mixture (1 mol% each).

For the determination of the best catalyst by deconvolution, next, the ten catalysts were divided into five batches with two catalysts each. From these five reactions, only the batch containing BF₃·Et₂O and Bi(OTf)₃ showed a good yield and conversion under these catalytic conditions (1 mol% loading) (Figure 4.21 (a)). After splitting these two catalysts for another screening cycle, only Bi(OTf)₃ showed good catalytic activity towards limonene oxide **27** conversion (Figure 4.21 (b)). After 3 h, a yield of 79.8% was achieved at full conversion of the starting material. Compared to the results reported in the literature, the conditions developed in this work with 1 mol% of Bi(OTf)₃ gave a slightly higher yield of dihydrocarvone **19**. Indeed, a higher yield was only reported for the use of heteropoly acids (82% yield of dihydrocarvone **19** with 0.1 mol% catalyst loading)^[169] as well as for the stoichiometric use of LiClO₄ (90% yield).^[168] The success of Bi(OTf)₃ is in good agreement with other results published in the literature, as the application of Bismuth was already shown to be efficient in several chemical transformations of terpenes, such as oxidation or acylation of alcohols, Wagner-Meerwein rearrangements and others,^[292] as well as in epoxide rearrangements of aromatic substrates.^[293] Moreover, other triflates have shown to be active in the Meinwald rearrangement, *e.g.* Erbium triflate.^[167]

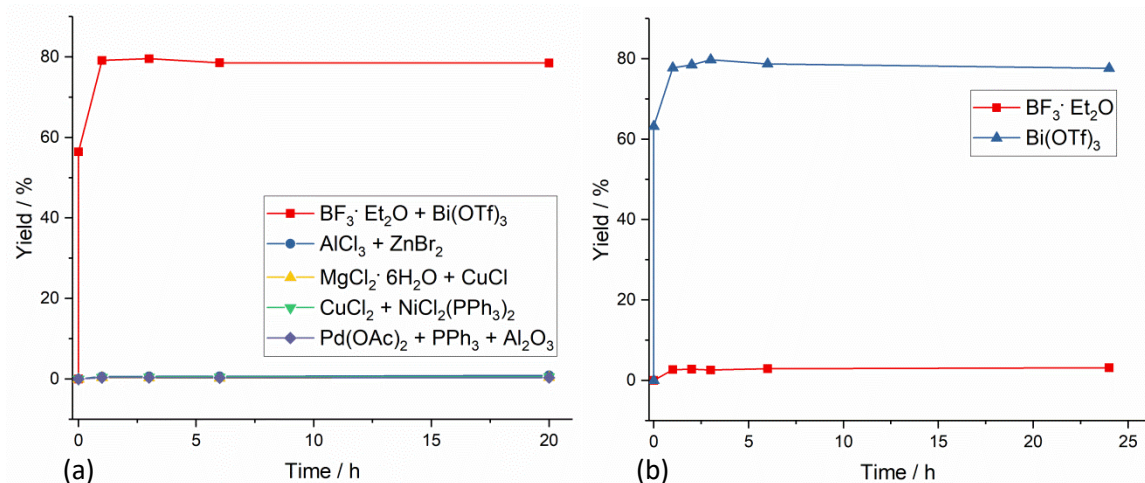
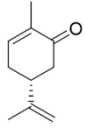
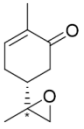
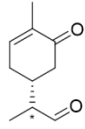
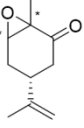
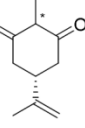
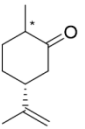
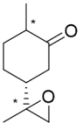
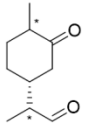
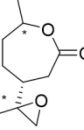
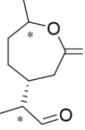
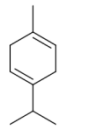
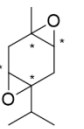
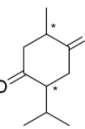
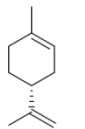
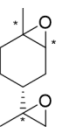
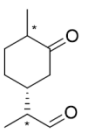


Figure 4.21 Yield of dihydrocarvone **19** obtained from the deconvolution of different catalyst combinations (a) and final deconvolution step with $\text{BF}_3 \cdot \text{Et}_2\text{O}$ and $\text{Bi}(\text{OTf})_3$ (b).

4.2.2.2 Substrate broadening

The optimized conditions identified from the deconvolution approach (1 mol% $\text{Bi}(\text{OTf})_3$, 0.2M THF and 40 °C) were applied to the other terpene-based epoxides described in chapter 4.2.1 in order to broaden the scope of substrates and increase the structural diversity. The obtained results are summarized in Table 4.4.

Table 4.4 Epoxidation of selected terpenes to mono- and bisepoxides and subsequent rearrangement to biscarbonyl compounds.

Starting Material	Epoxide (Isolated Yield)	Rearrangement Product	Reaction Time	GC Yield / % (Isolated Yield)
 22 (R)-(-)-Carvone	 23 (77%)	 28	1 h	92.3 (62)
	 24 (42%)	 29	4 h	0
 19 (+)-Dihydrocarvone	 20 (39%)	 30	1 min	90.6 ^a (60)
	 21 (58%)	 31	1 h	77.7 (30)
 25 γ-Terpinene	 26 (76%)	 32	1 h	34.5 ^a (29)
 33 (R)-(+)-Limonene	 34 (72%)	 30	2 h	57.6 ^b

General conditions rearrangement: 1 mol% Bi(OTf)₃, 0.2M THF, 40 °C.

^a 2 mol% Bi(OTf)₃; ^b 0.1 mol% Bi(OTf)₃, 0.2M in 2-MeTHF, 60 °C.

First, carvone-1,2-oxide **24**, differing from limonene oxide **27** only by the presence of a carbonyl in α-position to the epoxide, was tested as a substrate. However, when the rearrangement with Bi(OTf)₃ was attempted, no conversion of the starting material was observed. The replacement of Bi(OTf)₃ by different catalysts, such as FeCl₃, CuCl, MgCl₂·6H₂O, CuBr₂, ZnBr₂, BF₃·Et₂O, AlCl₃,

Al_2O_3 , InCl_3 , $\text{NiCl}_2(\text{PPh}_3)_2$ and LiBr , in another deconvolution approach did not result in a noticeable conversion of carvone-1,2-oxide **24** under the chosen reaction conditions (1 mol% catalyst, 40 °C, THF). An interaction of the epoxide with the adjacent carbonyl group seems to stabilize the molecule and, interestingly, fully impedes a Lewis acid-induced rearrangement.

To investigate the reactivity of the *exo*-cyclic epoxide **23**, the reaction conditions obtained from the deconvolution step were applied. Contrary to the result obtained with terpene **24**, the aldehyde **28** was obtained in a 92.3% yield in 1 h. After isolation, the product was analyzed by NMR spectroscopy (Figure 4.22). In the ^1H -NMR spectrum, the aldehyde (signal 9 at 9.65 ppm) and the double bond (signal 2 at 6.72 ppm) could be distinguished. Both expected diastereoisomers were observed in the ^{13}C -NMR spectrum, for example in two peaks of the carbonyl group (signal 6 at 198.92 and 198.89 ppm) or the double bond (signal 2 at 144.29 and 144.25 ppm). As the yield was already high, no further optimization was necessary for this substrate. In the literature, this rearrangement has only been reported using $\text{BF}_3\cdot\text{Et}_2\text{O}$ as catalyst: Engel *et al.* reported a yield of 70% with an amount of 1.30 eq of $\text{BF}_3\cdot\text{Et}_2\text{O}$,^[294] whereas Torosyan and Miftakhov reached an isolated yield of 88% using 10.0 eq of reactant.^[295] That high amount of toxic reagent strongly diminishes the sustainability of the reaction compared to the established procedure of this work.

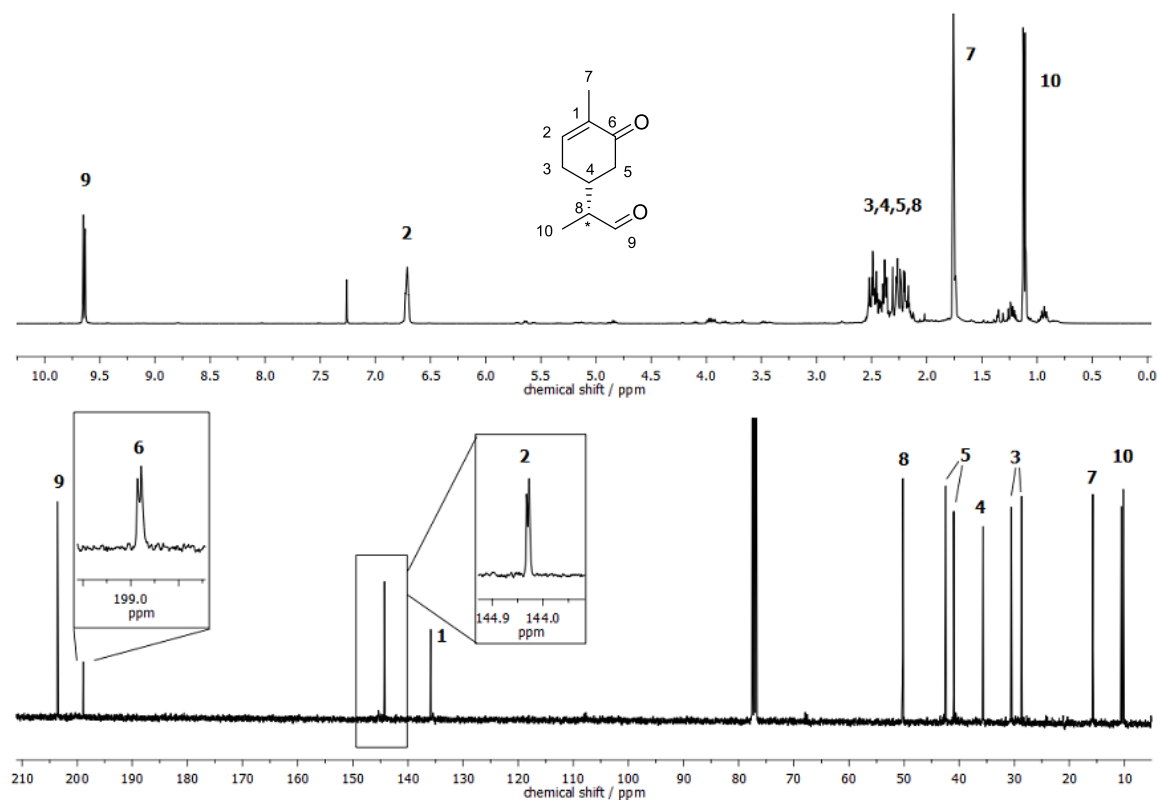


Figure 4.22 ^1H - and ^{13}C -NMR spectra of carvone-derived aldehyde **28** in CDCl_3 .

In a similar fashion, the rearrangement of (+)-dihydrocarvone oxide **20** under optimized conditions (1 mol% catalyst) resulted in a 77.8% yield in 1 h. The yield could not be improved by extending the reaction time, but reached 90.6% by increasing the catalyst loading to 2 mol%. In both reactions, the starting material was fully converted, thus, a higher catalyst loading was beneficial for enhancing the selectivity towards the desired product **30**. Figure 4.23 shows the NMR spectra of product **30**. In the ^1H -NMR spectrum, the aldehyde peak at 9.62 ppm (signal 9) was visible. As expected, all four possible diastereoisomers were observed in the ^{13}C -NMR spectrum. The rearrangement also took place with the epoxy lactone **21**. Applying the standard conditions, 77.7% yield of lactone aldehyde **31** was achieved.

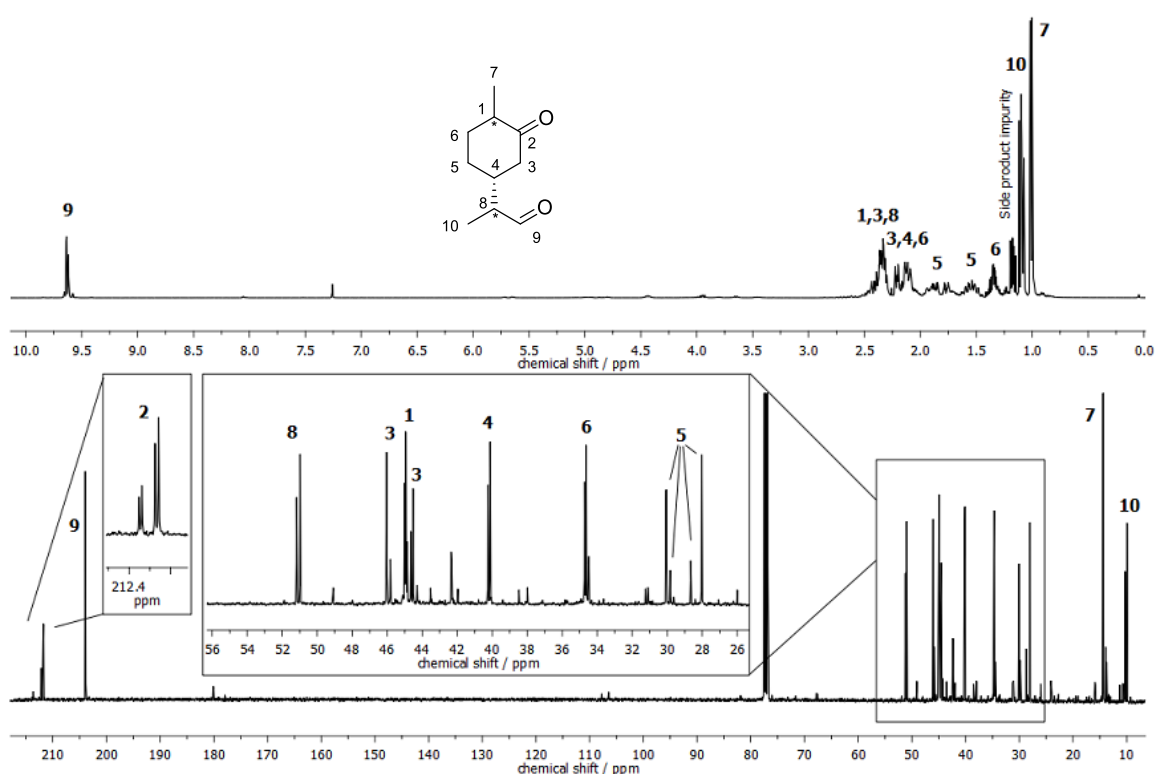


Figure 4.23 ^1H - and ^{13}C -NMR spectra of (+)-dihydrocarvone-based biscarbonyl **30** in CDCl_3 .

To diversify the biscarbonyl structures, also the reactivity of γ -terpinene dioxide **26** was studied. The desired product **32** was obtained in a yield of 25.1% after 3 h reaction time, with full conversion of the starting material, employing the standard conditions. An increase of the catalyst loading up to 2 mol% reduced the reaction time to 1 h for a slightly increased yield of 34.5%. Unfortunately, increasing the catalyst loading to 5 mol% did not further increase the product yield. This low yield could be explained by the formation of a by-product in a selectivity of around 36%. Indeed, an allylic alcohol with a double bond in conjugation with the carbonyl functionality (4-hydroxy-3-isopropyl-6-methylcyclohex-2-en-1-one) was identified as by-product

in the rearrangement step (see chapter 6.3.2 for analytical data). As this molecular structure constitutes an electronically stabilized isomer, this reaction pathway competes with the desired double rearrangement and prevents a higher selectivity. The ^1H and ^{13}C -NMR spectra of γ -terpinene derived biscarbonyl **32** are shown in Figure 4.24. The ^{13}C -NMR spectrum shows double signals of the two diastereoisomeric pairs of the product. Moreover, the peaks belonging to the carbonyl groups at 210 ppm (signals 2 and 5) are clearly visible. All signals could be assigned to the respective carbon atoms; however, assigning the respective isomers was not possible with the performed NMR experiments. Biscarbonyl **32** was obtained as a mixture of two diastereoisomers. As the reaction was carried out with only one diastereoisomer of γ -terpinene dioxide **26**, this confirmed the existence of an ionic intermediate in the reaction pathway, yielding all four possible reaction products. In the literature, biscarbonyl **32** has already been reported in 1964 and 1971, but was not synthesized from renewable resources or in a sustainable fashion. The authors used a pathway starting from 2,5-dimethoxy-*p*-cymene applying lithium and ammonia in ethanol^[296] or the oxidation of the corresponding diols *via* Jones oxidation applying highly toxic and carcinogenic chromium trioxide.^[297] The synthesis *via* a double rearrangement starting from bio-based γ -terpinene dioxide does not seem to have been reported before. By using renewable feedstock as well as catalytic and mild reaction conditions, this synthetic procedure represents a great improvement in terms of sustainability.

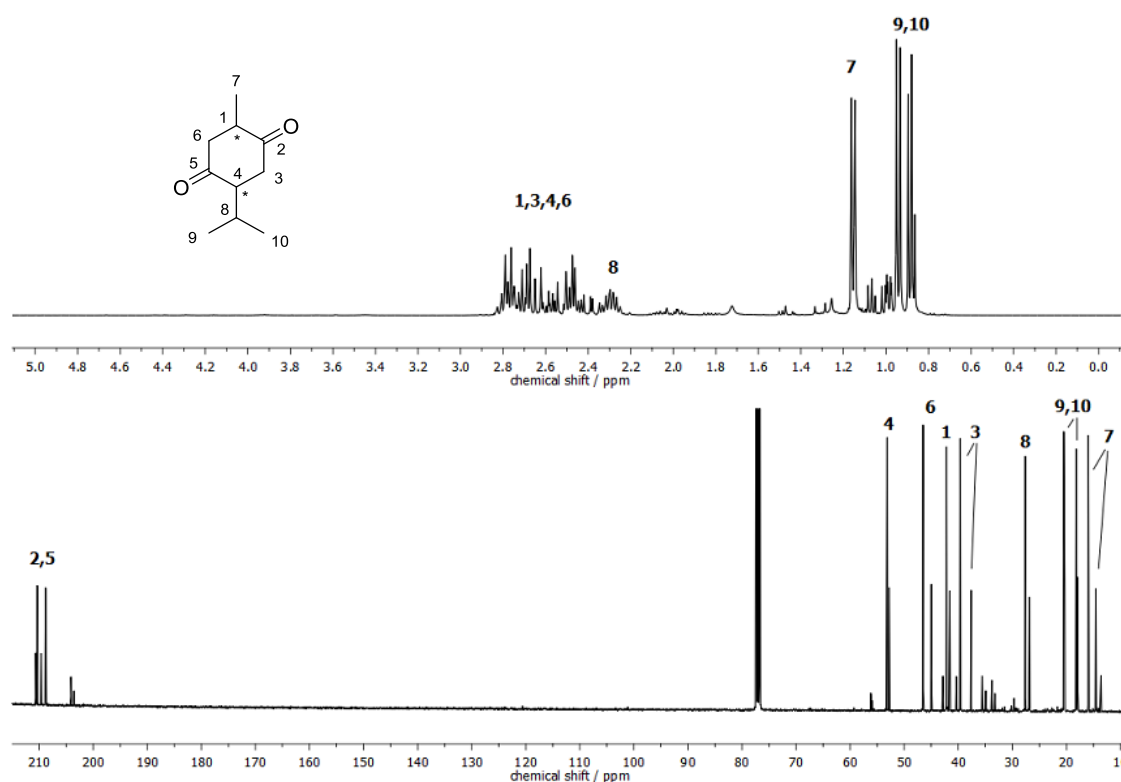


Figure 4.24 ^1H and ^{13}C spectra of γ -terpinene-derived biscarbonyl **32**.

As the rearrangement of limonene oxide **27** and dihydrocarvone oxide **20** proved to be successful, the direct double rearrangement of limonene dioxide **34** (mixture of four diastereoisomers, obtained by the epoxidation of (*R*)-(+)-limonene) was attempted to prepare biscarbonyl **30**, which can be a useful monomer precursor in polymer science. Following this strategy, a reaction step will be saved, since dihydrocarvone **19** is synthesized from either limonene or carvone.^[288] Moreover, as limonene is a cheap and abundant renewable resource, a direct synthesis from limonene dioxide represents a more desirable route. As a double rearrangement has to occur, possibly resulting in more side-products, a lower yield was expected. The biscarbonyl **30** was obtained in a yield of 51.7% after 0.5 h employing the optimized conditions of 1 mol% Bi(OTf)₃ at 40 °C in THF. An extension of the reaction time up to 5 h did not lead to an increased yield. Interestingly, a similar result was achieved with an even lower catalyst loading of 0.1 mol%, which further increases the sustainability of the process. In order to improve the yield for this reaction further, a screening with other catalysts and conditions was conducted. During the optimization process, it turned out that an elevated temperature of 60 °C as well as metal triflates can be an efficient combination for this particular epoxide rearrangement. Therefore, more triflates (In(OTf)₃, AgOTf, Yb(OTf)₃ and Zn(OTf)₂) were tested besides Bi(OTf)₃ in a subsequent reaction at 60 °C, in THF, with a low catalyst loading of 0.1 mol%, see Figure 4.25 (a).

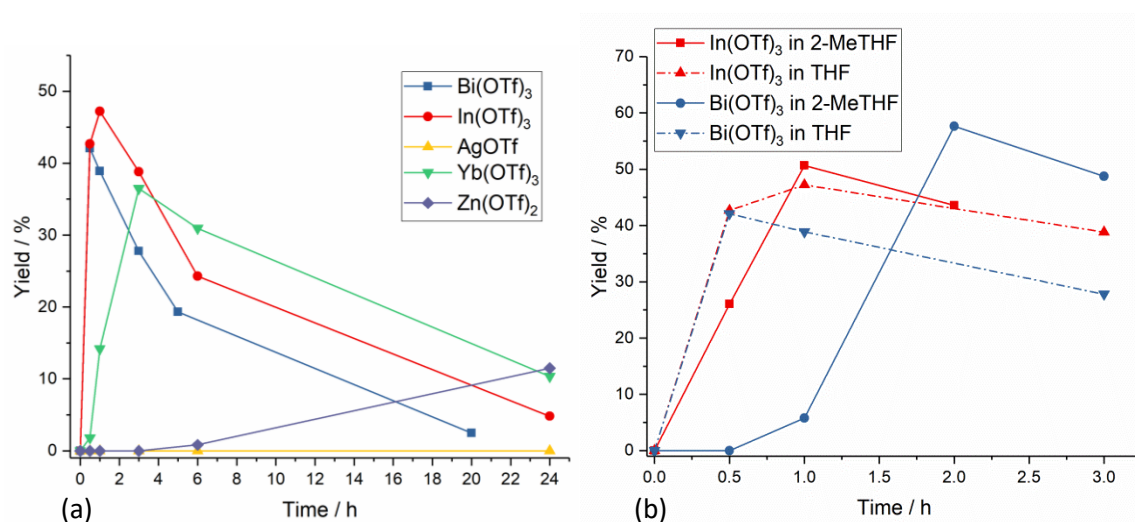


Figure 4.25 Rearrangement of limonene dioxide **33** to aldehyde **30**: Test of different catalysts (a) and solvents with In(OTf)₃ and Bi(OTf)₃ (b).

The best yield of 47.2% was reached after 1 h reaction time, using 0.1 mol% of In(OTf)₃. This result is slightly better than the value obtained for Bi(OTf)₃. Yb(OTf)₃ also showed an interesting catalytic activity towards limonene dioxide **34**, but with a lower yield of 36.5%. In the three cases, a short reaction time was beneficial, as the desired product **30** does degrade or isomerize

at prolonged reaction times under these conditions. However, under the chosen reaction conditions, silver triflate and zinc triflate exhibited a low catalytic activity. Moreover, to find a more sustainable substitute to THF, the reactions employing the most active catalysts, *i.e.* In(OTf)₃ and Bi(OTf)₃, were performed in 2-MeTHF (see Figure 4.25 (b)). In 2-MeTHF, Bi(OTf)₃ showed the highest yield of 57.6% after 2 h reaction time. Interestingly, in this and other reactions, for example with Zn(OTf)₂ in THF, a mono-rearranged product from the transformation of the *endo*-cyclic epoxide (epoxidized dihydrocarvone) could be detected as intermediate product, which was consumed shortly after being formed. Overall, besides improving the catalytic efficiency of the system, the use of 2-MeTHF also improves the sustainability of the process, as it is considered as a greener and less toxic alternative to THF that can be prepared from the lignocellulosic biomass.^{[298][299]} In the literature, the same reaction has been reported by Sudha and Sankararaman, who reached a yield of 70%; however, as mentioned before, lithium perchlorate was used in stoichiometric amounts.^[168]

In the course of the rearrangement study, all products were isolated and carefully characterized. Carvone-derived aldehyde **28** was obtained with an isolated yield of 72%, the dihydrocarvone-based aldehyde **30** in a yield of 60%, lactone **31** in a yield of 30% and biscarbonyl **32** with 29% isolated yield.

In conclusion, a deconvolution approach was successfully applied as a fast and easy method for screening catalysts and reaction conditions to obtain Bi(OTf)₃ as suitable catalyst, while using THF as solvent at moderate temperatures of 40 °C for the Meinwald rearrangement of terpene-based epoxides. The optimized conditions were subsequently applied to other terpene-based mono- and bisepoxides. Monoepoxides, such as carvone-8,9-oxide **23** and epoxidized dihydrocarvone **20**, rearranged with high yields to the desired aldehyde structures **28** and **30**. In a similar fashion, bisepoxides were rearranged. The bisepoxide derived from γ -terpinene containing two *endo*-cyclic epoxide groups **26** rearranged with moderate yields, whereas higher yields (up to 57.6%) were obtained for the rearrangement of limonene dioxide **34**. The reaction was optimized by replacing THF with the more sustainable alternative 2-MeTHF and decreasing the catalyst loading down to 0.1 mol%. Thus, the use of bismuth triflate in catalytic amounts gave access to valuable bio-based biscarbonyl structures, which are interesting molecules for the synthesis of renewable polymers.

4.2.3 Reductive Amination of Terpene-based Biscarbonyl Substrates

After the successful establishment of a reaction protocol for the rearrangement of terpene-based epoxides, the reductive amination of the formed biscarbonyls was investigated. In a first step, dihydrocarvone-based aldehyde **30** and carvone-based aldehyde **28** were examined. The applied reaction conditions are shown in Figure 4.26.

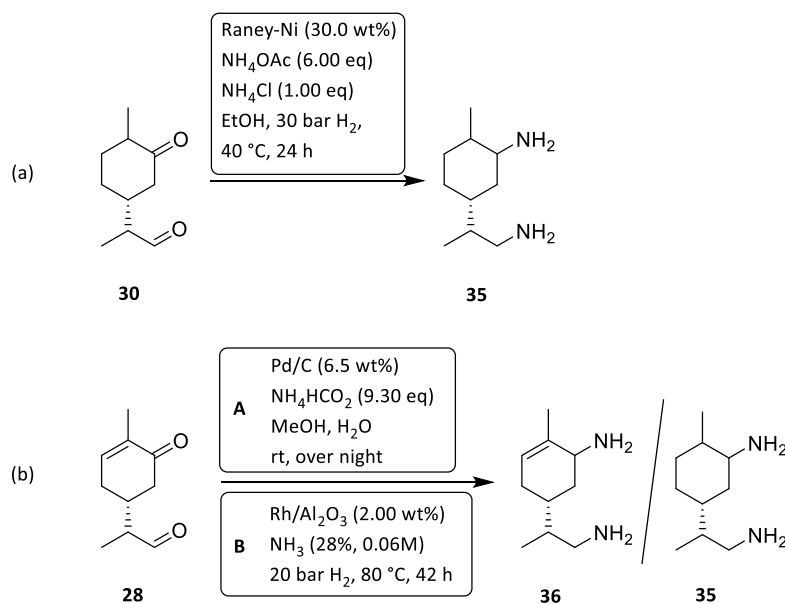


Figure 4.26 Reaction conditions for the reductive amination of dihydrocarvone aldehyde **30** (a) and carvone aldehyde **28** (b).

A reaction protocol using Raney-Ni, ammonium acetate and ammonium chloride that had been established before in the group on other substrates was used on the biscarbonyl **30**.^[300] The substrate (500 mg) was dissolved in 7.50 mL ethanol with 6.00 eq ammonium acetate and 1.00 eq ammonium chloride. Subsequently, 30.0 wt% Raney-Ni were added and the mixture was heated to 40 °C under 30 bar hydrogen pressure for 24 h (Figure 4.26 (a)). Then, the catalyst was filtered off, rinsed with dichloromethane and neutralized with hydrochloric acid. The organic phase was washed, dried over sodium sulfate and the solvent was removed under reduced pressure. The obtained crude product was analyzed *via* NMR spectroscopy. However, the spectrum revealed a multitude of proton and carbon signals, which did not allow for peak assignment. Therefore, precipitation of the amine using hydrogen chloride solution in dioxane as well as column chromatography were attempted in order to isolate the product. Unfortunately, it was not possible to isolate a product that could be properly analyzed. More research is needed to find a selective process for the conversion of aldehyde **30** into the desired diamine structure.

As alternative substrate, carvone-based aldehyde **28** was investigated.* Two synthesis protocols were tested, which are shown in Figure 4.26 (b). Protocol A uses palladium on activated charcoal as catalyst and ammonium formate as nitrogen source and was reported by Allegretti *et al.* as efficient tool for the reductive amination of sterically demanding substrates.^[301] For the reaction, 100 mg of **28** were dissolved in 1.50 mL methanol, and 9.30 eq ammonium formate and 173 μL H_2O were added. After the addition of 6.50 wt% Pd/C, the reaction mixture was stirred at room temperature overnight. The second protocol B follows a common reaction pathway *via* imine formation using ammonia solution, followed by hydrogenation with molecular hydrogen catalyzed by rhodium on alumina.^[302] For that, 100 mg of **28** were mixed with 10 mL ammonia solution (28%) and 2.00 wt% Rh/ Al_2O_3 . The mixture was heated to 80 °C under 20 bar hydrogen pressure for 42 h. Both reactions were monitored by gas-chromatography mass-spectrometry (GC-MS) measurements. The results are shown in Figure 4.27.

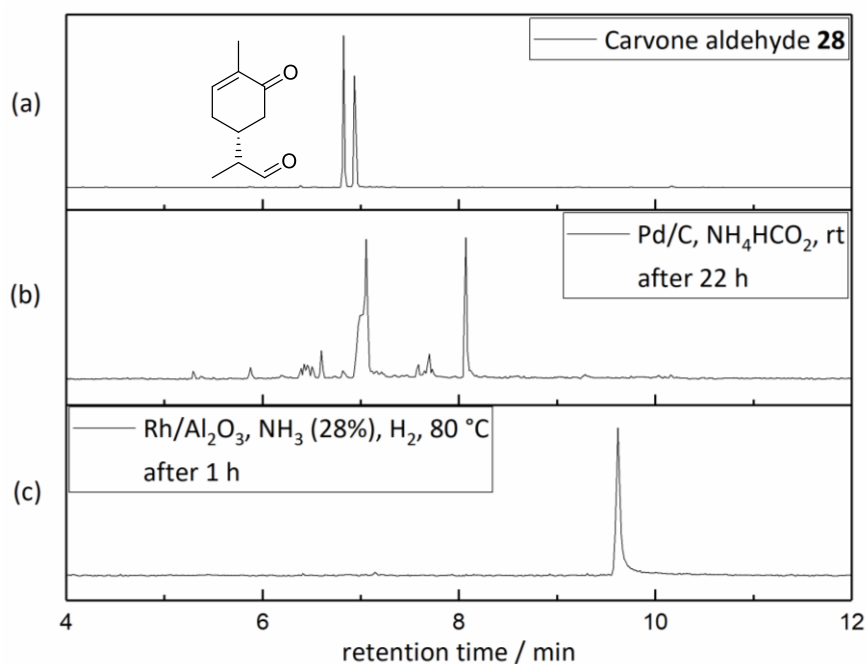


Figure 4.27 GC-MS chromatogram of the reductive amination of carvone-based aldehyde **28**: (a) starting material, (b) reaction applying Pd/C and ammonium formate after 22 h, (c) reaction applying Rh/ Al_2O_3 , ammonia and hydrogen after 1 h reaction time.

As can be seen in Figure 4.27 (b), in the reaction using Pd/C and ammonium formate, full conversion was achieved after 22 h reaction time and mainly two products were formed. During the aqueous work-up, different solubilities were observed, as the product with a retention time of around 7 min showed a higher solubility in the aqueous phase, while the product at around

* The reactions were carried out by Tim Trumler in the scope of his bachelor thesis “Synthesis of bio-based epoxides and diamines” under my co-supervision.

8 min was better soluble in the organic phase. However, also in this case, it was not possible to isolate and characterize the products. In the Rhodium-catalyzed reaction (Figure 4.27 (c)), full conversion was achieved after one hour reaction time. One product was formed selectively according to the GC-MS chromatogram. As the product was not soluble in the organic phase, the water phase was evaporated and the product was analyzed by NMR spectroscopy. In contrast to the GC-MS chromatogram, a diastereomeric pair and one additional molecule were observed. Even if clear structural assignment of the product mixture was not possible, some conclusions were gathered from the spectra. During the reaction, the aldehyde group and the double bond were completely transformed, as no signals were visible in the respective regions in the $^1\text{H-NMR}$ spectrum. Signals at 178 and 179 ppm in the $^{13}\text{C-NMR}$ spectrum indicated that the carbonyl group remained unreacted. Therefore, the desired structures **35** or **36** were most likely not formed during the reaction. However, also for aldehyde **28**, more research is needed to clearly identify the products in order to find suitable reaction conditions for the reductive amination.

The reductive amination of thymoquinone **37** was tested as an alternative. Thymoquinone is a natural substance and can be obtained from the essential oils of plants such as *Nigella sativa*.^[303] It can also be obtained through the oxidation of the cheaper and more readily available thymol and carvacrol, which can be found in oregano essential oil.^[304] The oxidation can for example be carried out using molecular oxygen as sustainable and cheap oxidant, catalyzed by a cobalt-salen complex.^[305] The reaction conditions applied during the reductive amination of thymoquinone are depicted in Figure 4.28.

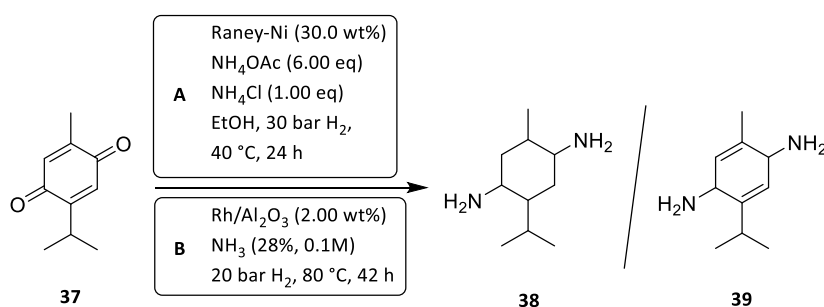


Figure 4.28 Reaction conditions for the reductive amination of thymoquinone **37**.

The reductive amination using Raney-Ni, ammonium acetate, ammonium chloride and molecular hydrogen already used for the reductive amination of dihydrocarvone aldehyde **30** was tested first (route A). Thymoquinone (500 mg) was dissolved in 8.00 mL ethanol with 6.00 eq ammonium acetate and 1.00 eq ammonium chloride, and then 30.0 wt% Raney-Ni was added. The mixture was stirred at 40 °C under 30 bar hydrogen pressure for 24 h. After filtering off the catalyst and rinsing with dichloromethane, the organic phase was washed with water, dried over

sodium sulfate and the solvent was removed under reduced pressure. The crude product was analyzed with GC-MS (Figure 4.29 (b)). Besides the starting material, mainly one peak is present in the chromatogram. After isolation *via* column chromatography, the product was identified as the corresponding aromatic diol. The formation of this product could be explained by the hydrogenation of one double bond, followed by a keto-enol tautomerism of the carbonyl groups. In addition, the imine formation could be hindered by the existence of the Michael systems, which alter the electrophilic character of the carbonyl group, favoring a nucleophilic attack of the double bond. Therefore, a second procedure (Figure 4.28 B) applying Rhodium on activated alumina as catalyst, aqueous ammonia as nitrogen source and molecular hydrogen was tested.* After mixing all reactants (200 mg thymoquinone, 2.00 wt% Rh/Al₂O₃, 10.0 mL NH₃ (28%)), the mixture was heated to 80 °C under 20 bar hydrogen pressure for 42 h. The reaction was followed again by GC-MS, the results are shown in Figure 4.29 (c) - (e).

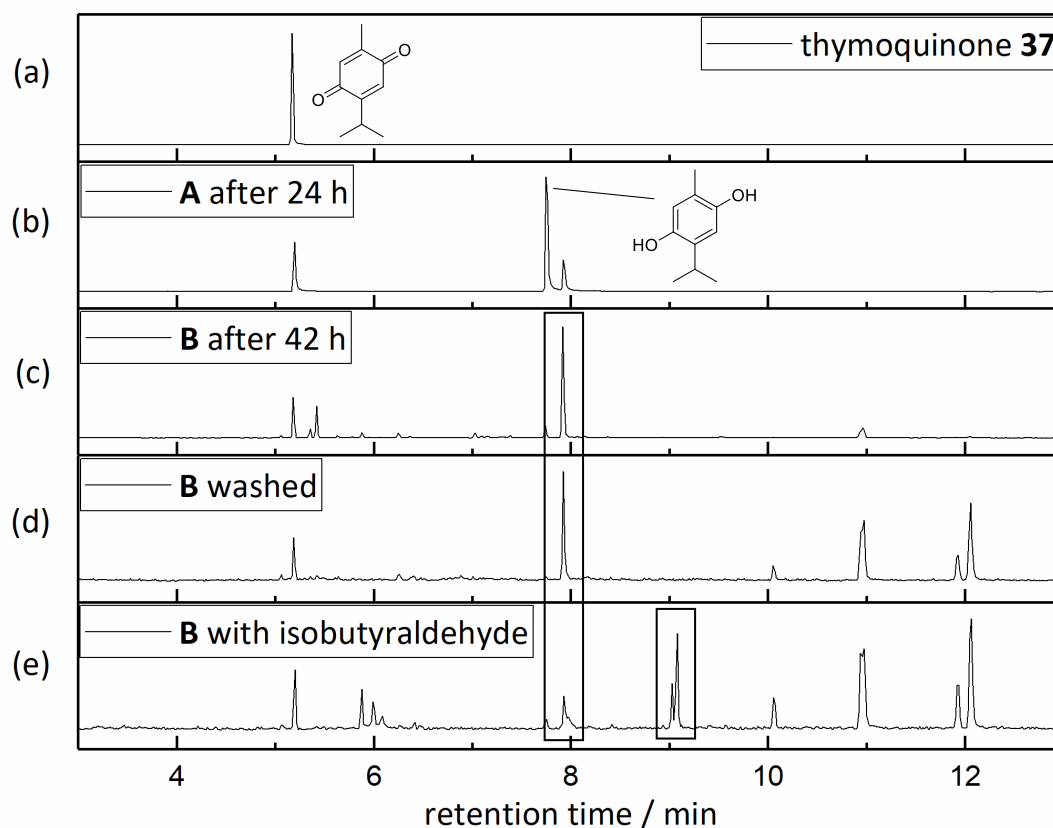


Figure 4.29 GC-MS chromatogram of the reductive amination of thymoquinone **37** shown in Figure 4.28: (a) starting material, (b) reaction applying Raney-Ni, NH₄OAc, NH₄Cl and H₂ (30 bar) after 24 h, (c) reaction applying Rh/Al₂O₃, ammonia and hydrogen (20 bar) after 42 h reaction time, (d) products after washing, (e) product mixture after the addition of isobutyraldehyde.

* The reaction was carried out by Tim Trumler in the scope of his bachelor thesis “Synthesis of bio-based epoxides and diamines” under my co-supervision.

After 42 h, almost full conversion was reached and a different selectivity compared to approach A was observed. Besides very small amounts of the aromatic diol, mainly one product with a similar retention time of around 8 min was formed. After aqueous work-up, the decreased intensity in the chromatogram compared to the other peaks showed that the product was at least partly soluble in water and was washed out during the work-up. To gain more information about the product and to confirm whether an amine had been formed, 3.00 eq isobutyraldehyde were added for imine formation with the possibly formed amine product. In the GC-MS chromatogram, a reduction of the product peak intensity and the formation of a new structure with a retention time of around 9 min were observed (Figure 4.29 (e)). According to the mass spectrum, the newly formed product exhibited a mass of 219 g/mol, which correlates to the existence of a mono-aminated product forming an imine with one isobutyraldehyde molecule. This result indicates that a mono-amination occurred. However, further research is required to identify all the products and to improve the reaction procedure to form the diamine.

Different reaction protocols for the reductive amination of different terpene-based biscarbonyls were investigated. The procedures showed varying selectivities towards the substrates; but the formation of the desired diamines was not observed and this part requires a deeper investigation. The reaction applying Rhodium on activated alumina showed promising results and should be tested with other substrates, *e.g.* dihydrocarvone aldehyde **30** or γ -terpinene-based biscarbonyl **32**. As the reductive amination proved difficult, the aminolysis of epoxides with ammonia was explored as alternative reaction pathway to synthesize terpene-based diamines. The results of this study are discussed in the following chapter.

4.2.4 Aminolysis of Terpene-based Bisepoxides

The ring-opening reaction of epoxides with ammonia as nucleophile was investigated for the synthesis of primary amines as alternative to the reductive amination of carbonyl groups for the synthesis of primary amines. This approach was reported in 2016 by Blattmann and Mülhaupt on limonene dioxide as bio-based substrate.^[203] The authors used aqueous ammonia solution in ethanol at 100 °C. After 15 h reaction time, one diastereoisomer was isolated by recrystallization from acetonitrile. To obtain a deeper insight into the reaction and the products formed during the ring-opening, the reaction was analyzed in detail in this work. The reaction scheme is shown in Figure 4.30. Instead of aqueous ammonia, a methanolic ammonia solution was used to facilitate the work-up, which consists of evaporating all solvents and reactants after the indicated reaction time. The reaction time was increased to 24 h to ensure full conversion of the starting material.

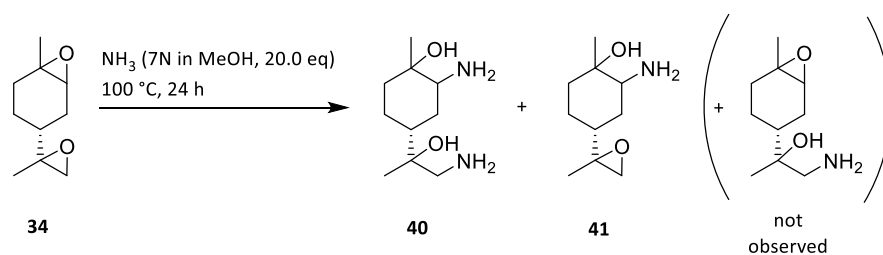


Figure 4.30 Reaction conditions for the aminolysis of limonene dioxide using ammonia (adapted from ^[203]).

After completion of the reaction, the crude product mixture was analyzed *via* GC (Figure 4.31 (a)). The chromatogram showed full conversion of the starting material as well as the formation of two products with similar retention times at around 7.7 min and a third product at around 9.9 min. As indicated in the literature, a recrystallization from acetonitrile was performed. At the same time, column chromatography was performed with a separate batch to isolate the products observed in the GC chromatogram. The GC chromatograms of the three obtained fractions are shown in Figure 4.31 (b) – (d).

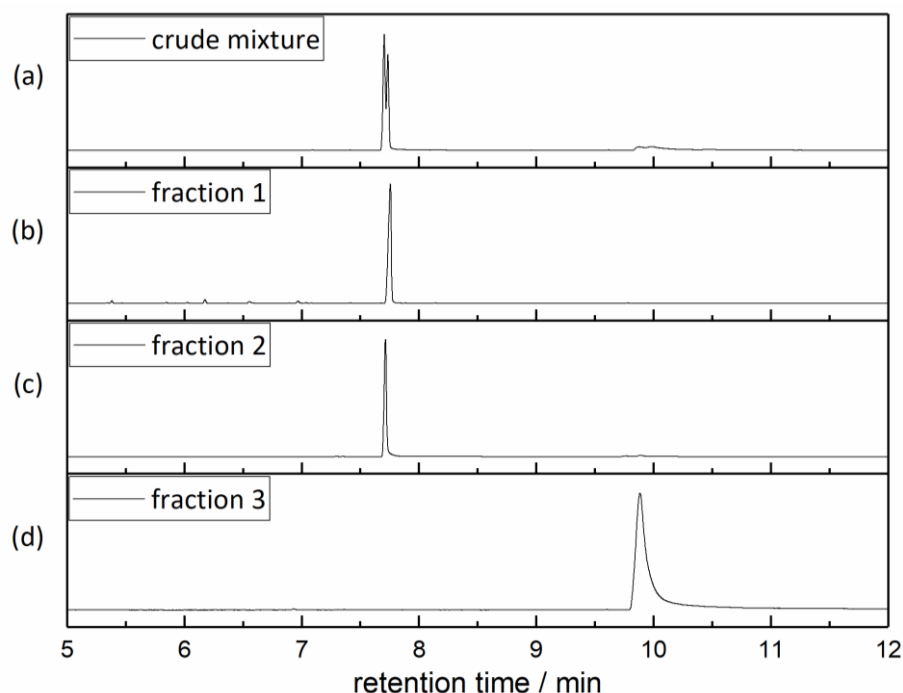


Figure 4.31 GC chromatograms of the aminolysis of limonene dioxide **34** before and after column chromatography: (a) crude product mixture, (b) fraction 1, (c) fraction 2, (d) fraction 3.

As can be seen in Figure 4.31, fraction 1 and 2 correspond to the double peak observed in the crude reaction mixture. Fraction 2 also corresponds to the product isolated during the recrystallization procedure. Fraction 3 was obtained in an isolated yield of 47% after column chromatography. All three fractions were thoroughly analyzed *via* 2D NMR spectroscopy and

mass spectrometry. Fractions 1 (27% yield) and fraction 2 (25% yield) were identified as mono-reacted products, whereas fraction 3 (47% yield) was identified as the desired diamine structure **40** (full analytical data can be found in chapter 6.3.2). The ^{13}C -NMR spectra of all fractions are depicted in Figure 4.32. Fractions 1 and 2 (Figure 4.32 (a) and (b)) show a similar ^{13}C -spectrum compared to fraction 3 (Figure 4.32 (c)). The carbon signals 1 and 2, belonging to the former *endo*-cyclic epoxide, show a similar chemical shift in all three fractions. In contrast, the signals 8 and 9, belonging to the former *exo*-cyclic epoxide, exhibit a different chemical shift in fraction 3 compared to fraction 1 and 2. In the spectrum of fraction 3, double peaks indicate the presence of two stereoisomers. Furthermore, all signals could be assigned, for instance signal 8 at 75.19 and 74.99 ppm or signal 1 at 72.12 and 72.08 ppm. As a result, fractions 1 and 2 were identified as two isomers of the mono-reacted product **41**, where only the *endo*-cyclic epoxide was converted to the respective aminoalcohol.

In a next step, reaching full conversion towards the diamine was attempted by increasing the reaction time to four days; however, no change in the product composition was achieved. As fraction 3 contained two diastereoisomers, whereas fractions 1 and 2 each consisted of a single isomer, it can be assumed that from the four isomers of limonene dioxide, only two diastereoisomers react to the desired product **40**. In the other two isomers, the reaction of the *exo*-cyclic epoxide group seems to be sterically inhibited, which prevents the reaction to reach full conversion of all epoxide groups. This is an interesting selectivity and can also be synthetically useful. However, the exact stereoisomers could not be assigned with the performed NMR measurements.

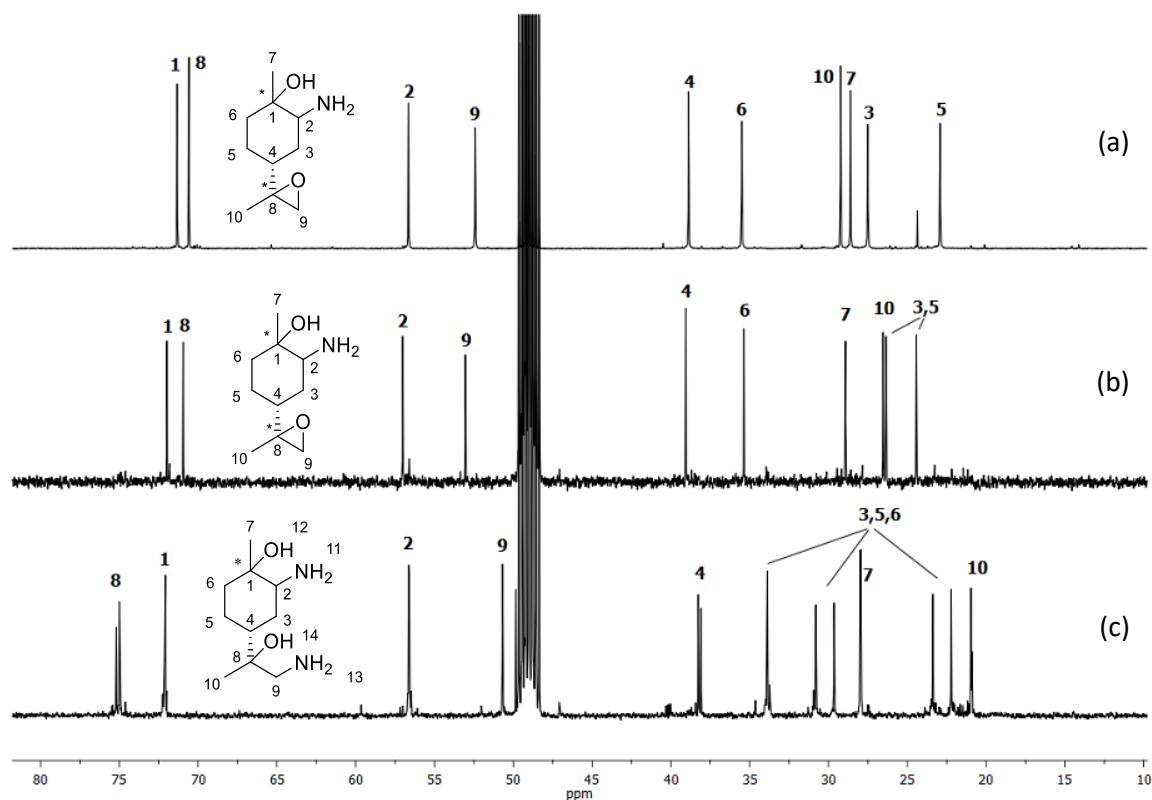


Figure 4.32 ^{13}C -NMR spectra of the aminolysis of limonene dioxide after column chromatography: (a) fraction 1, (b) fraction 2, (c) fraction 3.

To further confirm the obtained results, benzylation of the amine and hydroxyl groups was attempted as indirect quantification method (Figure 4.33). Fractions 2 and 3 as well as the crude product were individually mixed with 20.0 eq benzyl bromide and few milliliters dimethyl formamide (DMF). The mixtures were stirred at room temperature for 24 h. Subsequently, unreacted benzyl bromide and DMF were removed under high vacuum at 100 °C and the products were analyzed *via* NMR spectroscopy. The spectra can be found in chapter 6.3.2. The values obtained for the integration of the aromatic proton signals are listed in Table 4.5.

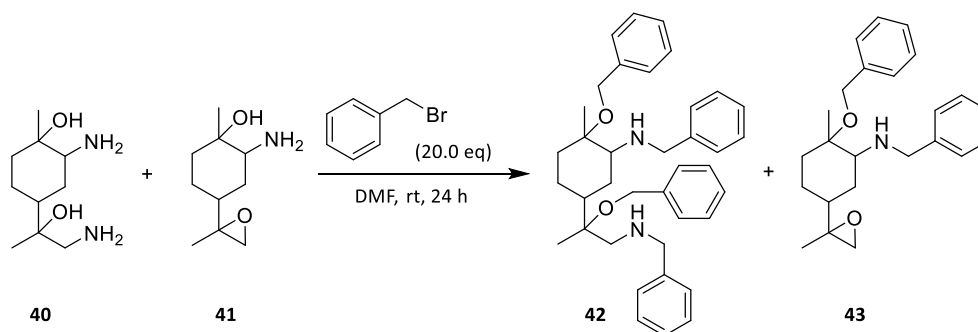


Figure 4.33 Benzylation of limonene dioxide-derived aminoalcohols as tool to confirm the structural assignment derived from NMR spectra.

Table 4.5 Results for the benzylation of limonene-dioxide-derived aminoalcohols.

Entry	Sample	Σ aromatic protons ^a	Product formed
1	Fraction 2	9.68	43
2	Fraction 3	19.3	42
3	Crude mixture	14.7	42 + 43 (50:50)

^a Signals were normalized to the methyl group signals between 1.15 and 1.40 ppm.

The benzylation of fraction 2 (Table 4.5, entry 1) led to the incorporation of two benzyl groups, as indicated by the integral of 9.68 aromatic protons. In contrast, in the benzylation of fraction 3, 19.3 aromatic protons were detected, correlating to a full conversion of both epoxide groups. When the crude product mixture was subjected to benzylation, a value of 14.7 protons was achieved, which indicates a 50:50 mixture of mono- and bisfunctional products. The data obtained by benzylation thus confirms the results obtained by NMR spectroscopy. As a further proof, in mass spectrometry measurements of fraction 1-3, high resolution masses of the three products were found. Thus, the post-modification with benzyl bromide to determine the number of alcohol and amine groups is useful for sterically hindered structure motifs like the terpene derivatives **40** and **41**. A transfer to sterically less demanding structures might lead to an over-benzylation of the amine groups, leading to a false number of functional groups.

To broaden the substrate scope of the aminolysis reaction, 1,4-cyclohexane dioxide **45** as another potentially bio-based bisepoxide was examined. Substrate **45** was synthesized from 1,4-cyclohexadiene, which can be obtained from plant oils *via* olefin metathesis reaction.^[306] The epoxidation was carried out using Oxone[®], sodium bicarbonate and acetone analogously to the epoxidation of terpenes described in chapter 4.2.1. After epoxidation, the crude product mixture was purified by column chromatography for structural analysis. The *trans*-isomer **45a** was identified as main reaction product (80.8% GC yield after 1 h), whereas smaller amounts of the *cis*-isomer **45b** were formed (17.3% GC yield). Detailed analytic information is given in chapter 6.3.2. Subsequently, both stereoisomers were subjected to the ring-opening reaction applying ammonia solution (Figure 4.34).

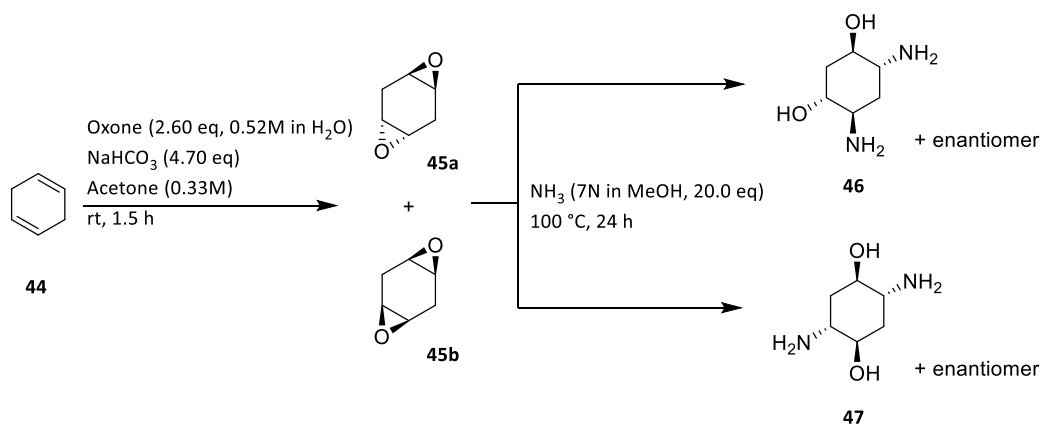


Figure 4.34 Epoxidation of 1,4-cyclohexadiene **44** applying Oxone®, sodium bicarbonate and acetone and subsequent aminolysis with methanolic ammonia solution to the two regioisomeric diamines **46** and **47**.

The dioxides **45a** and **45b** were heated to 100 °C for 24 h in methanolic ammonia solution. Then, the solvent was removed and the products were analyzed *via* NMR spectroscopy. The obtained ¹³C-NMR spectra are shown in Figure 4.35.

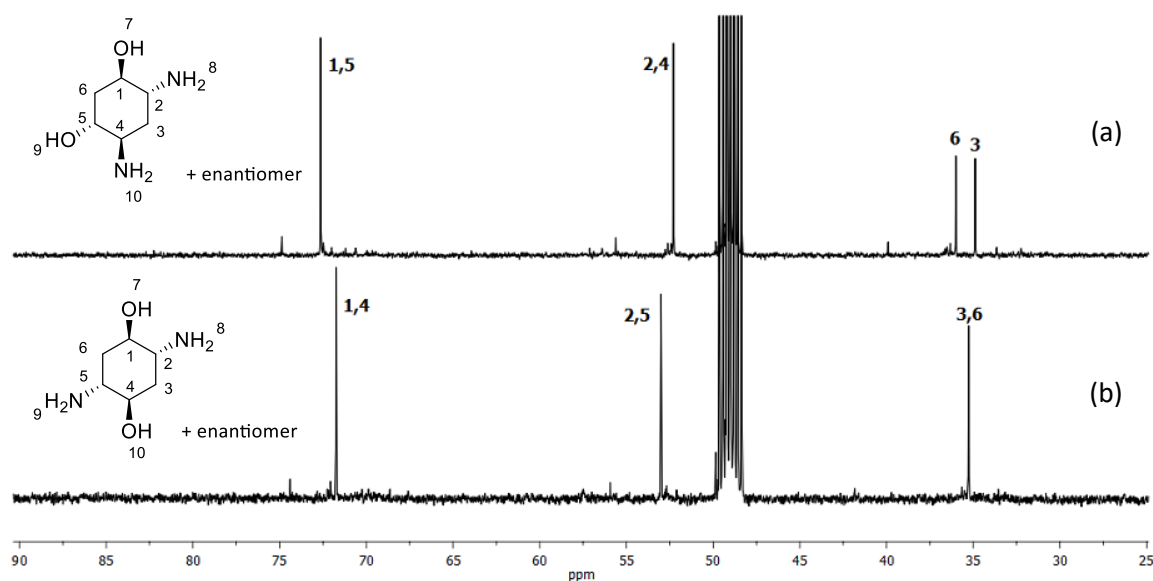


Figure 4.35 ¹³C-NMR spectra of the aminolysis of the two 1,4-cyclohexane dioxide diastereoisomers: (a) product of the *trans*-isomer, (b) product of the *cis*-isomer.

Figure 4.35 (a) shows the ¹³C-NMR spectrum of the product obtained from the *trans*-isomer **45a**. In both cases, only one regioisomer was formed during the ring-opening reaction. Due to the existence of two separate signals 3 and 6, the product was identified as 4,6-diaminocyclohexane-1,3-diol **46**. The ring-opening of the *cis*-isomer **45b** led to a different regioselectivity, as only one signal is observed for the atoms 3 and 6 in the ¹³C-NMR spectrum (Figure 4.35 (b)). This indicates the formation of 2,5-diaminocyclohexane-1,4-diol **47**, which exhibits the same chemical periphery for both carbon atoms 3 and 6. The ring-opening of *cis*- and *trans*-1,4-cyclohexadiene

dioxide with different nucleophiles has already been reported in literature. When nucleophiles such as aqueous acids or bases, hydrogen bromide or sodium bromide were used, the same regioselectivity as with ammonia solution was observed.^[307] The observed regioselectivity arises from an axial attack of the ammonia to the first epoxide group. Subsequently, the structure inverts to an all-equatorial conformation, which is then ring-opened by an axial attack of another ammonia nucleophile. The synthesis of aminoalcohols from 1,4-cyclohexane dioxide has already been reported.^[308] However, the ring-opening was carried out using sodium azide and *p*-TSA, followed by hydrogenation to the respective amine. Compared to this procedure, the ring-opening with ammonia solution constitutes a more sustainable pathway for the synthesis of aminoalcohols **46** and **47**.

In summary, the aminolysis of bisepoxides using ammonia solution represents an easy and efficient tool for the synthesis of diamine hardeners. In the case of limonene dioxide **34**, only two of the four diastereoisomers were converted to the desired product. Only the mono-reacted products were obtained from the other two isomers. The second ring-opening seems to be sterically inhibited and could also not be achieved by a prolonged reaction time. However, in the case of 1,4-cyclohexane dioxide **45**, full conversion was achieved. Substrates **45a** and **45b** showed different regioselectivities during the ring-opening reaction, leading to an amine functionalization in 1,3- and 1,4-position, respectively. Nevertheless, both products can be used as hardeners in epoxy resins, so a separation of the isomers is not necessary after the initial epoxidation step. In terms of sustainability, the aminolysis is relevant, as it does not need additional purification steps.

In conclusion, terpenes were investigated for the synthesis of bio-based amine hardeners in epoxy resins. In a first step, different literature-known procedures were applied for the epoxidation of dihydrocarvone, carvone and γ -terpinene. Especially Oxone[®] proved to be a good oxidant for the selective and efficient epoxidation of the sterically demanding terpene substrates. Next, the Meinwald rearrangement of the synthesized epoxides to the corresponding carbonyl groups was explored. Bismuth triflate showed good selectivities and yields, thus enabling an easy synthesis of bio-based biscarbonyl monomers. The reductive amination of the biscarbonyl substrates proved to be challenging. More research is needed to further exploit this reaction path, for instance by using other catalysts, amine sources or reduction protocols. Therefore, the aminolysis of bisepoxides with ammonia was investigated as sustainable alternative for the synthesis of diamines. Diamines based on limonene dioxide and 1,4-cyclohexane dioxide were synthesized using that procedure, which could in a next step be transferred to other bio-based bisepoxides, for instance γ -terpinene dioxide.

4.3 Polymerization of Bis-allyl Ether Monomers

4.3.1 Synthesis of Linear Polymers

The reactivity of the coupled monomers was first investigated for the synthesis of linear polymers. The linear polymers would be useful models to study the degradation of the cleavable monomers. Starting from the coupled bis-allyl ether monomers described in chapter 4.1.2, polymerization *via* acyclic diene metathesis (ADMET) as well as thiol-ene was attempted (Figure 4.36). For the ADMET polymerization (Figure 4.36, top), 200 mg AVA carbonate **10** and 3.10 mg *p*-benzoquinone (6.00 mol%) were dissolved in 300-400 μ L Polarclean. The mixture was heated to 80 °C until the dispersion became homogeneous. Subsequently, 6.10 mg Hoveyda-Grubbs II (HG II, 2 mol%) or 5.80 mg Hoveyda-Grubbs I (HG I, 2 mol%) catalyst were added. The solution was stirred at 80 °C under reduced pressure (50 mbar) for 5 h. The resulting crude product was analyzed *via* size exclusion chromatography (SEC). Unfortunately, with both catalysts, only low molecular weight oligomers were obtained ($M_n < 2,000$ Da, SEC system A). These results are in accordance with literature, as allyl ethers have been reported to exhibit a low reactivity in ADMET polymerizations.^[98] Therefore, thiol-ene polymerization was investigated as alternative route for the polymerization of bis-allyl ether **10** (Figure 4.36, bottom).

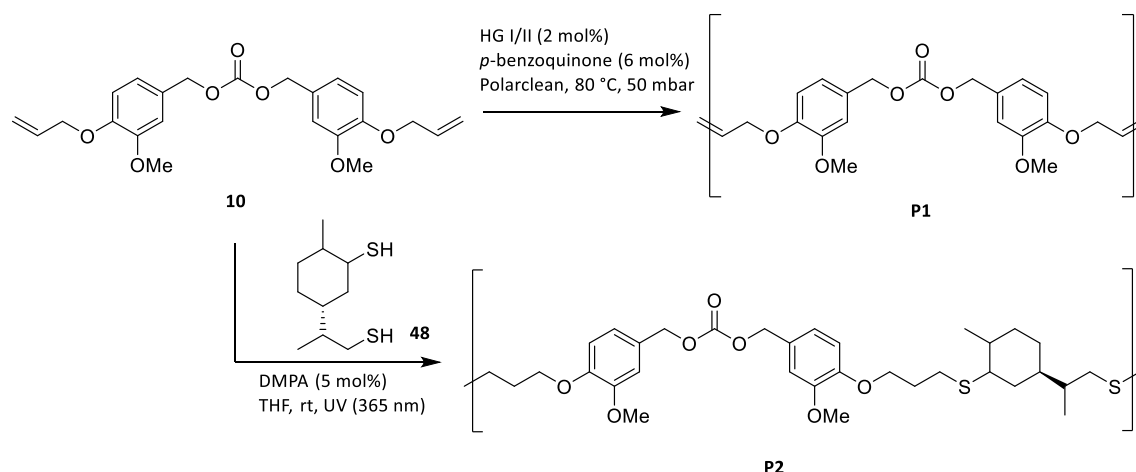


Figure 4.36 Synthesis of linear polymers from AVA carbonate **10** *via* ADMET and thiol-ene polymerization with the limonene-based dithiol **48**.

For the formation of linear thiol-ene polymers **P2**, the bio-based dithiol **48** was synthesized from limonene as starting material, according to a literature procedure.^[195] (*R*)-(+)-Limonene was thus reacted with thioacetic acid and the formed thioester groups were subsequently cleaved

applying TBD and methanol. After column chromatography, limonene dithiol **48** was obtained in a yield of 98.9% (the detailed synthesis procedure is listed in chapter 6.3.3). The synthesized dithiol was subsequently used in the thiol-ene polymerization of diene **10**. The dithiol was used in a slight excess to compensate for the possible formation of disulfide linkages during the polymerization. Polymerizations were carried out by mixing substrates **10** and **48** in 250 μL THF in a round bottom flask. The initiator 2,2-dimethoxy-2-phenylacetophenone (DMPA, 5 mol%) was added and the reaction was stirred at room temperature under UV irradiation (365 nm) for 6-8 h. Afterwards, the crude mixture was precipitated in cold MeOH and the obtained products were analyzed by SEC measurements. Different ratios, *i.e.* 1.05, 1.07 and 1.10 eq of limonene dithiol **48** compared to the diene **10** were tested. Figure 4.37 (a) shows the hexafluoroisopropanol (HFIP)-SEC traces (SEC system C) of all three experiments compared to the starting material **10**.

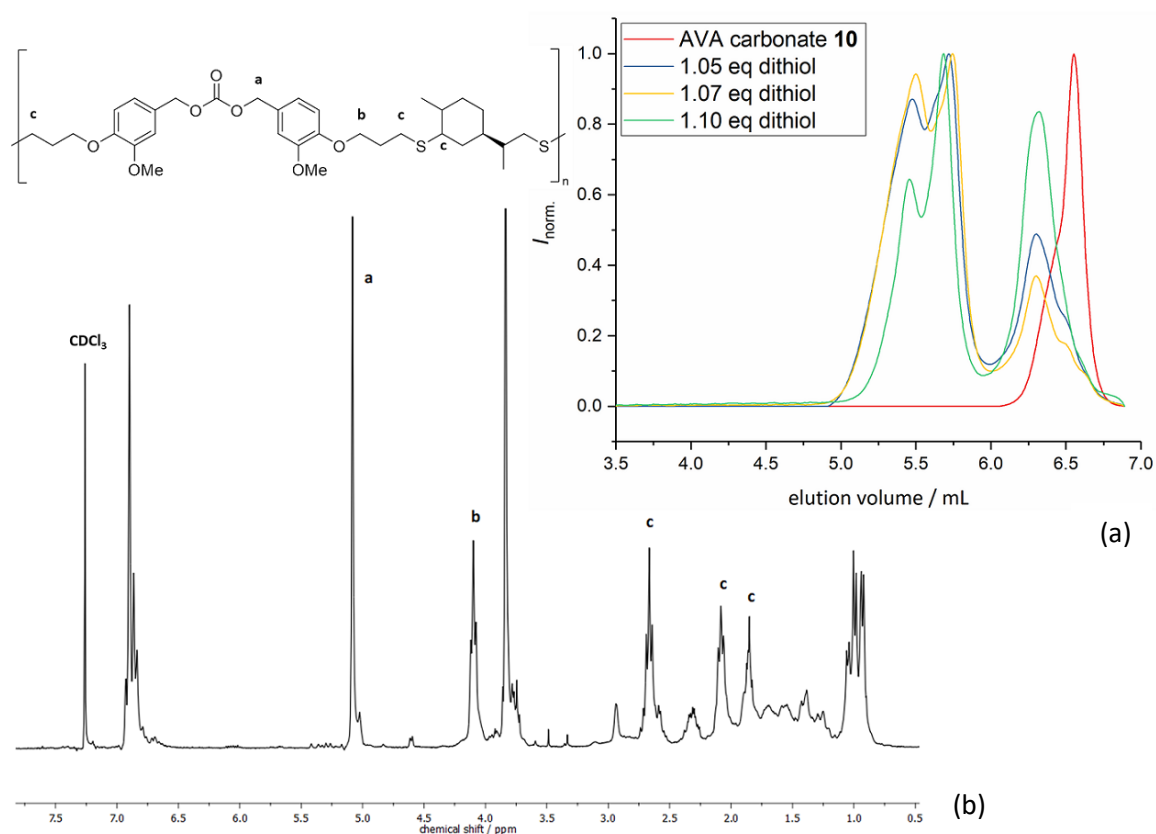


Figure 4.37 HFIP-SEC traces for the thiol-ene polymerization of AVA carbonate **10** and limonene-based dithiol **48** (a) (SEC system C), $^1\text{H-NMR}$ spectrum of **P2** with 1.07 eq dithiol **48** (b).

As depicted in Figure 4.37 (a), two populations were observed for all three polymerizations. Besides some low molecular weight products, oligomeric species with a molecular weight of $M_n = 4,000\text{-}6,000$ Da were formed. Comparing the different amounts of dithiol, no trend was

visible regarding the molecular weight of the obtained oligomers. An excess of 1.07 eq dithiol resulted in the lowest proportion of low-molecular by-products. Therefore, the oligomers obtained in the reaction with 1.07 eq dithiol ($M_n = 6,000$ Da, $\mathcal{D} = 1.35$) were analyzed by NMR spectroscopy. The $^1\text{H-NMR}$ spectrum is shown in Figure 4.37 (b). The occurrence of thiol-ene coupling is confirmed by the absence of double bond signals in the region between 5.2 and 6.5 ppm. Signal **b** at 4.10 ppm can be attributed to the CH_2 group adjacent to the ether group. Additionally, signals **c** (2.67, 2.08 and 1.85 ppm) belonging to the protons next to the newly formed thioether groups are observed. The carbonate group was conserved during the reaction, which is confirmed by the existence of signal **a** at 5.08 ppm belonging to the CH_2 group of the coupled vanillyl alcohol.

To see whether a higher molecular weight could be achieved with a less bulky dithiol, the reaction was repeated with the linear 1,6-hexanedithiol (Figure 4.38, blue trace). However, compared to the reaction with limonene dithiol (yellow trace), no improvement was achieved. With the linear dithiol, besides the low molecular weight fraction, molecular weights of $M_n = 4,900$ Da ($\mathcal{D} = 1.1$) were obtained. Thus, the steric hindrance of limonene dithiol **48** is not the cause for the low molecular weight in the polymerization. Performing the reaction with allyl eugenol **7** and limonene dithiol **48** (Figure 4.38, green trace), resulted in a broad molecular weight distribution consisting of mainly oligomeric species ($M_n = 1,100$ Da, $\mathcal{D} = 6.7$). Regarding that result, the carbonate group of AVA carbonate **10** does not seem to influence the obtained molecular weight. However, the synthesis of high molecular weight polymers was not possible with the chosen substrates and reaction conditions. Further investigations are required to find suitable reaction conditions, such as the use of a more powerful UV lamp.

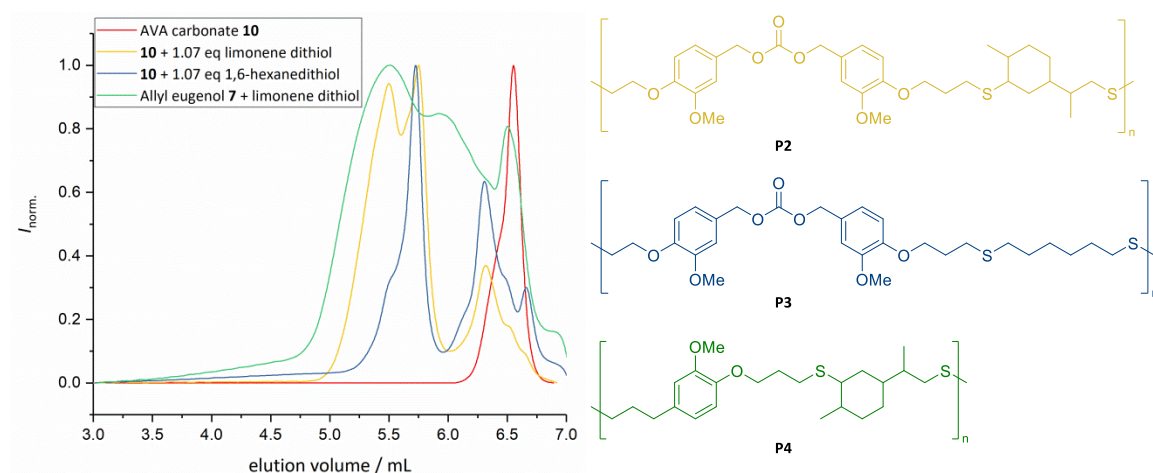


Figure 4.38 HFIP-SEC traces for the thiol-ene polymerization of AVA carbonate **10** with limonene dithiol **48** (**P2**), 1,6-hexanedithiol (**P3**) and of allyl eugenol **7** with limonene dithiol (**P4**) (SEC system C).

4.3.2 Synthesis of Cross-linked Thiol-Ene Films

As the synthesis of linear, high molecular weight polymers from diallyl ether monomers was not successful, in a next step, the formation of cross-linked thiol-ene films was attempted. A bio-based trithiol was synthesized from myrcene **49** applying the same procedure as for the synthesis of limonene dithiol **48** (Figure 4.39). In a first step, myrcene **49** was reacted with thioacetic acid by stirring the mixture at room temperature for 23 h. Subsequently, unreacted thioacetic acid was removed under reduced pressure. TBD and methanol were added and the solution was stirred at 75 °C for 25 h to cleave the formed thioester groups. Finally, the solvent was removed and trithiol **50** was obtained in a yield of 58.6% after column chromatography. The reaction was monitored by GC-MS, the chromatograms are shown in Figure 4.40.

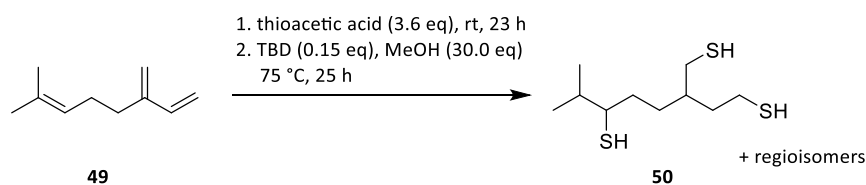


Figure 4.39 Synthesis of myrcene-based trithiol **50** in a two-step procedure applying thioacetic acid followed by saponification of the resulting ester groups using TBD in methanol.

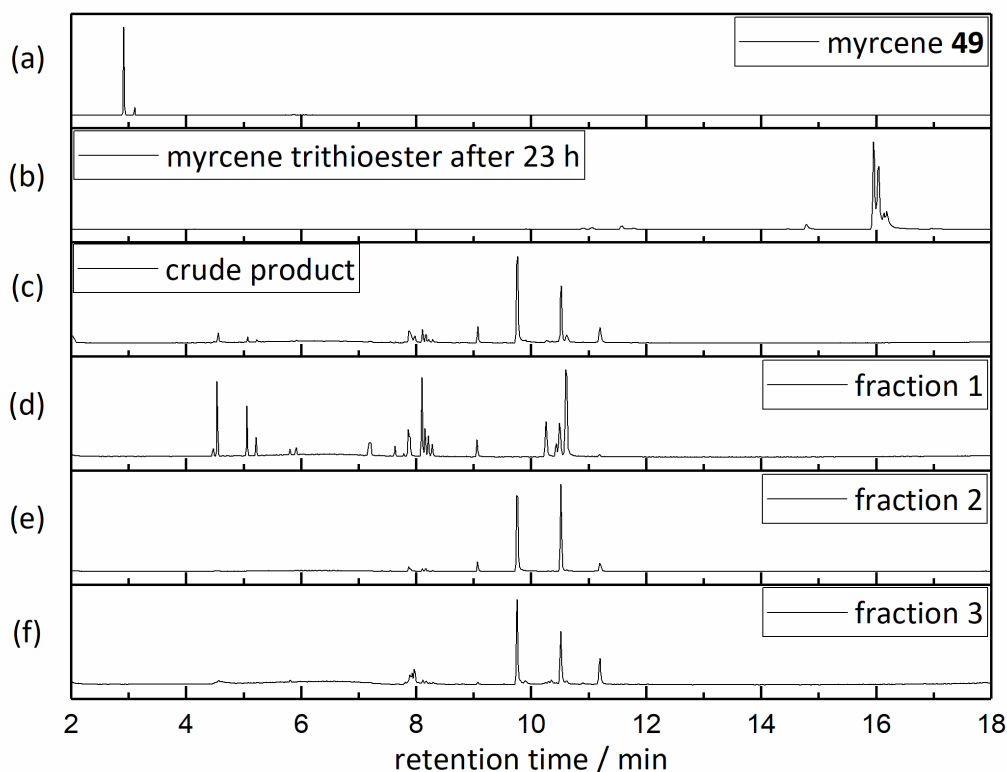


Figure 4.40 GC-MS chromatograms for the synthesis of myrcene-based trithiol **50**: (a) starting material myrcene, (b) reaction mixture after reaction with thioacetic acid for 23 h, (c) crude product after thioester hydrolysis, (d) fraction 1, (e) fraction 2 and (f) fraction 3 after column chromatography.

After the addition of thioacetic acid and stirring for 23 h (Figure 4.40 (b)), complete conversion of myrcene **49** (Figure 4.40 (a)) was achieved. After the saponification step (c), three main products were obtained (9.8, 10.5 and 11.2 min retention time). For a more detailed analysis, separation of the products by column chromatography was attempted. Fraction 1 (d) mostly contained by-products, whereas the main products were not separable by column chromatography and were eluted together. Therefore, fractions 2 (e) and 3 (f) both contained a mixture of the main products, which most probably consist of regioisomeric structures. Thus, fractions 2 and 3 were used for subsequent syntheses. Since a mixture of molecules was obtained, no clear structural assignment was possible by 2D-NMR spectroscopy. Therefore, trithiol **50** was characterized by mass spectrometry (showing masses of the trithiol **50** and the respective fragmentation products) and elemental analysis ($C_{10}H_{22}S_3$, calculated: C 50.37%, H 9.30%, S 40.33%; found: C 50.67%, H 8.61%, S 38.67%). In the literature, the synthesis of **50** has very recently been reported in a US patent.^[309] In this case, thiol formation was achieved by radical and acid-catalyzed sulfhydration of myrcene using H_2S as sulfur source. After distillation, the product was also obtained as a mixture of regioisomers in a purity of 98%.

With the bio-based trithiol **50** in hands, the formation of films *via* thiol-ene polymerization was investigated. The coupled diene monomers **10-12** as well as the Biginelli product **14** and allyl eugenol **7** were used as substrates (Figure 4.41).

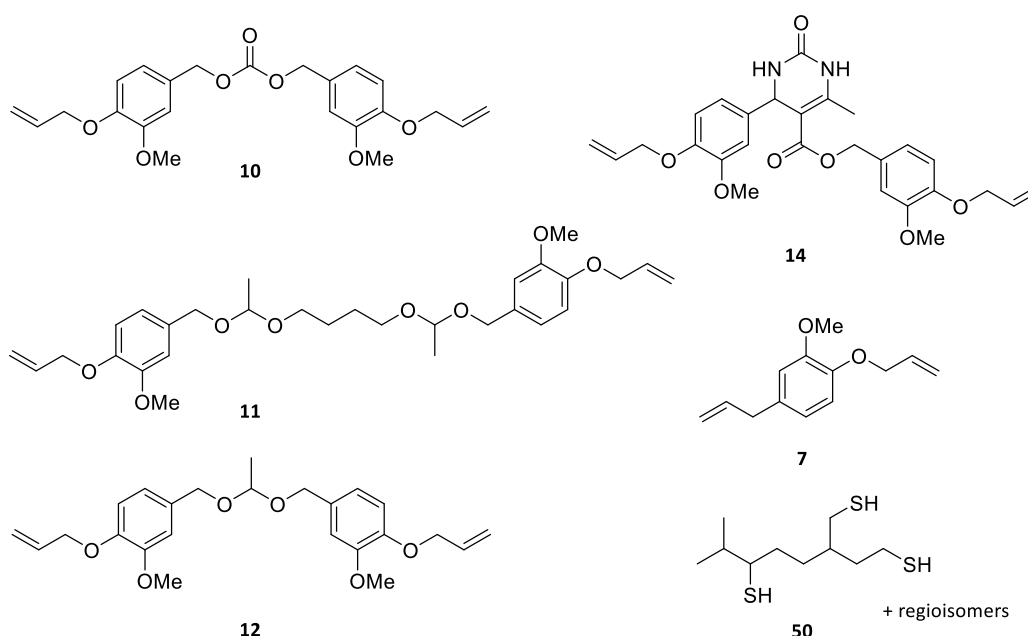


Figure 4.41 Structures of dienes used for the formation of thiol-ene films with myrcene-based trithiol **50**.

For the curing of thiol-ene films, the respective dienes were mixed with the myrcene-based trithiol **50** (the ratio of double bond to thiol was 1:1 in all samples). Subsequently, DMPA

(5 mol% per double bond) was added. After thorough mixing, the mixture was transferred to a glass plate with tape boundaries (1 cm x 2.5 cm). Solid samples were gently melted using a heatgun to ensure homogeneous film formation. The hot samples were placed in the curing oven and the curing was carried out under UV irradiation (365 nm, ~750 mW/cm², 50% power) for 10 min. Products were obtained as clear and mostly translucent films (Figure 4.42 (b)) that were removed from the glass surface with a sharp blade. The films were analyzed by differential scanning calorimetry (DSC) measurements for the determination of the glass transition temperature and by thermogravimetric analysis (TGA) to obtain the degradation temperature $T_{d\ 5\%}$. Furthermore, soluble parts were determined by immersion of the samples in THF for 24 h to estimate the efficiency of the cross-linking reaction. All results are summarized in Table 4.6.

Table 4.6 Summarized results for the thiol-ene film formation of dienes **10-12**, **14** and **7** with myrcene-based trithiol **50**.

Entry	Monomer	$T_g^a / ^\circ\text{C}$	$T_{d\ 5\%}^b / ^\circ\text{C}$	Soluble parts ^c / %
P5	10	14	202	14.2
P6	11	-23	134	65.3
P7	12	-13	171	62.2
P8	14	37	182	100
P9	7	-5	226	14.8

^a DSC system A, ^b determined by TGA, ^c Soluble parts = $100 \times (1 - m_D/m_0)$.

As a first step, the percentage of soluble parts of the cured films was determined. The dry polymer samples were weighed (m_0) before immersion in THF for 24 h. After removing the soluble part, the films were dried under vacuum and weighed again (m_D). The obtained values for the soluble parts give an indication about the degree of cross-linking in the material. Biginelly-based polymer **P8** was completely soluble in THF. This indicates a poor cross-linking during the polymerization, which might be caused by the rigid and bulky structure of monomer **14**. With a soluble part of 62.2% and 65.3%, respectively, the acetal resins **P7** and **P6** also show insufficient cross-linking. One possible explanation for that result is the potential attack of the acetal linkage by the thiol group. This leads to a cleavage of the linker and a lower cross-linking density. Indeed, transthioacetalization reactions have been reported in literature, for example catalyzed by vanadyl triflate (VO(OTf)₂) or indium(III) chloride.^{[310][311]} In contrast, better results were obtained for the carbonate-based resin **P5** and for the polymerization of allyl eugenol (**P9**). With 14.2% and 14.8%, respectively, only small parts of the obtained films were soluble, indicating good cross-linking and a successful resin formation.

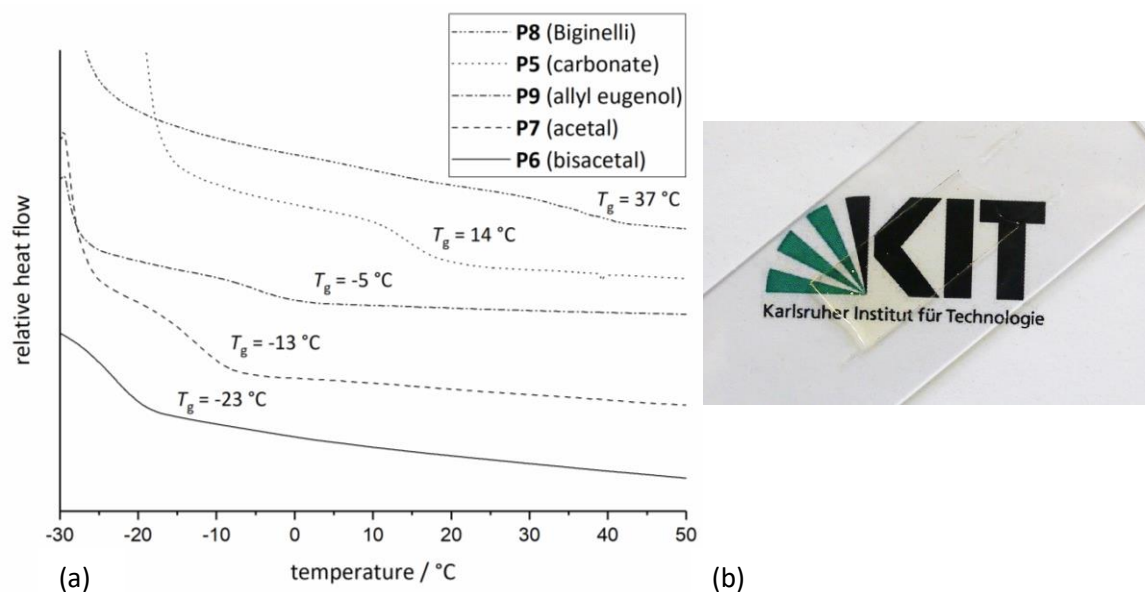


Figure 4.42 DSC graphs indicating the glass transition temperatures for the polymers **P5-P9** (a), photo of polymer film **P5** (b) (DSC system A).

Figure 4.42 (a) shows the stacked DSC thermograms of the polymers **P5-P9** and the obtained glass transition temperatures. The lowest T_g (-23 °C) was obtained for the films using bisacetal **11** (**P6**). Indeed, after polymerization, very soft and sticky films were obtained, which can be explained by the flexible aliphatic linker unit of the monomer and a high amount of unreacted monomers that act as plasticizer. A slightly higher T_g of -13 °C was achieved by applying monoacetal **12** (**P7**), which does not bear the additional aliphatic linker, but still contains high amounts of low molecular weight species. Films from allyl eugenol **7** (**P9**) exhibit a lower glass transition temperature (T_g = -5 °C) compared to carbonate **10** (**P5**, T_g = 14 °C). The highest T_g of 37 °C was obtained using Biginelli monomer **14** (**P8**), which can be attributed to the rigid structure of the monomer and intramolecular hydrogen bonding, as low cross-linking was achieved during the polymerization. Indeed, in this case, very brittle films were obtained that could not be removed from the glass plate without breaking. The thermal stability of all samples was investigated by TGA. The results are shown in Figure 4.43.

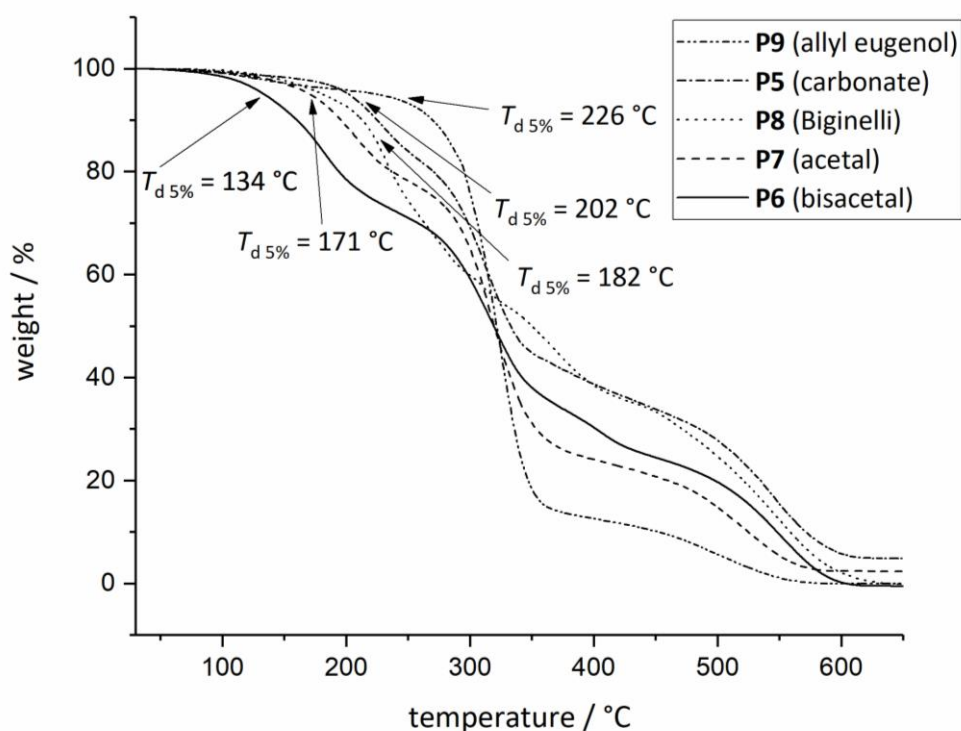


Figure 4.43 TGA analyses of the obtained thiol-ene films and the respective degradation onset temperature at a weight loss of 5%.

Acetal-based polymers **P6** and **P7** showed the lowest thermal stability, exhibiting $T_{d\ 5\%}$ -values of 134 °C and 171 °C, respectively. A slightly higher value of 182 °C was obtained for the Biginelli polymer **P8**. An improved thermal stability is observed for the two films exhibiting the highest cross-linking density (lowest proportion of soluble parts). The highest thermal stability was achieved with the cross-linked allyl eugenol (**P9**), which exhibited a degradation temperature of $T_{d\ 5\%} = 226$ °C followed by the carbonate-based polymer **P5** ($T_{d\ 5\%} = 202$ °C). The lower stability of **P5** is presumably caused by the carbonate linker, which is cleaved first at elevated temperatures. This is visible in the TGA thermograms. Indeed, for **P5**, a stepwise degradation is observed, while the eugenol-based polymer **P9** is mostly degrading in one step.

Furthermore, all films were analyzed by IR spectroscopy (Figure 4.44).

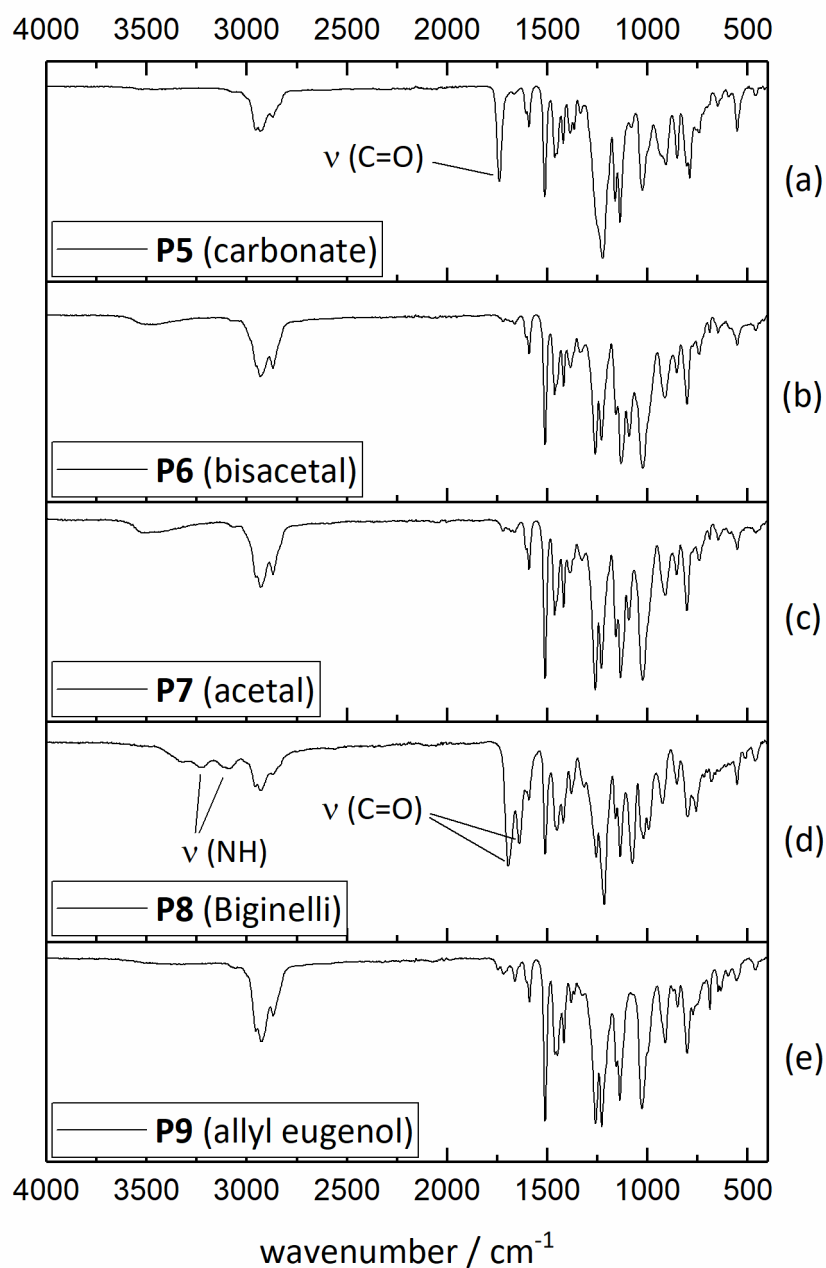


Figure 4.44 IR spectra of the thiol-ene films **P5-P9**.

The stretching band of the carbonyl group $\nu(\text{C}=\text{O})$ at 1738 cm^{-1} can be distinguished in the IR spectrum of carbonate-based film **P5** (Figure 4.44 (a)). Thus, the carbonate group is unaffected by the thiol-ene polymerization, which is in accordance with the results obtained by the solubility tests. In the spectrum of **P8**, the stretching of the carbonyl groups is visible at 1695 cm^{-1} and 1641 cm^{-1} and signals for the N-H stretching can be observed at 3231 and 3087 cm^{-1} . Thus, in this case, the Biginelli structure remains intact and the poor cross-linking is not caused by a degradation of the monomer. Unfortunately, the IR spectra of the acetal polymers **P6** and **P7** did

not allow for a confirmation of a reaction between the acetal group and the thiol, as no respective vibration mode was clearly distinguishable.

The stable and well cross-linked polymer films **P5** (carbonate-coupled monomer **10**) and **P9** (allyl eugenol **7**) were analyzed by stress-strain measurements to gain information on their mechanical properties. Several identical films were synthesized and analyzed. The combined stress-strain curves are shown in Figure 4.45 (a) and (b), respectively. The initial slope of the curves was used to calculate the Young's modulus. Furthermore, the elongation at break and ultimate tensile strength were determined. All results are summarized in Table 4.7.

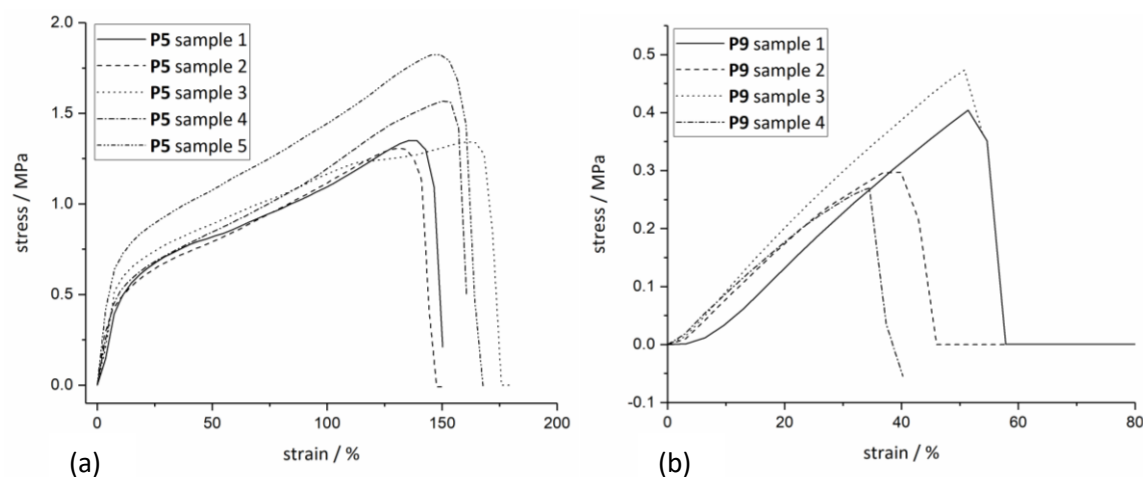


Figure 4.45 Stress-strain measurements of thiol-ene films **P5** and **P9**: Combined measurements of the carbonate film **P5** (a), combined measurements of the allyl eugenol film **P9** (b).

Table 4.7 Mechanical properties of polymer films **P5** and **P9** obtained from stress-strain measurements.

Sample	Young's modulus / MPa	Elongation at break / %	Ultimate tensile strength / MPa
P5	6.87 ± 1.29	148 ± 10.7	1.48 ± 0.194
P9	0.850 ± 0.0730	44.2 ± 7.21	0.361 ± 0.0815

Polymer film **P5** based on AVA carbonate **10** showed reproducible results and an elastomeric behavior. From all measurements, an average Young's modulus of 6.87 MPa was calculated. Furthermore, samples showed an elongation at break of 148% and an ultimate tensile strength of 1.48 MPa. These values are significantly higher compared to allyl eugenol-based polymer film **P9**. With a lower Young's modulus of 0.850 MPa, the samples showed poor mechanical properties. This was also reflected in the lower values of the ultimate tensile strength

(0.361 Mpa) and elongation at break (44.2%). A comparison of representative measurements of each polymer is shown in Figure 4.46.

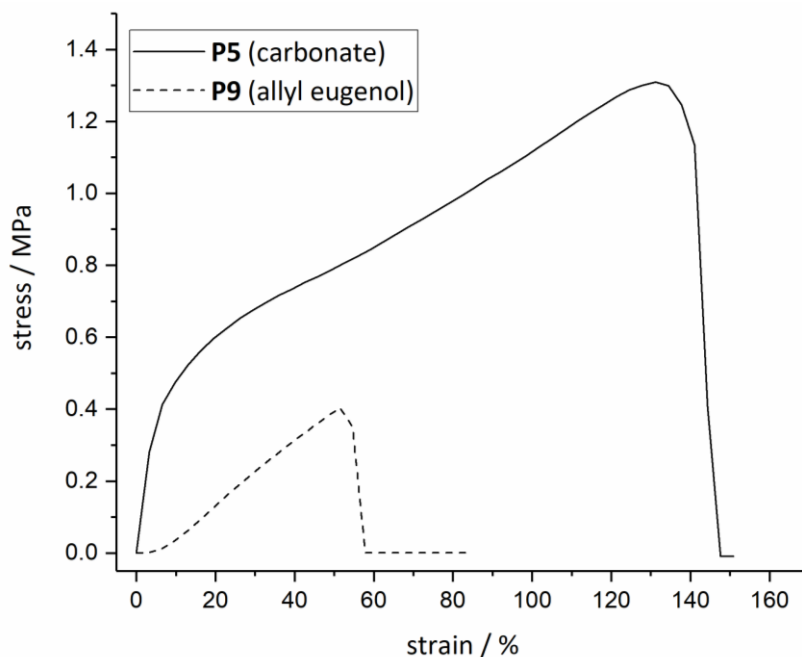


Figure 4.46 Comparison of stress-strain measurements of polymer films **P5** and **P9**.

In the literature, similar resins based on thiol-ene cross-linking have been reported. For example, Cheng and Zhang coupled itaconic acid with eugenol, synthesizing an aromatic structure containing three double bonds.^[312] The monomer was cross-linked with mercaptopropionate-based di-, tri- and tetrathiols. Applying the dithiols, which corresponds to the monomer functionality in this work, a T_g of 12.0 °C was achieved. Furthermore, the authors reported a thermal stability of 320 °C, a tensile modulus of 10.0 MPa, an ultimate tensile strength of 6.5 MPa and an elongation at break of 91.3%. The material shows slightly higher thermomechanical properties compared to polymer **P5**, which exhibits a higher elongation at break and a lower thermal stability. Similarly, Robertson *et al.* allylated renewable phenolic acids to introduce alkene groups.^[313] The monomers were subsequently cross-linked to stable networks using a tetrathiol. The obtained networks exhibited glass transition temperatures between -7 °C and 7 °C, tensile strengths between 1.8 and 3.7 MPa, tensile moduli between 8.5 and 12.5 MPa and elongations at break between 20 and 30%. Thus, glass transition temperatures are comparable to the results obtained for **P5** and **P9**. However, also in this case, slightly higher mechanical properties were reported. Allyl eugenol has also been used in thiol-ene resins. Shibata and co-workers reacted allyl eugenol with a commercial isocyanurate-based trithiol.^[314] The resin exhibited a T_g of 4.1 °C, a thermal stability of 350 °C, a tensile modulus of

2.1 MPa, tensile strength of 0.97 MPa and an elongation at break of 58.7%. These values are higher than the results obtained for polymer film **P9**. Therefore, in a next step, more research is needed to investigate whether the polymer properties can be improved, for instance by using a tetra-thiol to substitute myrcene-based trithiol **50** or by decreasing the film thickness to increase the efficiency of irradiation and the resulting cross-linking density.

In conclusion, the diene monomers synthesized in chapters 4.1.1 and 4.1.2 were polymerized by ADMET and thiol-ene reactions. During ADMET polymerization of AVA carbonate **10**, only low molecular weight oligomers were obtained. Using thiol-ene polymerization and a sustainable, limonene-based dithiol, better results were obtained. Polymerization with a slight excess of 1.07 eq dithiol led to the formation of oligomers with a molecular weight of $M_n = 6,000$ Da and a dispersity of $D = 1.35$. However, higher molecular weights seem to be limited by the allyl group, as the use of a sterically less demanding linear dithiol did not lead to higher molecular weight polymers. The use of allyl eugenol did also not improve this result. As an alternative, cross-linked films were prepared by reacting the diene monomers with a trithiol synthesized from bio-based myrcene. Presumably due to its sterically demanding structure and intramolecular hydrogen bonding, Biginelli-based diene **14** showed poor cross-linking in the thiol-ene polymerization. Slightly better results were obtained for the acetal-containing monomers **11** and **12**. However, the acetal group seems to react with the thiol groups, leading to polymers with high amounts of soluble fractions and comparably low thermal stability. Better results were obtained for the polymerization of carbonate-based monomer **10** and allyl eugenol **7**. After cross-linking, stable and translucent films with a good cross-linking density, as indicated by solubility tests, were obtained. Furthermore, both films exhibited acceptable thermal stabilities of 202 °C and 226 °C, respectively. The films were also tested in stress-strain measurements. The polymer film based on AVA carbonate (**P5**) exhibited good mechanical properties and showed elastomeric behavior. Allyl eugenol-based films (**P9**) showed poor mechanical properties with a lower Young's modulus and elongation at break. Therefore, more research is needed to increase the cross-linking and to improve the thermomechanical properties of the obtained films. Nevertheless, the results represent a promising basis for the implementation of the renewable and cleavable monomers in thiol-ene polymerizations.

4.4 Synthesis of Epoxy Resins from Diglycidyl Ether Monomers

In this chapter, the synthesis of epoxy resins based on the epoxy monomers described in chapter 4.1.3 and the amine hardeners described in chapter 4.2.4 is discussed. As a first step, the reactivity of the carbonate linker towards a nucleophilic attack of the amine curing agent was investigated. Then, a first curing test of GVA carbonate **16** applying commercially available Priamine® was performed. After successful polymer formation, the study was expanded to the remaining bisepoxides and amine curing agents. The obtained results were compared to the commercial monomers DGEBA and IPDA.

4.4.1 Reactivity Test of Carbonate Linker with Amines

Before investigating the synthesis of epoxy resins, the susceptibility of the carbonate linker, present in monomer **16**, towards a nucleophilic attack by the amine curing agent was evaluated. For easier monitoring, AVA carbonate **10** was used, as no reaction is expected between the diene monomer and the amine. To prevent evaporation of the amine during the test, the higher boiling octylamine was used. Reactions were carried out in a sealed pressure tube by mixing the substrate with octylamine and heating the mixture for a specific time. Reactions were followed by NMR, an example is shown in Figure 4.47. A degradation of the carbonate group should result in a decrease of the proton signal of the CH₂ group adjacent to the carbonate (signal 11 at 5.06 ppm). Different amounts of octylamine and temperatures were investigated; the obtained results are listed in Table 4.8.

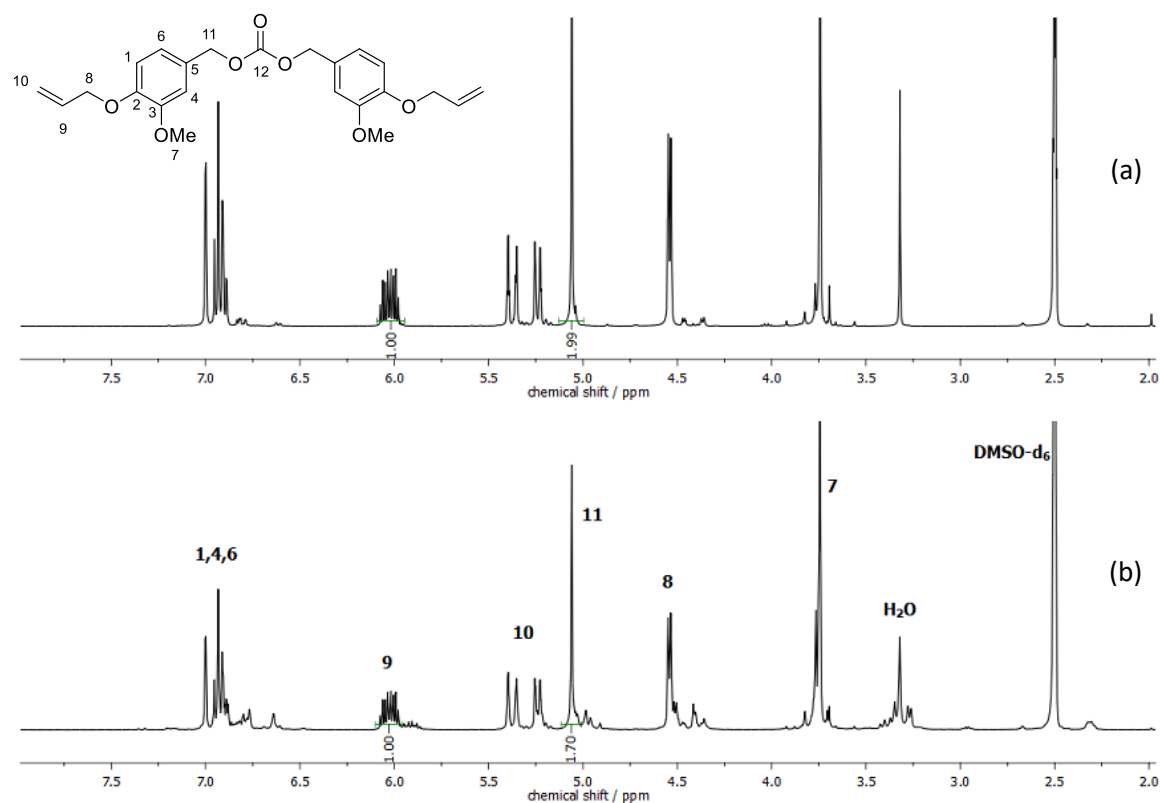


Figure 4.47 $^1\text{H-NMR}$ spectra of AVA carbonate **10** before (a) and after the reactivity test (b) with octylamine (entry 5 in Table 4.8).

Table 4.8 Reactivity test of the carbonate linker monomers **10** and **16** with varying amounts of octylamine.

Entry	Substrate	Octylamine / eq	Temperature / °C	Time / h	Degradation ^a / %
1	10	1.00	100	2	0
2	10	2.00	100	2	2.5
3	16	4.00	100	2	27.5
4	10	-	80 + 170	2 + 2	0
5	10	1.00	80 + 170	2 + 2	14.6

^a Degradation was determined by integrating the benzylic protons in the $^1\text{H-NMR}$ spectrum and comparing the value to the respective value at the beginning of the test.

In a first attempt, AVA carbonate **10** was mixed with 1.00 eq octylamine, corresponding to the ratio of an actual curing, where one amine group reacts with two epoxide moieties. After heating the mixture to 100 °C for 2 h, no decrease of the benzylic proton signal was observed in the $^1\text{H-NMR}$ spectrum (Table 4.8, entry 1). Thus, in a next step, the reaction was repeated with a higher amount of octylamine of 2.00 eq (entry 2). In this case, after 2 h at 100 °C, a slight degradation of 2.5% was observed. Thus, to further explore the extent of carbonate degradation

in presence of epoxide groups, GVA carbonate **16** was reacted with an excess of 4.00 eq octylamine. The mixture was again heated to 100 °C for 2 h, resulting in a complete conversion of the epoxide groups according to ¹H-NMR spectra. Additionally, a degradation of the carbonate group of 27.5% was observed (entry 3). This indicates that the ring-opening of the epoxide group through the amine is preferred over the degradation of the carbonate linker. However, using higher excesses of octylamine, a reaction with the carbonate group could not be avoided. The first tests were carried out at 100 °C. However, during the resin formation, higher temperatures are required to ensure proper post-curing of the network. Therefore, to investigate the carbonate stability at high temperatures, two more experiments were performed with a temperature program imitating the final curing conditions. First, AVA carbonate **10** was heated to 80 °C for 2 h without the addition of octylamine, simulating the pre-curing step. Then, the temperature was increased to 170 °C for additional 2 h (entry 4). No degradation was observed, excluding a degradation of the carbonate group due to elevated temperatures. Subsequently, the experiment was repeated in the presence of 1.00 eq octylamine. In this case, after 2 h at 80 °C, as already observed, the carbonate group remained intact. However, after another 2 h at 170 °C, no clear result was obtained. Depending on the reference signal in the NMR spectrum, different conclusions could be drawn. Taking the aromatic signals as reference, no degradation was detectable when compared to the integral of the benzylic protons. However, when referencing to the double bond signal, a decrease of 14.6% was calculated (Figure 4.47). In addition, minor additional signals were visible in the NMR spectrum.

To conclude, the reactivity tests showed a preferential reaction of the amine towards the epoxide groups. With stoichiometric amounts of amine, the carbonate group proved to be stable under pre-curing conditions. Using an excess of amine, the cleavage of the carbonate linker was induced. The linker remained stable at higher temperatures of 170 °C; however, in the presence of the amine, a degradation reaction with the linker could not be completely excluded. Therefore, the amount of linker degradation needs to be further investigated in the final epoxy resins, as a pre-curing at lower temperatures also results in a decrease of primary amine groups, reducing the possibility for carbonate degradation.

4.4.2 First Curing Test with Priamine®

A first test curing was performed with GVA carbonate **16** and the commercial, fatty acid-based hardener Priamine® **51** before using the sterically more demanding terpene-based diamine hardeners. In a first attempt, the curing was performed during a DSC measurement. **16** and **51** were mixed in a molar ratio of 2:1 and the mixture was transferred into a DSC aluminium pan.

The curing was carried out by heating to 300 °C with a heating rate of 10 °K/min. The DSC thermogram of the curing of **16** and **51** is shown in Figure 4.48. Upon heating, two exothermic peaks at 136 °C and 248 °C were observed, indicating curing reactions between the amine hardener and the epoxide monomer. The first curing step occurred after the melting (endothermic peak) of **16** at 129 °C.

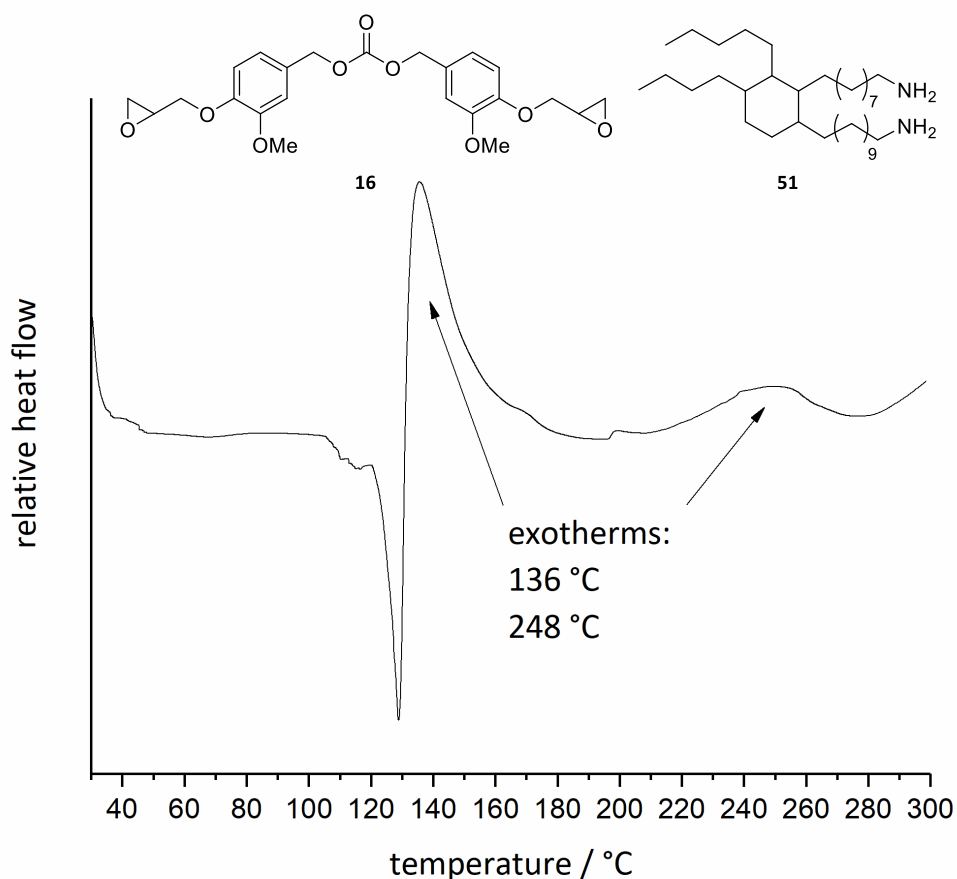


Figure 4.48 DSC curing of GVA carbonate **16** with the fatty acid-based Priamine® hardener (DSC system A).

The temperatures obtained from the exotherms in Figure 4.48 were subsequently used to determine the optimal curing conditions for the polymerization of **16** and **51**. As a result, the sample was pre-cured at 130 °C for 1 h. Then, the temperature was increased, and post-curing was carried out at 230 °C for 1 h. After curing, the obtained polymer was analyzed by DSC. No exotherms were observed, indicating a complete curing of the sample in the oven. The resulting polymer exhibited a glass transition temperature of 30°C. Additionally, the sample was analyzed by TGA and DMA. The results are shown in Figure 4.49. Analyzing the TGA thermogram (Figure 4.49 (a)), a degradation temperature of $T_{d5\%} = 329$ °C was determined. The DMA measurement (Figure 4.49 (b)) resulted in a storage modulus of $E' = 0.787$ GPa. Moreover, a T_g of 34 °C was identified *via* the maximum of the $\tan \delta$ peak. These values are lower compared to the

commercial DGEBA/IPDA systems, for which glass transition temperatures of 152 °C and 166 °C as well as storage moduli of 1.7 GPa and 1.9 GPa have been reported.^{[217][214]} The lower thermomechanical properties can be attributed to the long aliphatic segments of the Priamine® hardener, which are not present in IPDA. Nevertheless, the first curing tests gave promising results. Thus, a more detailed study was carried out using the synthesized epoxide monomers.

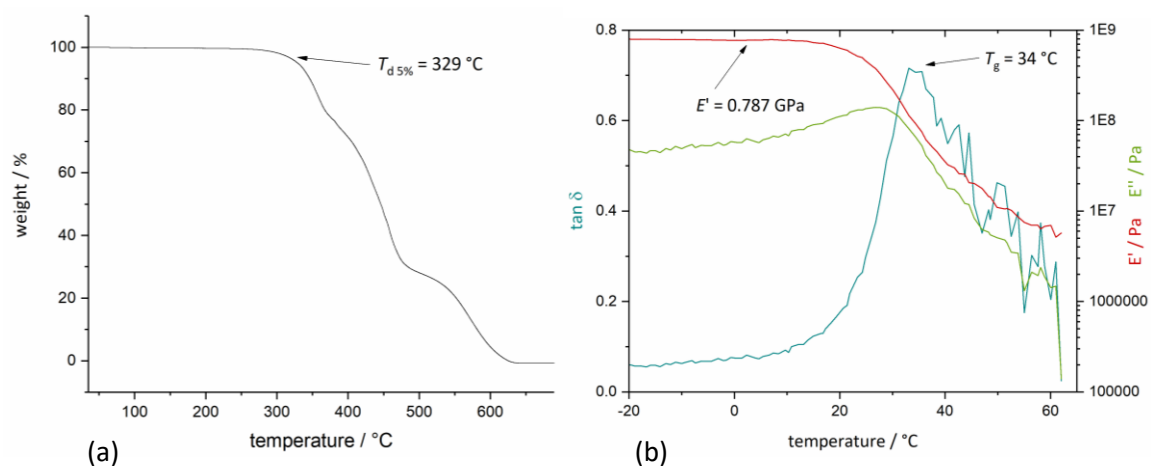


Figure 4.49 Thermomechanical analysis after curing GVA carbonate **16** with Priamine®: Onset degradation temperature ($T_{d5\%}$) obtained by TGA (a), storage modulus E' and T_g obtained by DMA analysis (b).

4.4.3 Epoxy Resin Studies

The synthesized epoxy monomers GVA carbonate **16**, GVA bisacetal **17** and the non-cleavable epoxidized allyl eugenol **18** as well as the reference monomer DGEBA **52** were studied for the preparation of epoxy resins with the limonene-based diamine synthesized in chapter 4.2.4 and IPDA as reference. The synthesized limonene bis-amino alcohol **40** was used as crude mixture (**40/41**) containing 50% of mono-reacted **41** and as pure monomer. All monomers are depicted in Figure 4.50.

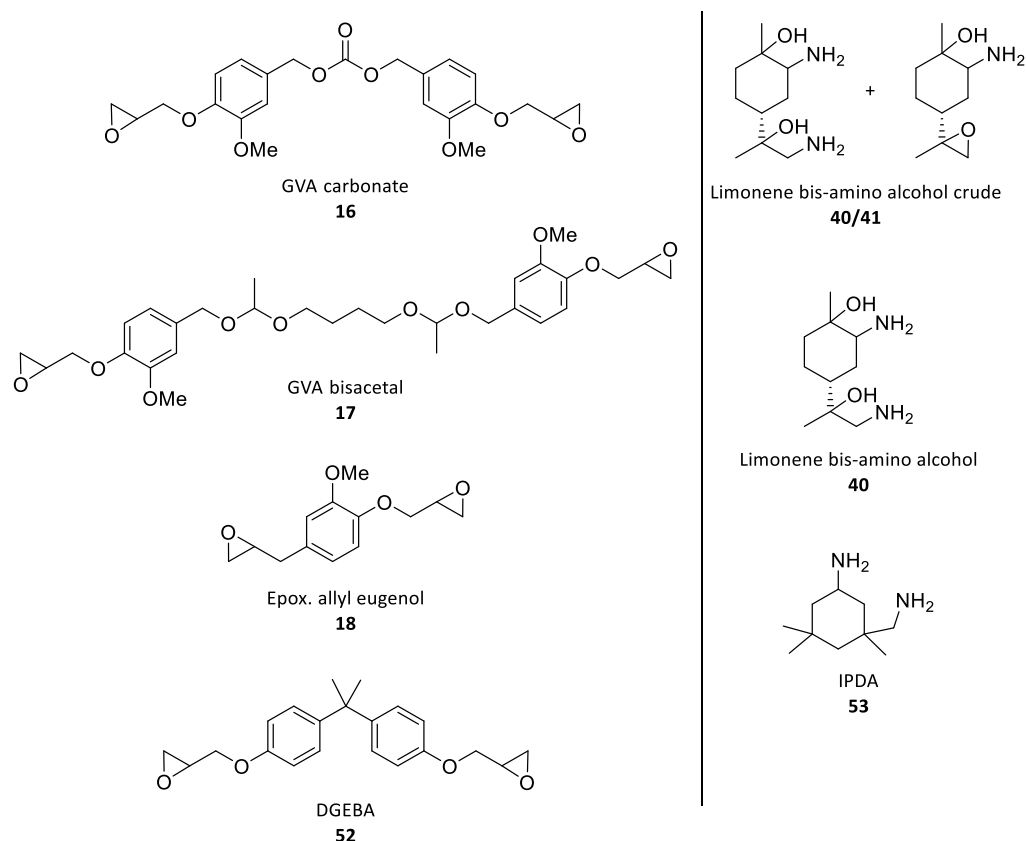


Figure 4.50 Monomers tested in the epoxy resin curing study: bisepoxides **16**, **17**, **18** and commercial DGEBA **52** (left), crude limonene bis-amino alcohol **40/41**, pure limonene bis-amino alcohol **40** and commercial IPDA **53** (right).

As a first step, the curing of all monomers was investigated *via* DSC measurements in order to determine the temperature of the curing exotherms. These values were used to establish the oven program to cure each sample. In all cases, only one exotherm was observed. Curings were carried out for 2 h at the onset temperature of the curing exotherm, followed by a 2 h post-curing at the upper limit of the exothermic peak. Detailed curing procedures are listed in chapter 6.3.4. The cured samples were analyzed by DSC, DMA and TGA to characterize their thermomechanical properties. The soluble part, giving information about the cross-linking density, was determined by weighing the samples before (m_0) and after immersion in THF for 24 h followed by drying (m_D). All obtained results are summarized in Table 4.9.

Table 4.9 Results for the epoxy resin study using the monomers depicted in Figure 4.50.

Sample	Epoxide	Amine	T_g DSC ^a / °C	T_g DMA ^b / °C	E'' ^c / GPa	Soluble part ^d / %	$T_{d 5\%}$ ^e / °C
P10	16	40/41	52	n.a.	n.a.	73.6	266
P11	16	40	51	62	1.55	91.6	241
P12	16	53	58	57	1.26	53.7	274
P13	17	40/41	11	n.a.	n.a.	43.2	261
P14	17	40	3	14	0.665	34.0	250
P15	17	53	39	36	0.542	14.9	235
P16	18	40/41	52	n.a.	n.a.	87.4	282
P17	18	40	91	88	1.86	0.40	293
P18	18	53	122	122	1.62	4.37	331
P19	52	40/41	89	n.a.	n.a.	n.a.	278
P20	52	40	49	51	1.56	32.5	n.a.
P21	52	53	90	91	1.31	10.7	299

^a DSC system A, ^b The T_g was obtained from the maximum of the E'' curve, ^c Determined by DMA, ^d Soluble parts = $100 \times (1 - m_D/m_0)$, ^e Obtained by TGA.

All samples cured with the crude limonene bis-amino alcohol **40/41** exhibited high soluble fractions, for example cured GVA carbonate (**P10**, 73.6%) or epoxidized eugenol (**P16**, 87.4%). This indicates an incomplete curing, which can be attributed to the high amount of the mono-functional amine **41** present in the mixture. Therefore, the crude amine mixture **40/41** is not suitable for epoxy resin curing, conclusions could not be drawn out of the DSC and TGA results and the resulting samples were not further analyzed by DMA.

Better results were obtained using the pure limonene bis-amino alcohol **40** (**P11**, **P14**, **P17** and **P20**). In this case, only GVA carbonate (**P11**) showed poor cross-linking, indicated by a high soluble fraction of 91.6%. This low cross-linking resulted from a poor mixing of the monomers, which hindered the formation of homogeneous samples, and from the potential reaction of the amine with the carbonate moiety. GVA bisacetal and DGEBA exhibited soluble fractions of around 30% (**P14**, 34.0% and **P20**, 32.5%), while the highest cross-linking density was reached for epoxidized eugenol (**P17**) with 0.40% soluble parts. The samples **P14**, **P17** and **P20** were analyzed by DSC, as shown in Figure 4.51 (a). The reference sample of DGEBA (**P20**) showed a T_g of 49 °C. A lower T_g of 3 °C was obtained for GVA bisacetal (**P14**), which can be explained by the

aliphatic spacer of the monomer. The polymer prepared from epoxidized eugenol (**P17**) showed a comparably high glass transition temperature of 91 °C, which is higher than for the DGEBA reference. All three samples were further analyzed by DMA, the results are shown in Figure 4.51 (b). The same trend as in the DSC was observed, with the bisacetal (**P14**) showing the lowest mechanical and thermal properties ($E' = 0.665$ GPa, $T_g = 14$ °C), followed by DGEBA (**P20**) with a storage modulus of 1.56 GPa and a T_g of 51 °C. Exhibiting a storage modulus of 1.86 GPa and a T_g of 88 °C, epoxidized eugenol (**P17**) showed the highest thermomechanical properties.

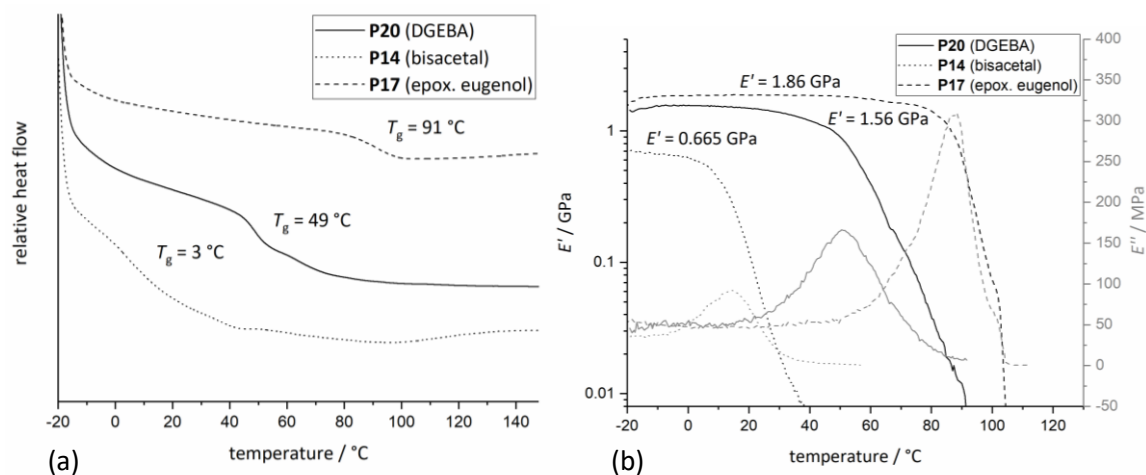


Figure 4.51 Thermomechanical properties of the samples cured with pure limonene bis-amino alcohol **40**: DSC traces (a) and storage moduli obtained by DMA (b).

The same trend in solubility was observed for the samples cured with IPDA (**P12**, **P15**, **P18** and **P21**), as well as for the samples cured with amine **40**. With a soluble fraction of 53.7%, GVA carbonate (**P12**) showed the lowest cross-linking. GVA bisacetal (**P15**, 14.9%) and DGEBA (**P21**, 10.7%) showed high cross-linking and the best result was obtained for epoxidized eugenol (**P18**, 4.73%). The DSC traces obtained for the samples cured with the commercial hardener IPDA are shown in Figure 4.52 (a). The lowest T_g , attributed to the flexible linker, was obtained for GVA bisacetal (**P15**, $T_g = 39$ °C). GVA carbonate (**P12**) showed a higher T_g of 58 °C, which is still lower than the value obtained for the DGEBA reference (**P21**, $T_g = 90$ °C). The highest glass transition temperature of 122 °C was achieved with epoxidized eugenol (**P18**). All samples were also analyzed by DMA measurements; the results are shown in Figure 4.52 (b). DMA traces showed the same trend, as GVA bisacetal (**P15**) exhibited the lowest values for the storage modulus ($E' = 0.542$ GPa) and the glass transition temperature (36 °C), followed by GVA carbonate (**P12**, $E' = 1.26$ GPa, $T_g = 57$ °C) and DGEBA (**P21**, $E' = 1.31$ GPa, $T_g = 91$ °C). The highest values were obtained for epoxidized eugenol (**P18**, $E' = 1.62$ GPa, $T_g = 122$ °C).

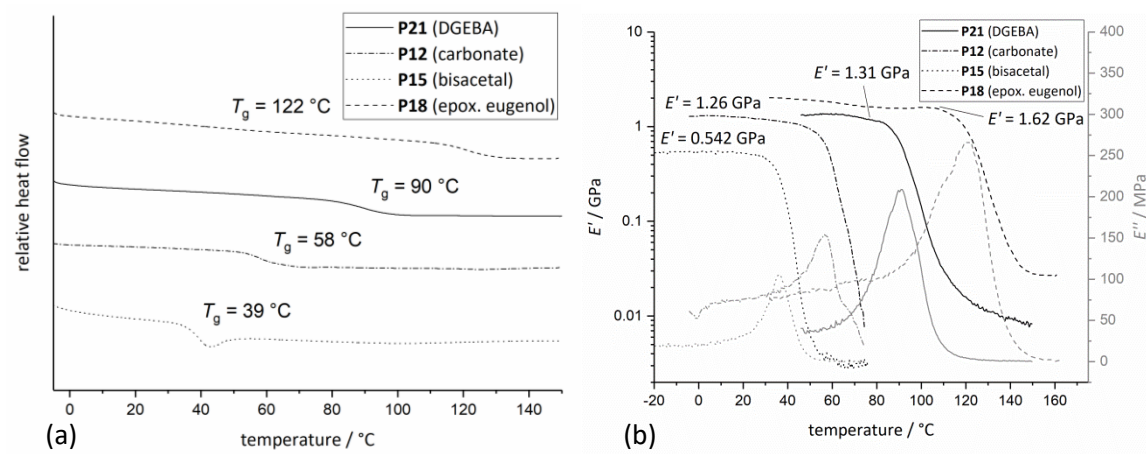


Figure 4.52 Thermomechanical properties of the monomers cured with IPDA **53**: DSC traces (a) and storage moduli obtained by DMA (b).

All cured samples were analyzed by TGA to determine their thermal stability. The combined results are shown in Figure 4.53. With $T_{d5\%}$ values between 235 °C and 331 °C, all samples showed satisfying thermal stabilities. Lower thermal stabilities were obtained for samples with a low cross-linking, for example for **P11** with $T_{d5\%} = 241\text{ °C}$ as well as for the samples of GVA bisacetal **17** (**P15** with $T_{d5\%} = 235\text{ °C}$ or **P14** with $T_{d5\%} = 250\text{ °C}$). Higher thermal stabilities were observed for samples with a high cross-linking, such as sample **P18** from epoxidized eugenol cured with IPDA ($T_{d5\%} = 331\text{ °C}$).

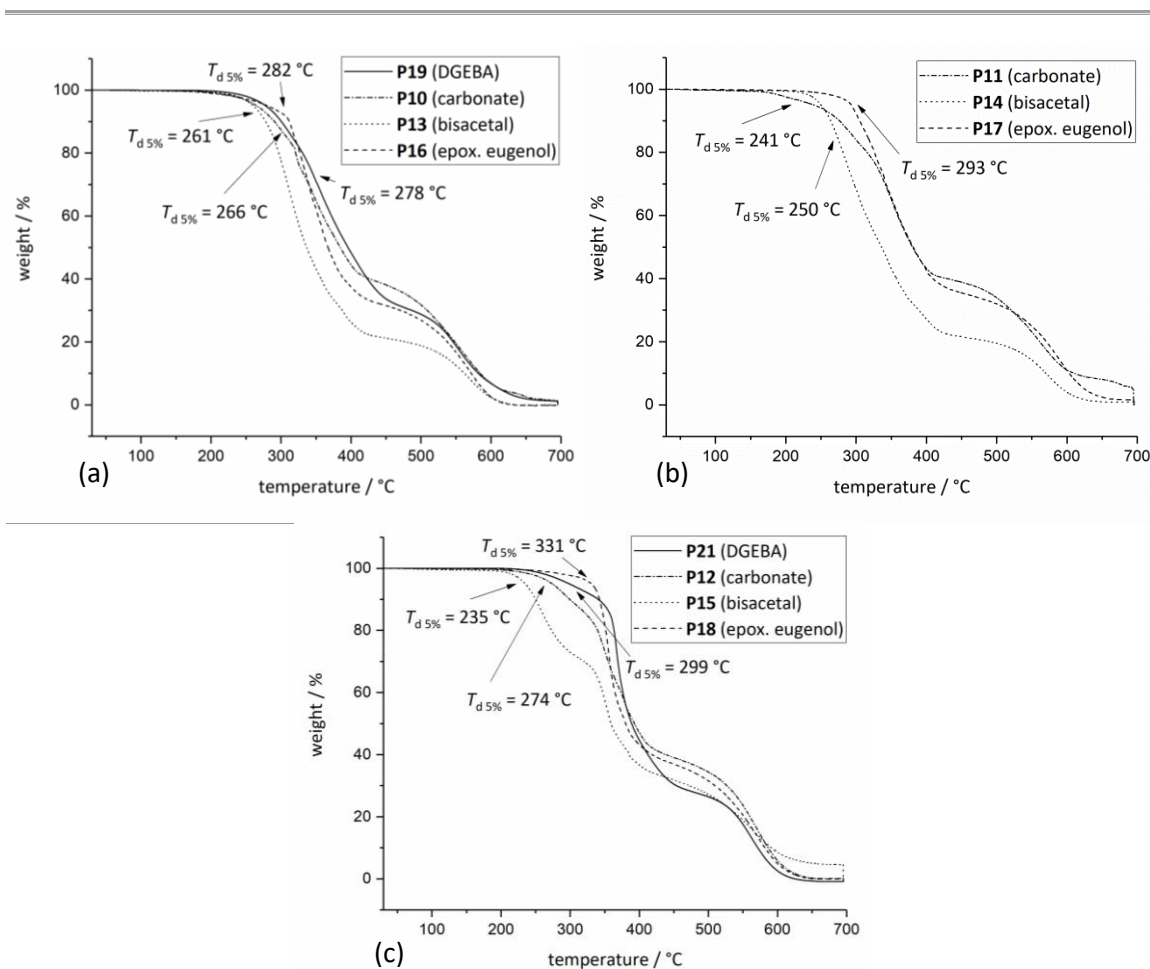


Figure 4.53 TGA traces for the synthesized epoxy resins: samples cured with crude limonene bis-amino alcohol **40/41** (a), samples cured with pure limonene bis-amino alcohol **40** (b) and samples cured with IPDA **53** (c).

Comparing the samples cured with pure limonene bis-amino alcohol **40** to the samples cured with IPDA, which are used as reference, generally lower glass transition temperatures were obtained (49 °C vs. 90 °C for DGEBA, 51 °C vs. 58 °C for GVA carbonate, 3 °C vs. 39 °C for GVA bisacetal and 91 °C vs. 122 °C for epoxidized eugenol). However, these results might be optimized by changing the curing conditions, as the solid pure limonene bis-amino alcohol **40** proved to be difficult to mix with the bisepoxide monomers. Thus, the formation of homogeneously cured samples was challenging, which can presumably be improved by adding small amounts of solvent. However, despite the lower glass transition temperatures, all samples cured with the bio-based amine **40** showed comparable mechanical properties in DMA measurements compared to the respective samples cured with IPDA (for example 1.56 GPa vs. 1.31 GPa for DGEBA, 0.665 GPa vs. 0.542 GPa for GVA bisacetal or 1.86 GPa vs. 1.62 GPa for epoxidized eugenol). Thus, limonene bis-amino alcohol **40** represents a potential alternative to IPDA, which can be synthesized from the abundant terpene limonene in a sustainable reaction

pathway. However, the crude diamine mixture was not suitable for epoxy resin curing. The high amount of monofunctional monomer prevented a sufficient cross-linking density and resulted in samples with a high percentage of soluble parts. Thus, a purification step is required to isolate the product **40**. GVA carbonate **16** also showed poor cross-linking with all amine hardeners, yielding polymers with high solubilities. A possible explanation for these results is the reaction of the amine hardener with the carbonate linker group, which was already observed to a minor degree in the reactivity tests described in chapter 4.4.1. The reaction between carbonate group and amine leads to a cleavage of the monomer and a decrease in amine groups available for the curing reaction, resulting in a poor cross-linking density and inferior thermomechanical properties. However, this monomer might be suitable for other polymerization methods, for instance cationic epoxy resin curing. This alternative pathway needs to be investigated in future studies. GVA bisacetal **17** showed better cross-linking than the carbonate monomer. Due to the aliphatic linker, lower thermomechanical properties were achieved compared to the DGEBA reference. However, monomer **17** represents a possible alternative for applications that do not require high thermal and mechanical properties. Epoxidized eugenol **18** proved to be a good non-recyclable alternative for DGEBA in combination with the investigated amine hardeners. Compared to DGEBA, superior glass transition temperatures and similar storage moduli were obtained, and the low percentage of soluble parts indicates a high cross-linking density. Furthermore, it can be synthesized in two reaction steps from renewable eugenol. Thus, a replacement of DGEBA with this renewable alternative can be envisioned.

4.5 Degradation Studies

4.5.1 Establishment of Degradation Conditions

In this chapter, degradation tests for the synthesized cleavable monomers are discussed. One goal of this PhD work is to find solutions for the problem of thermoset recycling. As thermosetting polymers exhibit a highly cross-linked structure, mechanical recycling through melt processing is not feasible. As discussed in chapter 2.4, different options have been found to introduce recyclability into thermosets. These include solvent-assisted depolymerization or the use of covalent adaptable networks. In this chapter, the solvent-assisted depolymerization approach combined with a recovery of the obtained degradation products for the synthesis of new polymers is discussed. The establishment of degradation conditions suitable for the thiolene films and epoxy resins synthesized in chapter 4.3.2 and 4.4.3 was attempted first. To facilitate the monitoring of the degradation progress, the coupled bis-allyl ethers **10**, **11** and **12**

were chosen as test substrates, as their degradation will form the easily detectable AVA **5** (Figure 4.54). As AVA carbonate **10** was expected to bear the most stable linker unit, it was used as model substrate to establish the degradation conditions.

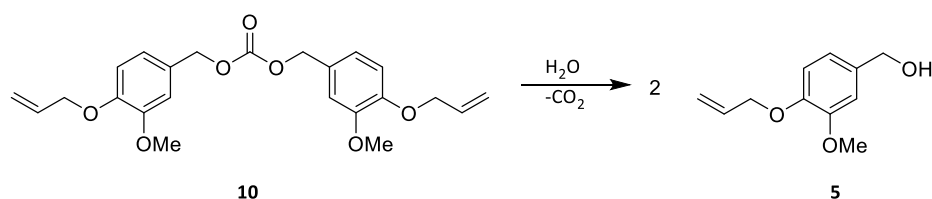


Figure 4.54 Degradation of AVA carbonate **10** to AVA **5** to establish degradation conditions.

In a first step, to confirm the formation of **5** during the degradation, 26 mg AVA carbonate **10** were immersed in 2 mL water in a sealable pressure tube. The mixture was heated to 150 °C for 3 h. Afterwards, 20 mL ethyl acetate were added, and the organic phase was dried over sodium sulfate. The solvent was removed under reduced pressure and the obtained product was analyzed by GC-MS measurements. Figure 4.55 shows the GC-MS traces and the respective mass spectrum of the degradation product (a) and of pure AVA **5** (b). The GC-MS trace (a) shows the formation of two products during the degradation of **10**. The main product was AVA **5**, which was also confirmed by comparing the mass spectrum to the spectrum of **5** (Figure 4.55, right). The second product (at slightly higher retention times) could not be identified; however, the mass spectrum showed the same mass as AVA **5**. Thus, presumably, an isomer of AVA **5** was formed, *e.g.* through a Claisen rearrangement, which would shift the allyl group to the aromatic ring. However, this side reaction can be neglected in the case of resin degradation, as the epoxy resins do not contain relevant amounts of free allyl groups. However, GC-MS analyses did not allow the quantification of the degradation, as no reference was used and the starting material was not detectable. Therefore, a SEC measurement was performed. The chromatogram showed the formation of AVA **5** as well as small amounts of remaining coupled monomer **10**.

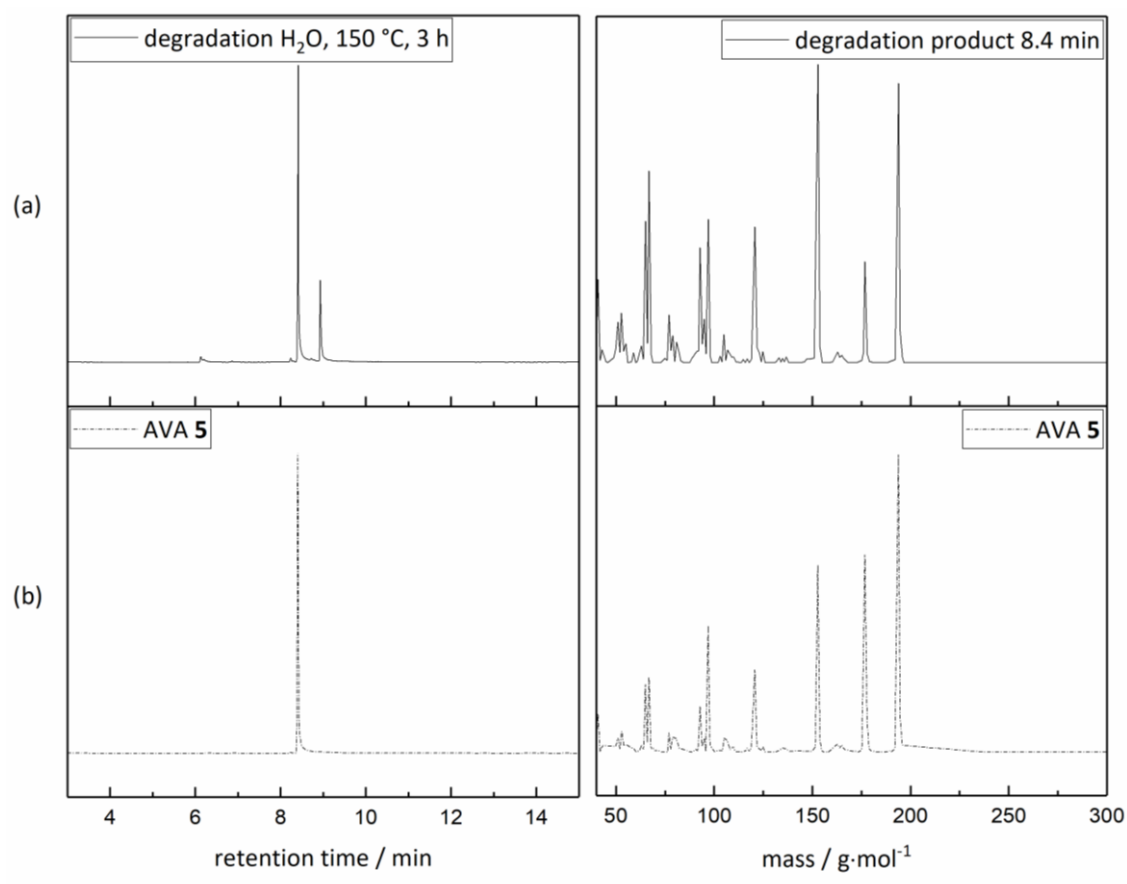


Figure 4.55 Degradation test of AVA carbonate **10** in water at 150 °C: GC-MS chromatogram after 3 h and the corresponding GC-MS mass spectrum (a), chromatogram and mass spectrum of the AVA **5** reference (b).

As the degradation test in water did not lead to full conversion according to SEC measurements, different degradation conditions were tested. Both the carbonate linker as well as the acetal linkers are acid-labile functional groups. During the degradation, an organic solvent is beneficial for the solubilization of the degradation products and should lead to better results. The summarized results are shown in Figure 4.56 (a). The progress of the degradation was monitored by SEC analysis. The percentage of degradation was determined by integrating the signal area of the coupled starting material and comparing it to the signal area of the product, AVA **5**. First, 0.25 mmol AVA carbonate **10** were dissolved in 1.25 mL of an acetonitrile solution (0.2M) and brought to pH = 3 using 500 μ L of a phosphate buffer solution. The solution was stirred at 50 °C for 10 h (green trace). However, the chosen conditions proved to be too mild to degrade carbonate **10** and no degradation products were observed in the SEC chromatogram after 10 h. Thus, in a next step, the reaction was repeated by dissolving **10** in a 0.2M mixture of THF and buffer (pH = 2, 1:1) and slightly higher temperatures of 80 °C were applied (yellow trace). After 6 h, also in this case, no degradation was observed. The best result was obtained when 0.2 mmol of substrate were dissolved in 1.00 mL DMF and 42.0 μ L concentrated hydrochloric acid solution

(0.5M in relation to DMF). The solution was heated to 100 °C, leading to 55% degradation after 72 h (red trace). The DMF/HCl system also led to better results than a comparable aqueous system, which was obtained by bringing water to a pH of 2 with concentrated hydrochloric acid (blue trace). In this case, a lower degradation of 27% was obtained after 48 h reaction time.

The SEC chromatogram for the degradation of AVA carbonate **10** in the DMF/HCl system is shown in Figure 4.56 (b). The signal at 20.2 min retention time, belonging to the coupled product **10**, decreased over time. At the same time, AVA **5** was formed, indicated by an increase of the corresponding signal at 21.4 min retention time.

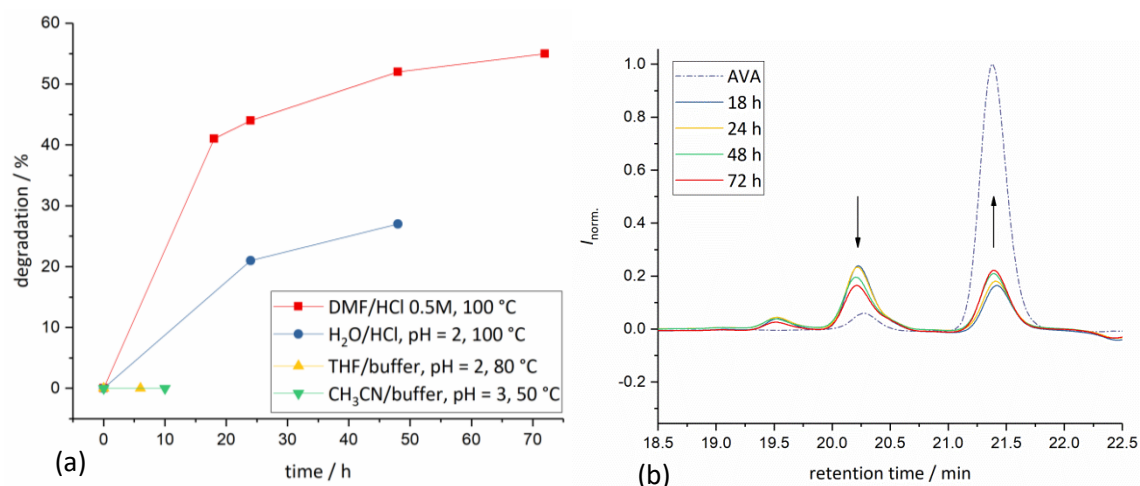


Figure 4.56 Establishment of degradation conditions for AVA carbonate **10**: test of different reaction conditions (a), monitoring of the degradation *via* SEC applying the DMF/HCl system (b) (SEC system B).

Comparing the different degradation conditions, the DMF/HCl system was chosen as most suitable procedure for the degradation of thiol-ene and epoxy resins. Buffer solutions did not lead to a fast degradation of the carbonate linker. Although the aqueous system led to a partial degradation of **10**, an organic solution is advantageous, as it enables a dissolution of the formed degradation product.

After the establishment of a degradation procedure for AVA carbonate **10**, the degradation of the acetal monomers **11** and **12** was also attempted (Figure 4.57).

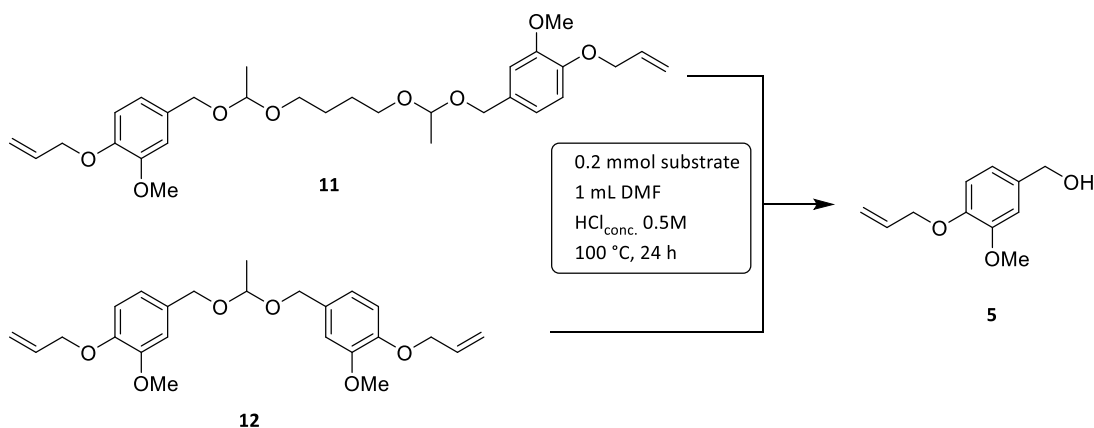


Figure 4.57 Degradation of acetal monomers **11** and **12** to AVA **5** using the established degradation conditions for the DMF/HCl system.

Analogous to the carbonate monomer, 0.2 mmol of the monomers were dissolved in 1.00 mL DMF and 42 μ L concentrated hydrochloric acid in a pressure tube. Subsequently, the vial was sealed and heated to 100 °C for 24 h. The SEC traces of the obtained products are shown in Figure 4.58. Complete degradation of the bisacetal **11** (a) and of the monoacetal monomer **12** (b) was observed after 24 h. AVA **5** was formed as main degradation product in both cases. However, in both SEC traces, the formation of a second degradation product with higher molecular weight is visible. The formed products were not isolated or analyzed; but two possible by-products are conceivable. In the case of bisacetal **11**, the existence of the mono-cleaved product consisting of the allyl vanillyl alcohol still bearing one acetal linker and the C4 carbon spacer is possible. However, as complete degradation was observed for the acetal groups, and a product with the same retention time is also visible in the SEC chromatogram of AVA acetal **12**, this seems unlikely. Another explanation is the formation of the ether-coupled product, which was also observed as side reaction in several coupling reaction attempts. In strong acidic environment, the benzylic alcohol showed an increased tendency for ether formation, which is highly probable in this case.

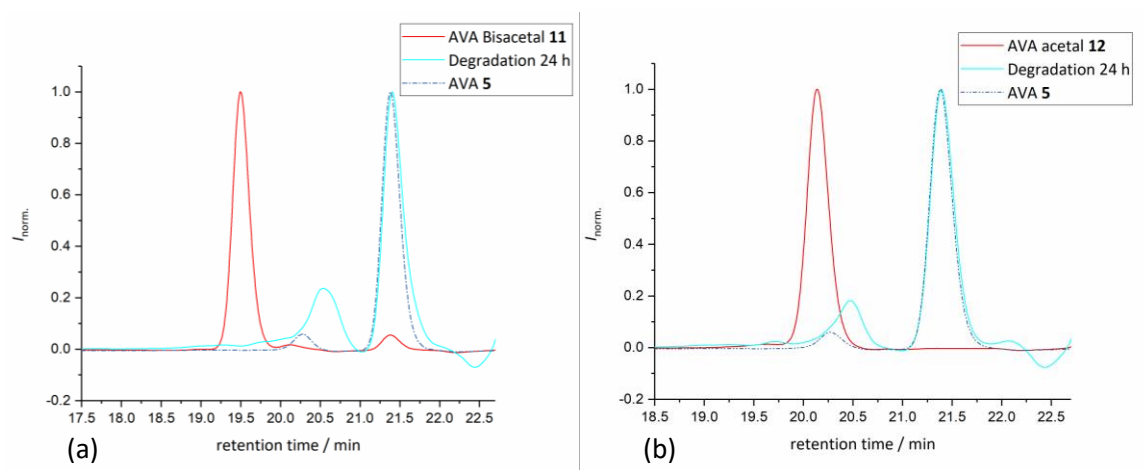


Figure 4.58 Degradation of AVA bisacetal **11** (a) and AVA acetal **12** (b) applying the established degradation conditions (DMF 0.2M, HCl_{conc} 0.5M, 100 °C, 24 h) (SEC system B).

4.5.2 Degradation of Thiol-Ene Film P5

After the successful establishment of degradation conditions of the monomers, the procedure was tested on the thiol-ene polymer film **P5** based on AVA carbonate **10** and myrcene trithiol **50**. The theoretical main product is shown in Figure 4.59. In a glass pressure tube, 34.4 mg of polymer film **P5** were immersed in 1.00 mL DMF and 42.0 μL concentrated hydrochloric acid. The sealed pressure tube was heated to 100 °C and the reaction time was prolonged to 48 h to ensure complete conversion. After 48 h, the polymer was completely soluble. The solvent was removed under reduced pressure and the resulting powder was analyzed by ESI-MS. The obtained mass spectrum is shown in Figure 4.60.

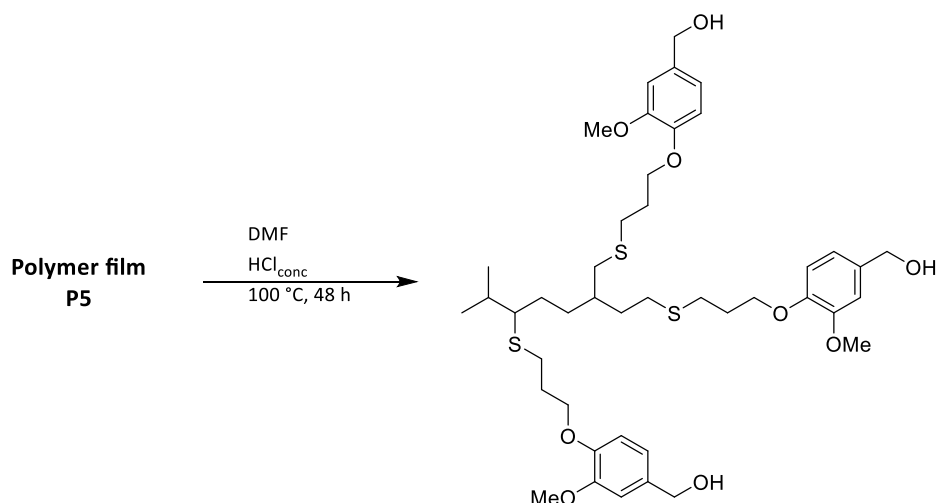


Figure 4.59 Degradation of polymer film **P5** applying the established degradation conditions (DMF, HCl_{conc} , 100 °C).

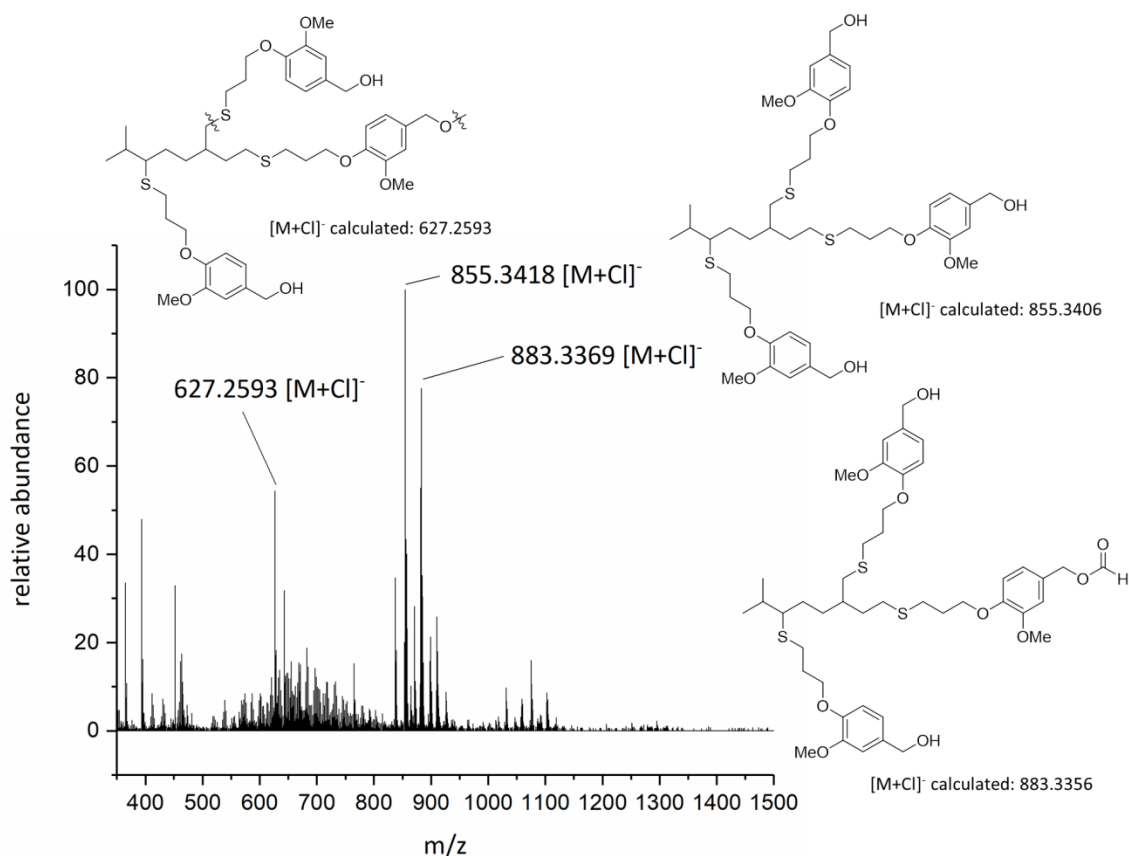


Figure 4.60 ESI-MS spectrum of degraded polymer film **P5** (negative mode) and proposed structures for the most intense peak signals.

The mass spectrum of the degraded polymer **P5** shows degradation products with m/z up to 1,100. The three most intense peaks were analyzed and the proposed structures are shown in Figure 4.60. The most intense peak was assigned to the expected degradation product as shown in Figure 4.59, consisting of the myrcene trithiol linked to three allyl vanillyl alcohol moieties. The second peak exhibited a slightly higher mass. The proposed structure contains the same structure, including the rest of the former carbonate group. The third peak could be assigned to a fragment containing the myrcene backbone and two attached allyl vanillyl ether groups. Besides the three main signals, the spectrum also showed a broad variety of products in the mass range of the di- and trifunctionalized myrcene, indicating a successful degradation of the polymer resin. To confirm the structure of the main degradation product with 855.3418 g/mol, the measured and the calculated isotopic patterns of the proposed structure were compared, the spectra are shown in Figure 4.61. The high agreement of the isotopic patterns proves the formation of the expected degradation product.

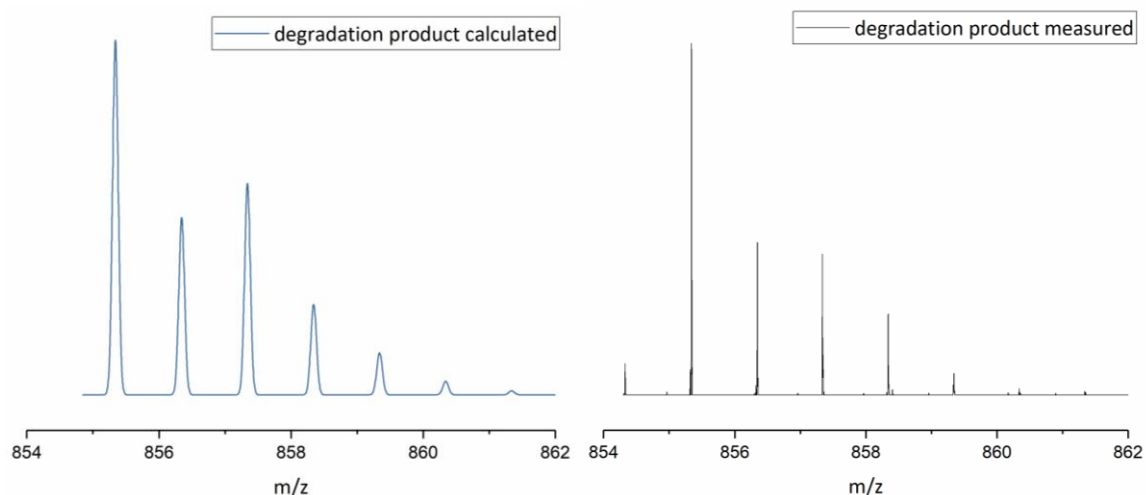


Figure 4.61 Main degradation product of polymer film **P5**: calculated isotopic pattern (left), measured isotopic pattern (right).

In summary, with a degradation of 55% after 72 h, the DMF/HCl system gave the best result of the tested systems for the degradation of AVA carbonate **10**. When the same conditions were applied to the acetal monomers **11** and **12**, full degradation was obtained after 24 h. However, another side product was formed, which presumably consists of the ether-coupled AVA dimer. The formation of this ether linkage might be prevented by performing the degradations at higher dilutions and by using less hydrochloric acid. In contrast, the degradation of AVA carbonate **10** might be improved by increasing the amount of HCl solution. However, also in this case, the formation of the ether side product needs to be considered. The established degradation conditions were subsequently transferred to the thiol-ene polymer film **P5** obtained by the reaction of AVA carbonate **10** and myrcene trithiol **50**. After 48 h at 100 °C, the polymer film was completely dissolved. In the mass spectrum, degradation products in the mass range of 500-1,100 g/mol were identified. The most intense mass peak was identified as the predicted degradation product resulting from the cleavage of the carbonate linker groups. In a next step, the product mixture obtained after degradation needs to be further analyzed (by SEC, NMR and titration) in order to be used for a second polymerization cycle, for instance in polyurethane synthesis, but the results described in this chapter are promising. After successfully establishing the degradation of polymer film **P5**, the recycling of the other cured resins should be investigated in following studies. The sustainability of the degradation conditions should be improved by the replacement of DMF, which is not considered as a green solvent. A more sustainable alternative would increase the overall sustainability of the degradable thermoset system.

5

Conclusion and Outlook

The development of a more sustainable polymer production requires a shift towards renewable resources and environmentally benign synthetic procedures. This is especially relevant for thermosetting polymers, which conventionally are not easily recyclable. Therefore, in this work, new routes for the sustainable synthesis of recyclable thermosets were investigated. In the first part, vanillyl alcohol was used for the synthesis of cleavable monomers that can replace the commercial monomer DGEBA. First, vanillyl alcohol and eugenol were allylated at the phenolic hydroxyl groups using a benign reaction protocol employing palladium nanoparticles in water and allyl methyl carbonate. In a next step, reaction procedures were established for the coupling of vanillyl alcohol at the unreacted benzylic hydroxyl group, introducing acid-labile carbonate and acetal groups. Thus, bis-allylated monomers were obtained. The synthesis of bisepoxide monomers was performed through the epoxidation of allylated vanillyl alcohol employing the sustainable oxidation agent hydrogen peroxide, and coupling reactions following the previously developed procedures. Furthermore, terpenes were investigated for the synthesis of bio-based amine curing agents as a replacement for the commercial hardener IPDA. A synthesis route entailing the epoxidation of terpene double bonds followed by a rearrangement to the respective carbonyl groups was pursued. After screening, bismuth triflate was selected as efficient catalyst for the rearrangement reactions. Thus, the sustainable transformation of terpenes into different biscarbonyl structures was demonstrated. These structures constitute

interesting substrates for polymer synthesis and should be further investigated. As the reductive amination of the biscarbonyls was not efficient, the aminolysis of the epoxides using ammonia solution was used as alternative pathway for the synthesis of diamines. The reaction of limonene dioxide with ammonia was explored in detail and the reaction products (the desired diamine and the mono-amine resulting from the ring-opening of the *endo*-cyclic epoxide) were identified. The same reaction was transferred to the potentially bio-based 1,4-cyclohexane dioxide. In this case, depending on the employed isomer, two regioisomeric products were obtained. Due to the easy synthesis protocol of the aminolysis reaction, this pathway represents an attractive route for the formation of amine hardeners and could be transferred to a multitude of promising substrates.

The synthesized diene monomers were polymerized by thiol-ene polymerizations. The reaction with a dithiol based on limonene yielded low molecular weight oligomers ($M_n = 6,000$ Da, $\bar{D} = 1.35$). As an alternative, the polymerization with a myrcene-based trithiol was performed and led to the formation of translucent cross-linked polymer films. The polymers resulting from monomers containing acetal linkers showed a low cross-linking density, while the monomer featuring a carbonate moiety and allylated eugenol resulted in higher cross-linking densities. Thermal analyses showed glass transition temperatures of 14 °C and -5 °C, respectively. The carbonate film, with a Young's modulus of 6.87 MPa, an ultimate tensile strength of 1.48 MPa and an ultimate elongation at break of 148%, showed promising thermomechanical properties of an elastomeric behavior. Thus, thiol-ene polymerization showed a good potential for the synthesis of sustainable cross-linked polymers, as many renewable molecules, especially terpenes, bear double bonds and can be transformed into polythiol monomers.

The cleavable bisepoxides were investigated as monomers in the synthesis of epoxy resins using the synthesized limonene-based bis-amino alcohol as hardener. In this case, the monomer containing a carbonate linker showed an insufficient cross-linking density and other polymerization pathways, such as cationic curing, should be investigated. Even if an increased cross-linking density was reached applying the acetal linker group, lower thermomechanical properties compared to DGEBA were achieved due to the aliphatic character of the linker. In contrast, epoxidized allyl eugenol showed good thermomechanical properties and could be used as a non-recyclable alternative to DGEBA. The use of limonene bis-amino alcohol as curing agent resulted in polymers with slightly lower glass transition temperatures, but similar mechanical properties compared to IPDA.

In general, degradable linker groups represent a good alternative to introduce recyclability into cross-linked networks. However, the compatibility of the linker groups with each polymerization

technique has to be considered. For instance, the carbonate group was suitable for thiol-ene polymerization, while only low cross-linking densities were achieved in epoxy resin curings. On the other hand, the acetal-coupled monomers did not give satisfactory results in thiol-ene reactions, but showed to be suitable for epoxy resin curings.

Finally, reaction conditions for the degradation of the synthesized cross-linked polymers were established. Using the cleavable monomers, several degradation conditions were tested. A mixture of DMF and hydrochloric acid and a reaction temperature of 100 °C were found to be the most efficient system. Subsequently, the established degradation conditions were transferred to the thiol-ene polymer film containing carbonate linker groups. After 48 h, the polymer was completely dissolved and the most intense peaks in the mass spectrum of the resulting residue could be assigned to the expected degradation products, *i.e.* a polyol, showing the successful degradation of the polymer network.

In a next step, the degradation of the other synthesized resins needs to be investigated. The degradation products need to be further analyzed to assess their functionality and to establish synthesis routes for a follow-up polymerization step and thus a second life cycle of the material. For instance, the synthesis of polyurethanes or polyesters is envisaged. Another interesting application for the terpene-based biscarbonyl structures is the use in covalent adaptable networks, such as imine vitrimers, which constitutes an attractive pathway for the synthesis of recyclable thermosets. If reacted with a co-monomer bearing at least three amine groups, a polyimine network is formed. Promising first results were already obtained within the scope of this thesis for biscarbonyl **30**, as shown in Figure 5.1 (top).^{*} The synthesis of polyfunctional amine monomers was performed by a reaction of linseed oil with cysteamine hydrochloride (CAHC) in a thiol-ene reaction applying reaction conditions reported in literature for the transformation of grapeseed oil (Figure 5.1, bottom).^[315] Experimental details can be found in chapter 6.3.5. An average functionalization of three amine groups per molecule was estimated according to the decrease of double bond signals in the ¹H-NMR spectrum.

^{*} The study was carried out by Alina Wagner in the scope of her Bachelor thesis “Synthese bio-basierter Polyamine für Polymeranwendungen” under my co-supervision.

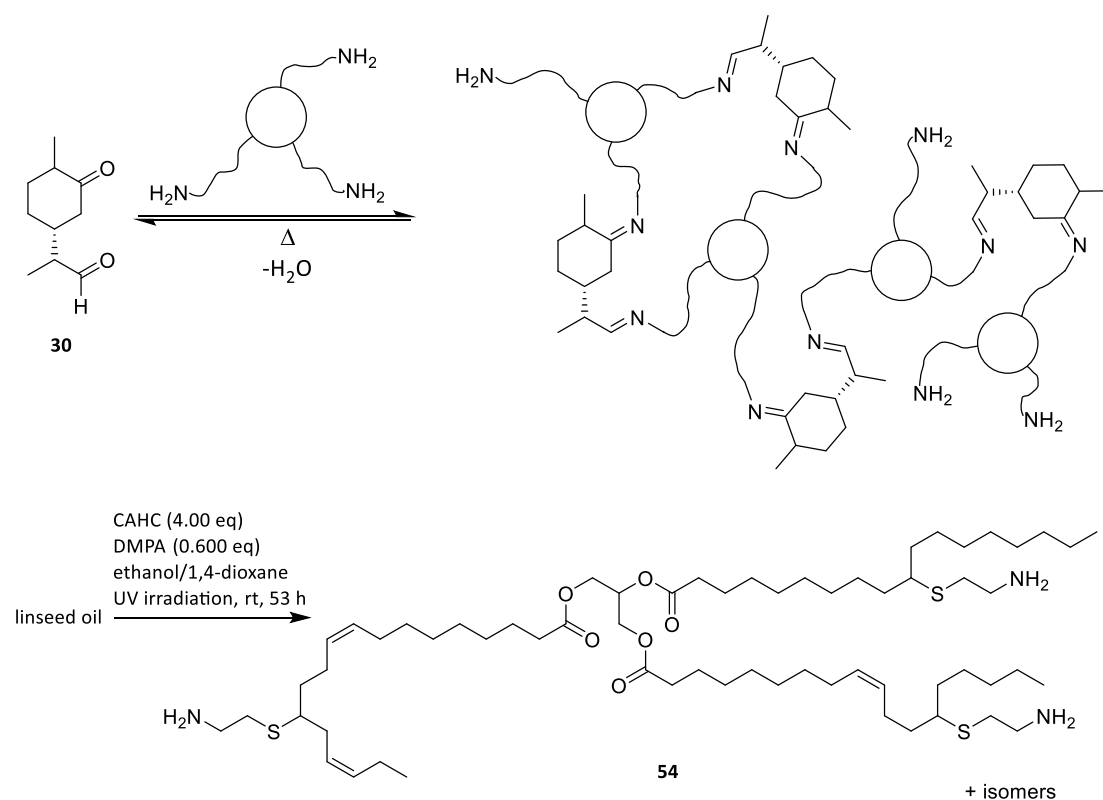


Figure 5.1 General scheme for the formation of imine vitrimer networks from bis-carbonyl **30** (top) and representative structure of the amine **54** obtained from linseed oil *via* thiol-ene reaction applying cysteamine hydrochloride (bottom).

In a first step, a curing in the DSC instrument was carried out to determine the reactivity of the mixture and the glass transition temperature of the resulting material. The bis-carbonyl **30** and the polyamine **54** were mixed in equimolar ratios regarding the amount of functional groups. The curing in the DSC was carried out by heating the sample to 180 °C, cooling down to -20 °C and again heating to 180 °C at a heating rate of 10 K/min. In the first heating cycle, no clear exothermic curing could be distinguished. However, in the second heating cycle, a T_g of 63 °C was observed (Figure 5.2, bold line).

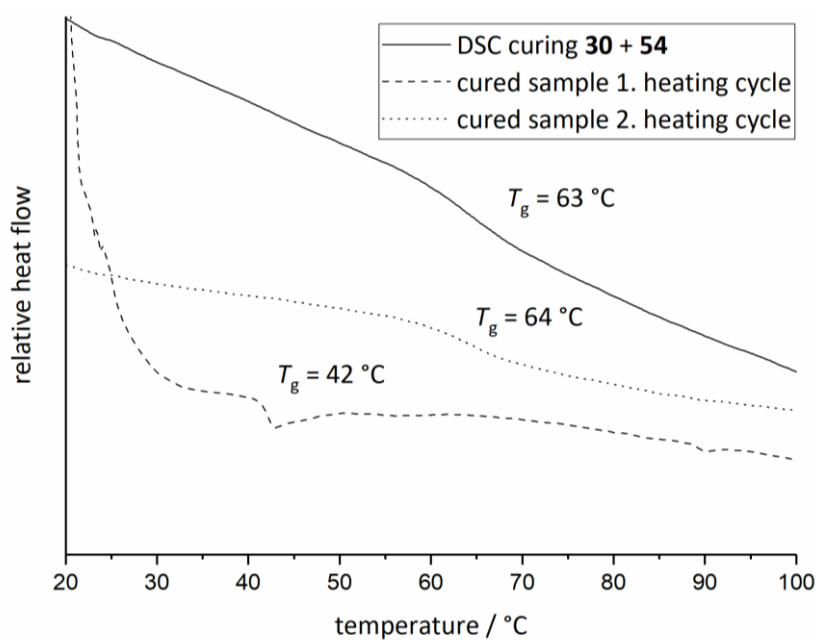


Figure 5.2 DSC curing measurement of biscarbonyl **30** with amine **54** (bold line) and the DSC analysis of the cured sample (dashed lines) (DSC system B).

In a next step, amine **54** was used for a curing with biscarbonyl **30** in the vacuum oven. 18.6 mg (0.111 mmol) of biscarbonyl **30** were mixed with 82.2 mg (74.0 μmol calculated for a triamine) **54** and the curing was carried out at 80 °C for 16 h in the vacuum oven to remove the formed water from the network. As a result, a soft material was obtained, which was analyzed by DSC measurements. The DSC traces of the first and second heating cycle are shown in Figure 5.2 (dashed lines). In the first heating cycle, a comparably low T_g of 42 °C was obtained, whereas in the second heating cycle, a higher T_g of 64 °C was observed. This result clearly shows that the chosen curing program was not sufficient to reach complete curing of the material. In a next step, the curing procedure needs to be improved to reach a fully cured imine polymer. Then, mechanical properties and the reshaping of the material needs to be tested to confirm the recyclability of the polymer network. Nevertheless, the study represents a promising first result for the vitrimer synthesis from terpene-based biscarbonyls. The obtained results can be used as basis for further research to improve the reaction protocol and to transfer the optimized reaction conditions to the other terpene-based biscarbonyl structures, opening up a new application field for these versatile molecules.

Overall, in this work, novel routes for the synthesis of recyclable bio-based thermosets were presented. The Twelve Principles of Green Chemistry were used as guidelines to establish benign synthesis routes and to achieve sustainable transformations of renewable resources into valuable monomers and polymers.

6

Experimental Section

6.1 Materials

All solvents were used without further purification. Water, when used in the synthesis, was de-ionised.

The following chemicals were used as received:

cerium(IV)-sulfate (99%, Sigma-Aldrich), chloroform-d (CDCl_3 , 99.8 atom-% D, Euriso-Top), dimethyl sulfoxide-d₆ (99.8 atom-% D, Euriso-Top), ethyl vinyl ether (99%, Sigma-Aldrich), phosphomolybdic acid hydrate (99%, Sigma-Aldrich), silica gel 60 (0.040-0.063, Sigma-Aldrich), sodium sulfate (99%, Bernd Kraft), TLC silica F₂₅₄ (Sigma-Aldrich), hydrogen peroxide (30 wt% in H₂O, Sigma-Aldrich), limonene dioxide (mixture of cis-(+) and trans(+) isomers, 98%, Rheinmetall Nitrochemie), (*R*)-(+)-limonene (97%, Sigma-Aldrich), cysteamine hydrochloride (>97%, Fluka), 2,2-dimethoxy-2-phenylacetophenon (DMPA, 99%, Sigma-Aldrich), ninhydrin (95%, ChemPur), sodium chloride (99.5%, Fisher chemical), (+)-dihydrocarvone (98%, Sigma-Aldrich), sodium hydrogen carbonate (>95%, Sigma-Aldrich), Oxone® (Sigma-Aldrich), (*R*)-(-)-carvone (98%, Sigma-Aldrich), acetone (>99.5%, Sigma-Aldrich), sodium hydroxide (98%, Sigma-Aldrich), γ -terpinene (>97%, Sigma-Aldrich), tetradecane (99%, Sigma-Aldrich), boron trifluoride etherate (46-51% BF₃, Sigma-Aldrich), aluminium chloride (98.5%, Acros Organics), zinc bromide (98%, Sigma-Aldrich), magnesium chloride hexahydrate (99%, Sigma-Aldrich), copper(I) chloride (97%, Sigma-Aldrich), copper(II) chloride (97%, Sigma-Aldrich), dichlorobis(triphenylphosphine)nickel(II) (98%, Sigma-

Aldrich), palladium acetate (98%, Sigma-Aldrich), triphenylphosphine (n.a.), aluminium oxide (Brockmann I, Acros Organics), bismuth triflate (99%, Alfa Aesar), indium triflate (Sigma-Aldrich), silver triflate (>99%, Sigma-Aldrich), ytterbium triflate (99.9%, Acros Organics), zinc triflate (98%, Sigma-Aldrich), allyl alcohol (99%, Acros Organics), dimethyl carbonate (>99%, Sigma-Aldrich), 1,5,7-Triazabicyclo(4.4.0)dec-5-en (TBD, 98%, Sigma-Aldrich), vanillyl alcohol (99%, Acros Organics), palladium nanoparticles (Pd_{NP}@PVP, particles were synthesized by Dr. Silke Behrens (IKFT) and analyzed by TEM, DLS and AES-ICP,^[79] palladium content: 0.0404 mmol/mL), pyridinium *p*-toluenesulfonate (PPTS, >99%, Fluka), 1,4-butanediol divinyl ether (98%, Sigma-Aldrich), dichloromethane (99.8%, Fisher Scientific), ethanol (>99.8%, Fisher Scientific), ammonium bicarbonate (>99%, Sigma-Aldrich), acetonitrile (>99.9%, Fisher Scientific), sodium sulfite (technical grade, Carl Roth), methanol (HPLC grade, VWR chemicals), 2-methyl tetrahydrofuran (>99.5%, Sigma-Aldrich), eugenol (99%, Acros Organics), *tert*-butyl acetoacetate (97%, Acros Organics), vanillin (99%, Acros Organics), urea (technical grade), *p*-toluenesulfonic acid monohydrate (99%, Acros Organics), triethyl amine (>99.5%, Fisher Scientific), tetrahydrofuran (>99.7%, VWR chemicals), NH₃ (7N in MeOH, Sigma-Aldrich), high oleic sunflower oil (Cargill), linseed oil (cold-pressed, Brändle), 1,4-dioxane (99%, Acros Organics), chloroform (>99.8%, Fisher Scientific), sodium carbonate (technical grade, Solvay), thioacetic acid (96%, Sigma-Aldrich), myrcene (90%, Acros Organics), bisphenol A diglycidyl ether (DGEBA, Sigma-Aldrich), isophorone diamine (IPDA, *cis*- and *trans*-mixture, >99%, TCI), Raney-Ni[®] (slurry in H₂O, Sigma-Aldrich), Octylamine (99%, Alfa Aesar), sodium tungstate (99%, Sigma-Aldrich), peracetic acid (38–40% in acetic acid, Merck), *Candida Antarctica* lipase B (immobilized on acrylic resin, Sigma-Aldrich), Aliquat[®] 336 (Sigma-Aldrich), methyltrioxorhenium (MTO, Re: 71-76%, Sigma-Aldrich), phosphoric acid (40%, Sigma-Aldrich), ammonium acetate (99.6%, Fisher Scientific), ammonium chloride (technical grade), ammonium formate (97%, Sigma-Aldrich), ammonia (28%, Acros Organics), palladium on activated charcoal (10% palladium basis, Sigma-Aldrich), Rh/Al₂O₃ (5 wt% Rh, Sigma-Aldrich), *p*-benzoquinone (>99%, Sigma-Aldrich), Hoveyda-Grubbs catalyst 2nd generation (97%, Sigma-Aldrich), hydrochloric acid (37%, Fisher chemical), molecular sieve (3Å, Sigma-Aldrich), *N,N*-dimethylformamide (99.8%, Sigma-Aldrich), benzyl bromide (98%, Acros Organics), di-*tert*-butyl dicarbonate (≥98 %, Fluka), Priamine[®] (Croda), urea-hydrogen peroxide (97%, Sigma-Aldrich), Hoveyda-Grubbs first generation (Sigma-Aldrich), 1,6-hexanedithiol (97%, Alfa Aesar).

6.2 Characterization Methods

Thin layer chromatography was carried out on silica gel coated aluminium foil (TLC silica gel F254, Sigma-Aldrich). Compounds were visualized by staining with Seebach-solution (mixture of phosphomolybdic acid hydrate, cerium(IV) sulfate, sulfuric acid and water).

High pressure reactions were performed in a high-pressure laboratory reactor (BR-100) from Berghof products + instruments.

UV Curings were carried out with an Awelcure UV-LED Curing System using a lamp with 1000 mW/cm² and a wavelength of 365 nm. At the applied distance of 9 cm, an intensity of around 750 mW/cm² was achieved according to spectral data provided by the manufacturer. Samples were cured at 50% power for 10 min.

Curings were carried out in a Thermo Scientific VacuTherm VT6025 oven attached to a high vacuum pump.

NMR spectra were recorded on BRUKER Advance DPX spectrometers (Billerica, MA) with a 5-mm dual proton/carbon probe operating at 300 MHz or 400 MHz for ¹H spectra and 75.5 MHz or 101 MHz for ¹³C spectra, respectively. CDCl₃, DMSO-d₆ or MeOD were used as solvent and the resonance signals at 7.26 ppm, 2.50 ppm and 3.31 ppm (¹H) and 77.16 ppm, 39.52 ppm and 49.00 ppm (¹³C) served as reference, respectively for ¹H and ¹³C NMR, for the chemical shift δ . The spin multiplicity and corresponding signal patterns were abbreviated as follows: s = singlet, d = doublet, t = triplet, q = quartet, quint. = quintet, m = multiplet Coupling constants *J* were noted in Hz. Furthermore, 2D NMR methods, *e.g.* heteronuclear single quantum coherence (HSQC), heteronuclear multiple bond correlation (HMBC) and correlated spectroscopy (COSY) were carried out, if necessary, for signal assignment and structure elucidation.

GC chromatograms were recorded with a Bruker 430 GC instrument with a capillary column FactorFourTM VF-5ms (30 m × 0.25 mm × 0.25 mm) and a flame ionization detector (FID). Tetradecane was used as internal standard. Heating program: Start at 95 °C, heating to 200 °C with 15 °C/min. Hold at 200 °C for 4 min. Heating to 300 °C with 15 °C/min. Hold at 300 °C for 2 min. To calculate the conversion, the ratio of the product peak area divided by the reference peak area (tetradecane) at a given reaction time (*t*) was compared to the respective ratio at the beginning of the reaction (*t*₀). The non-isolated yields were estimated by dividing the product peak area by the total area of all peaks (excluding the tetradecane reference). For selectivity, the

product peak area was divided by the area of all product peak areas, without the starting material and the tetradecane reference.

GC-MS (electron impact (EI)) measurements were performed on the following system: a Varian 431 GC instrument with a capillary column FactorFour VF-5 ms (30 m × 0.25 mm × 0.25 mm) and a Varian 210 ion trap mass detector. Scans were performed from 40 to 650 m/z at rate of 1.0 scans/s. The oven temperature program was: initial temperature 95 °C, hold for 1 min, ramp at 15 °C/min to 220 °C, hold for 4 min, ramp at 15 °C/min to 300 °C, hold for 2 min. The injector transfer line temperature was set to 250 °C. Measurements were performed in the split-split mode (split ratio 50:1) using helium as carrier gas (flow rate 1.0 mL/min).

Fast atom bombardment (**FAB**) and Electron Ionisation (**EI**) mass spectra were recorded on a Finnigan MAT 95 instrument.

Orbitrap Electrospray-Ionisation Mass Spectrometry (**ESI-MS**) mass spectra were recorded on a Q Exactive (Orbitrap) mass spectrometer (Thermo Fisher Scientific, San Jose, CA, USA) equipped with an atmospheric pressure ionisation source operating in the nebuliser assisted electrospray mode. The instrument was calibrated in the m/z-range 150-2000 using a standard containing caffeine, Met-Arg-Phe-Ala acetate (MRFA) and a mixture of fluorinated phosphazenes (Ultramark 1621, all from Sigma Aldrich). A constant spray voltage of 3.5 kV, a dimensionless sheath gas of 6, and a sweep gas flow rate of 2 were applied. The capillary voltage and the S-lens RF level were set to 68.0 V and 320°C, respectively.

Infrared spectra (**IR**) were recorded on a Bruker Alpha-p instrument in a frequency range from 3997.21 to 373.942 cm⁻¹ applying ATR-technology.

Size exclusion chromatography (**SEC**) analyses were performed either on system A, system B or system C:

System A: A Shimadzu LS 20A system equipped with a SIL-20A autosampler and a RID-10A refractive index detector was used with the solvent THF (flow rate 1mL min⁻¹) at 40 °C as the mobile phase. The analysis was performed on the following column system: main column PSS SDV analytical (5 µm, 300 × 8.0 mm, 10,000 Å) with a PSS SDV analytical precolumn (5 µm, 50 × 8.0 mm). For the calibration, narrow linear poly(methyl methacrylate) standards (Polymer Standards Service, PPS, Germany) ranging from 1,100 to 981,000 g/mol were used.

System B: Measurements were performed on a SHIMADZU Size Exclusion Chromatography (SEC) system equipped with a SHIMADZU isocratic pump (LC-20AD), a SHIMADZU refractive index detector (24 °C) (RID-20A), a SHIMADZU autosampler (SIL-20A) and a VARIAN column oven (510,

50 °C). For separation, a three-column setup was used with one SDV 3 μm , 8 \times 50 mm precolumn and two SDV 3 μm , 1000 \AA , 3 \times 300 mm columns supplied by PSS, Germany. Tetrahydrofuran (THF) stabilized with 250 ppm butylated hydroxytoluene (BHT, $\geq 99.9\%$) supplied by SIGMA-ALDRICH was used at a flow rate of 1.0 mL min^{-1} . Calibration was carried out by injection of eight narrow polymethylmethacrylate standards ranging from 102 to 58300 kDa.

System C: Measurements were performed in HFIP containing 0.1 wt% potassium trifluoroacetate with Tosoh EcoSEC HLC-8320 SEC system. The solvent flow was 0.40 mL \cdot min $^{-1}$ at 30 °C and the concentration of the samples was 1 mg \cdot mL $^{-1}$. The analysis was performed on a three column system: PSS PFG Micro precolumn (3.0 \times 0.46 cm, 10,000 \AA), PSS PFG Micro (25.0 \times 0.46cm, 1000 \AA) and PSS PFG Micro (25.0 \times 0.46cm, 100 \AA). The system was calibrated with linear poly(methylmethacrylate) standards (Polymer Standard Service, Mp:102-981 kDa).

Differential Scanning Calorimetry (**DSC**) measurements were performed on either system A or system B:

System A: Measurements were performed on DSC Q100 (TA Instruments). For curing reactions, samples were heated from 20 °C to 250 °C at a rate of 10 °C \cdot min $^{-1}$. Consecutive cooling and the second heating run were also performed at 10 °C \cdot min $^{-1}$. The glass transition temperatures were calculated from the second heating run. For the analysis of the cured resins, samples were heated from -10 °C to 150 °C at a rate of 10 °C \cdot min $^{-1}$. For the analysis of cured thiol-ene films, samples were heated from -30 °C to 150 °C at a rate of 10 °C \cdot min $^{-1}$ to determine the glass transition temperature.

System B: Experiments were carried out using a Mettler Toledo DSC star^e system. The DSC experiments were carried out under nitrogen atmosphere using 40 μl aluminium crucibles. Samples were heated from 20 °C to 180 °C with a heating rate of 10 °C \cdot min $^{-1}$. Consecutive cooling to -20 °C and the second heating cycle were also performed at 10 °C \cdot min $^{-1}$. For curing reactions in the DSC, the glass transition temperatures were calculated from the second heating run.

Thermogravimetric analyses (**TGA**) were performed on TGA-Q500 system from TA instruments under air atmosphere. Starting at room temperature, samples were heated to 700 °C with a heating rate of 10 °C \cdot min $^{-1}$.

Dynamic Mechanical Analysis (**DMA**) measurements were performed on a DMA RSA 3 (TA instrument) equipped with a liquid nitrogen cooling system. Forced strain was used on a rectangular tensile geometry at a frequency of 1 Hz, a strain of 0.02% and a temperature range between -40 °C and $T_g + 10$ °C at a rate of 3 °C \cdot min $^{-1}$.

To determine the mechanical properties of the polymers, **tensile stress** and **tensile strain** were obtained using a DMA apparatus in traction transient mode at a rate of 10 mm/min. Tensile tests were performed on polymers processed into films. The effective length, width, and thickness of the specimens were generally 8, 5, and 0.1 mm, respectively. Four to five replicated measurements were taken for each sample.

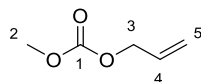
Swelling properties of weighed bar samples (m_0) of the cross-linked polymers were analyzed. After immersion in THF for 24 h, the swollen samples were dried under vacuum at 100 °C over night and weighed again (m_D) to obtain the soluble part of the networks:

$$\text{Soluble part / \%} = 100 \times (1 - m_D/m_0)$$

6.3 Experimental Procedures

6.3.1 Experimental Procedures for Chapter 4.1

Allyl methyl carbonate **3**



The synthesis of allyl methyl carbonate was carried out according to literature.^[79]

A mixture of 68.3 mL (58.1 g, 1.00 mol, 1.00 eq) allyl alcohol and 631 mL (676 g, 7.50 mol, 7.50 eq) dimethyl carbonate was stirred at 80 °C in a round bottom flask for five minutes. Subsequently, 1.39 g (10.0 mmol, 0.01 eq) TBD was added to the flask. The reaction was run for 1 h. A mixture of dimethyl carbonate, allyl methyl carbonate and diallyl carbonate was obtained and separated by distillation. The product was distilled at 100 mbar and 70 °C.

Yield: 28%

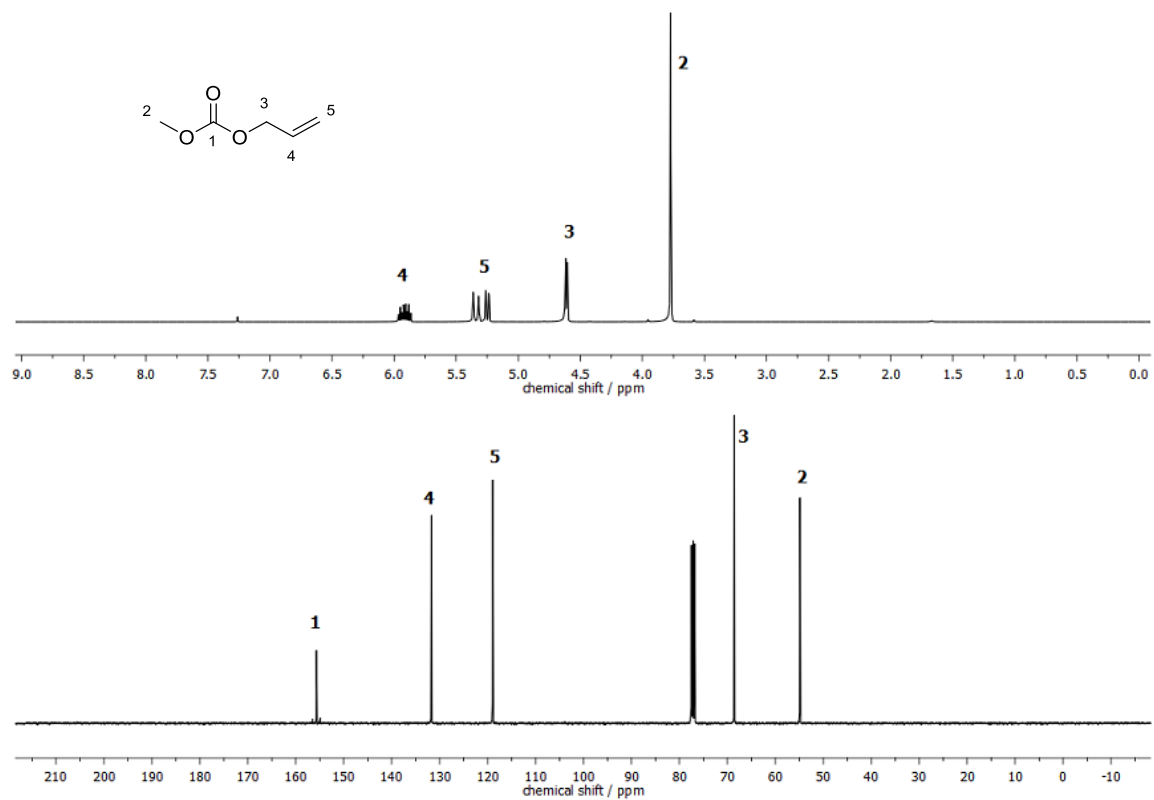
¹H-NMR (400 MHz, CDCl₃) δ / ppm = 5.96-5.87 (m, 1H, H4), 5.37-5.23 (m, 2H, H5), 4.62-4.60 (m, 2H, H3), 3.77 (s, 3H, H2).

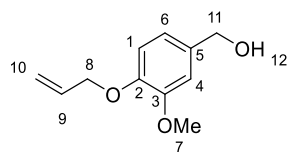
¹³C-NMR (101 MHz, CDCl₃) δ / ppm = 155.70, 131.70, 118.91, 68.56, 54.88.

IR (ATR platinum diamond): ν / cm⁻¹ = 2959.3, 1745.5, 1650.6, 1444.1, 1365.1, 1249.1, 965.0, 927.5, 790.8, 555.2.

The NMR spectra are in accordance with the literature.^[79]

Experimental Section



Allylated vanillyl alcohol ((4-(allyloxy)-3-methoxyphenyl)methanol) 5

The synthesis of allylated vanillyl alcohol was carried out according to literature.^[79]

In a round bottom flask, 10.0 g (64.9 mmol, 1.00 eq) vanillyl alcohol were mixed with 18.8 g (162 mmol, 2.50 eq) allyl methyl carbonate and 851 mg (3.25 mmol, 0.05 eq) triphenylphosphine in 90 mL water. Palladium nanoparticles stabilized in water (Pd_{NP}@PVP, 0.10 mol%, 64.9 μmol, 1.60 mL) were added to the mixture and the reaction was stirred at 90 °C for 16 h. The reaction mixture was poured in a separation funnel and extracted with ethyl acetate. The combined organic phases were dried over sodium sulfate and the solvent was removed under reduced pressure. The crude mixture was purified by column chromatography (30% EtOAc/CH).

Yield: 75%

R_f = 0.45 (50% EtOAc/CH)

¹H-NMR (300 MHz, DMSO-d₆) δ / ppm = 6.93-6.63 (m, 3H, H1+H4+H6), 6.09-5.96 (m, 1H, H9), 5.40-5.21 (m, 2H, H10), 5.07 (t, *J* = 5.7 Hz, 1H, H12), 4.51 (d, *J* = 3.9 Hz, 2H, H8), 4.41 (d, *J* = 5.5 Hz, 2H, H11), 3.75 (s, 3H, H7).

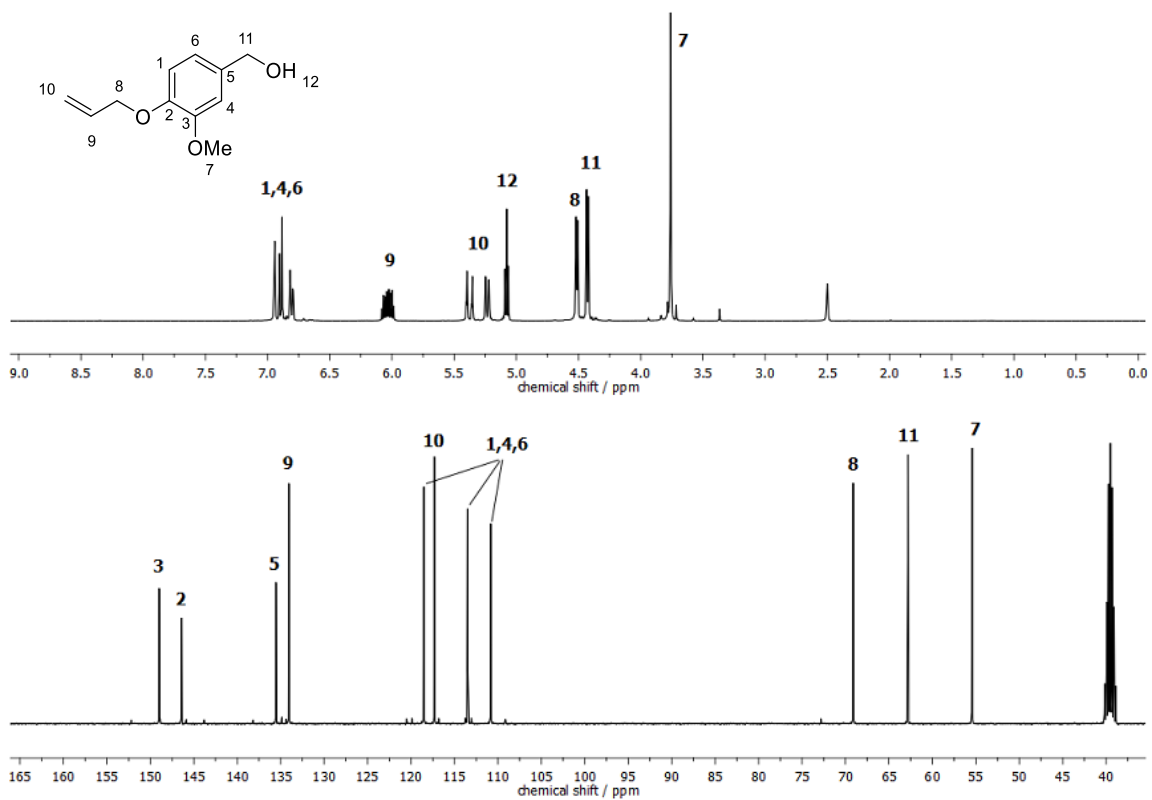
¹³C-NMR (75 MHz, DMSO-d₆) δ / ppm = 148.93, 146.38, 135.51, 134.06, 118.49, 117.33, 113.44, 110.80, 69.09, 62.78, 55.42.

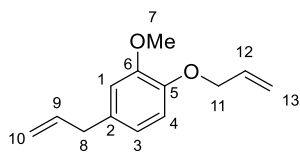
IR (ATR platinum diamond): ν / cm⁻¹ = 3330.9, 2993.4, 2906.2, 2856.2, 2354.3, 2157.7, 2033.5, 1860.9, 1646.6, 1591.6, 1512.7, 1454.9, 1417.9, 1365.1, 1319.3, 1294.0, 1252.2, 1232.6, 1136.9, 1059.6, 1022.8, 1005.0, 989.0, 925.7, 916.5, 853.5, 820.2, 802.6, 739.7, 642.2, 606.0, 592.4, 575.2, 522.1, 462.538, 409.7.

EI-HRMS of C₁₁H₁₄O₃ [M]⁺ calculated: 194.0937, found: 194.0937.

The NMR spectra are in accordance with the literature.^[79]

Experimental Section



Allylated eugenol (4-allyl-1-(allyloxy)-2-methoxybenzene)* 7

The synthesis of allylated eugenol was carried out according to literature.^[79]

In a round bottom flask, 10.0 g (60.9 mmol, 1.00 eq) eugenol were mixed with 14.1 g (122 mmol, 2.00 eq) allyl methyl carbonate and 799 mg (3.05 mmol, 0.05 eq) triphenyl phosphine in 70 mL water. Palladium nanoparticles stabilized in water (Pd_{NP}@PVP, 0.10 mol%, 60.9 μmol, 1.51 mL) were added to the mixture and the reaction was stirred at 90 °C for 4 h. The reaction mixture was poured in a separation funnel and extracted with ethyl acetate. The combined organic phases were dried over sodium sulfate and the solvent was removed under reduced pressure. The crude mixture was purified by column chromatography (25% EtOAc/CH).

Yield: 96%

R_f = 0.58 (10% EtOAc/CH)

¹H-NMR (400 MHz, DMSO-d₆) δ / ppm = 6.88-6.66 (m, 3H, H1+H3+H4), 6.07-5.89 (m, 2H, H9+H12), 5.39-5.21 (m, 2H, H13), 5.09-5.01 (m, 2H, H10), 4.50 (d, *J* = 5.3 Hz, 2H, H11), 3.74 (s, 3H, H7), 3.29 (d, *J* = 6.7 Hz, 2H, H8).

¹³C-NMR (101 MHz, DMSO-d₆) δ / ppm = 149.05, 145.94, 137.93, 134.05, 132.59, 120.14, 117.25, 115.47, 113.80, 112.55, 69.09, 55.43, 39.09.

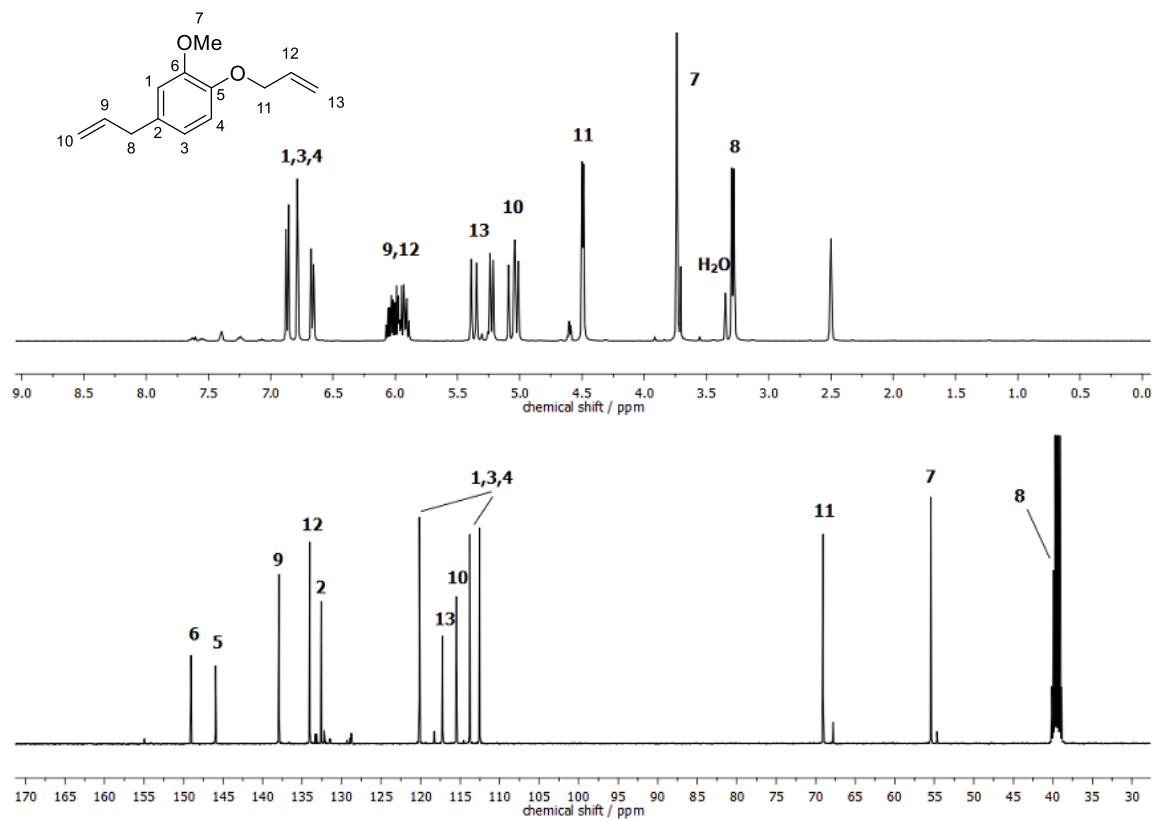
IR (ATR platinum diamond): ν / cm⁻¹ = 3077.7, 2907.2, 1638.2, 1589.7, 1508.6, 1463.0, 1419.4, 1361.9, 1257.6, 1227.6, 1139.2, 1023.3, 992.9, 913.5, 849.5, 801.0, 746.6, 722.1, 696.8, 657.0, 599.0, 541.7, 459.3.

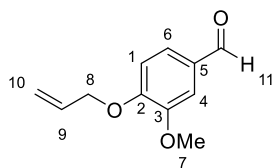
EI-HRMS of C₁₃H₁₆O₂ [M]⁺ calculated: 204.1145, found: 204.1149.

The NMR spectra are in accordance with the literature.^[79]

* This reaction was performed by Annika Nutz in the scope of an internship under my co-supervision.

Experimental Section



Allylated vanillin (4-(allyloxy)-3-methoxybenzaldehyde) 9

The synthesis of allylated vanillin was carried out according to a literature known procedure.^[79]

In a round bottom flask, 15.0 g vanillin (98.6 mmol, 1.00 eq) were mixed with 28.6 g allyl methyl carbonate (247 mmol, 2.50 eq) and 1.29 g triphenyl phosphine (4.93 mmol, 0.05 eq) in 140 mL water. Palladium nanoparticles stabilized in water (0.10 mol%, 98.6 μ mol, 2.44 mL) were added to the mixture and the reaction was stirred at 90 °C for 22 h. The reaction mixture was poured in a separation funnel and extracted with ethyl acetate. The combined organic phases were dried over sodium sulfate and the solvent was removed under reduced pressure. The crude mixture was purified by column chromatography (10- \rightarrow 20% EtOAc/CH).

Yield: 76%

R_f = 0.56 (40% EtOAc/CH)

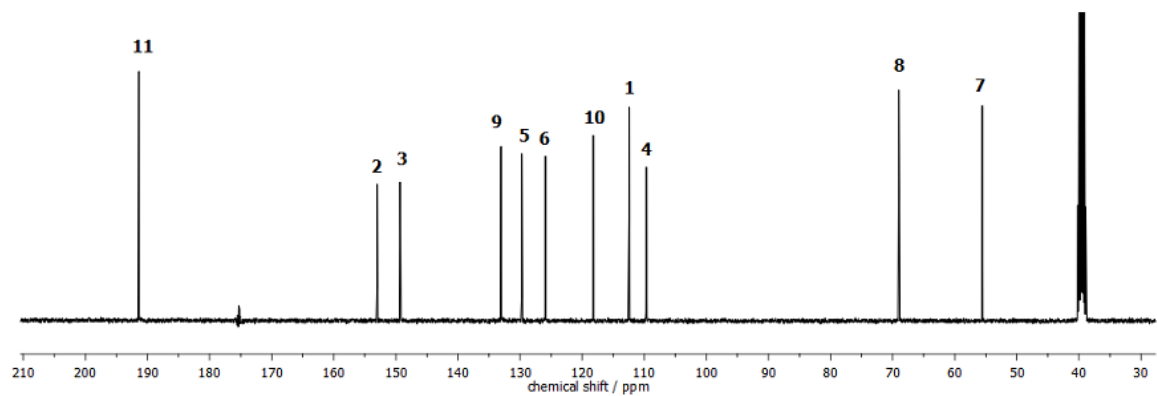
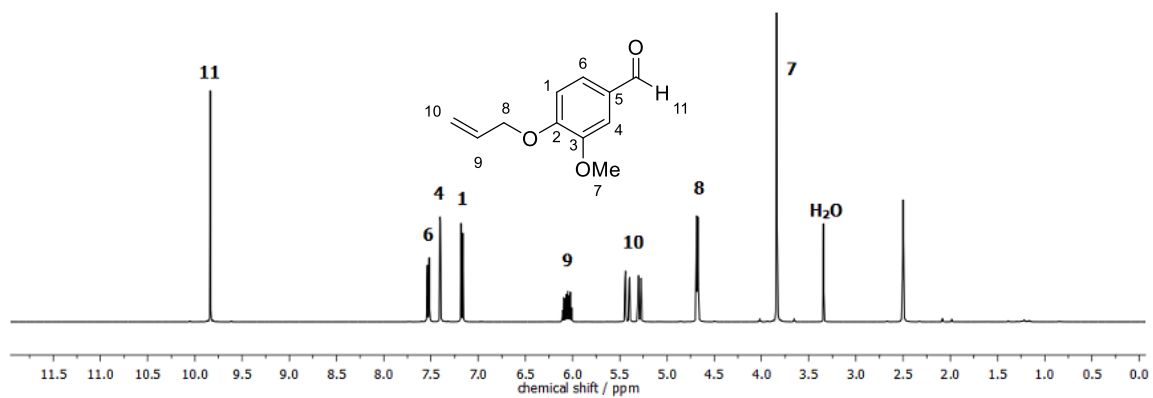
¹H-NMR (400 MHz, DMSO-*d*₆) δ / ppm = 9.84 (s, 1H, H11), 7.53 (dd, *J* = 8.2, 1.9 Hz, 1H, H6), 7.40 (d, *J* = 1.8 Hz, 1H, H4), 7.17 (d, *J* = 8.3 Hz, 1H, H1), 6.11-6.01 (m, 1H, H9), 5.45-5.27 (m, 2H, H10), 4.68 (dt, *J* = 5.3, 1.3 Hz, 2H, H8), 3.84 (s, 3H, H7).

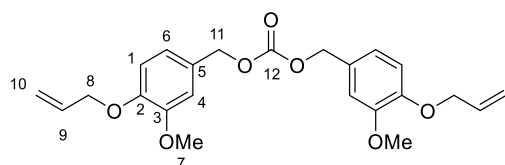
¹³C-NMR (101 MHz, DMSO-*d*₆) δ / ppm = 191.40, 153.01, 149.32, 133.06, 129.74, 125.92, 118.23, 112.54, 109.68, 69.00, 55.69.

IR (ATR platinum diamond): ν / cm⁻¹ = 2937.9, 2834.2, 1678.6, 1583.7, 1505.3, 1463.2, 1422.4, 1395.1, 1338.0, 1262.0, 1230.8, 1194.5, 1158.3, 1132.0, 1030.7, 991.7, 929.1, 865.3, 805.9, 780.8, 729.3, 659.7, 631.0, 588.8, 567.4, 427.5.

EI-HRMS of C₁₁H₁₂O₃ [M]⁺ calculated: 192.0781, found: 192.0787.

Experimental Section



AVA carbonate (bis(4-(allyloxy)-3-methoxybenzyl) carbonate) 10

1.00 g (5.15 mmol, 1.00 eq) AVA **5** was dissolved in 4.64 g (51.5 mmol, 10.0 eq) dimethyl carbonate. To this solution, 35.8 mg (258 μmol , 5.00 mol%) TBD were added and the mixture was heated to 80 °C under reflux for 6 hours. The progress of the reaction was checked *via* TLC. Unreacted dimethyl carbonate was removed with the rotary evaporator. Then, 1.05 g (5.41 mmol, 1.05 eq) AVA were added and the mixture was heated to 100 °C under reflux for 24 hours. Again, the progress of the reaction was monitored using TLC. After completion of the reaction, 30 mL of ethyl acetate were added. The organic phase was washed with water (3 \times 30 mL) and brine (30 mL), dried over sodium sulfate and the solvent was removed under vacuum. The product was purified *via* column chromatography (5% \rightarrow 30% EtOAc/CH) and obtained as a white solid.

Yield: 67%

R_f = 0.56 (40% EtOAc/CH)

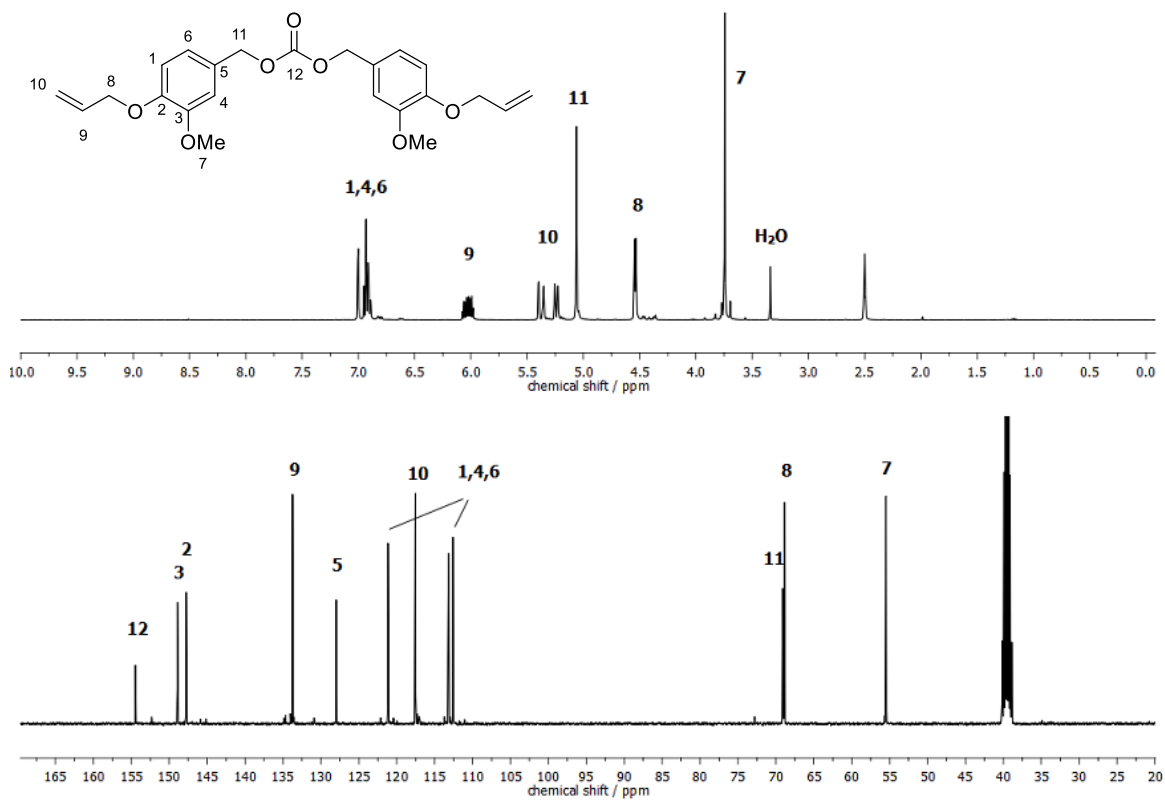
$^1\text{H-NMR}$ (400 MHz, DMSO- d_6) δ / ppm = 7.00-6.89 (m, 6H, H1+H4+H6), 6.07-5.98 (m, 2H, H9), 5.40-5.22 (m, 4H, H10), 5.06 (s, 4H, H11), 4.54 (dt, J = 5.3, 1.4 Hz, 4H, H8), 3.74 (s, 6H, H7).

$^{13}\text{C-NMR}$ (101 MHz, DMSO- d_6) δ / ppm = 154.46, 148.91, 147.77, 133.75, 128.00, 121.15, 117.55, 113.18, 112.60, 69.10, 68.90, 55.50.

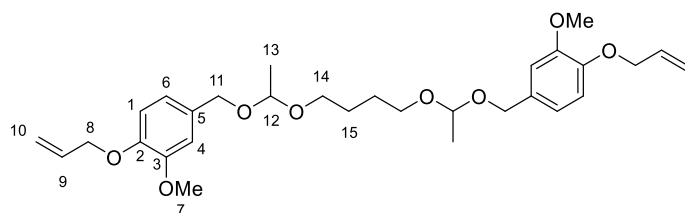
IR (ATR platinum diamond): ν / cm^{-1} = 2963.1, 2835.8, 1742.3, 1649.6, 1604.8, 1590.6, 1513.4, 1453.5, 1421.5, 1376.3, 1328.9, 1253.0, 1223.6, 1195.1, 1165.2, 1134.0, 1021.5, 917.4, 905.1, 886.3, 852.6, 801.3, 787.2, 738.2, 663.0, 633.3, 617.0, 550.7, 518.8, 468.1, 420.2.

FAB-HRMS of $\text{C}_{23}\text{H}_{26}\text{O}_7$ $[\text{M}]^+$ calculated: 414.1673, found: 414.1674.

Experimental Section



AVA bisacetal (1,12-bis(4-(allyloxy)-3-methoxyphenyl)-3,10-dimethyl-2,4,9,11-tetraoxa dodecane) 11



In a round bottom flask, 2.00 g (10.3 mmol, 1.00 eq) allylated vanillyl alcohol **5** and 732 mg (5.15 mmol, 0.50 eq) 1,4-butanediol divinyl ether were dissolved in 21 mL DCM (0.5M). To the solution, 129 mg (0.515 mmol, 0.05 eq) pyridinium *p*-toluenesulfonate (PPTS) were added and the mixture was stirred at 0 °C for 5 h. The solution was washed with water, dried over sodium sulfate and the solvent was removed under vacuum. The product was purified *via* column chromatography (10% EtOAc/CH).

Yield: 64%

R_f = 0.50 (40% EtOAc/CH)

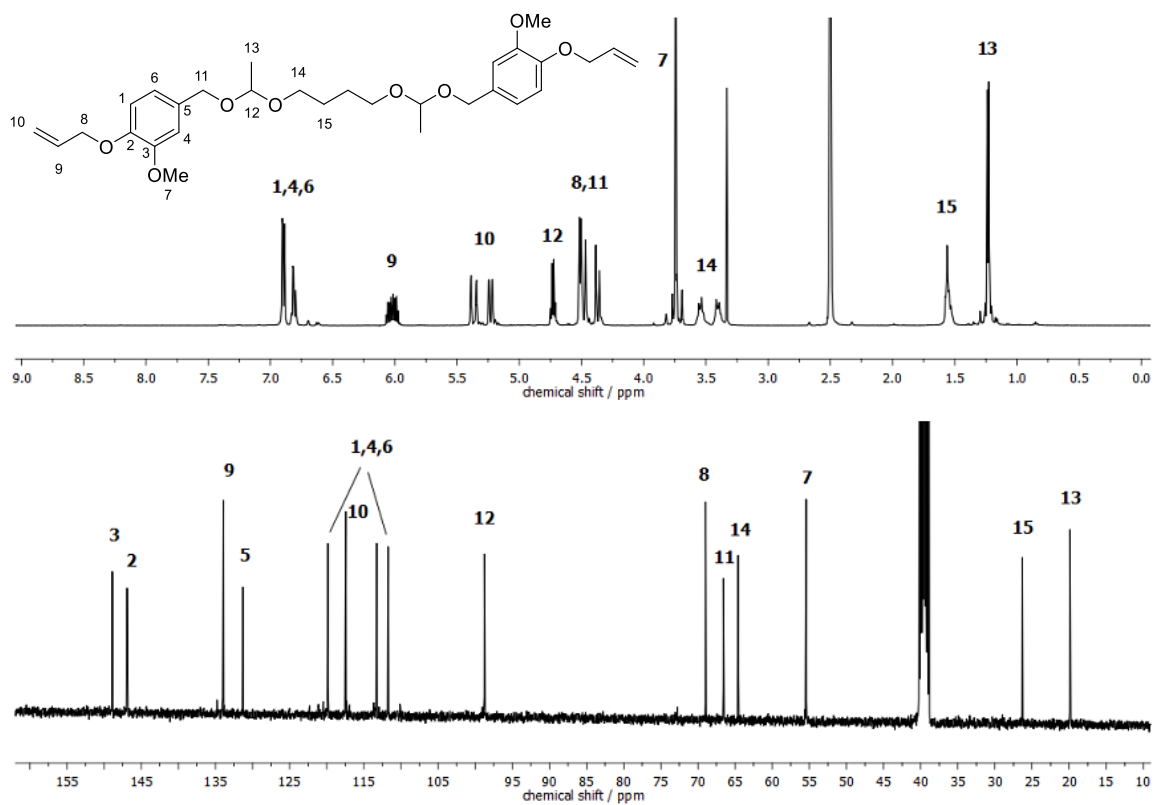
¹H-NMR (400 MHz, DMSO-*d*₆) δ / ppm = 6.90-6.79 (m, 6H, H1+H4+H6), 6.07-5.97 (m, 2H, H9), 5.39-5.21 (m, 4H, H10), 4.73 (q, *J* = 5.2 Hz, 2H, H12), 4.52-4.36 (m, 8H, H8+H11), 3.74 (s, 6H, H7), 3.57-3.49 (m, 2H, H14), 3.43-3.38 (m, 2H, H14), 1.57-1.53 (m, 4H, H15), 1.23 (d, *J* = 5.3 Hz, 6H, H13).

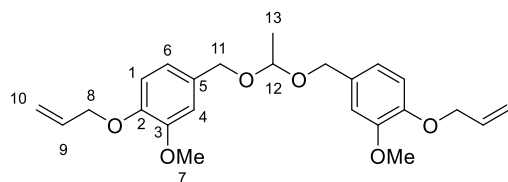
¹³C-NMR (101 MHz, DMSO-*d*₆) δ / ppm = 148.90, 146.90, 133.93, 131.30, 119.84, 117.44, 113.28, 111.72, 98.75, 68.98, 66.55, 64.58, 55.44, 26.31, 19.89.

IR (ATR platinum diamond): ν / cm⁻¹ = 3334.8, 2981.6, 2915.9, 2871.3, 1648.8, 1592.6, 1513.2, 1464.3, 1418.0, 1399.7, 1383.1, 1365.5, 1341.3, 1262.7, 1234.2, 1199.2, 1164.5, 1119.0, 1098.2, 1045.9, 1016.4, 969.7, 928.8, 913.3, 901.6, 863.0, 846.2, 809.5, 792.8, 742.7, 626.0, 595.9, 570.3, 522.0, 491.8, 463.8.

FAB-HRMS of C₃₀H₄₂O₈ [M]⁺ calculated: 530.2874, found: 530.2881.

Experimental Section



AVA acetal (4,4'-((ethane-1,1-diylbis(oxy))bis(methylene))bis(1-(allyloxy)-2-methoxybenzene))**12**

In a round bottom flask, 1.00 g (5.15 mmol, 1.00 eq) allylated vanillyl alcohol **5** was dissolved in 7.43 g (103 mmol, 20.0 eq) ethyl vinyl ether. Then, 259 mg (1.03 mmol, 0.20 eq) PPTS were added and the mixture was stirred at room temperature for 1 h. The excess of ethyl vinyl ether was removed with a rotary evaporator and again 1.00 g (5.15 mmol, 1.00 eq) allyl vanillyl alcohol and 10.0 mL 2-MeTHF were added. The solution was stirred at room temperature for 40 h. The crude product was purified *via* column chromatography (5-10% EtOAc/CH).

Yield: 37%**R_f** = 0.57 (40% EtOAc/CH)

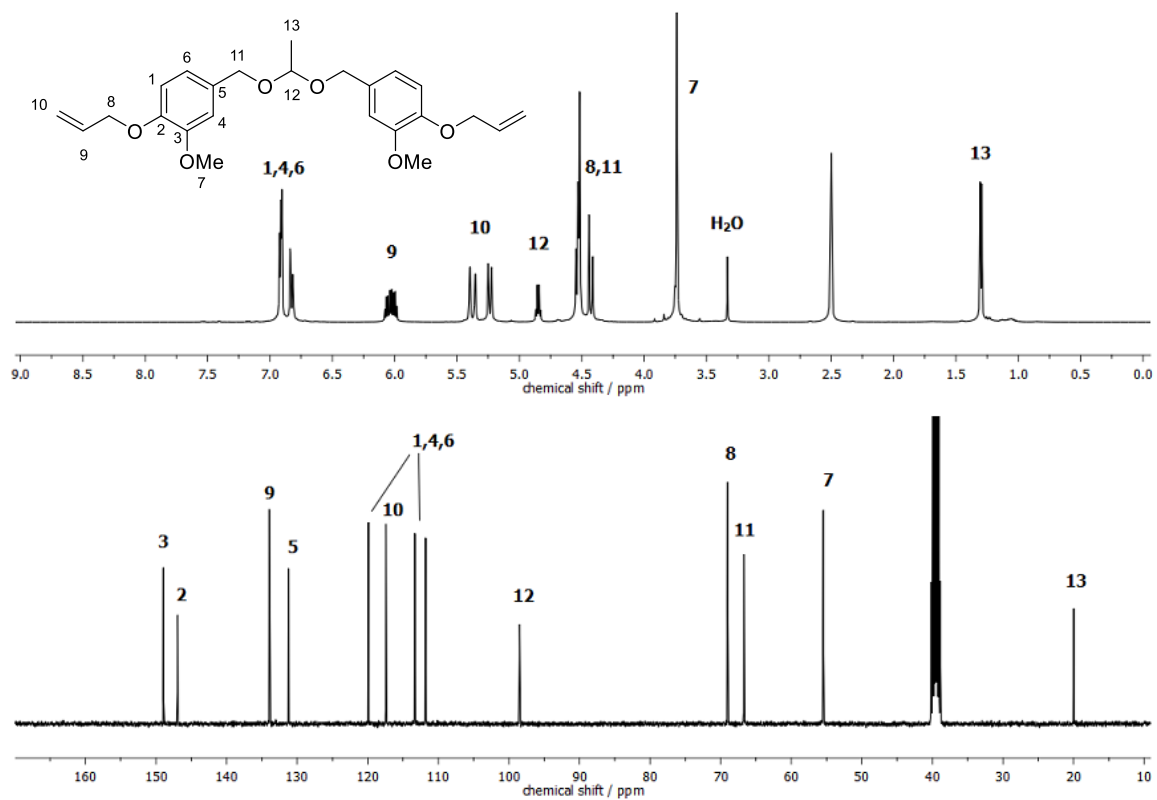
¹H-NMR (400 MHz, DMSO-*d*₆) δ / ppm = 6.92-6.82 (m, 6H, H1+H4+H6), 6.08-5.98 (m, 2H, H9), 5.40-5.22 (m, 4H, H10), 4.85 (q, *J* = 5.2 Hz, 1H, H12), 4.55-4.41 (m, 8H, H8+H11), 3.74 (s, 6H, H7), 1.30 (d, *J* = 5.3 Hz, 3H, H13).

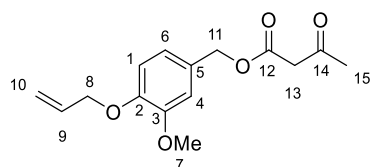
¹³C-NMR (101 MHz, DMSO-*d*₆) δ / ppm = 148.92, 146.95, 133.93, 131.25, 119.92, 117.42, 113.32, 111.80, 98.48, 68.99, 66.69, 55.45, 19.96.

IR (ATR platinum diamond): ν / cm⁻¹ = 2935.2, 2869.0, 1648.2, 1591.6, 1510.5, 1462.8, 1419.6, 1391.9, 1326.6, 1261.6, 1227.7, 1160.3, 1122.5, 1092.2, 1018.4, 993.6, 921.9, 853.5, 801.8, 765.7, 744.0, 648.4, 551.8, 460.6.

FAB-HRMS of C₂₄H₃₀O₆ [M]⁺ calculated: 414.2037, found: 414.2041.

Experimental Section



AVA acetoacetate (4-(allyloxy)-3-methoxybenzyl 3-oxobutanoate) 13

The synthesis of AVA acetoacetate was adapted from literature.^[316]

At a Zinke apparatus, 300 mg (1.55 mmol, 1.00 eq) AVA **5** and 641 μL (611 mg, 3.86 mmol, 2.50 eq) *tert*-butyl acetoacetate were heated to 150 °C for 6 h. Subsequently, the product was isolated *via* column chromatography (20- \rightarrow 30% EtOAc/CH).

Yield: 68%

R_f = 0.62 (50% EtOAc/CH)

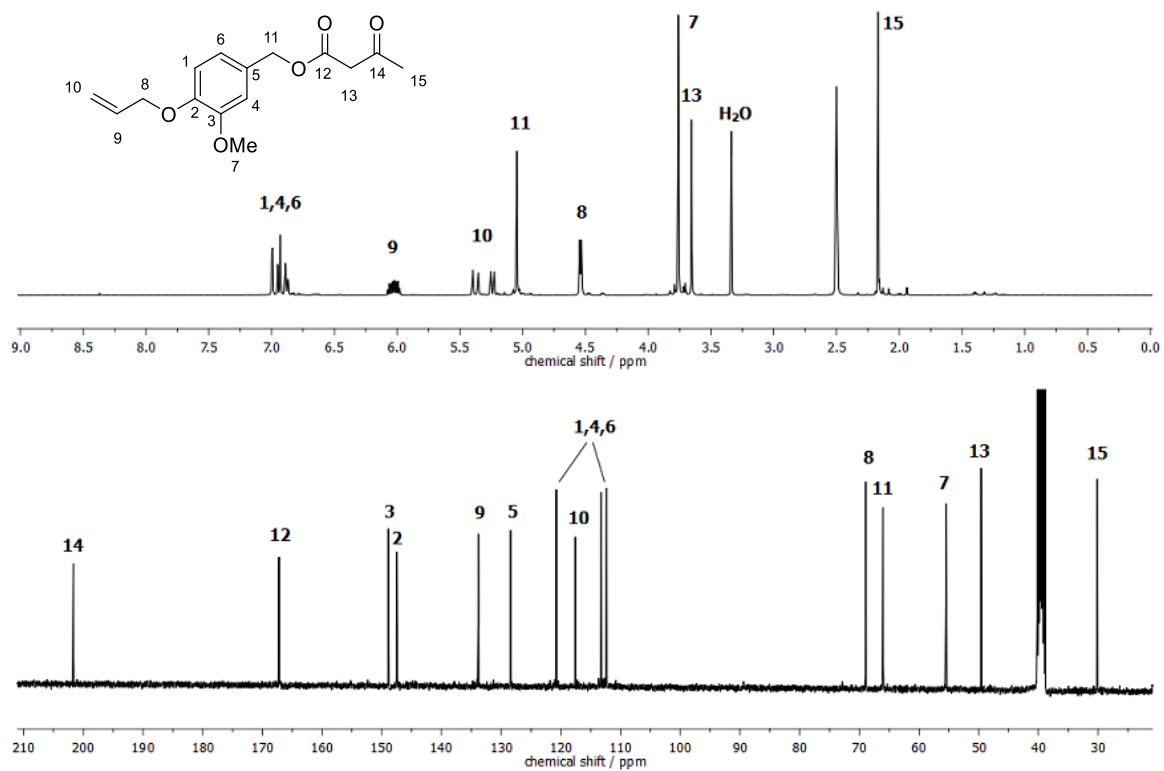
¹H-NMR (400 MHz, DMSO-*d*₆) δ / ppm = 6.99-6.87 (m, 3H, H1+H4+H6), 6.08-5.97 (m, 1H, H9), 5.40-5.23 (m, 2H, H10), 5.05 (s, 2H, H11), 4.54 (d, *J* = 5.3 Hz, 2H, H8), 3.76 (s, 3H, H7), 3.65 (s, 2H, H13), 2.17 (s, 3H, H15).

¹³C-NMR (101 MHz, DMSO-*d*₆) δ / ppm = 201.65, 167.21, 148.90, 147.51, 133.81, 128.42, 120.76, 117.57, 113.23, 112.34, 68.93, 66.04, 55.51, 49.60, 30.13.

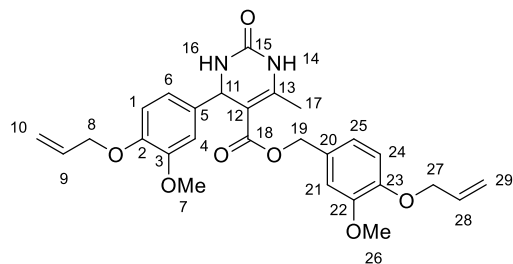
IR (ATR platinum diamond): ν / cm^{-1} = 2938.8, 1739.3, 1713.5, 1647.9, 1592.4, 1513.6, 1462.9, 1421.3, 1361.2, 1313.8, 1258.4, 1227.4, 1137.8, 1019.8, 994.1, 926.5, 852.9, 802.7, 755.5, 624.0, 552.2, 457.6.

EI-HRMS of C₁₅H₁₈O₅ [M]⁺ calculated: 278.1149, found: 278.1155.

Experimental Section



Biginelli product with AVA acetoacetate and allyl vanillin (4-(allyloxy)-3-methoxybenzyl 4-(4-(allyloxy)-3-methoxyphenyl)-6-methyl-2-oxo-1,2,3,4-tetrahydropyrimidine-5-carboxylate) 14



The reaction conditions were adapted from literature.^[317]

In a round bottom flask, 40.0 mg (208 μmol , 1.00 eq) allylated vanillin **9** were mixed with 15.0 mg (250 μmol , 1.20 eq) urea and 69.6 mg (250 μmol , 1.20 eq) AVA acetoacetate **13**. To the mixture, 4.00 mg (20.8 μmol , 0.10 eq) *p*-toluenesulfonic acid monohydrate were added and the reaction was run at 110 $^{\circ}\text{C}$ for 8 h. The product was isolated by column chromatography (1% Et_3N , 70% EtOAc/CH).

Yield: 38%

R_f = 0.54 (90% EtOAc/CH)

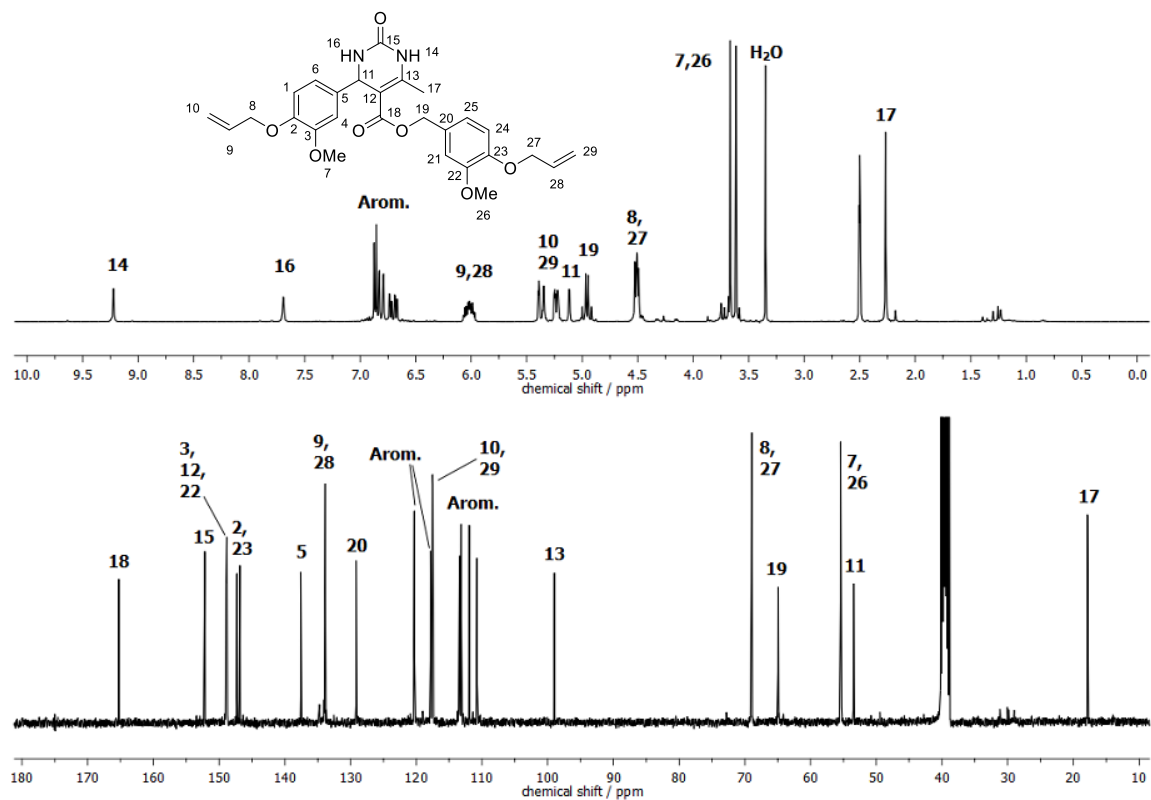
$^1\text{H-NMR}$ (400 MHz, DMSO-d_6) δ / ppm = 9.22 (d, J = 1.5 Hz, 1H, H14), 7.70-7.69 (m, 1H, H16), 6.98-6.66 (m, 6H, H1+H4+H6+H21+H24+H25), 6.07-5.97 (m, 2H, H9+H28), 5.40-5.34 (m, 2H, H10+H29), 5.25-5.21 (m, 2H, H10+H29), 5.12 (d, J = 3.3 Hz, 1H, H11), 4.96 (q, J = 12.4 Hz, 2H, H19), 4.53-4.49 (m, 4H, H8+H27), 3.67 (s, 3H, H7/H26), 3.62 (s, 3H, H7/26), 2.27 (s, 3H, H17).

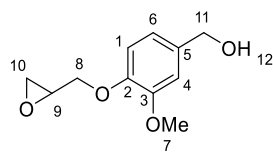
$^{13}\text{C-NMR}$ (101 MHz, DMSO-d_6) δ / ppm = 165.27, 152.18, 148.94, 148.85, 148.76, 147.29, 146.86, 137.55, 133.92, 133.85, 129.14, 120.28, 117.83, 117.54, 117.49, 113.42, 113.16, 111.93, 110.75, 98.96, 69.00, 68.95, 64.95, 55.42, 55.33, 53.44, 17.85.

IR (ATR platinum diamond): ν / cm^{-1} = 3355.0, 3224.3, 3106.5, 2924.6, 1690.5, 1642.0, 1593.5, 1511.9, 1455.7, 1420.2, 1376.8, 1320.6, 1257.0, 1218.6, 1158.0, 1137.8, 1086.6, 1022.8, 996.7, 938.2, 847.6, 795.8, 769.9, 755.7, 737.4, 676.5, 647.5, 556.7, 471.6, 412.3.

FAB-HRMS of $\text{C}_{27}\text{H}_{30}\text{N}_2\text{O}_7$ $[\text{M}]^+$ calculated: 494.2048, found: 494.2052.

Experimental Section



Glycidyl vanillyl alcohol ((3-methoxy-4-(oxiran-2-ylmethoxy)phenyl)methanol) 15

In a round bottom flask, 500 mg (2.57 mmol, 1.00 eq) AVA **5** and 406 mg (5.14 mmol, 2.00 eq) NH_4HCO_3 were dissolved in 13 mL $\text{H}_2\text{O}/\text{CH}_3\text{CN}$ (2:3, 5 mL H_2O and 8 mL CH_3CN , 0.2M). 2.91 g (25.7 mmol, 10.0 eq) hydrogen peroxide solution (30%) was added and the mixture was heated to 30°C for 20 h. The solution was extracted with ethyl acetate. The combined organic phases were washed with Na_2SO_3 -solution and water, dried over sodium sulfate and the solvent was removed under vacuum. The crude mixture was purified by column chromatography (10->70% EtOAc, 1% MeOH/CH).

Yield: 57%

$R_f = 0.33$ (70% EtOAc/CH)

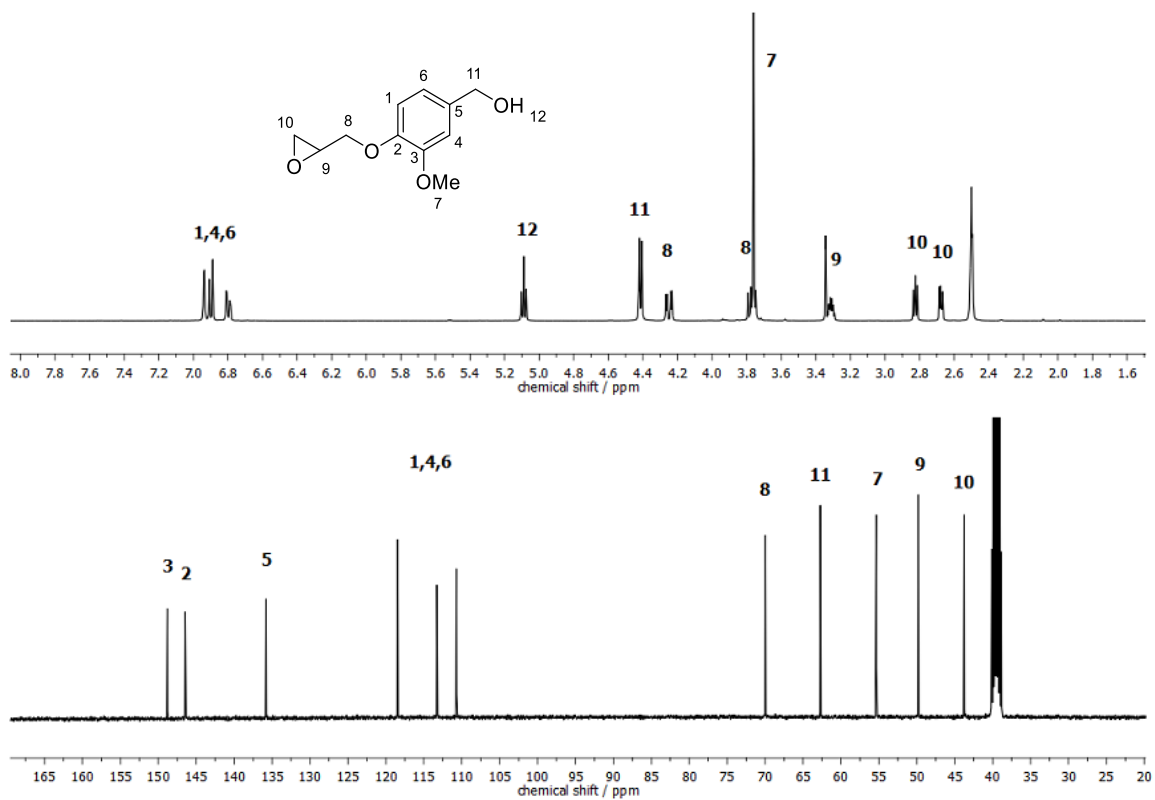
$^1\text{H-NMR}$ (400 MHz, DMSO-d_6) δ / ppm = 6.94-6.79 (m, 3H, H1+H4+H6), 5.09 (t, $J = 5.7$ Hz, 1H, H12), 4.42 (d, $J = 5.7$ Hz, 2H, H11), 4.25 (dd, $J = 11.4$ Hz, 2.7 Hz, 1H, H8), 3.79-3.75 (m, 4H, H7+H8), 3.33-3.29 (m, 1H, H9), 2.84-2.81 (m, 1H, H10), 2.68 (dd, $J = 5.1$ Hz, 2.7 Hz, 1H, H10).

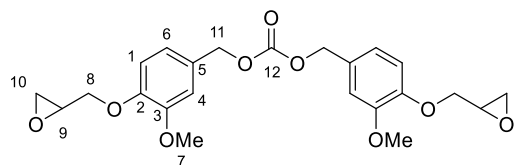
$^{13}\text{C-NMR}$ (101 MHz, DMSO-d_6) δ / ppm = 148.80, 146.45, 135.79, 118.44, 113.28, 110.69, 69.96, 62.71, 55.35, 49.80, 43.75.

IR (ATR platinum diamond): ν / cm^{-1} = 3313.0, 3003.3, 2921.2, 2865.5, 1592.4, 1512.6, 1465.0, 1416.7, 1372.7, 1345.5, 1309.7, 1258.6, 1232.8, 1196.2, 1157.0, 1128.4, 1057.3, 1023.8, 939.4, 917.7, 864.6, 853.4, 796.5, 755.9, 720.2, 635.8, 550.7, 450.0.

FAB-HRMS of $\text{C}_{11}\text{H}_{14}\text{O}_4$ $[\text{M}]^+$ calculated: 210.0887, found: 210.0893.

Experimental Section



GVA carbonate (bis(3-methoxy-4-(oxiran-2-ylmethoxy)benzyl) carbonate) 16

500 mg (2.38 mmol, 1.00 eq) GVA **15** were dissolved in 4.28 g (47.6 mmol, 20.0 eq) dimethyl carbonate. 16.6 mg (119 μ mol, 0.05 eq) TBD were added and the mixture was heated to 70 °C for 22 h. Unreacted dimethyl carbonate was removed with the rotary evaporator. Subsequently, another 500 mg of glycidyl vanillyl alcohol and 12 mL 2-MeTHF (0.2 M) were added and the mixture was heated to 70 °C for 23 h. Subsequently, the solvent was removed under reduced pressure. The product was purified by precipitation in ethyl acetate.

Yield: 68%

R_f = 0.52 (40% EtOAc/CH)

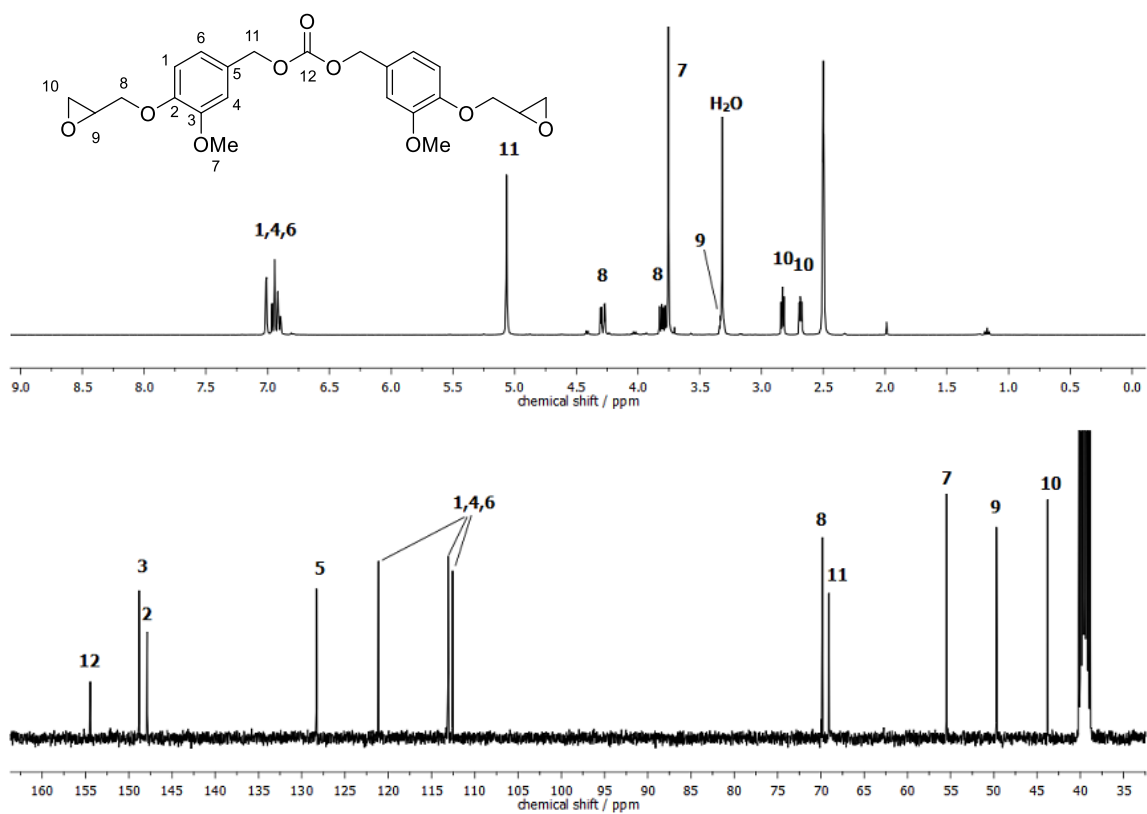
$^1\text{H-NMR}$ (400 MHz, DMSO- d_6) δ / ppm = 7.01-6.89 (m, 6H, H1+H4+H6), 5.07 (s, 4H, H11), 4.29 (dd, J = 11.4, 2.7 Hz, 2H, H8), 3.83-3.75 (m, 8H, H7+H8), 3.34-3.30 (m, 2H, H9), 2.84-2.82 (m, 2H, H10), 2.69-2.67 (m, 2H, H10).

$^{13}\text{C-NMR}$ (101 MHz, DMSO- d_6) δ / ppm = 154.44, 148.80, 147.86, 128.31, 121.13, 113.09, 112.56, 69.83, 69.06, 55.47, 49.71, 43.77.

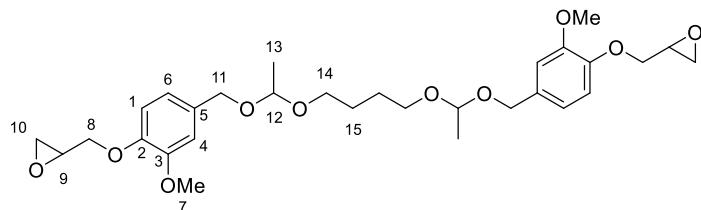
IR (ATR platinum diamond): ν / cm^{-1} = 2927.0, 1743.2, 1592.7, 1515.9, 1448.6, 1421.1, 1377.0, 1350.1, 1253.5, 1225.9, 1165.3, 1133.3, 1025.4, 942.0, 919.2, 904.9, 886.9, 863.8, 851.6, 801.0, 787.8, 764.2, 739.8, 661.2, 629.8, 594.3, 552.7, 466.8, 445.6, 410.2.

FAB-HRMS of $\text{C}_{23}\text{H}_{26}\text{O}_9$ [M] $^+$ calculated: 446.1571, found: 446.1578.

Experimental Section



GVA bisacetal (2,2'-(((3,10-dimethyl-2,4,9,11-tetraoxadodecane-1,12-diyl)bis(2-methoxy-4,1-phenylene))bis(oxy))bis(methylene))bis(oxirane))* 17



In a round bottom flask, 1.00 g (4.76 mmol, 1.00 eq) GVA **15** and 338 mg (2.38 mmol, 0.50 eq) 1,4-butanediol divinyl ether were dissolved in 9.5 mL DCM (0.5M). Then, 59.8 mg (238 μ mol, 0.05 eq) PPTS were added and the mixture was stirred at room temperature for 7 h. The solvent was removed and the product was purified *via* column chromatography (10% EtOAc, 2% MeOH/CH).

Yield: 72%

R_f = 0.54 (70% EtOAc/CH)

$^1\text{H-NMR}$ (400 MHz, DMSO- d_6) δ / ppm = 6.92-6.81 (m, 6H, H1+H4+H6), 4.73 (q, J = 5.3 Hz, 2H, H12), 4.44 (dd, J = 45.9, 11.6 Hz, 4H, H11), 4.25 (dd, J = 11.4, 2.7 Hz, 2H, H8), 3.79-3.75 (m, 8H, H7+H8), 3.58-3.53 (m, 2H, H14), 3.42-3.39 (m, 2H, H14), 3.33-3.29 (m, 2H, H9), 2.84-2.81 (m, 2H, H10), 2.69-2.67 (m, 2H, H10), 1.60-1.54 (m, 4H, H15), 1.24 (d, J = 5.3 Hz, 6H, H13).

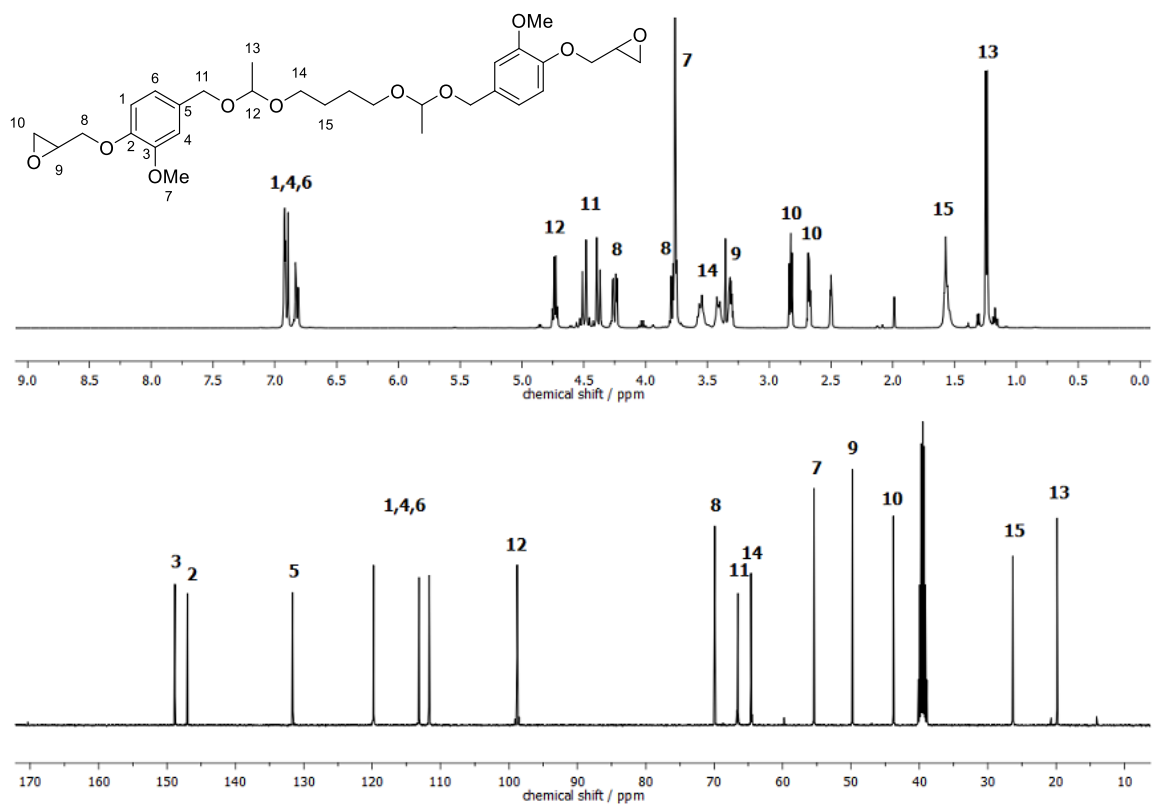
$^{13}\text{C-NMR}$ (101 MHz, DMSO- d_6) δ / ppm = 148.84, 147.03, 131.65, 119.82, 113.15, 111.65, 98.80, 69.92, 66.53, 64.62, 55.39, 49.79, 43.78, 26.35, 19.86.

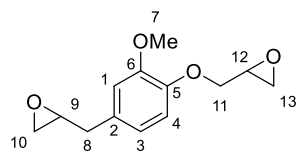
IR (ATR platinum diamond): ν / cm^{-1} = 2935.0, 2871.7, 1592.7, 1512.2, 1464.0, 1419.7, 1388.5, 1341.8, 1263.1, 1230.7, 1159.9, 1125.4, 1091.7, 1025.7, 908.8, 853.1, 801.2, 762.0, 554.5, 458.1.

ESI-HRMS of $\text{C}_{30}\text{H}_{42}\text{O}_{10}$ $[\text{M}]^+$ calculated: 562.2772, found: 562.2769.

* This reaction was performed by Bastian Pfeuffer in the bachelor thesis "Synthesis of cleavable monomers for bio-based, recyclable polymers" under my co-supervision.

Experimental Section



Epoxidized allyl eugenol (2-(3-methoxy-4-(oxiran-2-ylmethoxy)benzyl)oxirane)* 18

In a round bottom flask, 5.00 g (24.5 mmol, 1.00 eq) allylated eugenol **7** were mixed with 7.75 g (98.0 mmol, 4.00 eq) ammonium bicarbonate and dissolved in 123 mL H₂O/CH₃CN (2:3, 49 mL H₂O and 74 mL CH₃CN, 0.2M). To this mixture, 16.7 g (147 mmol, 6.00 eq) hydrogen peroxide solution (30%) was added and the mixture was heated to 30 °C for 21 h. To increase conversion, another 11.1 g (98.0 mmol, 4.00 eq) hydrogen peroxide solution (30%) was added and the reaction was continued to a total reaction time of 40 h. Subsequently, the reaction mixture was extracted with ethyl acetate. After removing the solvent under reduced pressure, the product was purified *via* column chromatography (40% EtOAc/CH).

Yield: 45%

R_f = 0.42 (40% EtOAc/CH)

¹H-NMR (400 MHz, DMSO-d₆) δ / ppm = 6.90-6.88 (m, 2H, H3 + H4), 6.76 (dd, *J* = 8.2, 1.9 Hz, 1H, H1), 4.25 (dd, *J* = 11.4, 2.8 Hz, 1H, H11), 3.79-3.72 (m, 4H, H11 + H7), 3.34-3.29 (m, 1H, H12), 3.12-3.07 (m 1H, H9), 2.82 (dd, *J* = 8.7, 4.4 Hz, 1H, H13), 2.73-2.70 (m, 3H, H8 + H10), 2.68 (dd, *J* = 5.1, 2.6 Hz, 1H, H13), 2.54 (dd, *J* = 5.1, 2.6 Hz, 1H, H10).

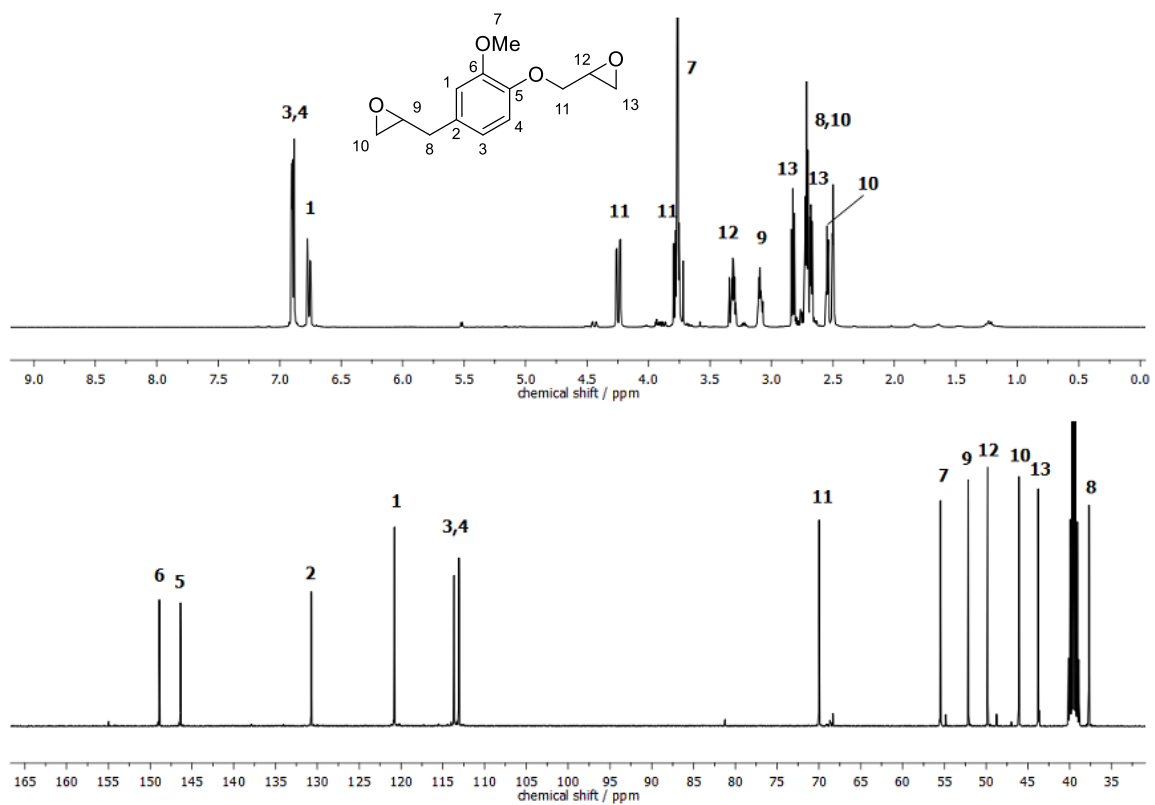
¹³C-NMR (101 MHz, DMSO-d₆) δ / ppm = 148.90, 146.38, 130.74, 120.78, 113.65, 113.07, 69.98, 55.45, 52.12, 49.82, 46.09, 43.77, 37.71.

IR (ATR platinum diamond): ν / cm⁻¹ = 3050.1, 3002.6, 2915.4, 2835.5, 1751.1, 1592.2, 1513.7, 1470.0, 1452.4, 1420.0, 1405.2, 1349.9, 1333.2, 1258.3, 1231.2, 1210.0, 1157.2, 1136.1, 1078.4, 1026.0, 952.4, 934.3, 912.7, 863.7, 853.5, 840.4, 796.1, 758.6, 744.9, 731.6, 630.4, 595.7, 556.7, 462.6, 438.4.

EI-HRMS of C₁₃H₁₆O₄ [M]⁺ calculated: 236.1043, found: 236.1050.

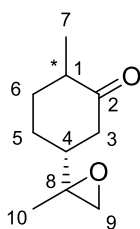
* This reaction was performed by Annika Nutz in the scope of an internship under my co-supervision.

Experimental Section



6.3.2 Experimental Procedures for Chapter 4.2

Dihydrocarvone oxide (2-methyl-5-(2-methyloxiran-2-yl)cyclohexan-1-one) 20



The synthesis was carried out following a literature known epoxidation procedure.^[290]

In a round bottom flask, 500 mg (3.28 mmol, 1.00 eq) of (+)-dihydrocarvone were mixed with 398 mg (984 μmol , 0.30 eq) Aliquat 336, 157 mg (656 μmol , 0.20 eq) $\text{Na}_2\text{WO}_4 \cdot 2\text{H}_2\text{O}$, 321 mg (1.31 mmol, 0.40 eq) H_3PO_4 solution (40% in H_2O) and 15.0 mL dichloromethane. To the solution, 1.49 g (13.1 mmol, 4.00 eq) hydrogen peroxide solution (30%) was added and the mixture was heated to 40 °C for 46 h. The mixture was extracted with ethyl acetate. The organic phase was washed with water, dried over sodium sulfate and the solvent was removed under reduced pressure. The crude mixture was purified by column chromatography (10% EtOAc/CH). The product was obtained as a mixture of two isomers.

Yield: 39%

$R_f = 0.60$ (40% EtOAc/CH)

$^1\text{H-NMR}$ (400 MHz, CDCl_3) δ / ppm = 2.64-2.53 (m, 2H, H9), 2.44-2.39 (m, 1H, H3), 2.35-2.28 (m, 1H, H1), 2.20-2.07 (m, 2H, H6+H3), 1.94-1.89 (m, 1H, H5), 1.78-1.47 (m, 2H, H4+H5), 1.35-1.24 (m, 1H, H6), 1.28+1.27 (s, 3H, H10), 1.00+0.98 (s, 3H, H7).

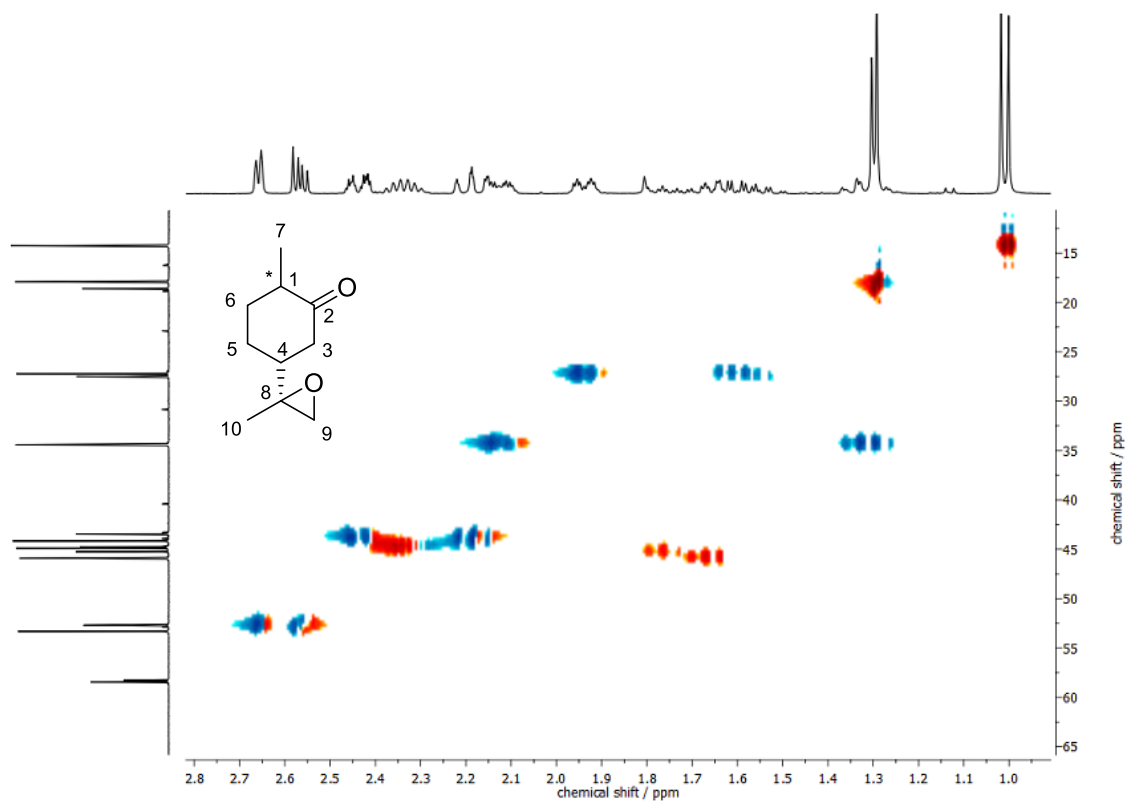
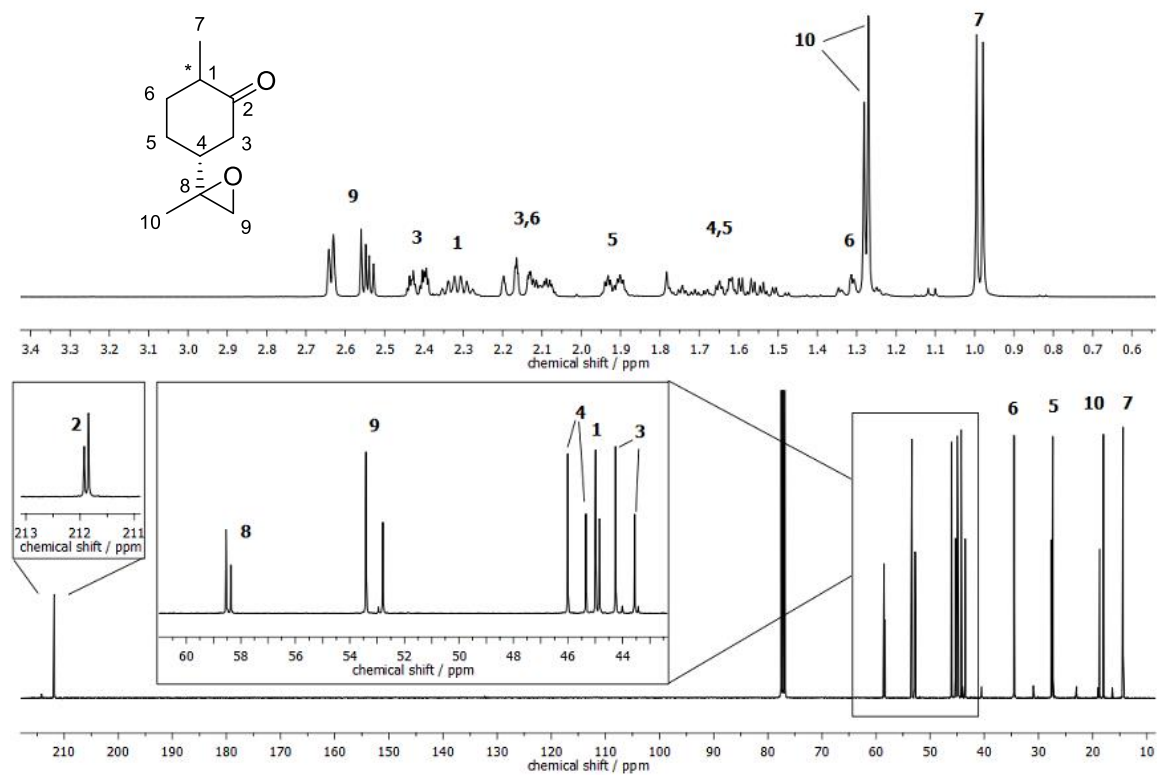
$^{13}\text{C-NMR}$ (101 MHz, CDCl_3) δ / ppm = 211.92, 211.84, 58.54, 58.37, 53.41, 52.79, 46.01, 45.34, 44.99, 44.85, 44.26, 43.56, 34.51, 34.46, 27.61, 27.32, 18.70, 18.02, 14.37, 14.36.

IR (ATR platinum diamond): ν / cm^{-1} = 2968.3, 2931.8, 2863.4, 1708.9, 1450.4, 1377.9, 1319.7, 1279.5, 1241.1, 1217.5, 1172.8, 1141.4, 1082.4, 1061.2, 1019.1, 968.2, 903.4, 889.9, 860.2, 844.5, 802.7, 724.3, 648.3, 603.3, 528.9, 481.5, 433.0.

EI-HRMS of $\text{C}_{10}\text{H}_{16}\text{O}_2$ $[\text{M}]^+$ calculated: 168.1145, found: 168.1151.

The NMR spectra are in accordance with the literature.^[128]

Experimental Section



Detailed reaction procedures for Table 4.1:**Entry 2:**

In a round bottom flask, 282 mg (1.45 mmol, 1.10 eq) peracetic acid solution (38-40% in acetic acid) were added to 4.40 mL dimethyl carbonate and the mixture was dried over 3Å molecular sieve for 3 h. The solution was then added dropwise to 200 mg (1.31 mmol, 1.00 eq) (+)-dihydrocarvone. The mixture was heated to 70 °C under argon and stirred for 16 h.

Entry 3:

In a round bottom flask, 10 mL dimethyl carbonate, 200 mg (1.31 mmol, 1.00 eq) (+)-dihydrocarvone and 262 mg lipase CALB (200 mg/mmol) were mixed. To the stirring mixture, 5 × 149 mg (6.55 mmol, 5.00 eq) hydrogen peroxide solution (30%) were added in steps of 1 h. The reaction was carried out at 40 °C for 28 h.

Entry 4:

In a round bottom flask, 200 mg (1.31 mmol, 1.00 eq) (+)-dihydrocarvone and 64.0 mg lipase CALB (50 mg/mmol) were dissolved in 2.80 mL ethyl acetate. To this solution, 136 mg urea-hydrogen peroxide (1.44 mmol, 1.10 eq) were added and the solution was stirred at 40 °C for 21 h.

Entry 5:

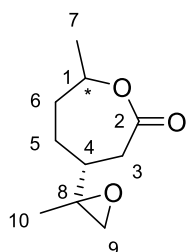
A portion of 200 mg (1.31 mmol, 1.00 eq) (+)-dihydrocarvone, 17.5 mg (393 µmol, 0.03 eq) Aliquat 336, 86.4 mg (262 µmol, 0.20 eq) Na₂WO₄·2H₂O, 128.5 mg (524 µmol, 0.40 eq) H₃PO₄ (40% in H₂O) and 594 mg (5.24 mmol, 4.00 eq) hydrogen peroxide solution (30% in H₂O) were dissolved in 6.50 mL chloroform and stirred at 40°C for 5 h.

Entry 6:

A portion of 200 mg (1.31 mmol, 1.00 eq) (+)-dihydrocarvone was dissolved in 1.30 mL dichloromethane. To this solution, 3.30 mg (13.1 µmol, 0.01 eq) methyltrioxorhenium and 223 mg (1.97 mmol, 1.50 eq) hydrogen peroxide solution (30% in H₂O) were added and the mixture was stirred at room temperature for 4 h.

Entry 7:

In a round bottom flask, 100 mg (657 µmol, 1.00 eq) (+)-dihydrocarvone, 2.60 mL (35.5 mmol, 54.0 eq) acetone and 265 mg (3.15 mmol, 4.80 eq) sodium bicarbonate were mixed. To the stirring mixture, 526 mg (1.71 mmol, 2.60 eq) Oxone[®] dissolved in 3.30 mL water were added with an addition rate of 1 mL/min and the mixture was stirred at room temperature for 1.5 h.

Epoxidized DHC lactone ((4R)-7-methyl-4-((R)-2-methyloxiran-2-yl)oxepan-2-one) 21

In a round bottom flask, 20 mL dimethyl carbonate and 6.41 g (32.9 mmol, 5.00 eq) peracetic acid (38-40% in acetic acid) were dried over 4Å molecular sieve for 2 h. Subsequently, the solution was added to 1.00 g (6.57 mmol, 1.00 eq) (+)-dihydrocarvone and the mixture was heated to 70 °C under argon for 6 h. After cooling to room temperature, 50 mL ethyl acetate were added and the solution was washed with sodium sulfite solution, water and brine. The organic phase was dried over sodium sulfate and the solvent was removed under reduced pressure. The product was purified *via* column chromatography (50% EtOAc/CH) and obtained as a mixture of two diastereoisomers.

Yield: 58%

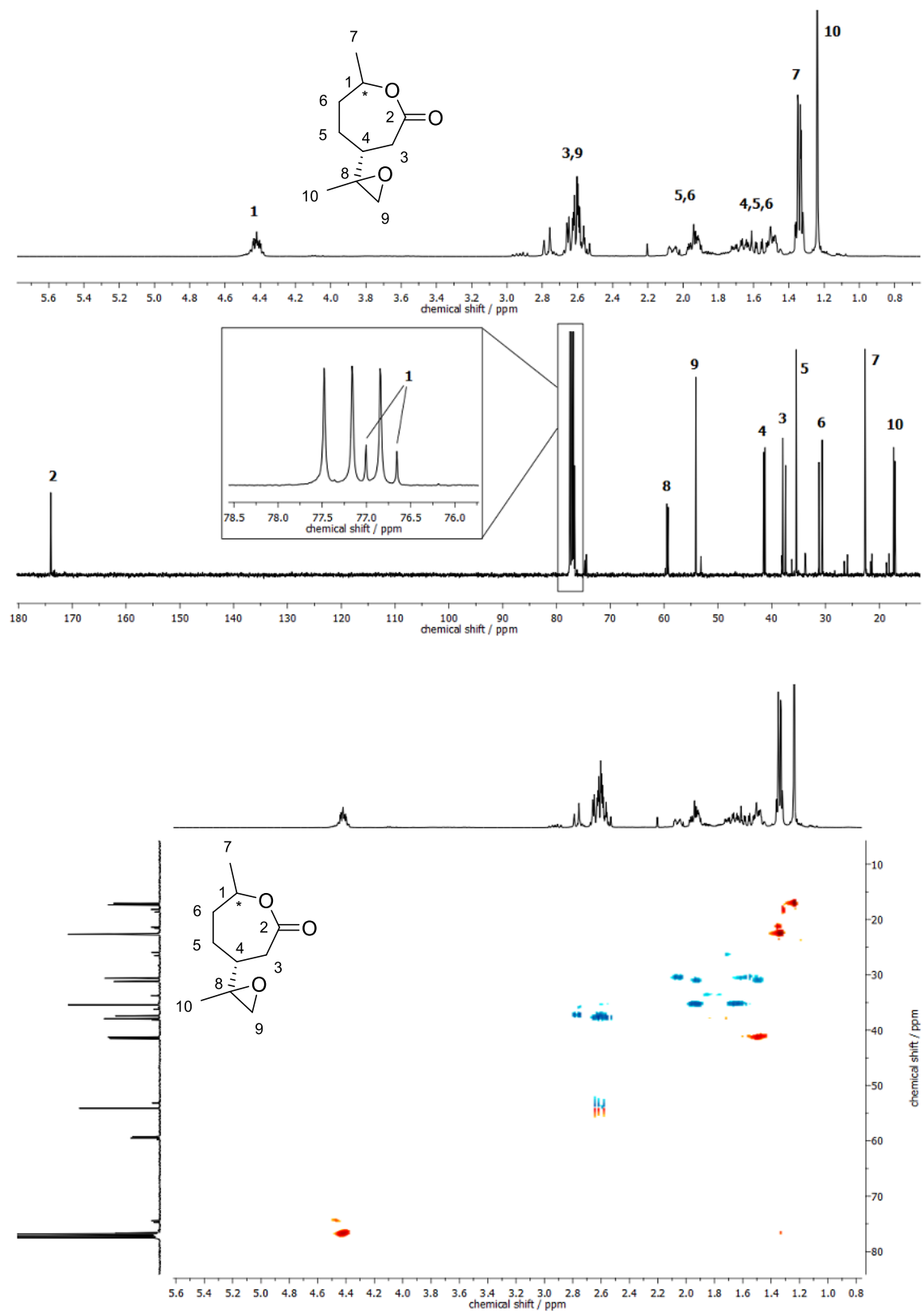
R_f = 0.50 (60% EtOAc/CH)

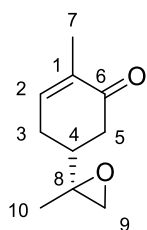
¹H-NMR (400 MHz, CDCl₃) δ / ppm = 4.51-4.38 (m, 1H, H1), 2.79-2.53 (m, 4H, H3+H9), 2.08-1.83 (m, 2H, H5+H6), 1.73-1.47 (m, 3H, H4+H5+H6), 1.36-1.32 (m, 3H, H7), 1.24 (s, 3H, H10).

¹³C-NMR (101 MHz, CDCl₃) δ / ppm = 173.98, 77.01, 76.66, 59.49, 59.23, 54.10, 41.51, 41.25, 37.93, 37.42, 35.43, 31.21, 30.62, 22.66, 17.33, 17.10.

IR (ATR platinum diamond): ν / cm⁻¹ = 3440.7, 2973.9, 2934.3, 1718.6, 1454.3, 1381.3, 1322.4, 1283.2, 1238.4, 1210.9, 1174.2, 1136.3, 1090.2, 1057.8, 1032.0, 1006.7, 987.8, 947.6, 897.4, 836.1, 821.6, 741.1, 671.0, 650.0, 619.4, 592.0, 543.1, 518.5, 489.9, 434.6.

EI-HRMS of C₁₀H₁₆O₃ [M]⁺ calculated: 184.1094, found: 184.1100.



Carvone-8,9-oxide (2-methyl-5-(2-methyloxiran-2-yl)cyclohex-2-en-1-one)* 23

The synthesis was carried out following a literature known epoxidation procedure.^[120]

5.00 g (33.3 mmol, 1.00 eq) (*R*)-(-)-carvone, 86.7 mL (1.80 mol, 54.0 eq) acetone and 13.4 g (160 mmol, 4.80 eq) sodium bicarbonate were mixed in a round bottom flask at room temperature. To the stirring mixture, 15.3 g (49.9 mmol, 1.50 eq) Oxone[®] dissolved in 96 mL water were added dropwise. After 45 min., the phases were extracted three times with 50 mL ethyl acetate. The combined organic phases were washed two times with 100 mL water and then dried over sodium sulfate. The solvent was removed under reduced pressure and the crude mixture was purified by column chromatography (10% EtOAc/CH). The product was obtained as a mixture of two isomers.

Yield: 77%

R_f = 0.59 (40% EtOAc/CH)

¹H-NMR (400 MHz, CDCl₃) δ / ppm = 6.74-6.71 (m, 1H, H2), 2.71-2.66 (m, 1H, H9), 2.60-2.52 (m, 2H, H5+H9), 2.44-2.36 (m, 1H, H3), 2.30-2.15 (m, 2H, H3+H5), 2.12-2.02 (m, 1H, H4), 1.77 (s, 3H, H7), 1.31 (d, *J* = 6.7 Hz, 3H, H10).

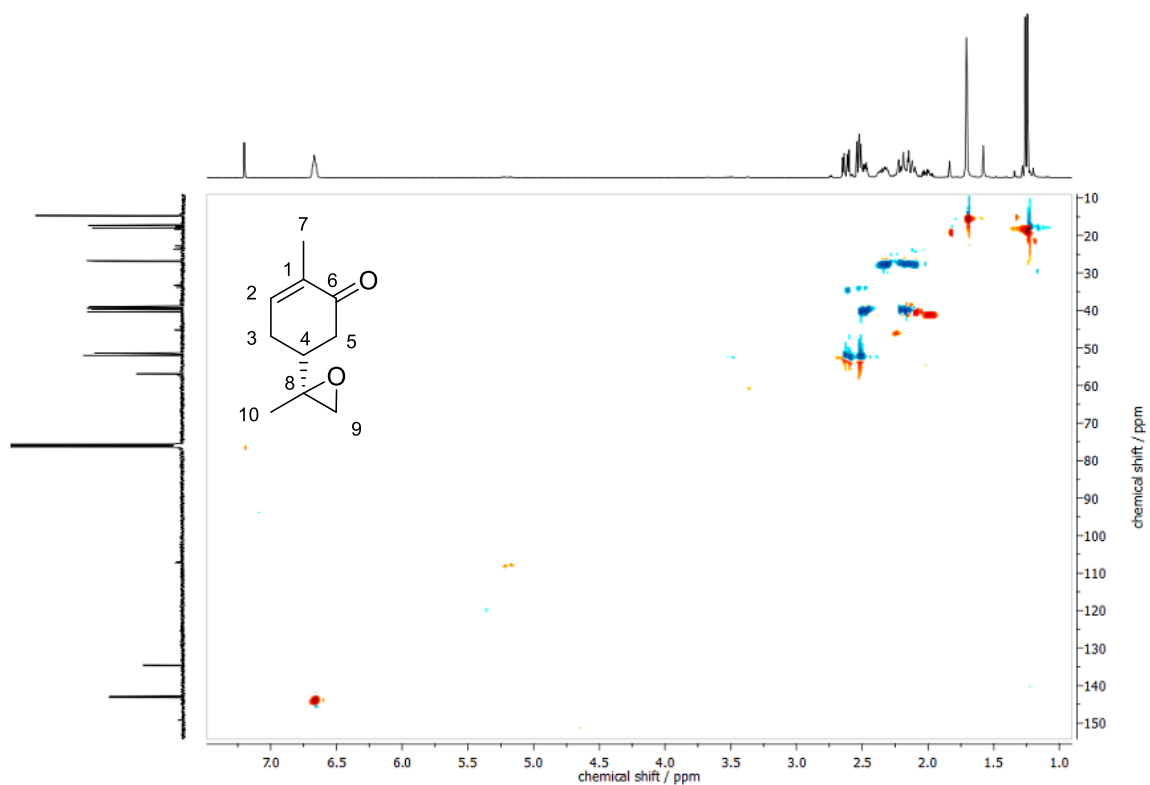
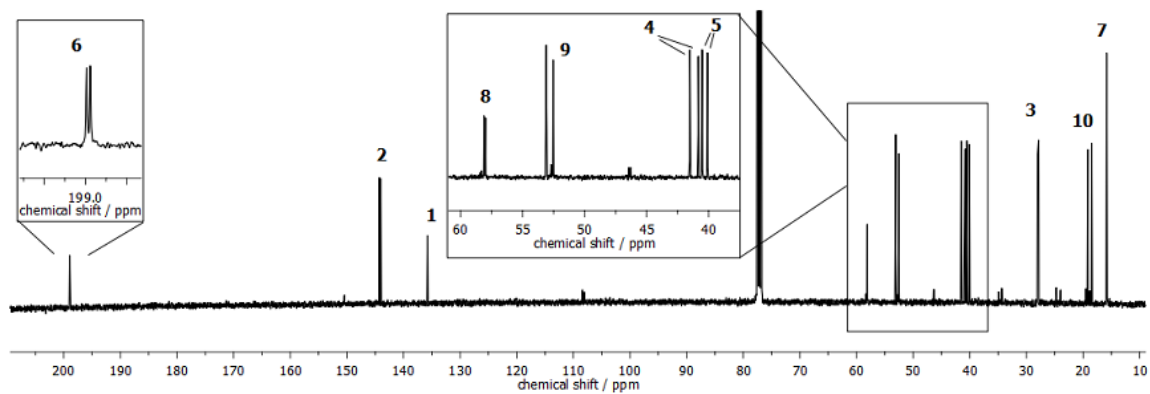
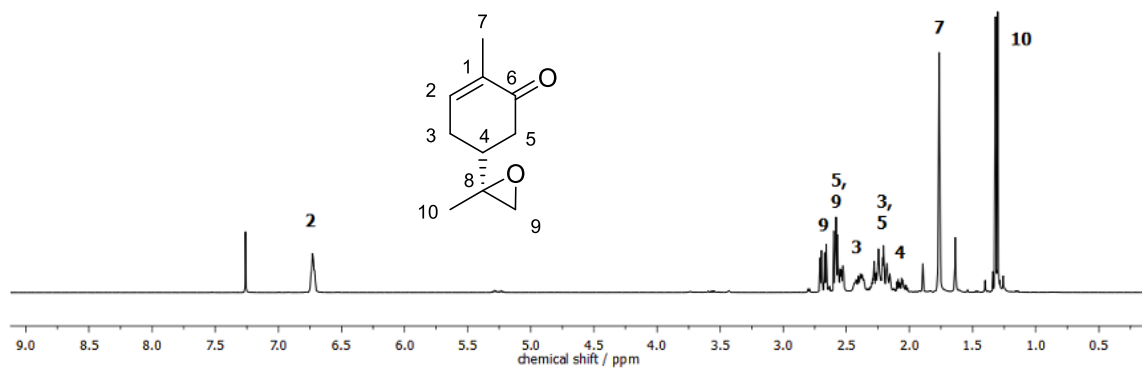
¹³C-NMR (101 MHz, CDCl₃) δ / ppm = 198.99, 198.94, 144.26, 144.02, 135.80, 135.74, 58.10, 58.00, 53.09, 52.53, 41.51, 40.83, 40.52, 40.09, 28.03, 27.85, 19.18, 18.48, 15.84.

IR (ATR platinum diamond): ν / cm⁻¹ = 2924.5, 1710.8, 1667.3, 1434.9, 1365.1, 1248.8, 1144.8, 1106.4, 1051.5, 992.6, 938.1, 902.7, 829.6, 802.8, 762.5, 704.6, 670.0, 563.3, 523.0, 488.5, 426.1.

EI-HRMS of C₁₀H₁₄O₂ [M]⁺ calculated: 166.0988, found: 166.0992.

The NMR spectra are in accordance with the literature.^[119]

* The reaction was carried out by Tim Trumler in the scope of his bachelor thesis "Synthesis of bio-based epoxides and diamines" under my co-supervision.



Detailed reaction procedures for Table 4.2:

Entry 1:

In a round bottom flask, 300 mg (2.00 mmol, 1.00 eq) (*R*)-(-)-carvone were dissolved in 3.30 mL methanol and cooled to 0 °C. A mixture of 2.27 g (20.0 mmol, 10.0 eq) hydrogen peroxide solution (30% in H₂O) and 4.20 mL (1.01 mg, 25.2 mmol, 12.6 eq) sodium hydroxide solution (6M) was added. The solution was stirred at 0 °C for 20 min and at 40 °C until a total reaction time of 4 h.

Entry 2:

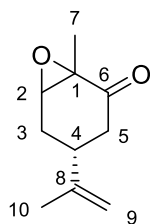
A portion of 200 mg (1.33 mmol, 1.00 eq) (*R*)-(-)-carvone and 266 mg lipase CALB (200 mg/mmol) were dissolved in 10.0 mL dimethyl carbonate. To this mixture, 5× 151 mg (6.65 mmol, 5.00 eq) hydrogen peroxide solution (30% in H₂O) was added in steps of 1 h and the solution was stirred at 40 °C for 51 h.

Entry 3:

A portion of 200 mg (1.33 mmol, 1.00 eq) (*R*)-(-)-carvone and 66.5 mg lipase CALB (50 mg/mmol) were dissolved in 2.80 mL ethyl acetate (0.5M). To this mixture, 138 mg (1.46 mmol, 1.10 eq) urea-hydrogen peroxide were added and the solution was stirred at 40 °C for 29 h.

Entry 4:

In a round bottom flask, 100 mg (666 μmol, 1.00 eq) (*R*)-(-)-carvone, 269 mg (3.20 mmol, 4.80 eq) sodium bicarbonate and 2.10 mL acetone were mixed in a round bottom flask. Under continuous stirring, 307 mg (999 μmol, 1.50 eq) Oxone® dissolved in 1.90 mL water were added using a syringe pump with a constant flow rate of 0.5 mL/min at room temperature. The reaction mixture was stirred at room temperature for 0.5 h.

Carvone-1,2-oxide (1-methyl-4-(prop-1-en-2-yl)-7-oxabicyclo[4.1.0]heptan-2-one) * 24

The synthesis was carried out following a literature known epoxidation procedure.^[119]

In a round bottom flask, 300 mg (*R*)-(-)-carvone (2.00 mmol, 1.00 eq) were dissolved in 3.30 mL methanol. The solution was cooled to 0 °C and 2.27 g (20.0 mmol, 10.0 eq) hydrogen peroxide solution (30% in H₂O) were added to the mixture while stirring. A 6M solution of NaOH (100 mg NaOH in 16.7 mL H₂O, 2.50 mmol, 1.25 eq) was added slowly and the reaction was stirred at 0 °C for ~20 min and additional 2.5 h at 40 °C. Afterwards, the reaction mixture was diluted with 10 mL DCM and washed with water. The organic phase was dried over sodium sulfate and the solvent was removed under reduced pressure. The crude mixture was purified by column chromatography (10% EtOAc/CH).

Yield: 42%

R_f = 0.76 (40% EtOAc/CH)

¹H-NMR (400 MHz, CDCl₃) δ / ppm = 4.73 (d, *J* = 27.6 Hz, 2H, H9), 3.42 (s, 1H, H2), 2.72-2.66 (m, 1H, H4), 2.56 (dd, *J* = 17.6, 4.5 Hz, 1H, H5), 2.34 (d, *J* = 14.0 Hz, 1H, H3), 2.04-1.96 (m, 1H, H5), 1.91-1.84 (m, 1H, H3), 1.69 (s, 3H, H10), 1.38 (s, 3H, H7).

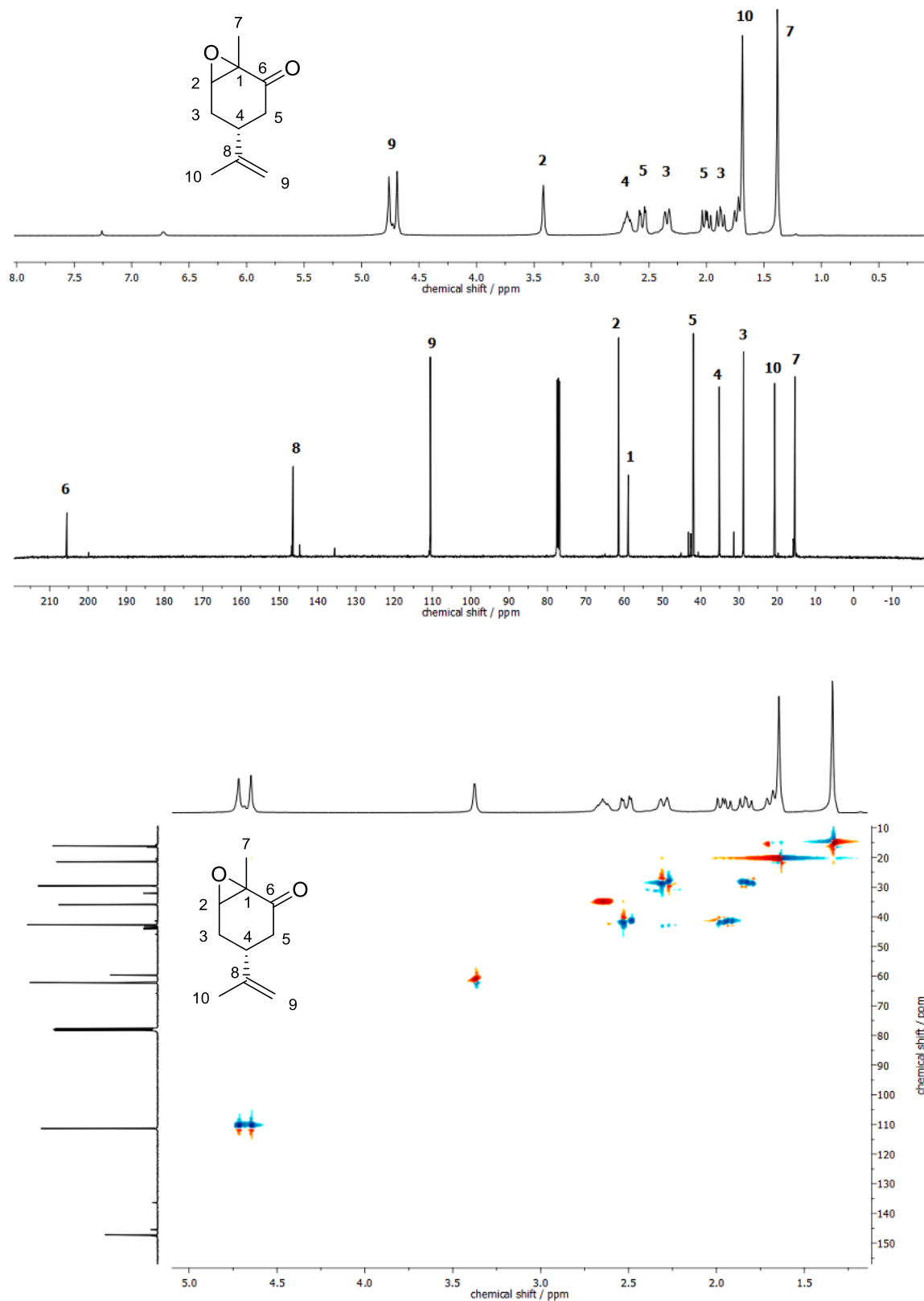
¹³C-NMR (101 MHz, CDCl₃) δ / ppm = 205.51, 146.44, 110.57, 61.43, 58.88, 41.89, 35.13, 28.80, 20.67, 15.37.

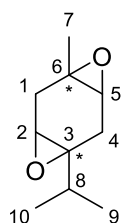
IR (ATR platinum diamond): ν / cm⁻¹ = 2976.6, 2934.1, 1704.8, 1672.0, 1645.1, 1438.3, 1376.2, 1322.3, 1177.7, 1106.7, 1043.1, 988.4, 953.0, 888.9, 813.4, 756.1, 651.5, 503.3, 473.9, 446.9, 428.6.

EI-HRMS of C₁₀H₁₄O₂ [M]⁺ calculated: 166.0988, found: 166.0996.

The NMR spectra are in accordance with the literature.^[119]

* The reaction was carried out by Pascal Rauthe in the scope of his Vertieferarbeit "Synthesis and optimization of terpene-based epoxides and their subsequent rearrangements" under my co-supervision.



γ -Terpinene dioxide (1-isopropyl-5-methyl-4,8-dioxatricyclo[5.1.0.0^{3,5}]octane) 26

The synthesis was carried out following a literature known epoxidation procedure.^[120]

5.00 g (36.7 mmol, 1.00 eq) γ -terpinene and 14.5 g (173 mmol, 4.70 eq) sodium bicarbonate were suspended in 110 mL acetone (0.33M). To the mixture, 29.3 g (95.4 mmol, 2.60 eq) Oxone[®] dissolved in 184 mL water was slowly added under ice cooling and stirring. Subsequently, the reaction was stirred at room temperature for 2 h. 100 mL ethyl acetate were added and the phases were separated. The aqueous phase was extracted with ethyl acetate, then the combined organic phases were washed with water, dried over sodium sulfate and the solvent was removed under reduced pressure. The two isomeric products were purified *via* column chromatography (5- \rightarrow 20% EtOAc/CH).

Fraction 1 (*cis* diastereoisomer according to ^[126]):

Yield: 49%.

R_f = 0.81 (40% EtOAc/CH).

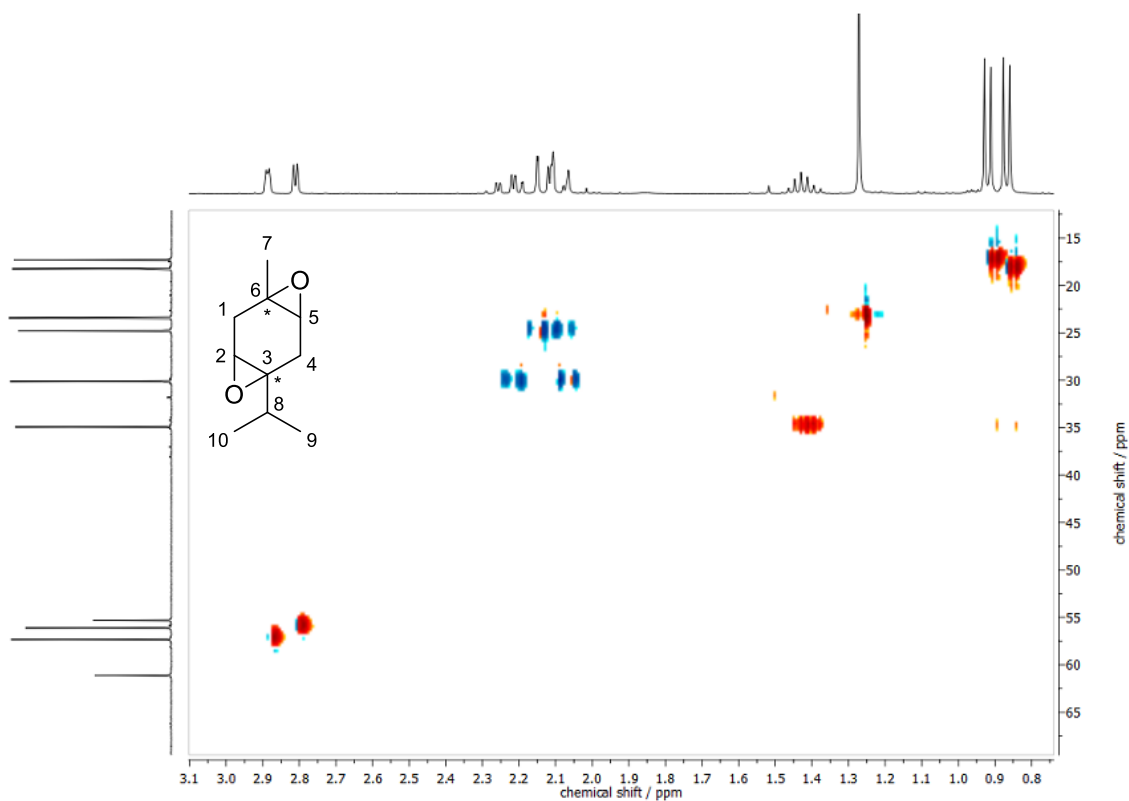
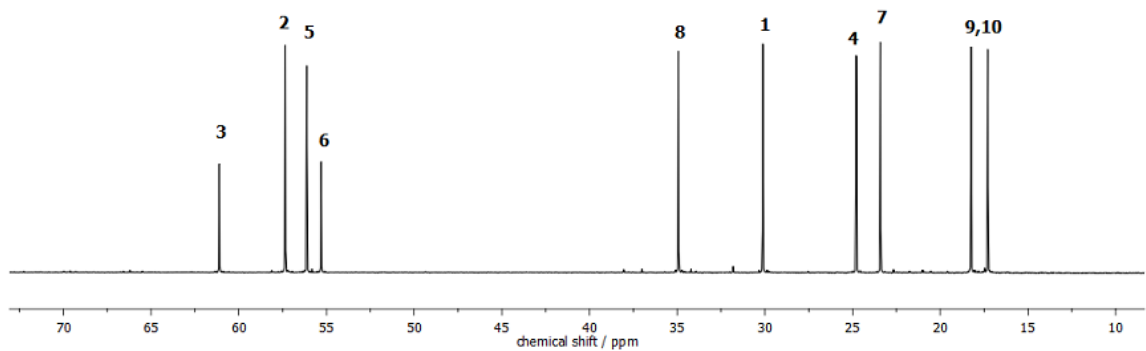
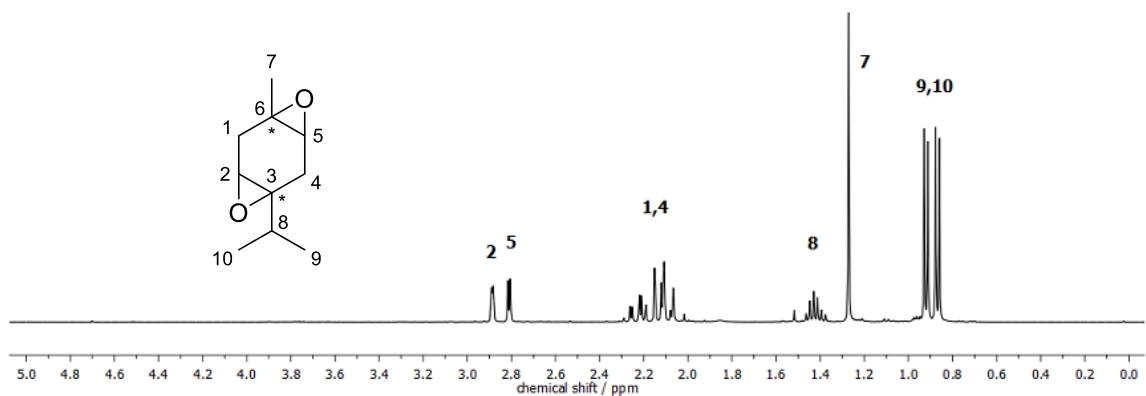
¹H-NMR (400 MHz, CDCl₃) δ / ppm = 2.89 (d, *J* = 3.2 Hz, 1H, H2), 2.82 (d, *J* = 4.0 Hz, 1H, H5), 2.29-2.07 (m, 4H, H1, H4), 1.46-1.38 (m, 1H, H8), 1.27 (s, 3H, H7), 0.92 (d, *J* = 6.8 Hz, 3H, H9/H10), 0.87 (d, *J* = 7.0 Hz, 3H, H9/H10).

¹³C-NMR (101 MHz, CDCl₃) δ / ppm = 61.11, 57.34, 56.12, 55.30, 34.93, 30.12, 24.79, 23.42, 18.25, 17.29.

IR (ATR platinum diamond): ν / cm⁻¹ = 2962.4, 2915.0, 1467.0, 1419.0, 1385.0, 1367.6, 1334.2, 1206.4, 1118.0, 1067.6, 1029.0, 1006.3, 936.2, 895.7, 875.3, 826.4, 733.6, 671.1, 642.6, 525.8, 491.5, 468.3, 430.3.

EI-HRMS of C₁₀H₁₆O₂ [M+H]⁺ calculated: 169.1223, found: 169.1228.

Experimental Section



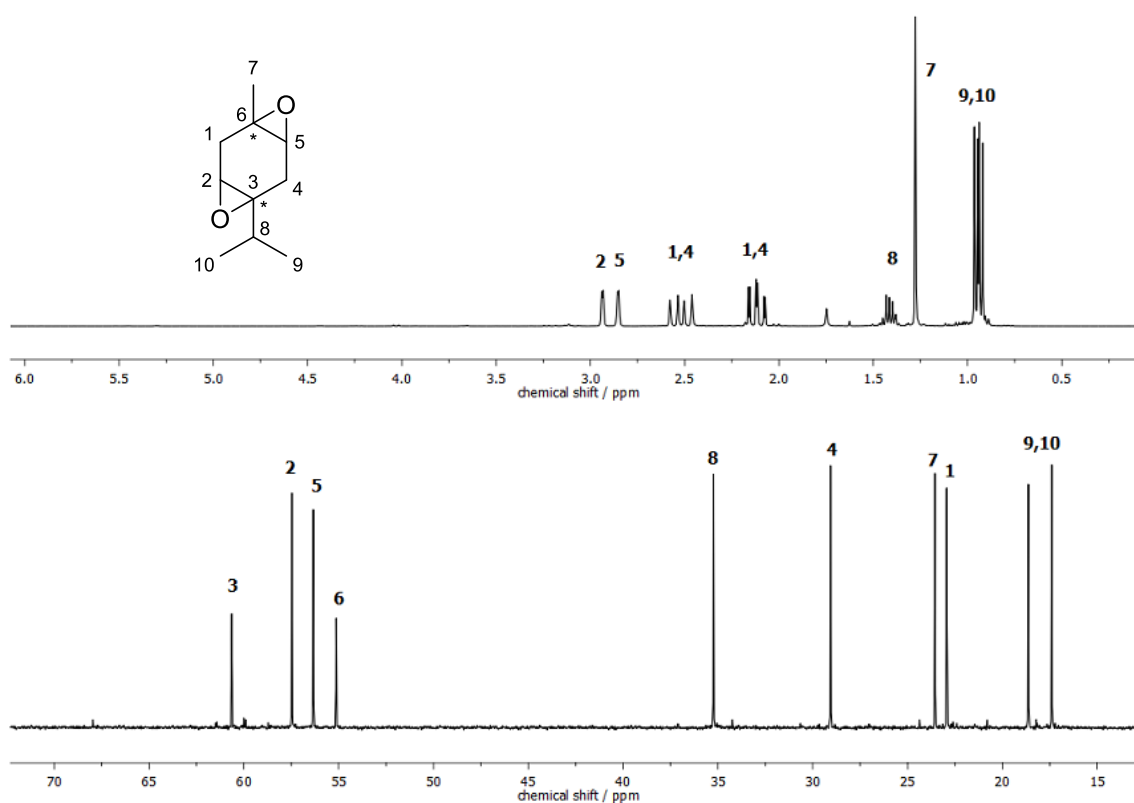
Fraction 2 (*trans* diastereoisomer):**Yield:** 27%**R_f** = 0.36 (40% EtOAc/CH)

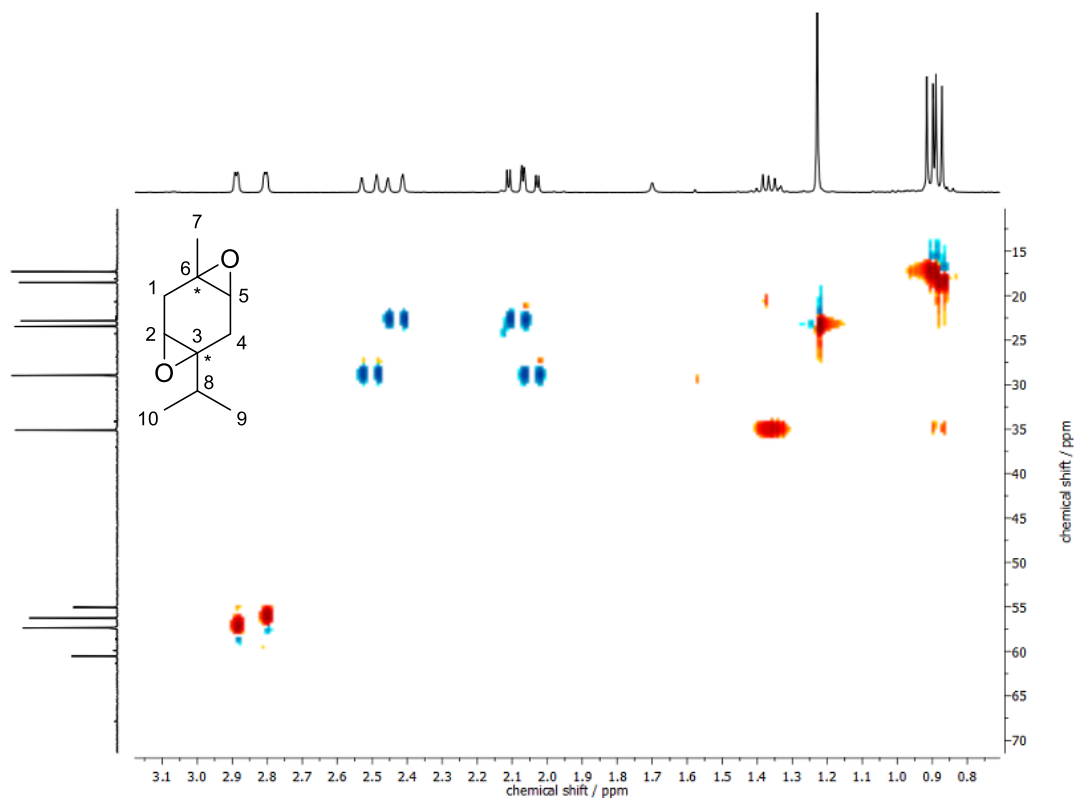
¹H-NMR (400 MHz, CDCl₃) δ / ppm = 2.94 (d, *J* = 2.8 Hz, 1H, H2), 2.85 (d, *J* = 2.3 Hz, 1H, H5), 2.58-2.46 (m, 2H, H1, H4), 2.18-2.07 (m, 2H, H1, H4), 1.46-1.36 (m, 1H, H8), 1.28 (s, 3H, H7), 0.95 (d, *J* = 6.9 Hz, 3H, H9/H10), 0.93 (d, *J* = 7.0 Hz, 3H, H9/H10).

¹³C-NMR (101 MHz, CDCl₃) δ / ppm = 60.64, 57.47, 56.34, 55.14, 35.23, 29.06, 23.55, 22.93, 18.63, 17.40.

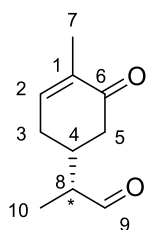
IR (ATR platinum diamond): ν / cm⁻¹ = 3479.5, 2961.5, 2903.6, 1466.8, 1416.1, 1373.2, 1340.1, 1312.8, 1281.9, 1208.5, 1106.7, 1070.1, 1040.6, 976.2, 957.3, 920.2, 873.5, 833.0, 770.2, 707.3, 671.3, 639.8, 597.8, 525.7, 488.0, 463.8, 416.5.

EI-HRMS of C₁₀H₁₆O₂ [M]⁺ calculated: 168.1145, found: 168.1149.



**Detailed reaction procedure for Table 4.3:****Entry 1:**

In a round bottom flask, 30.0 mL dimethyl carbonate and 17.2 g (88.2 mmol, 6.00 eq) peracetic acid (38-40% in acetic acid) were dried over 4Å-molecular sieve for 3 h. Subsequently, the solution was added to 2.00 g (14.7 mmol, 1.00 eq) γ -terpinene and the mixture was heated to 70 °C under argon for 19 h. After cooling to room temperature, 50 mL ethyl acetate were added and the solution was washed with sodium sulfite solution, water and brine. The organic phase was dried over sodium sulfate and the solvent was removed under reduced pressure. The product was purified *via* column chromatography (13% EtOAc/CH) and obtained in a yield of 27.8%.

Carvone-9-aldehyde (2-(4-methyl-5-oxocyclohex-3-en-1-yl)propanal) 28

1.00 g (6.02 mmol, 1.00 eq) of epoxidized (*R*)-(-)-carvone **23** was dissolved in 30 mL THF (0.2M). To the solution, 39.5 mg (60.2 μ mol, 0.01 eq) bismuth triflate was added and the reaction was heated to 40 °C for 1 h. The solution was then diluted with 50 mL ethyl acetate and the organic phase was washed two times with water and dried over sodium sulfate. The solvent was removed under reduced pressure. The crude mixture was purified by column chromatography (20% EtOAc/CH). The product was obtained as a mixture of two diastereoisomers.

Yield: 62%

R_f = 0.44 (40% EtOAc/CH)

¹H-NMR (400 MHz, CDCl₃) δ / ppm = 9.64 (dd, *J* = 7.2, 1.9 Hz, 1H, H9), 6.73-6.70 (m, 1H, H2), 2.53-2.12 (m, 6H, H3+H4+H5+H8), 1.76 (d, *J* = 1.2 Hz, 3H, H7), 1.11 (dd, *J* = 7.1, 2.5 Hz, 3H, H10).

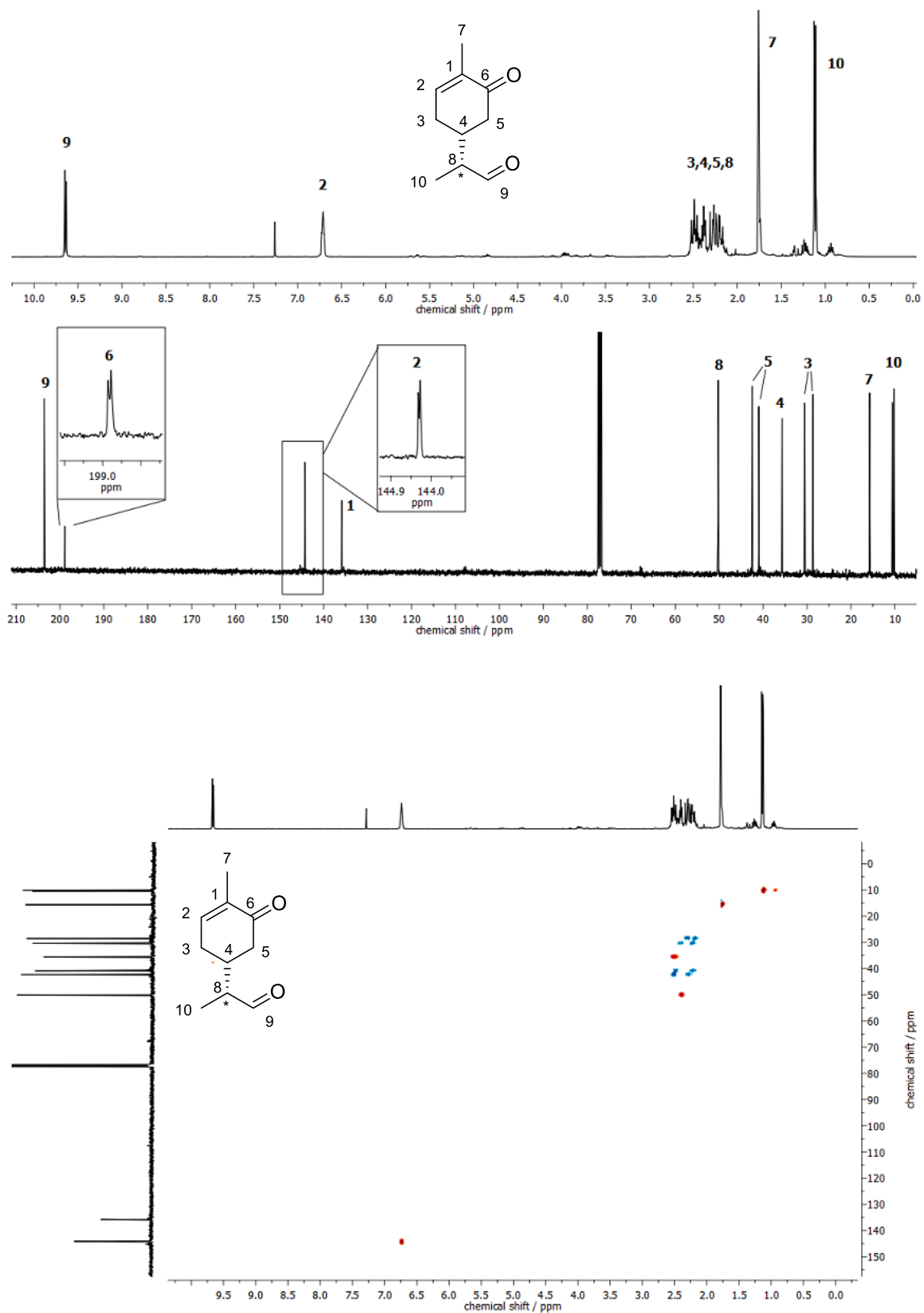
¹³C-NMR (101 MHz, CDCl₃) δ / ppm = 203.57, 198.93, 198.89, 144.29, 144.25, 135.90, 135.87, 50.23, 50.21, 42.46, 40.97, 35.74, 35.68, 30.52, 28.66, 15.77, 15.76, 10.59, 10.21.

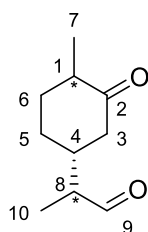
IR (ATR platinum diamond): ν / cm⁻¹ = 3393.8, 2921.7, 2851.4, 2713.7, 1720.8, 1668.8, 1451.8, 1366.0, 1246.2, 1105.4, 1071.7, 931.9, 903.5, 708.4, 551.6, 470.1.

EI-HRMS of C₁₀H₁₄O₂ [M]⁺ calculated: 166.0988, found: 166.0995.

The NMR spectra are in accordance with the literature.^[295]

Experimental Section



Dihydrocarvone-aldehyde (2-(4-methyl-3-oxocyclohexyl)propanal) 30

1.50 g (8.92 mmol, 1.00 eq) of epoxidized dihydrocarvone **20** were dissolved in 45 mL THF (0.2M). To the solution, 58.5 mg (89.2 μ mol, 0.01 eq) bismuth triflate was added and the reaction was heated to 40 °C for 1 h. The solution was then diluted with 50 mL ethyl acetate and the organic phase was washed two times with water and dried over sodium sulfate. The solvent was removed under reduced pressure. The crude mixture was purified by column chromatography (10->20% EtOAc/CH). The product was obtained as a mixture of four diastereoisomers. Due to the instability of the product, small impurities can always be found in the NMR spectrum.

Yield: 60%

R_f = 0.50 (40% EtOAc/CH)

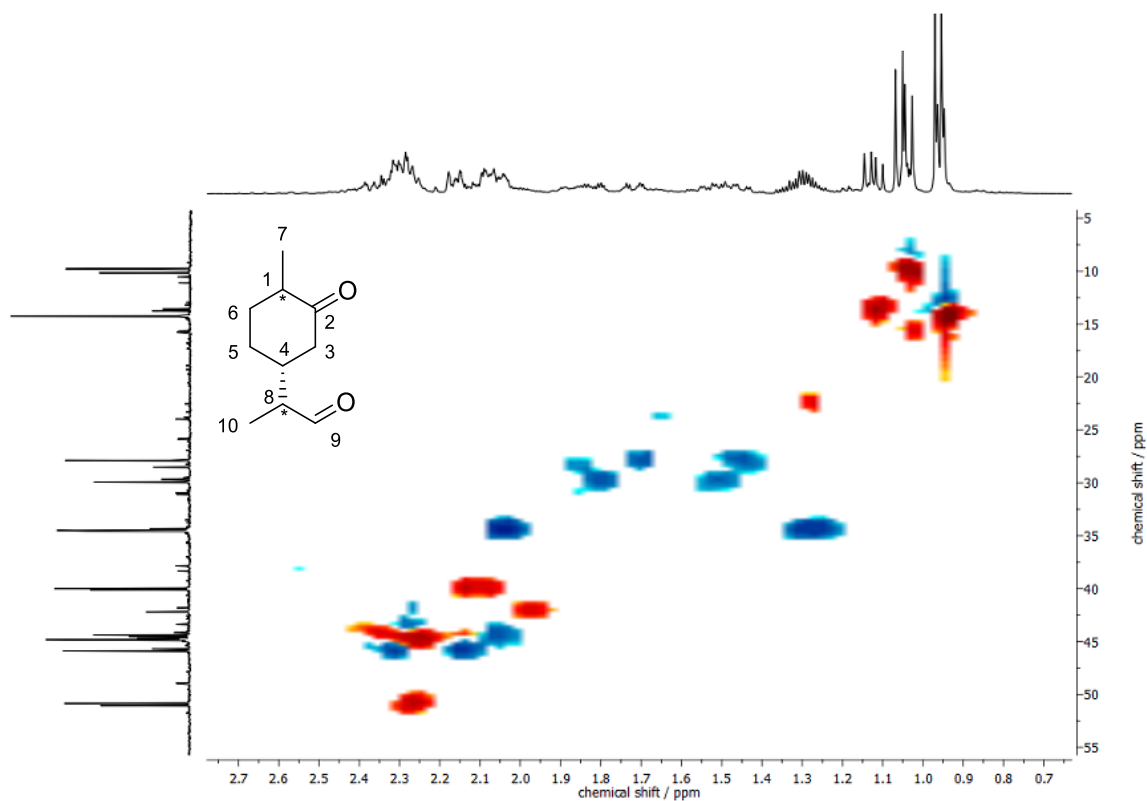
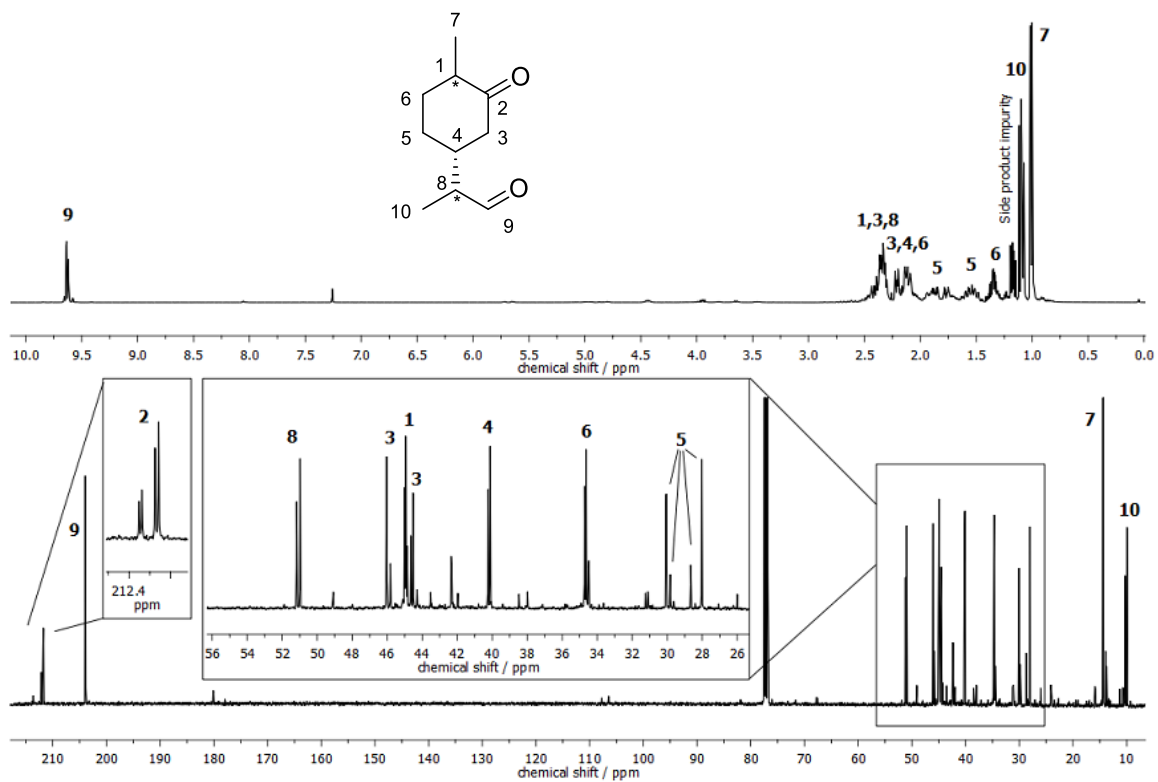
$^1\text{H-NMR}$ (400 MHz, CDCl_3) δ / ppm = 9.66-9.58 (m, 1H, H9), 2.44-2.30 (m, 3H, H1+H3+H8), 2.23-2.09 (m, 3H, H3+H4+H6), 1.94-1.74 (m, 1H, H5), 1.63-1.48 (m, 1H, H5), 1.41-1.29 (m, 1H, H6), 1.12-1.08 (m, 3H, H10), 1.02-1.00 (m, 3H, H7).

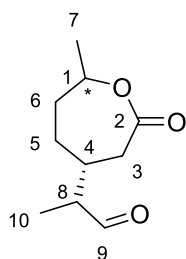
$^{13}\text{C-NMR}$ (101 MHz, CDCl_3) δ / ppm = 212.18, 212.12, 211.84, 211.76, 203.95, 51.17, 50.98, 46.03, 45.82, 45.00, 44.95, 44.86, 44.65, 44.52, 40.23, 40.12, 34.71, 34.64, 34.50, 34.48, 30.05, 29.82, 28.65, 28.03, 14.38, 10.29, 9.92.

IR (ATR platinum diamond): ν / cm^{-1} = 2967.8, 2931.2, 2861.1, 2715.0, 1707.6, 1452.5, 1376.0, 1221.0, 1187.2, 1079.3, 938.2, 885.1, 849.4, 730.2, 639.1, 506.5, 402.3.

EI-HRMS of $\text{C}_{10}\text{H}_{16}\text{O}_2$ $[\text{M}]^+$ calculated: 168.1145, found: 168.1152.

Experimental Section



DHC lactone aldehyde ((2S)-2-((4R)-7-methyl-2-oxooxepan-4-yl)propanal) 31

In a round bottom flask, 250 mg (1.48 mmol, 1.00 eq) epoxidized lactone **21** was dissolved in 7.50 mL THF. Then, 9.70 mg (14.8 μmol , 0.01 eq) bismuth triflate was added and the solution was stirred at 40 °C for 1 h. The solvent was removed and 10 mL ethyl acetate was added. The solution was washed with water, dried over sodium sulfate and the solvent was removed under reduced pressure. The product was purified *via* column chromatography (30% EtOAc/CH) and obtained as a mixture of two diastereoisomers.

Yield: 30%

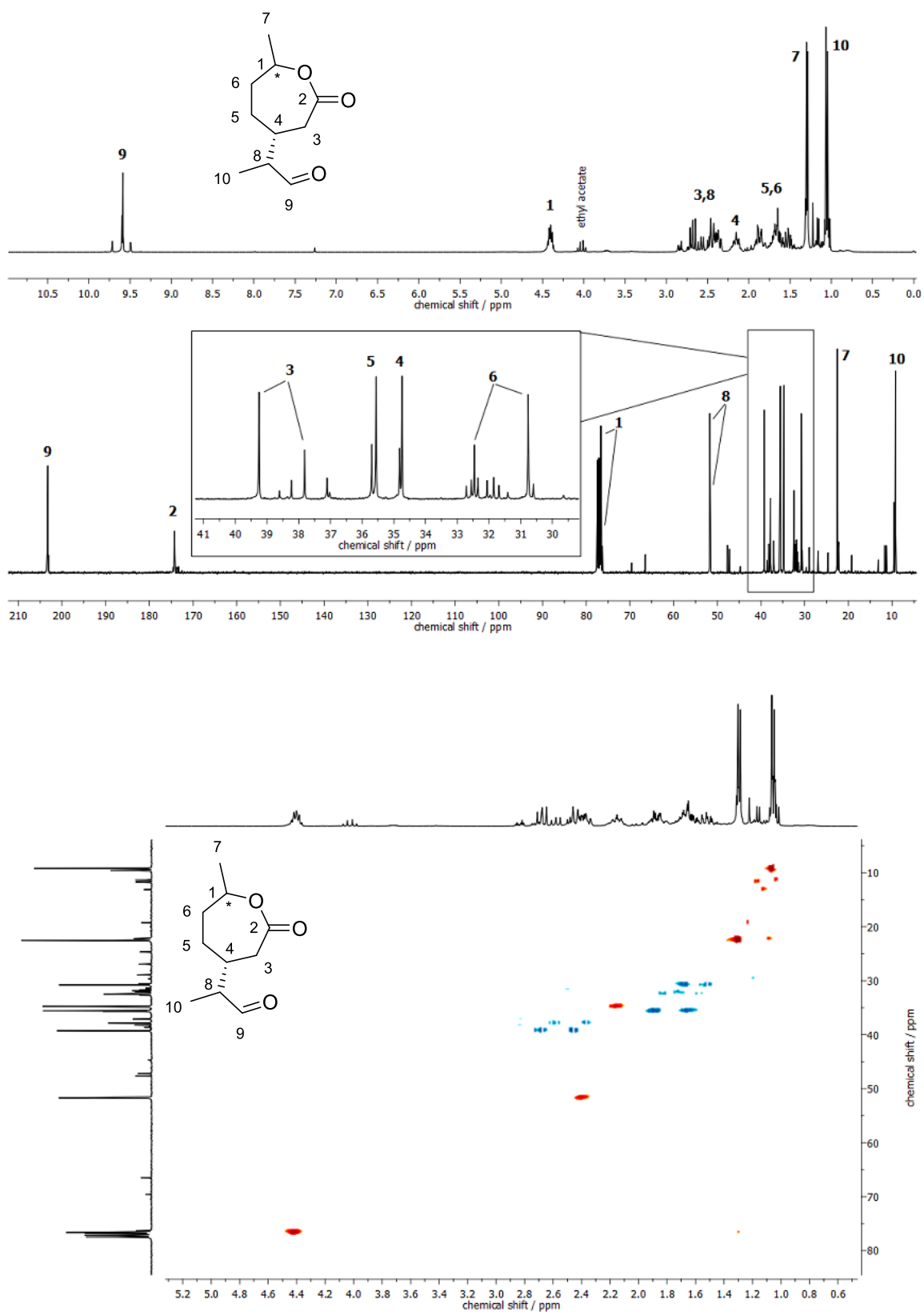
R_f = 0.55 (60% EtOAc/CH)

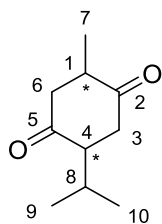
¹H-NMR (400 MHz, CDCl₃) δ / ppm = 9.60-9.59 (m, 1H, H9), 4.48-4.37 (m, 1H, H1), 2.75-2.32 (m, 3H, H3+H8), 2.22-2.10 (m, 1H, H4), 1.93-1.48 (m, 4H, H5+H6), 1.31-1.29 (m, 3H, H7), 1.08-1.03 (m, 3H, H10).

¹³C-NMR (101 MHz, CDCl₃) δ / ppm = 203.26, 203.24, 174.24, 174.14, 76.64, 76.53, 51.71, 51.60, 39.25, 37.81, 35.70, 35.56, 34.82, 34.74, 32.46, 30.76, 22.52, 9.57, 9.21.

IR (ATR platinum diamond): ν / cm⁻¹ = 3735.2, 2974.5, 2936.3, 2199.5, 2118.4, 2011.2, 1965.6, 1717.2, 1453.4, 1380.3, 1324.4, 1285.5, 1252.2, 1213.3, 1176.4, 1142.6, 1092.7, 1063.4, 1040.2, 988.7, 945.0, 907.9, 842.2, 682.8, 643.2 556.3, 438.6.

EI-HRMS of C₁₀H₁₆O₃ [M]⁺ calculated: 184.1094, found: 184.1098.



γ -Terpinene biscarbonyl (2-isopropyl-5-methylcyclohexane-1,4-dione) 32

500 mg (2.97 mmol, 1.00 eq) of epoxidized γ -terpinene were dissolved in 15 mL THF (0.2M). To the solution, 39.0 mg (59.4 μ mol, 0.02 eq) bismuth triflate was added and the reaction was heated to 40 °C for 3 h. The solution was then diluted with 20 mL ethyl acetate and the organic phase was washed two times with water and dried over sodium sulfate. The solvent was removed under reduced pressure. The crude mixture was purified by column chromatography (20- \rightarrow 25% EtOAc/CH). The product was obtained as a mixture of two diastereoisomers.

Yield: 29%

R_f = 0.56 (40% EtOAc/CH)

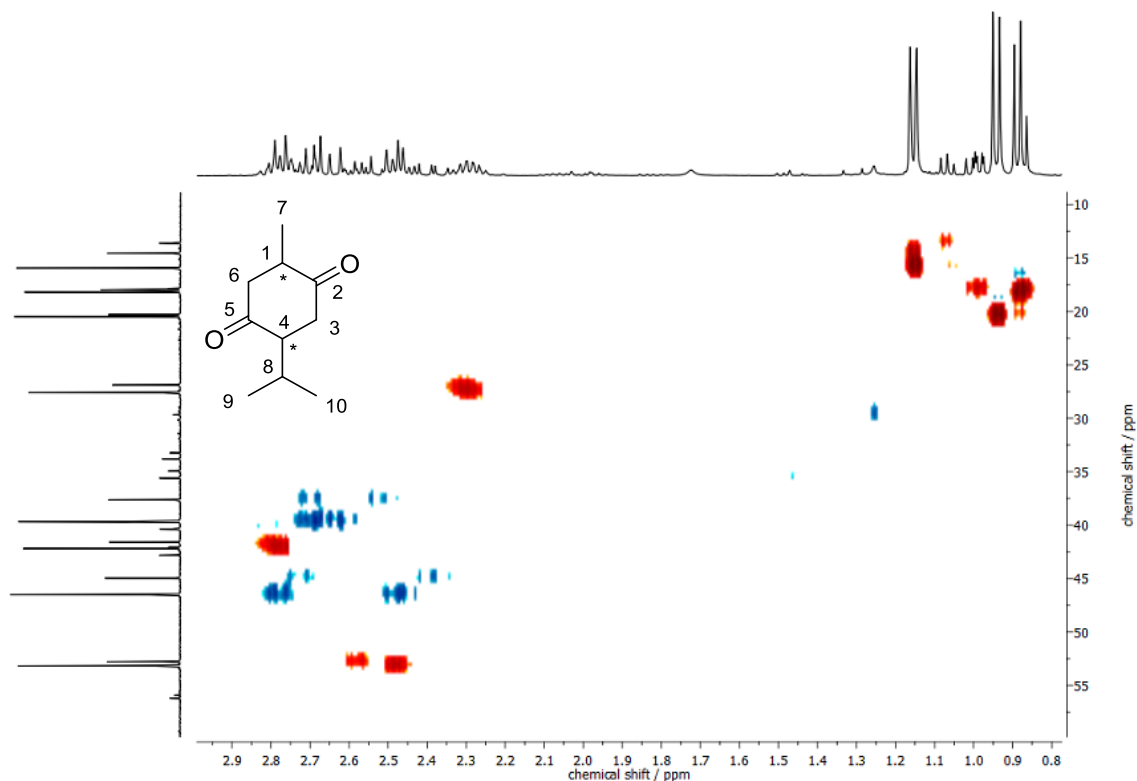
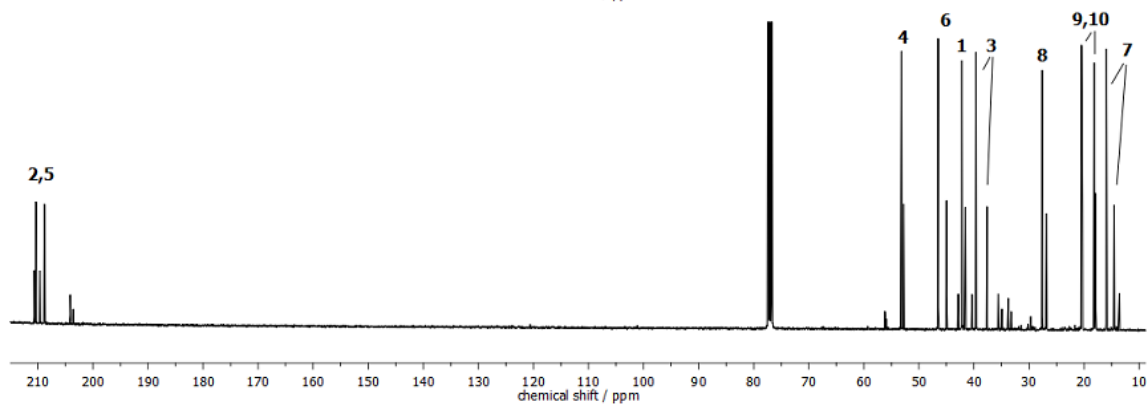
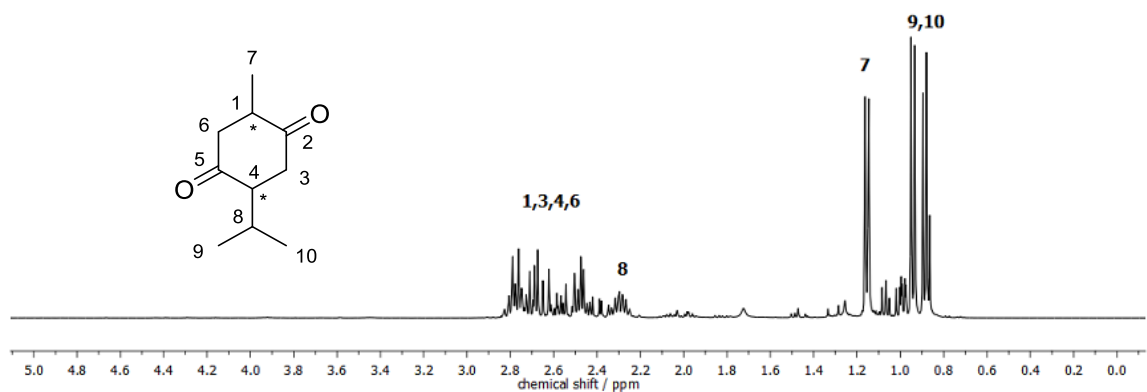
¹H-NMR (400 MHz, CDCl₃) δ / ppm = 2.79-2.34 (m, 6H, H1+H3+H4+H6), 2.31-2.21 (m, 1H, H8), 1.12 (dd, J = 6.6 Hz, 0.9 Hz, 3H, H7), 0.90 (d, J = 6.9 Hz, 3H, H9/10), 0.84 (t, J = 6.5 Hz, 3H, H9/10).

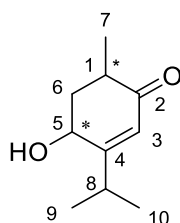
¹³C-NMR (101 MHz, CDCl₃) δ / ppm = 210.76, 210.42, 209.73, 208.90, 53.23, 52.83, 46.58, 45.02, 42.26, 41.66, 39.73, 37.70, 27.67, 26.96, 20.56, 20.39, 18.27, 18.05, 16.03, 14.65.

IR (ATR platinum diamond): ν / cm⁻¹ = 2962.1, 2874.6, 1708.6, 1458.0, 1371.2, 1292.5, 1247.4, 1143.1, 1086.7, 845.3, 775.7, 624.2, 503.9, 454.2, 432.8.

EI-HRMS of C₁₀H₁₆O₂ [M]⁺ calculated: 168.1145, found: 168.1149.

Experimental Section



Identified side product: 4-hydroxy-3-isopropyl-6-methylcyclohex-2-en-1-one

Yield: 17%

$R_f = 0.36$ (40% EtOAc/CH)

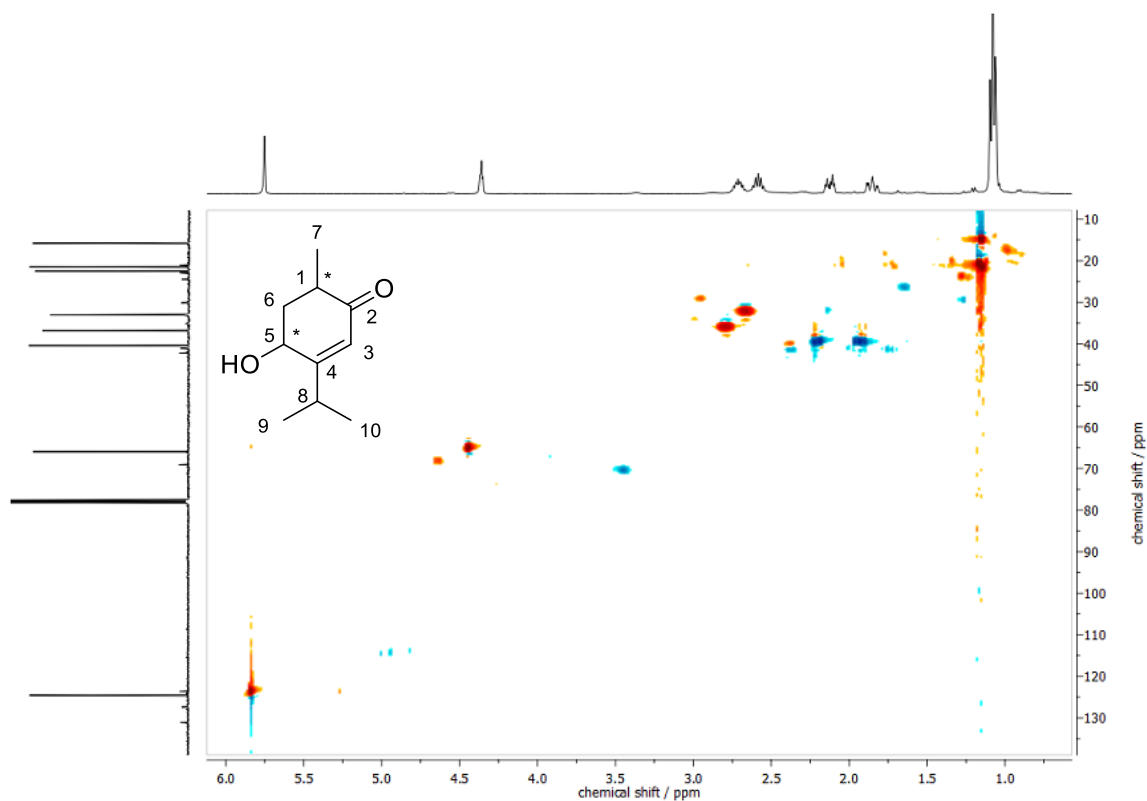
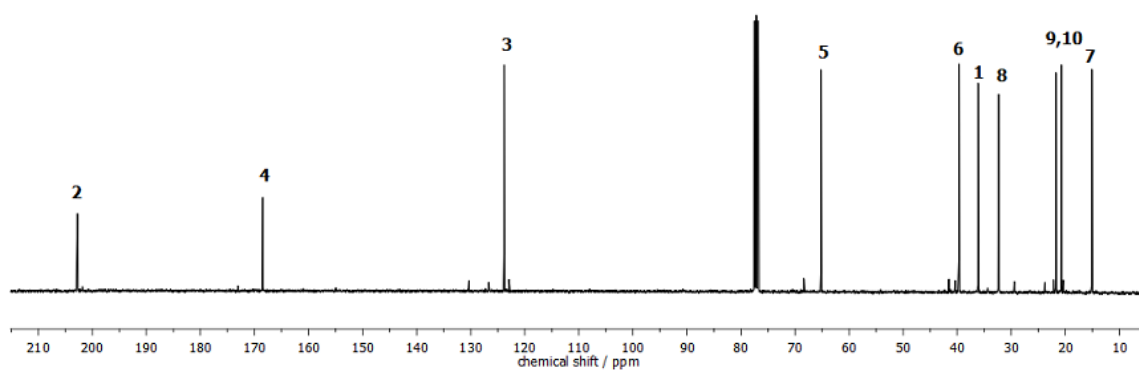
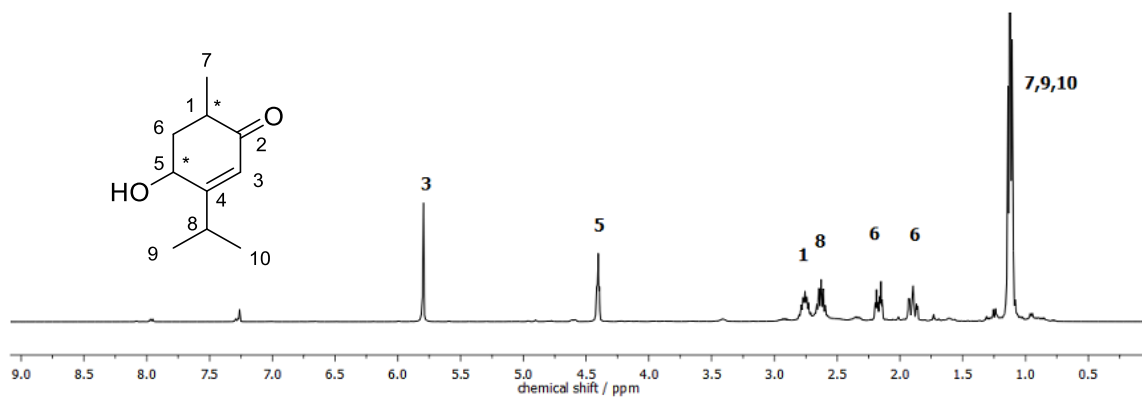
$^1\text{H-NMR}$ (400 MHz, CDCl_3) δ / ppm = 5.80 (s, 1H, H3), 4.40 (t, $J = 3.7$ Hz, 1H, H5), 2.80-2.71 (m, 1H, H1), 2.68-2.58 (m, 1H, H8), 2.20-2.14 (m, 1H, H6), 1.93-1.86 (m, 1H, H6), 1.14-1.11 (m, 9H, H7+H9+H10).

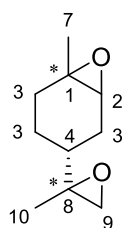
$^{13}\text{C-NMR}$ (101 MHz, CDCl_3) δ / ppm = 202.74, 168.48, 123.80, 65.22, 39.67, 36.11, 32.34, 21.76, 20.76, 15.08.

IR (ATR platinum diamond): ν / cm^{-1} = 3395.0, 2964.0, 2932.6, 2874.7, 1656.2, 1460.9, 1377.0, 1330.0, 1261.7, 1217.7, 1187.1, 1097.5, 1066.0, 1026.4, 970.2, 937.3, 893.3, 844.8, 752.7, 709.3, 579.6, 507.3.

EI-HRMS of $\text{C}_{10}\text{H}_{16}\text{O}_2$ $[\text{M}]^+$ calculated: 168.1145, found: 168.1151.

Experimental Section



Limonene dioxide (1-methyl-4-(2-methyloxiran-2-yl)-7-oxabicyclo[4.1.0]heptane) 34

The synthesis was carried out according to literature.^[120]

In a three-necked round bottom flask, 10.0 g (73.4 mmol, 1.00 eq) (*R*)-(+)-limonene were dissolved in 220 mL acetone. 29.0 g (345 mmol, 4.70 eq) sodium bicarbonate were added and the mixture was stirred at room temperature. 58.7 g (190.8 mmol, 2.60 eq) Oxone[®], dissolved in 367 mL water (0.52M), was slowly added to the reaction mixture using a dropping funnel. After the reaction (90 min), the product was extracted with diethyl ether, dried over sodium sulfate and the solvent was removed. The crude mixture was purified by column chromatography (10% EtOAc/CH). The product was obtained as a mixture of four isomers.

Yield: 72%.

R_f = 0.59 (40% EtOAc/CH)

¹H-NMR (400 MHz, CDCl₃) δ / ppm = 2.94-2.86 (m, 1H, H2), 2.51-2.38 (m, 2H, H9), 2.08-1.23 (m, 6H, H4+H3), 1.20 (s, 3H, H7), 1.13-1.10 (m, 3H, H10), 1.07-0.88 (m, 1H, H4+H3).

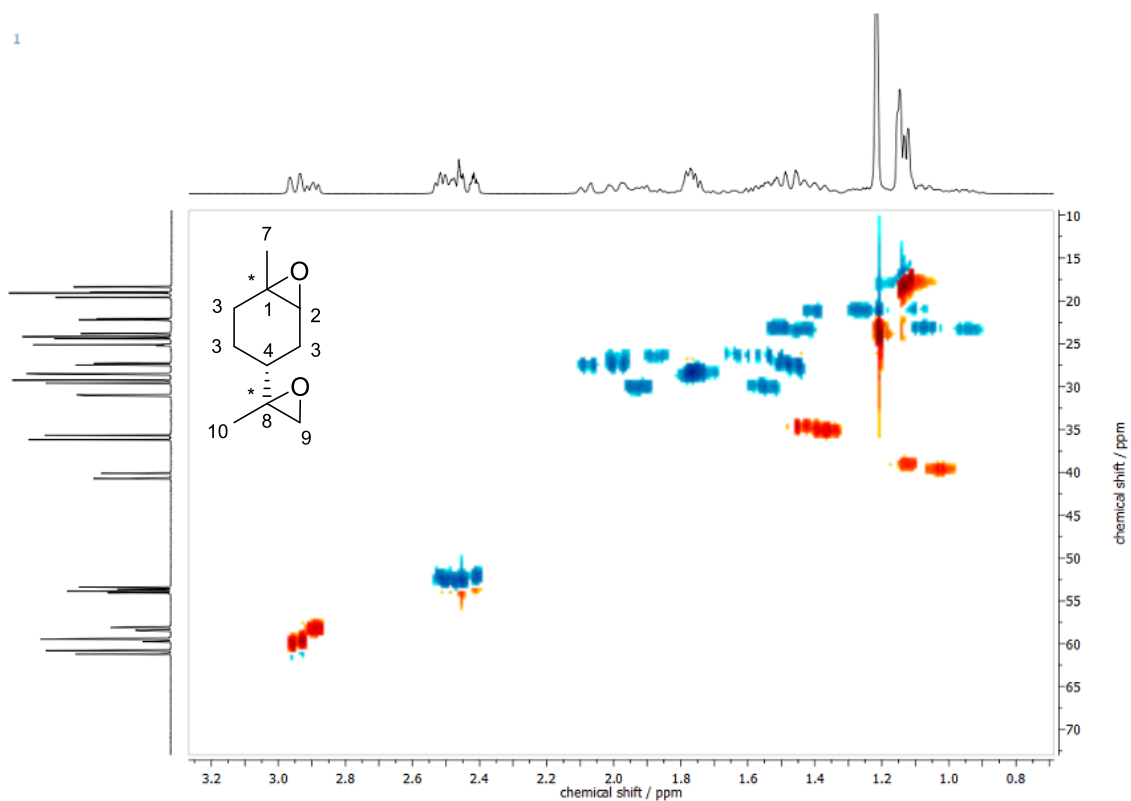
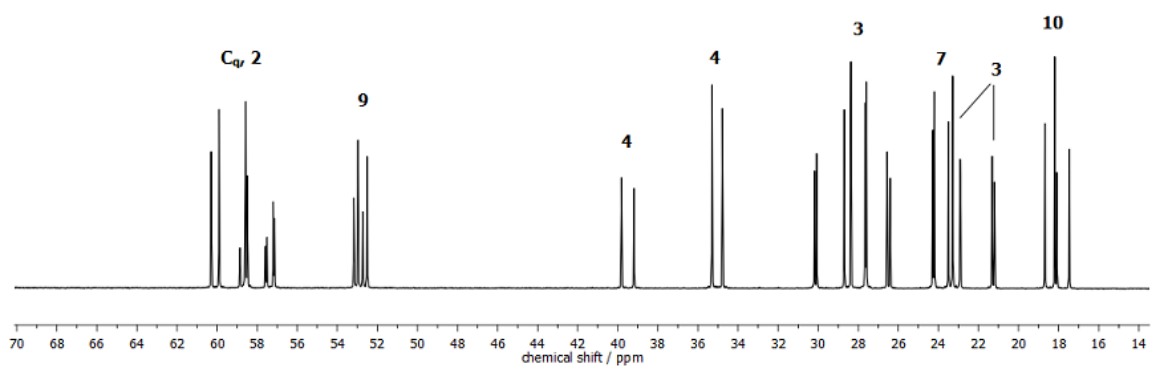
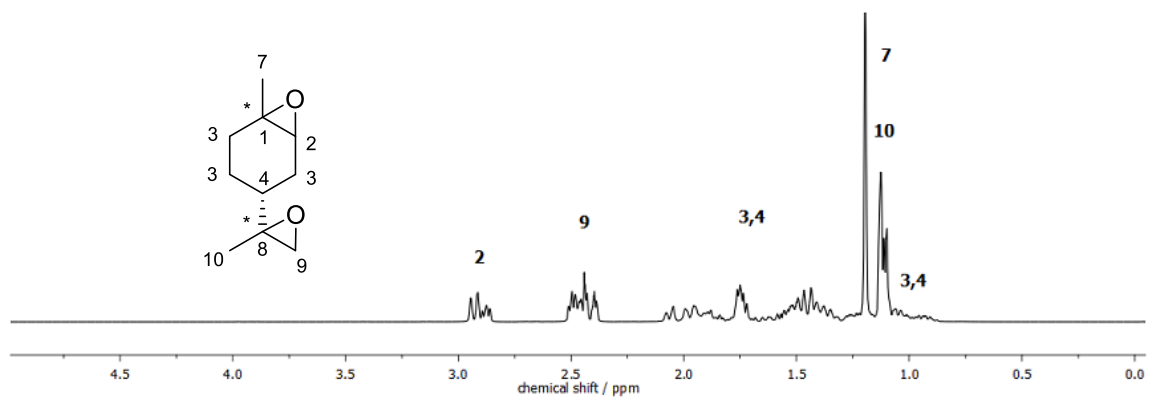
¹³C-NMR (101 MHz, CDCl₃) δ / ppm = 60.30, 59.90, 58.86, 58.61, 58.58, 58.49, 57.58, 57.52, 57.20, 57.14, 53.17, 52.96, 52.73, 52.52, 39.81, 39.19, 35.29, 34.77, 30.19, 30.07, 28.70, 28.36, 27.65, 27.60, 26.56, 26.41, 24.28, 24.20, 23.50, 23.29, 22.92, 22.90, 21.32, 21.20, 18.68, 18.19, 18.09, 17.47.

IR (ATR platinum diamond): ν / cm⁻¹ = 2927.6, 1435.5, 1380.3, 1358.1, 1282.5, 1210.8, 1181.8, 1124.9, 1106.0, 1068.5, 1038.5, 1021.7, 941.0, 902.8, 850.7, 835.9, 798.5, 762.2, 671.0, 617.2, 550.0, 497.7, 472.2, 454.7, 433.9.

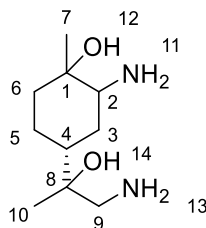
EI-HRMS of C₁₀H₁₆O₂ [M]⁺ calculated: 168.1145, found: 168.1151.

The NMR spectra are in accordance with the literature.^[120]

Experimental Section



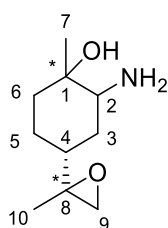
Limonene bis-amino alcohol (2-amino-4-(1-amino-2-hydroxypropan-2-yl)-1-methylcyclohexan-1-ol) 40



The synthesis was adapted from a literature known procedure.^[203]

In a pressure reactor flask, 5.00 g (29.7 mmol, 1.00 eq) limonene dioxide (obtained from epoxidation of (*R*)-(+)-limonene) were dissolved in 85 mL (594 mmol, 20.0 eq) ammonia solution (7N in MeOH). The mixture was heated at 100 °C for 48 h in the pressure reactor to prevent ammonia evaporation. The solvent was removed under reduced pressure and the product was purified *via* column chromatography (10% MeOH/EtOAc). (TLC plates were stained with a ninhydrin solution in ethanol).

Fraction 1 (one diastereoisomer):



Yield: 27%

R_f = 0.46 (100% MeOH)

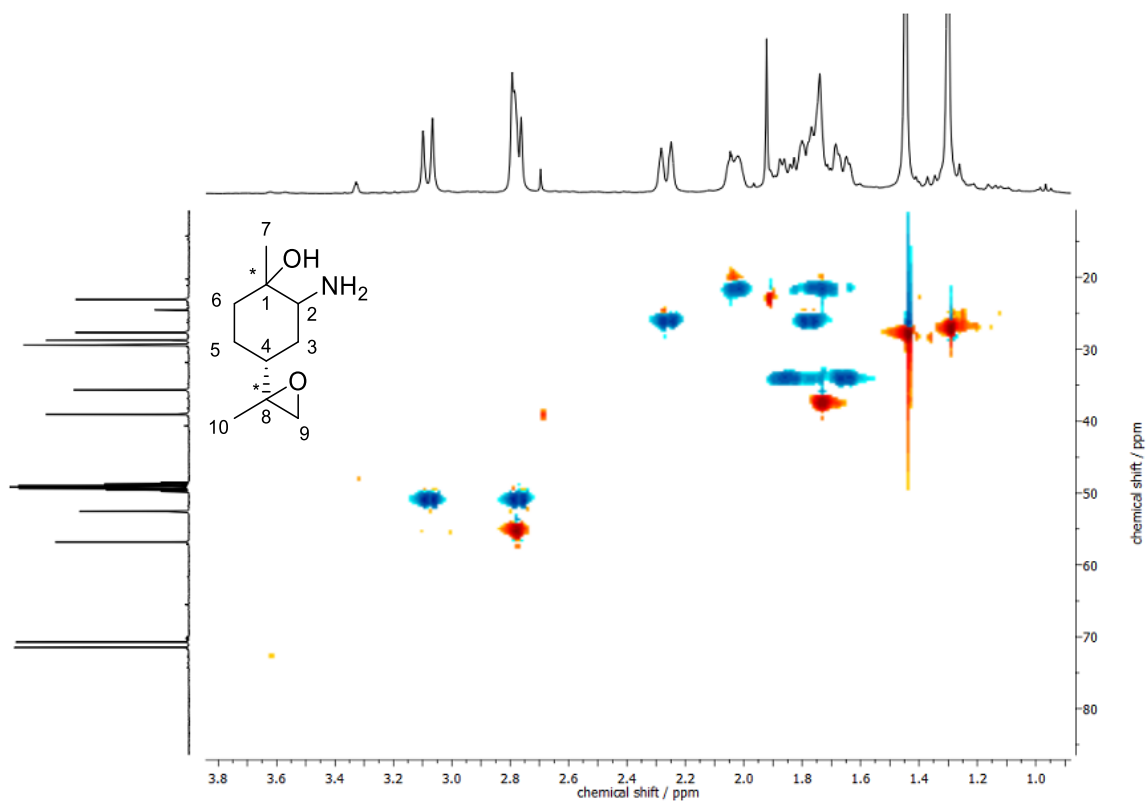
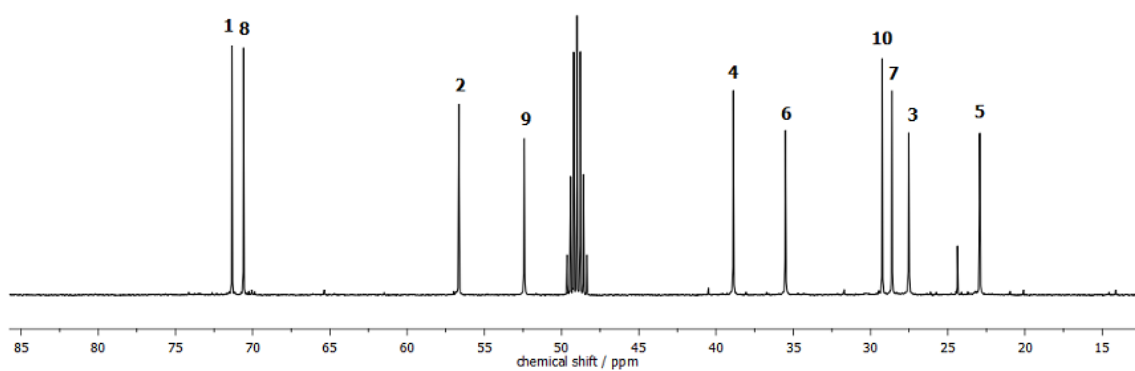
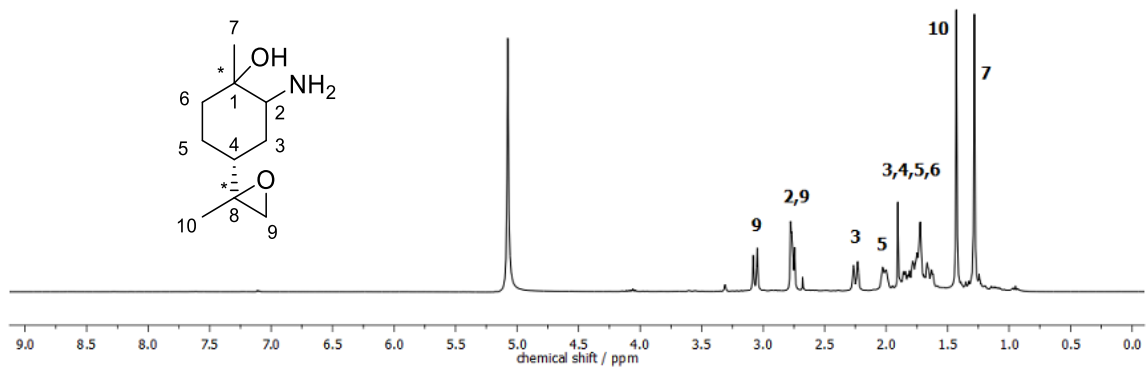
¹H-NMR (400 MHz, MeOH-d₄) δ / ppm = 3.08-3.05 (m, 1H, H₉), 2.78-2.74 (m, 2H, H₂+H₉), 2.26-2.23 (m, 1H, H₃), 2.03-2.00 (m, 1H, H₅), 1.86-1.62 (m, 5H, H₃+H₄+H₅+H₆), 1.43 (s, 3H, H₁₀), 1.28 (s, 3H, H₇).

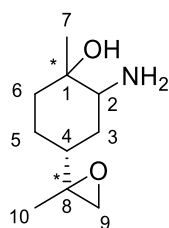
¹³C-NMR (101 MHz, MeOH-d₄) δ / ppm = 71.33, 70.59, 56.65, 52.41, 38.87, 35.50, 29.23, 28.61, 27.51, 22.92.

IR (ATR platinum diamond): ν / cm⁻¹ = 3303.4, 2936.8, 2826.0, 1659.2, 1447.8, 1374.4, 1210.4, 1126.4, 1087.9, 1026.9, 983.0, 971.2, 949.3, 922.0, 894.8, 855.4, 825.0, 631.5, 566.3.

ESI-HRMS of C₁₀H₁₉NO₂ [M+H]⁺ calculated: 186.1489, found: 186.1488.

Experimental Section



Fraction 2 (one diastereoisomer):

Yield: 25%

R_f = 0.23 (100% MeOH)

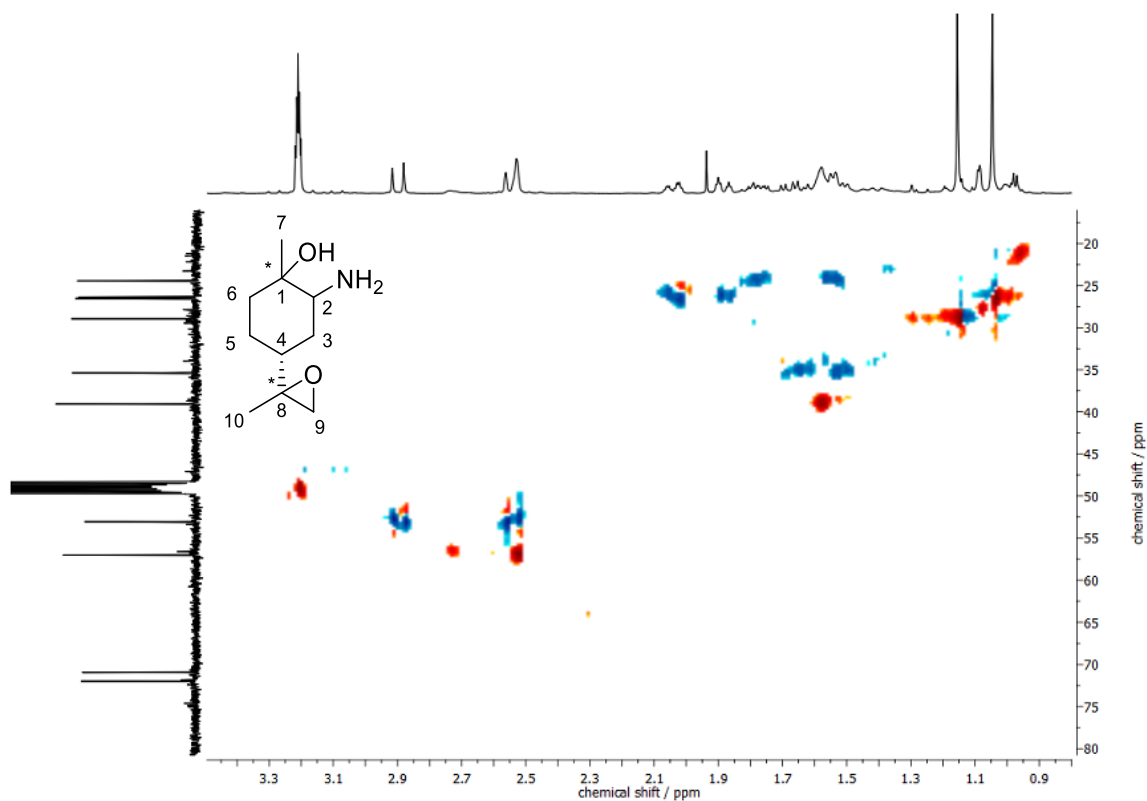
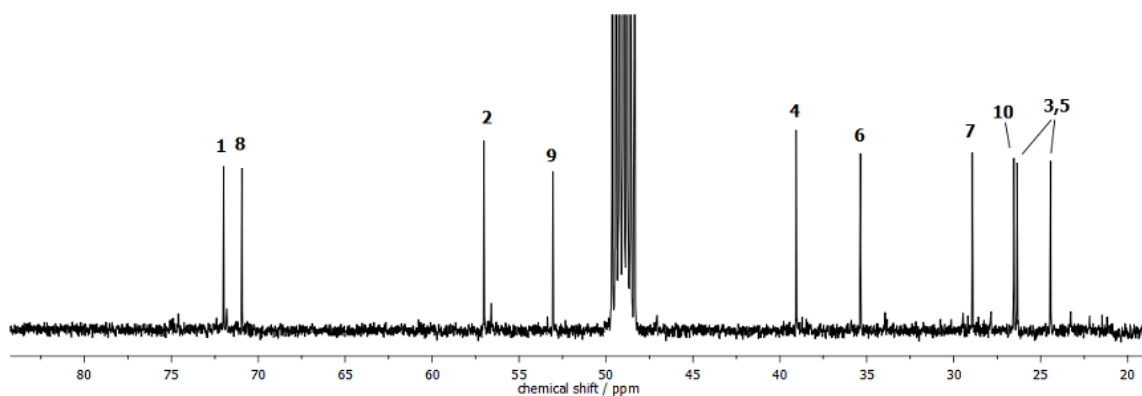
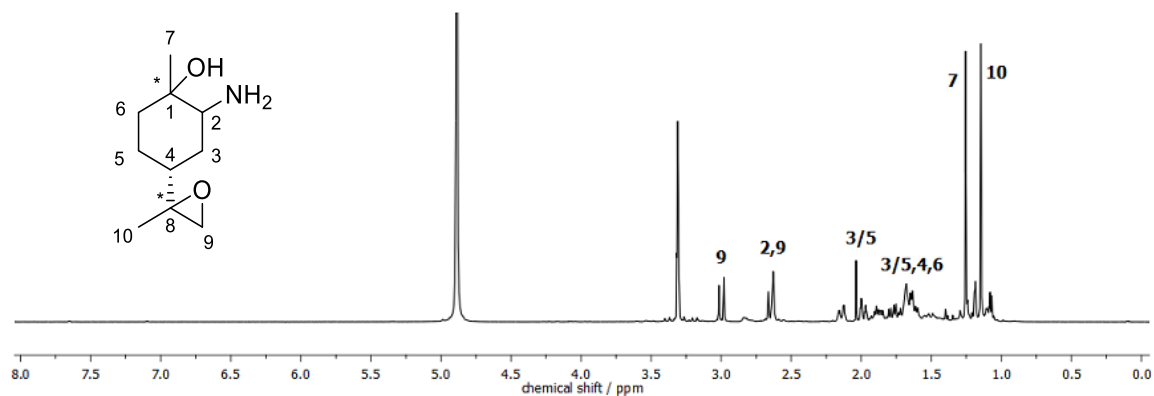
¹H-NMR (400 MHz, MeOH-d₄) δ / ppm = 3.02-2.98 (m, 1H, H9), 2.66-2.63 (m, 2H, H2+H9), 2.17-2.11 (m, 1H, H3/H5), 2.04-2.01 (m, 1H, H3/H5), 1.93-1.85 (m, 1H, H3/H5), 1.80-1.60 (m, 4H, H3/H5+H4+H6), 1.26 (s, 3H, H7), 1.15 (s, 3H, H10).

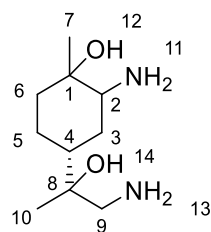
¹³C-NMR (101 MHz, MeOH-d₄) δ / ppm = 71.99, 70.94, 57.02, 53.04, 39.06, 35.36, 28.93, 26.54, 26.35, 24.43.

IR (ATR platinum diamond): ν / cm⁻¹ = 3299.6, 2965.7, 2939.8, 1947.5, 1575.3, 1466.2, 1408.8, 1370.7, 1306.1, 1262.0, 1244.1, 1213.1, 1181.7, 1146.1, 1114.4, 1095.2, 1045.9, 1004.2, 983.6, 970.3, 942.2, 925.6, 907.4, 870.3, 851.1, 795.9, 745.6, 678.8, 569.7, 519.3, 485.0, 422.2.

ESI-HRMS of C₁₀H₁₉NO₂ [M+H]⁺ calculated: 186.1489, found: 186.1489.

Experimental Section



Fraction 3 (two diastereoisomers):

Yield: 47%

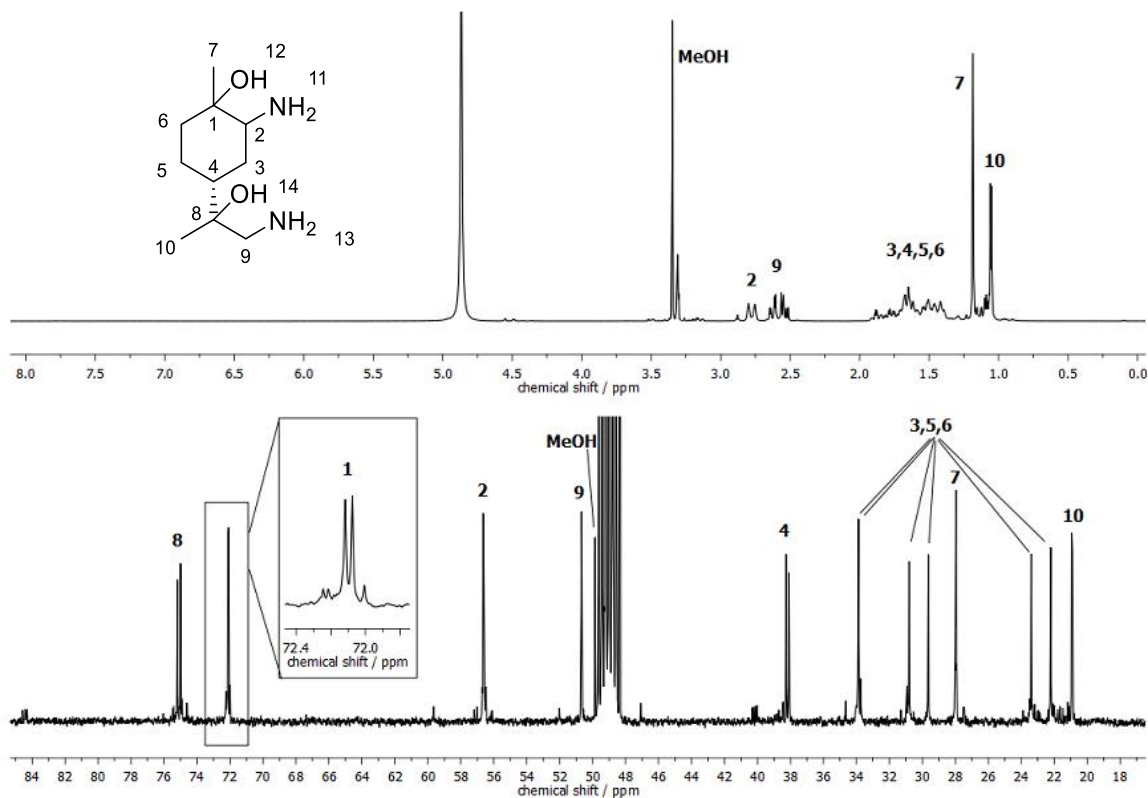
$R_f = 0.01$ (100% MeOH)

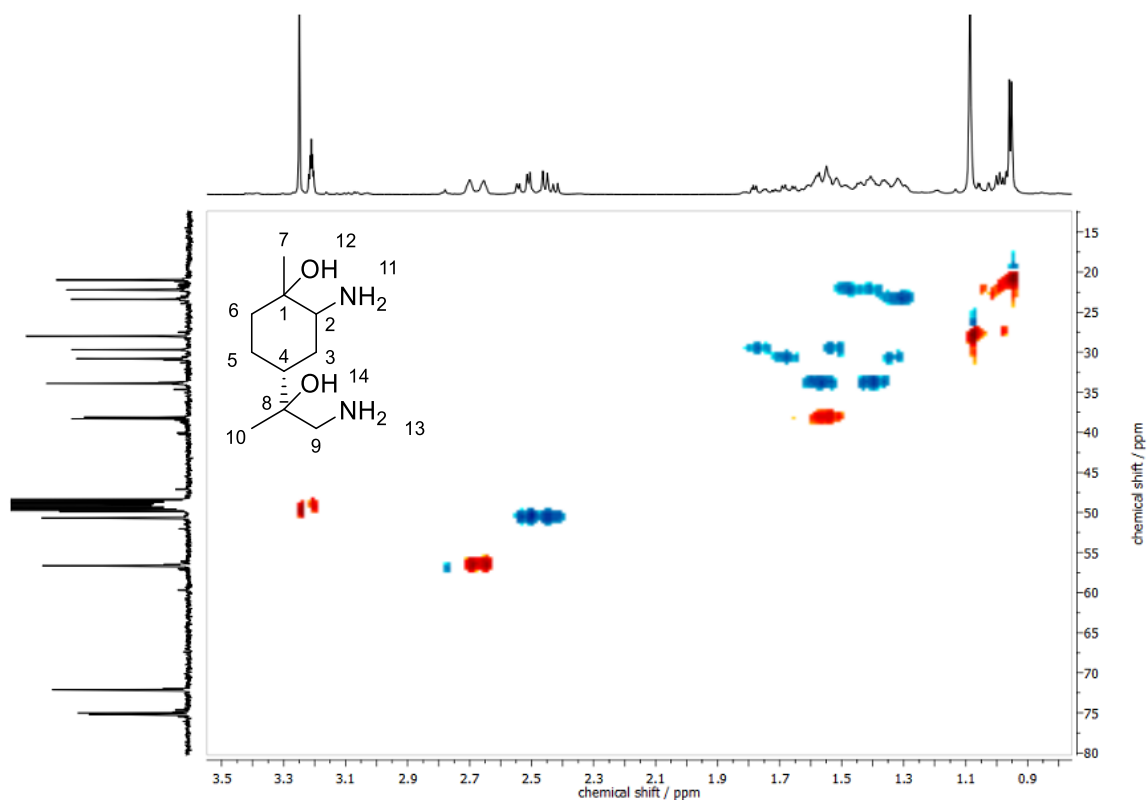
$^1\text{H-NMR}$ (400 MHz, MeOH- d_4) δ / ppm = 3.80-2.75 (m, 1H, H2), 2.65-2.51 (m, 2H, H9), 1.91-1.39 (m, 7H, H3+H4+H5+H6), 1.19 (s, 3H, H7), 1.05 (d, $J = 3.2$ Hz, 3H, H10).

$^{13}\text{C-NMR}$ (101 MHz, MeOH- d_4) δ / ppm = 75.19, 74.99, 72.12, 72.08, 56.64, 56.60, 50.68, 50.66, 38.27, 38.10, 33.90, 33.88, 30.80, 29.64, 27.99, 27.96, 23.39, 22.22, 20.95, 20.90.

IR (ATR platinum diamond): ν / cm^{-1} = 3291.7, 2932.9, 1583.9, 1458.0, 1374.3, 1173.2, 1122.0, 1033.1, 941.1, 907.5, 860.4, 817.8, 621.0, 420.9.

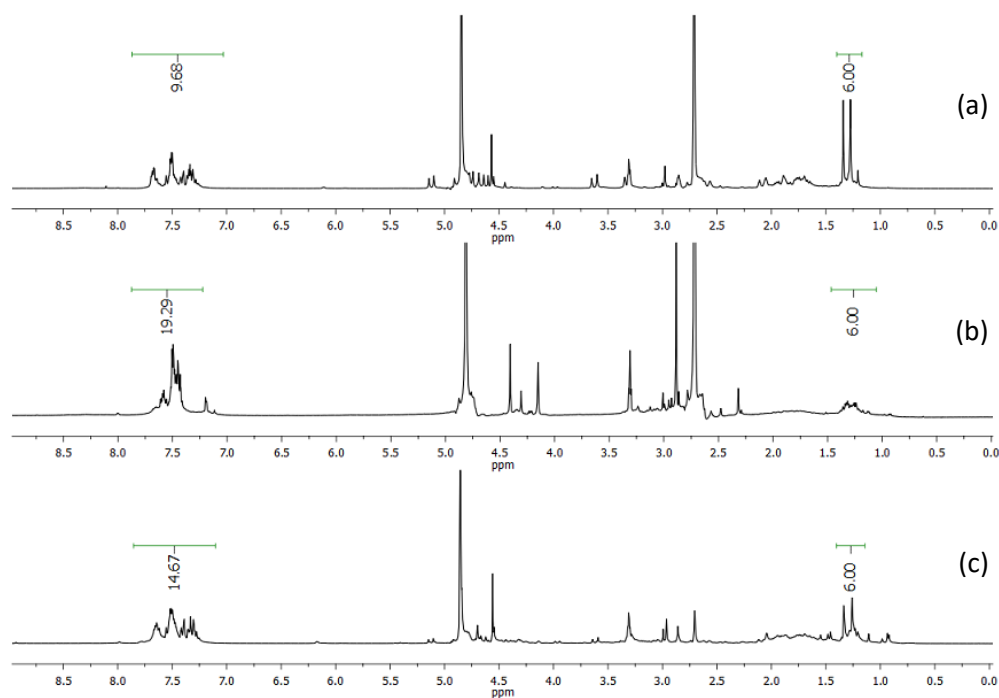
ESI-HRMS of $\text{C}_{10}\text{H}_{22}\text{N}_2\text{O}_2$ $[\text{M}+\text{H}]^+$ calculated: 203.1754, found: 203.1754.

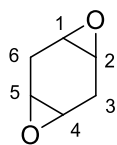




Benylation of limonene bis-amino alcohols:

Fractions 2 (a) and 3 (b) as well as the crude product (c) were mixed with 20.0 eq benzyl bromide and few mL of DMF. The mixtures were stirred at room temperature for 24 h. Subsequently, unreacted benzyl bromide and DMF were removed under high vacuum at 100 °C and the products were analyzed *via* NMR spectroscopy.



1,4-Cyclohexane dioxide (4,8-dioxatricyclo[5.1.0.0^{3,5}]octane) 45

The synthesis was carried out according to a literature known procedure.^[120]

In a three-necked flask, 5.00 g (62.4 mmol, 1.00 eq) 1,4-cyclohexadiene and 24.6 g (293 mmol, 4.70 eq) sodium bicarbonate were mixed with 189 mL acetone (0.33M). In a separate flask, 49.8 g (162 mmol, 2.60 eq) Oxone[®] were dissolved in 324 mL water (0.5M). The solution was slowly added to the reaction mixture under cooling. The reaction mixture was stirred at room temperature for 1.5 h. The product was extracted with ethyl acetate, dried over sodium sulfate and the solvent was removed under reduced pressure. The two isomeric products were then isolated *via* column chromatography (25-75% EtOAc/CH).

Fraction 1 (*trans*-isomer) 45a:

Yield: 30%

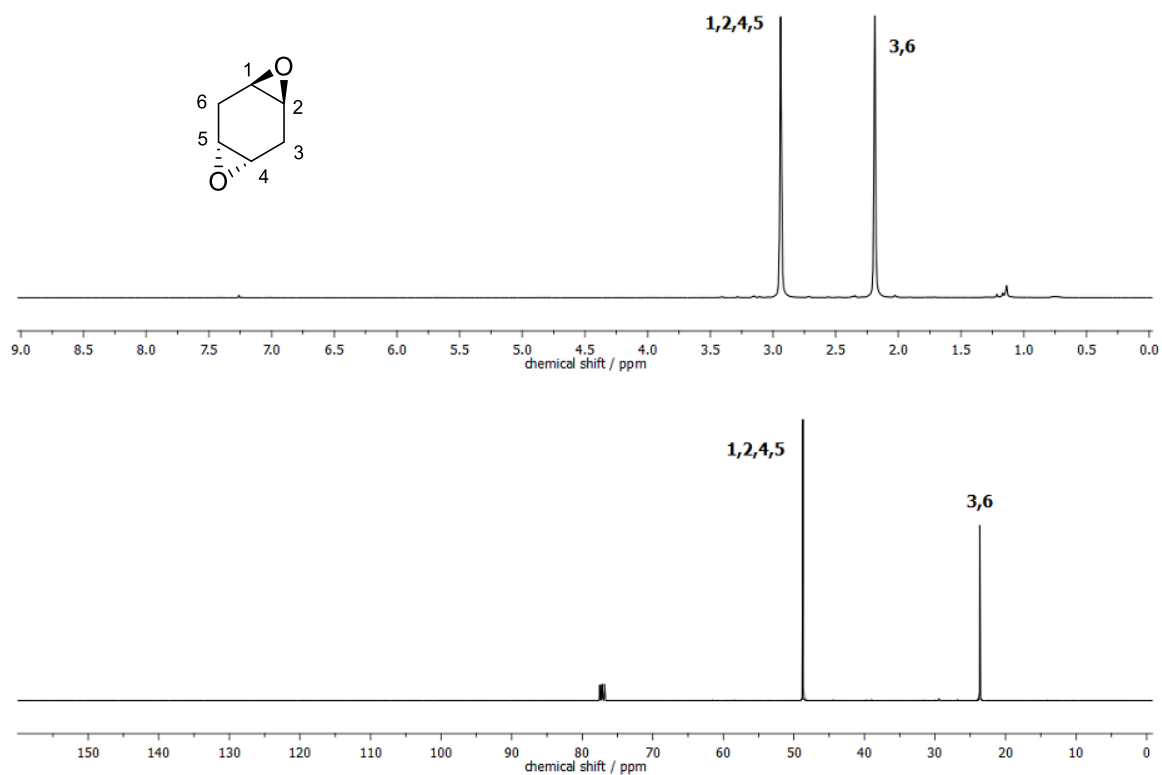
R_f = 0.42 (50% EtOAc/CH)

¹H-NMR (400 MHz, CDCl₃) δ / ppm = 2.94 (s, 4H, H1+H2+H4+H5), 2.19 (s, 4H, H3+H6).

¹³C-NMR (101 MHz, CDCl₃) δ / ppm = 48.73, 23.68.

IR (ATR platinum diamond): ν / cm⁻¹ = 3010.2, 2942.7, 2923.6, 2824.9, 1470.8, 1419.2, 1389.4, 1339.9, 1266.3, 1231.1, 1134.6, 1045.1, 930.0, 902.3, 859.0, 801.7, 718.2, 423.5.

EI-HRMS of C₆H₈O₂ [M]⁺ calculated: 112.0519, found: 112.0525. (mixture of both isomers)



Fraction 2 (*cis*-isomer) **45b:**

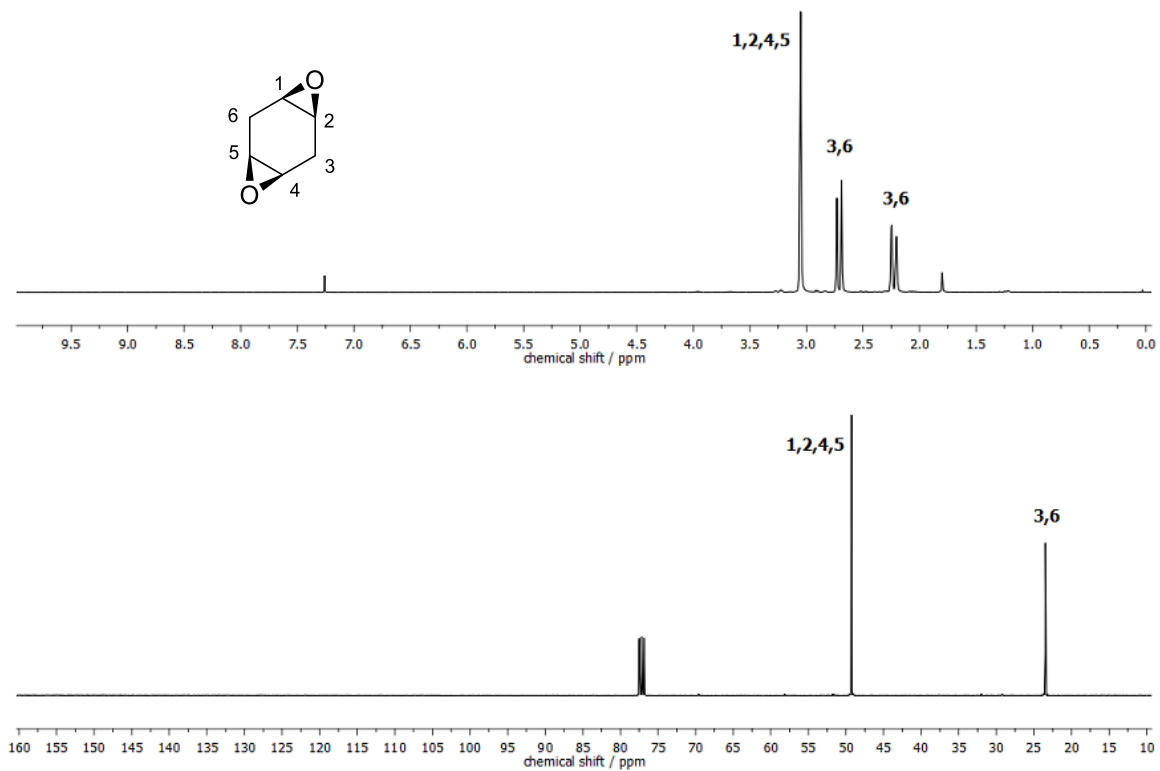
Yield: 5%

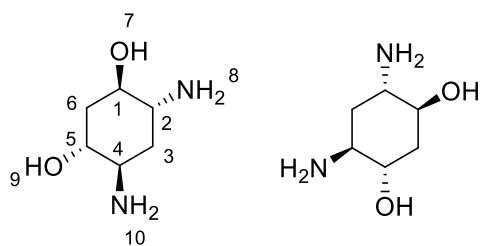
R_f = 0.11 (50% EtOAc/CH)

$^1\text{H-NMR}$ (400 MHz, CDCl_3) δ / ppm = 3.10-2.98 (m, 4H, H1+H2+H4+H5), 2.71 (d, J = 17.1 Hz, 2H, H3+H6), 2.27-2.16 (m, 2H, H3+H6).

$^{13}\text{C-NMR}$ (101 MHz, CDCl_3) δ / ppm = 49.25, 23.48.

IR (ATR platinum diamond): ν / cm^{-1} = 3009.6, 2912.2, 2360.3, 1469.2, 1422.2, 1353.1, 1263.4, 1094.2, 1019.5, 931.7, 896.1, 831.4, 808.0, 788.3, 768.5, 682.1, 591.8.



***trans*-1,4-Cyclohexadiene-derived aminoalcohol (4,6-diaminocyclohexane-1,3-diol) 46**

In a high pressure Teflon tube, 1.00 g (8.92 mmol, 1.00 eq) *trans*-cyclohexane dioxide **45a** was dissolved in 25.5 mL (178 mmol, 20.0 eq) ammonia solution (7N in MeOH). The solution was heated to 100 °C in the pressure reactor for 24 h. Subsequently, the excess of ammonia and the methanol was removed under reduced pressure.

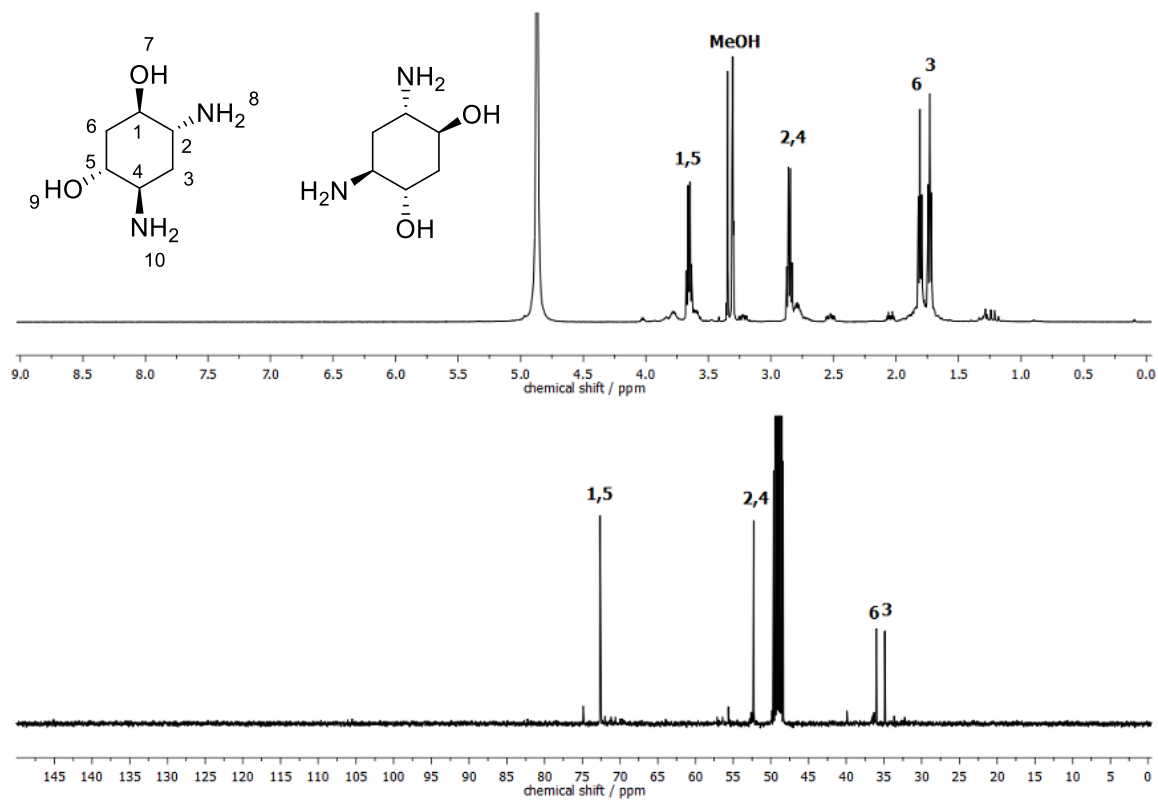
Yield: 91%

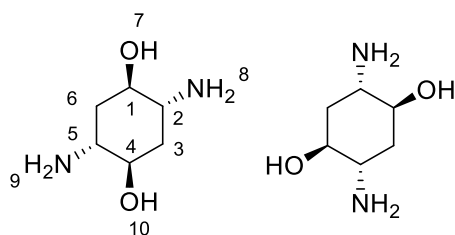
¹H-NMR (400 MHz, MeOH-*d*₄) δ / ppm = 3.65 (q, *J* = 5.7 Hz, 2H, H1+H5), 2.85 (q, *J* = 5.9 Hz, 2H, H2+H4), 1.81 (t, *J* = 5.5 Hz, 2H, H6), 1.73 (t, *J* = 5.8 Hz, 2H, H3) (including minor signals for OH- and NH₂-groups).

¹³C-NMR (101 MHz, MeOH-*d*₄) δ / ppm = 72.64, 52.29, 36.00, 34.89.

IR (ATR platinum diamond): ν / cm⁻¹ = 3313.3, 3273.8, 2922.3, 2856.5, 1602.5, 1439.8, 1360.0, 1340.2, 1304.7, 1287.2, 1209.1, 1193.1, 1142.2, 1115.8, 1097.1, 1035.9, 1010.3, 973.3, 948.3, 883.2, 810.9, 757.4, 584.2, 535.8, 498.1, 466.6, 441.3, 421.0.

EI-HRMS of C₆H₁₄N₂O₂ [M+H]⁺ calculated: 147.1128, found: 147.1132.



***cis*-1,4-Cyclohexadiene-derived aminoalcohol (2,5-diaminocyclohexane-1,4-diol) 47**

In a high pressure Teflon tube, 141 mg (1.26 mmol, 1.00 eq) *cis*-cyclohexane dioxide **45b** was dissolved in 3.60 mL (25.1 mmol, 20.0 eq) ammonia solution (7N in MeOH). The solution was heated to 100 °C in the pressure reactor for 15 h. Subsequently, the excess of ammonia and the methanol was removed under reduced pressure.

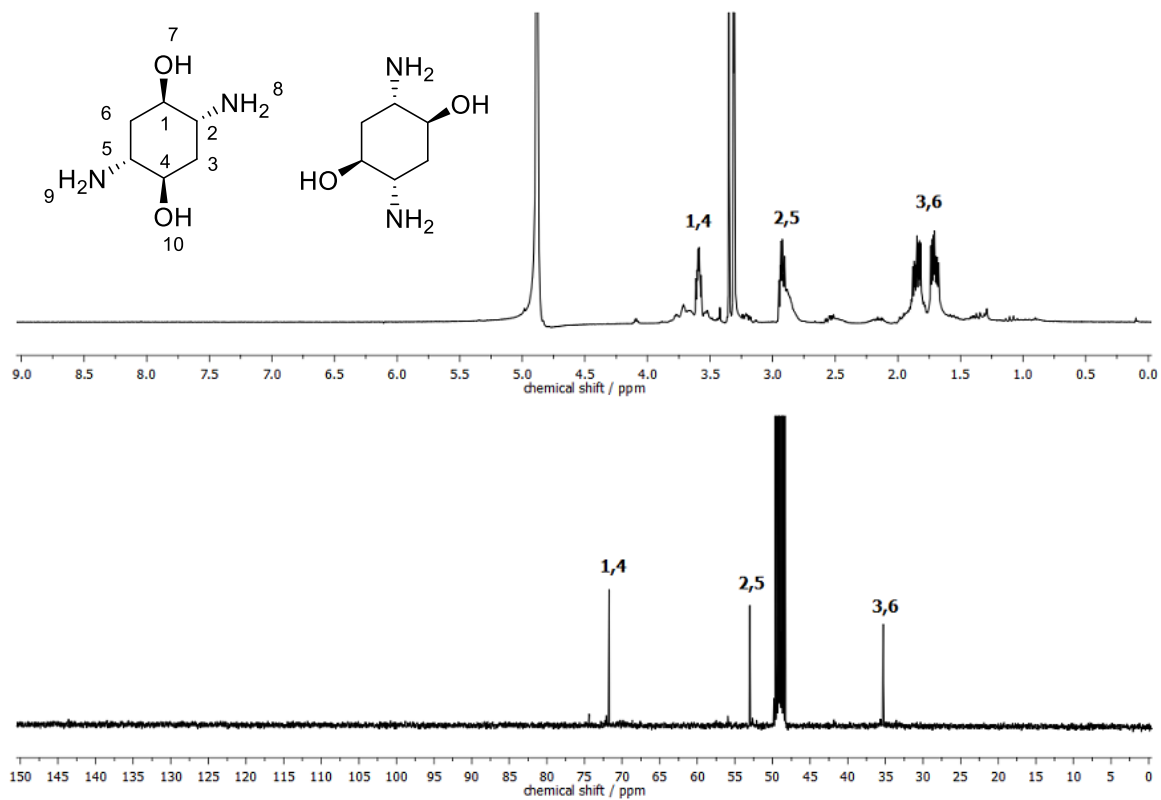
Yield: 84%

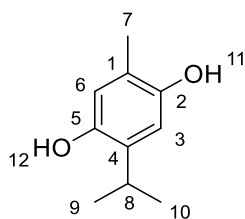
¹H-NMR (400 MHz, MeOH-*d*₄) δ / ppm = 3.61-3.57 (m, 2H, H1+H4), 2.95-2.91 (m, 2H, H2+H5), 1.88-1.82 (m, 2H, H3+H6), 1.74-1.68 (m, 2H, H3+H6) (including minor signals for OH- and NH₂-groups).

¹³C-NMR (101 MHz, MeOH-*d*₄) δ / ppm = 71.74, 53.00, 35.27.

IR (ATR platinum diamond): ν / cm⁻¹ = 3337.8, 3277.5, 2924.2, 1596.7, 1438.0, 1363.7, 1296.4, 1211.5, 1113.0, 1067.8, 1046.2, 1017.7, 972.8, 930.4, 887.9, 815.6, 765.6, 582.9, 530.5, 485.7, 445.9.

EI-HRMS of C₆H₁₄N₂O₂ [M]⁺ calculated: 146.1050, found: 146.1049.



2-Isopropyl-5-methylbenzene-1,4-diol

In a pressure reactor Teflon tube, 200 mg (1.22 mmol, 1.00 eq) thymoquinone were mixed with 20.0 mg (10 wt%) palladium on activated charcoal and 2.50 mL ethyl acetate. The reaction was run under 10 bar hydrogen atmosphere at 40 °C for 17 h. The catalyst was then filtered off and the solvent was removed under reduced pressure. The product was isolated *via* column chromatography (20% EtOAc/CH).

Yield: 62%

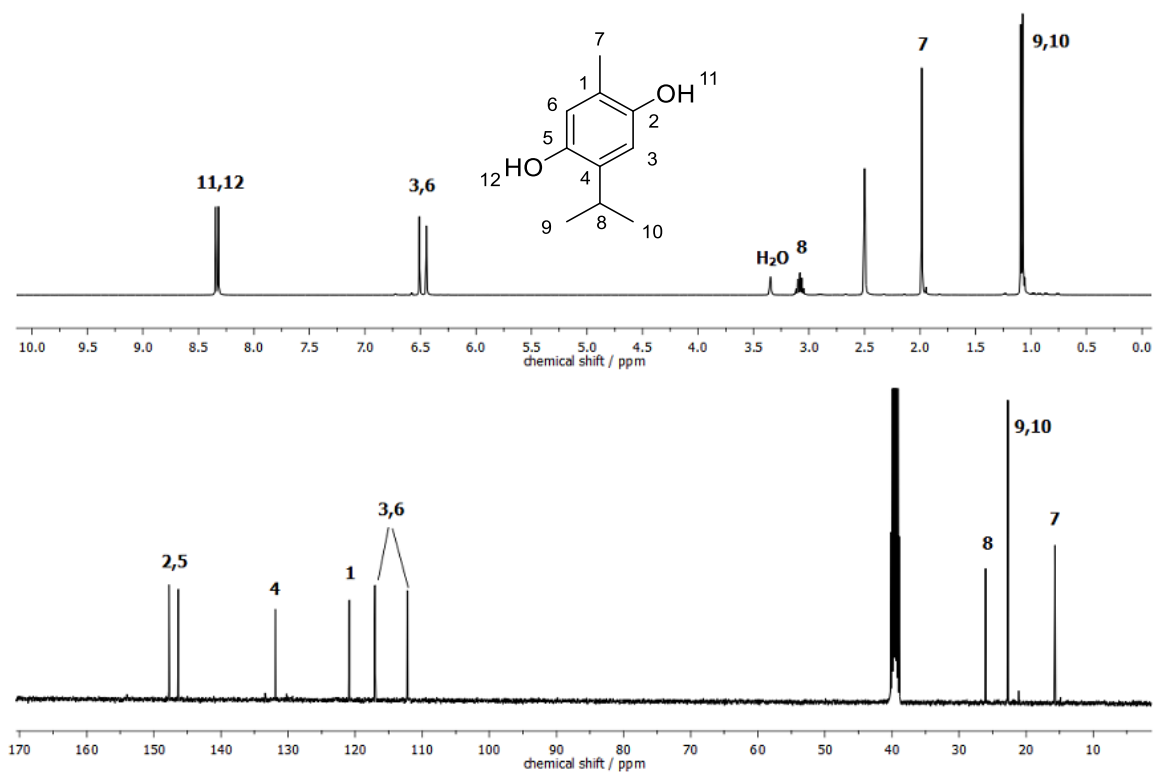
R_f = 0.59 (40% EtOAc/CH)

¹H-NMR (400 MHz, DMSO-d₆) δ / ppm = 8.35 (s, 1H, H11/H12), 8.32 (s, 1H, H11/H12), 6.51 (s, 1H, H3/H6), 6.45 (s, 1H, H3/H6), 3.13-3.03 (m, 1H, H8), 1.98 (s, 3H, H7), 1.09 (d, *J* = 6.9 Hz, 6H, H9+H10).

¹³C-NMR (101 MHz, DMSO-d₆ CDCl₃) δ / ppm = 147.73, 146.36, 131.88, 120.86, 117.05, 112.23, 26.04, 22.72, 15.69.

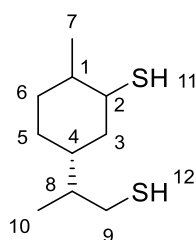
IR (ATR platinum diamond): ν / cm⁻¹ = 3255.2, 2966.1, 2207.3, 2034.7, 1987.6, 1697.9, 1529.3, 1419.7, 1378.7, 1362.4, 1243.3, 1175.0, 1142.4, 1108.4, 1094.6, 1038.3, 999.9, 870.0, 856.2, 817.2, 740.8, 677.8, 609.0, 573.6, 488.6, 424.1.

EI-HRMS of C₁₀H₁₄O₂ [M]⁺ calculated: 166.0988, found: 166.0993.



6.3.3 Experimental Procedures for Chapter 4.3

Limonene dithiol ((5*R*)-5-((*S*)-1-mercaptopropan-2-yl)-2-methylcyclohexane-1-thiol) 48



The synthesis was carried out according to literature.^[195]

In a round bottom flask, 10.0 g (73.4 mmol, 1.00 eq) (*R*)-(+)-limonene were mixed with 13.1 mL (14.0 g, 184 mmol, 2.50 eq) thioacetic acid under slight cooling. The mixture was stirred at room temperature for 26 h. The thioacetic acid was partly removed under reduced pressure. Subsequently, 1.01 g (7.34 mmol, 0.100 eq) TBD and 59 mL (47.0 g, 1.47 mol, 20.0 eq) methanol were added and the solution was stirred at 75 °C for 20 h. The solvent was then removed under reduced pressure and the product was isolated by column chromatography (5% EtOAc/CH). The product was obtained as a mixture of diastereoisomers.

Yield: 99%

R_f = 0.84 (20% EtOAc/CH)

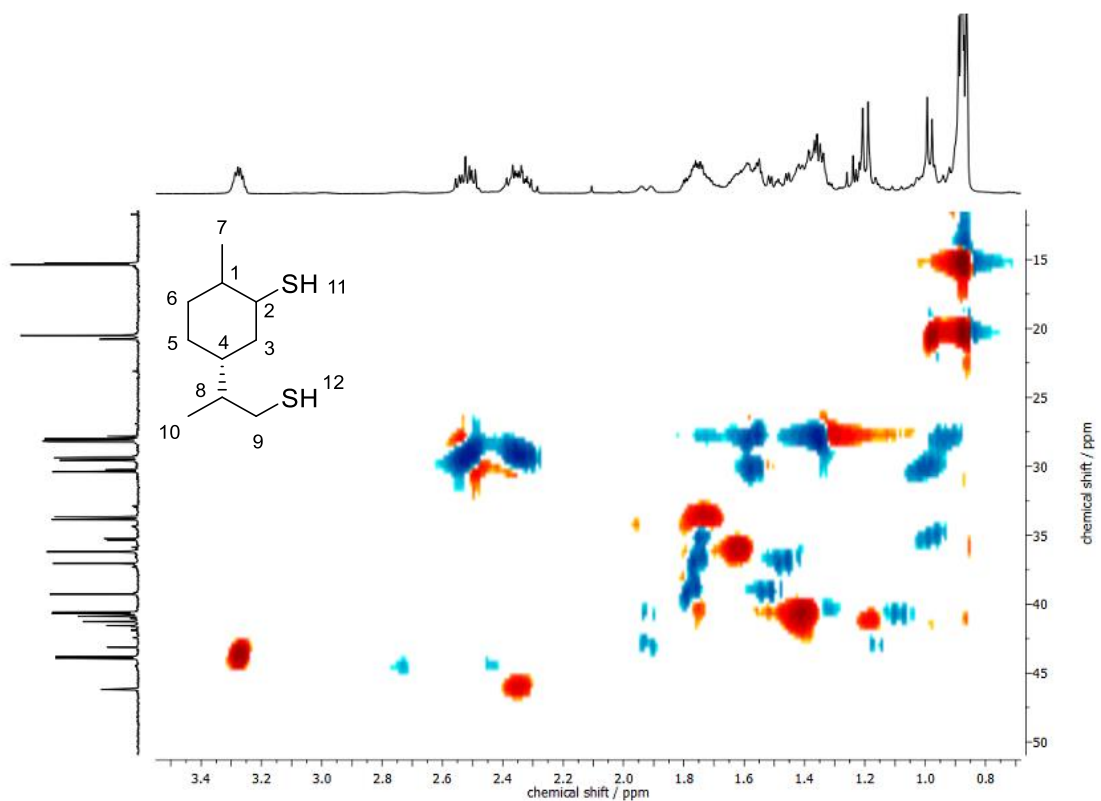
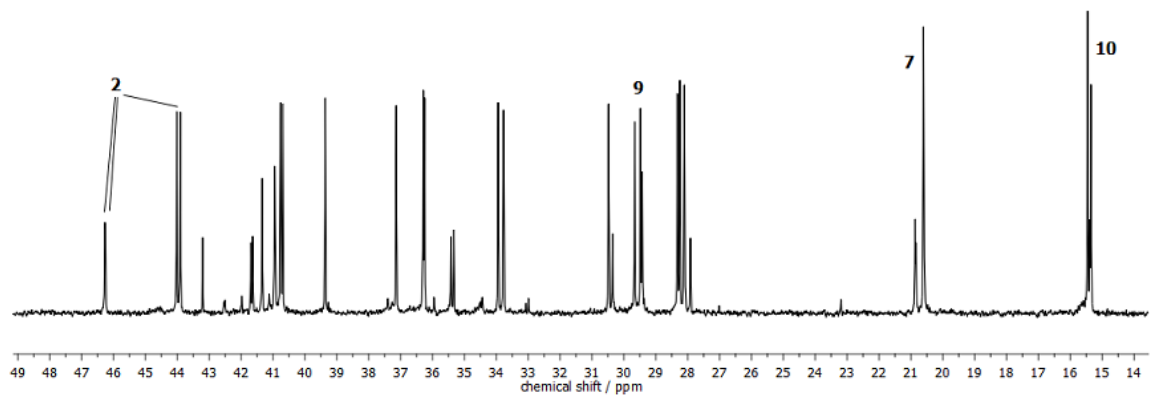
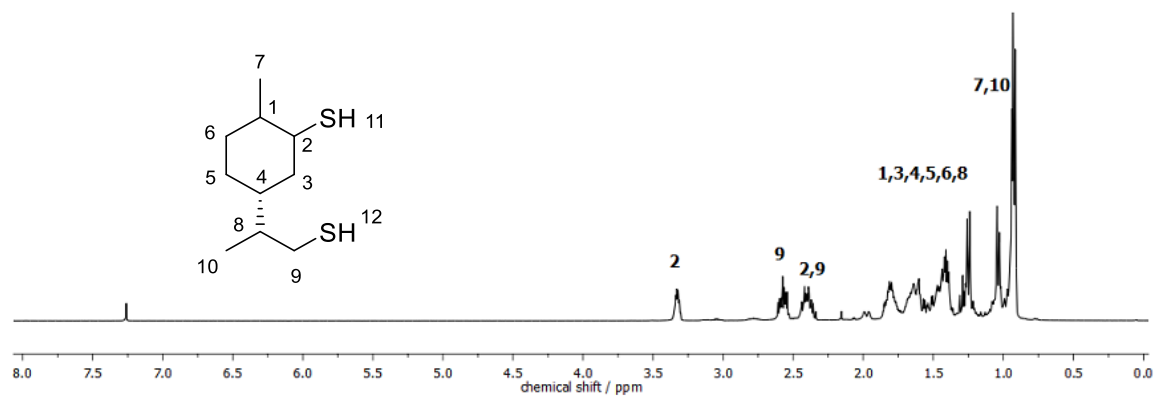
¹H-NMR (400 MHz, CDCl₃) δ / ppm = 3.35-3.30 (m, 1H, H2), 2.61-2.34 (m, 2H, H9), 1.86-1.22 (m, 9H, H1+H3+H4+H5+H6+H8), 1.07-0.92 (m, 6H, H7+H10).

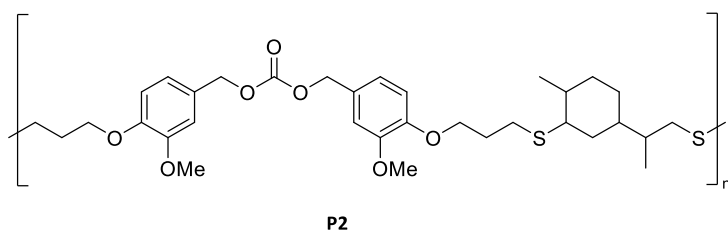
¹³C-NMR (101 MHz, CDCl₃) δ / ppm = 46.27, 46.26, 44.02, 43.91, 43.21, 41.34, 40.95, 40.93, 40.76, 40.69, 39.36, 37.14, 36.29, 36.25, 35.42, 35.33, 33.94, 33.77, 30.47, 30.35, 29.66, 29.48, 29.42, 28.32, 28.24, 28.10, 27.91, 20.87, 20.84, 20.60, 20.59, 15.45, 15.38, 15.35.

IR (ATR platinum diamond): ν / cm⁻¹ = 2955.2, 2918.8, 2868.1, 2851.7, 2561.6, 1452.2, 1375.5, 1292.2, 1251.6, 1105.0, 979.5, 938.5, 766.4, 719.2, 670.2, 623.4, 422.6.

EI-HRMS of C₁₀H₂₀S₂ [M]⁺ calculated: 204.1001, found: 204.1005.

The NMR spectra are in accordance with the literature.^[195]



Linear thiol-ene polymers from AVA carbonate **10 with limonene dithiol **48**:****1.05 eq **48**:**

100 mg (241 μmol , 1.00 eq) AVA carbonate **10** and 51.8 mg (253 μmol , 1.05 eq) limonene dithiol **48** were dissolved in 250 μL THF. 12.1 μL DMPA solution in THF (1M, 12.1 μmol , 0.05 eq) were added and the mixture was stirred at room temperature for 5 min until the mixture became homogeneous. Subsequently, the reaction was carried out by stirring at room temperature for 8 h under UV irradiation using two handheld UV lamps. The product was precipitated in cold methanol and analyzed by HFIP-SEC (SEC system C).

$M_n = 5,700$ Da, $D = 1.31$

1.07 eq **48:**

107 mg (257 μmol , 1.00 eq) AVA carbonate **10** and 56.2 mg (275 μmol , 1.07 eq) limonene dithiol **48** were dissolved in 250 μL THF. 12.9 μL DMPA solution in THF (1M, 12.9 μmol , 0.05 eq) were added and the mixture was stirred at room temperature for 5 min until the mixture became homogeneous. Subsequently, the reaction was carried out by stirring at room temperature for 6 h under UV irradiation using two handheld UV lamps. The product was precipitated in cold methanol and analyzed by HFIP-SEC (SEC system C).

$M_n = 6,000$ Da, $D = 1.55$

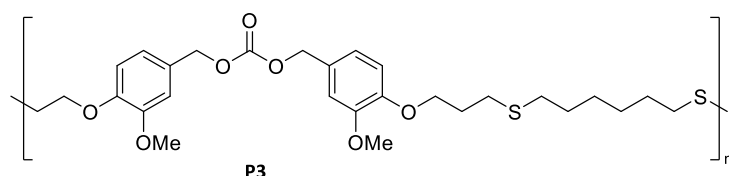
1.10 eq **48:**

104 mg (251 μmol , 1.00 eq) AVA carbonate **10** and 56.5 mg (276 μmol , 1.10 eq) limonene dithiol **48** were dissolved in 250 μL THF. 12.6 μL DMPA solution in THF (1M, 12.6 μmol , 0.05 eq) were added and the mixture was stirred at room temperature for 5 min until the mixture became homogeneous. Subsequently, the reaction was carried out by stirring at room temperature for

6.5 h under UV irradiation using two handheld UV lamps. The crude product was analyzed by HFIP-SEC (SEC system C).

$M_n = 7,200$ Da, $\mathcal{D} = 7.20$

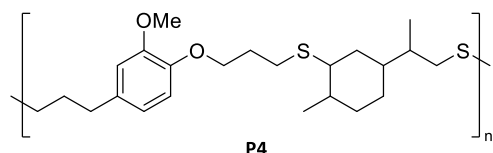
Linear thiol-ene polymers from AVA carbonate **10 with 1,6-hexanedithiol:**



121 mg (292 μmol , 1.00 eq) AVA carbonate **10** and 47.0 mg (313 μmol , 1.07 eq) 1,6-hexanedithiol were dissolved in 250 μL THF. 14.6 μL DMPA solution in THF (1M, 14.6 μmol , 0.05 eq) were added and the mixture was stirred at room temperature for 5 min until the mixture became homogeneous. Subsequently, the reaction was carried out by stirring at room temperature for 4 h under UV irradiation using two handheld UV lamps. The crude product was analyzed by HFIP-SEC (SEC system C).

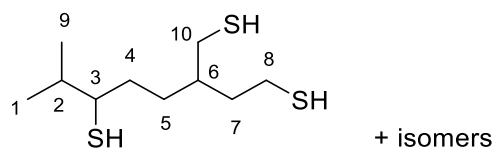
$M_n = 4,900$ Da, $\mathcal{D} = 1.10$

Linear thiol-ene polymers from allyl eugenol **7 with limonene dithiol **48**:**



204 mg (1.00 mmol, 1.00 eq) allyl eugenol **7** and 213 mg (1.00 mmol, 1.00 eq) limonene dithiol **48** were mixed in a round bottom flask. 12.8 mg (0.05 mmol, 0.05 eq) DMPA were added and the mixture was stirred at room temperature for 4 h under UV irradiation using two handheld UV lamps. The crude product was analyzed by HFIP-SEC (SEC system C).

$M_n = 1,100$ Da, $\mathcal{D} = 6.70$

Myrcene trithiol (3-(mercaptomethyl)-7-methyloctane-1,6-dithiol) 50

The synthesis of myrcene trithiol was carried out according to a literature known procedure.^[195]

In a round bottom flask, 5.00 g (36.7 mmol, 1.00 eq) myrcene were mixed with 9.44 mL (10.1 g, 132 mmol, 3.60 eq) thioacetic acid under ice cooling. The mixture was stirred at room temperature for 23 h. The thioacetic acid was partly removed under reduced pressure. Subsequently, 766 mg (5.51 mmol, 0.150 eq) TBD and 45 mL (35.3 g, 1.10 mol, 30.0 eq) methanol were added and the solution was stirred at 75 °C for 25 h. The solvent was removed under reduced pressure and the product was isolated by column chromatography (0.5->1% EtOAc/CH). The product was obtained as a mixture of isomers. Because of the indistinct NMR spectra (see spectra below), the product was identified *via* mass spectrometry and elemental analysis.

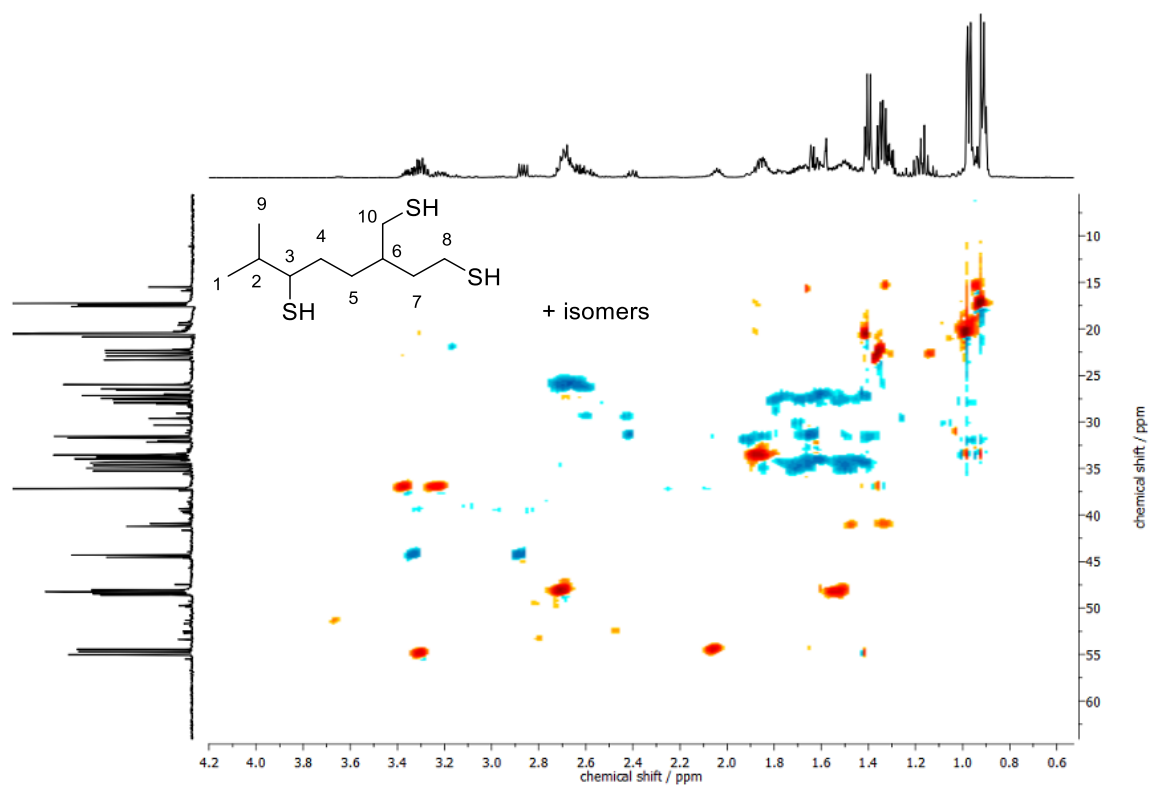
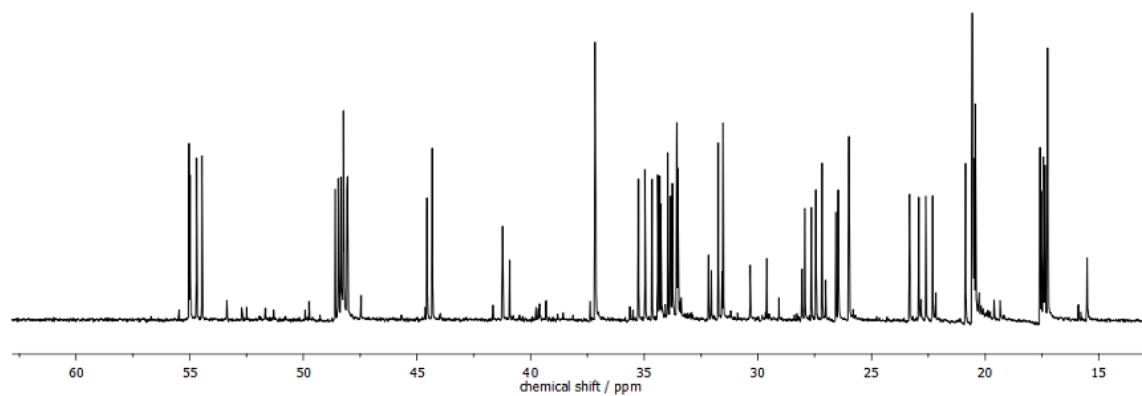
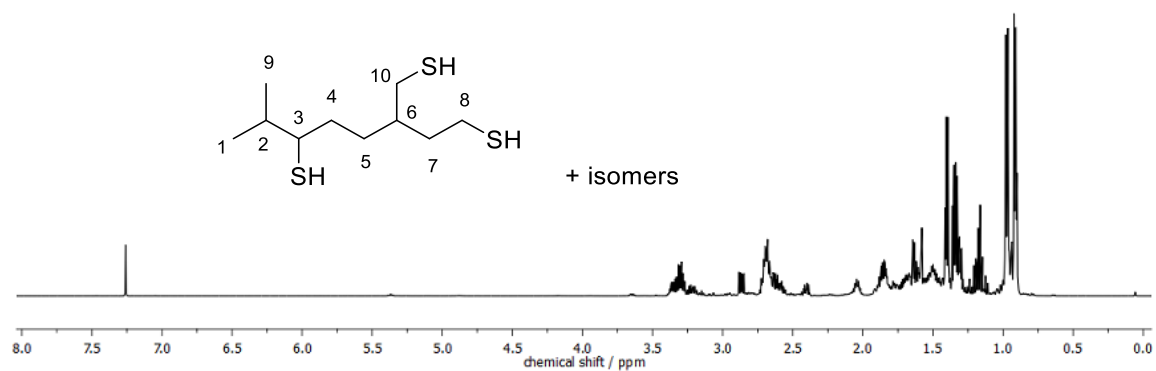
Yield: 59%

R_f = 0.61 (2% EtOAc/CH)

IR (ATR platinum diamond): ν / cm^{-1} = 2958.7, 2924.9, 2867.9, 2548.7, 1452.2, 1382.7, 1366.3, 1329.2, 1247.7, 1080.0, 921.6, 873.1, 809.4, 765.9, 713.5, 660.8, 468.9.

EI-HRMS of C₁₀H₂₂S₃ [M]⁺ calculated: 238.0878, found: 238.0882.

Elemental analysis: calculated: C 50.37%, H 9.30%, S 40.33; found: C 50.67%, H 8.61%, S 38.67%.



General procedure for the synthesis of thiol-ene resins

For the curing of thiol-ene films, the respective diene was mixed with the myrcene-based trithiol **50** (the ratio of double bond to thiol was 1:1 in all samples). Subsequently, DMPA (5 mol% per double bond) was added. After thorough mixing, the mixture was transferred to a glass plate with tape boundaries (1 cm x 2.5 cm). Solid samples were gently melted using a heatgun to ensure homogeneous film formation. The hot samples were placed into the curing oven and the curing was carried out under UV irradiation (365 nm, 50% power) for 10 min. DSC analyses were carried out using DSC system A.

Thiol-ene curing of AVA carbonate **10** with **50** (P5):

55.2 mg of **10** was mixed with 21.2 mg of **50** and 3.40 mg DMPA. The curing was carried out according to the general procedure described above.

DSC: $T_g = 14\text{ }^\circ\text{C}$

TGA: $T_{d\ 5\%} = 202\text{ }^\circ\text{C}$

IR (ATR platinum diamond): $\nu / \text{cm}^{-1} = 2931.7, 1738.9, 1592.2, 1513.3, 1462.6, 1421.1, 1386.2, 1366.0, 1334.6, 1224.3, 1162.1, 1138.0, 1026.5, 908.7, 852.0, 789.5, 650.0, 552.3, 461.2.$

Stress-strain measurements: Young's modulus: $6.87 \pm 1.29\text{ MPa}$, elongation at break: $148 \pm 10.7\%$, ultimate tensile strength: $1.48 \pm 0.194\text{ MPa}$.

Thiol-ene curing of AVA bisacetal **11** with **50** (P6):

56.2 mg of **11** was mixed with 16.8 mg of **50** and 2.70 mg DMPA. The curing was carried out according to the general procedure described above.

DSC: $T_g = -23\text{ }^\circ\text{C}$

TGA: $T_{d\ 5\%} = 134\text{ }^\circ\text{C}$

IR (ATR platinum diamond): $\nu / \text{cm}^{-1} = 3487.8, 2932.2, 2869.3, 1663.2, 1591.4, 1511.3, 1463.4, 1419.1, 1384.9, 1336.2, 1260.9, 1230.6, 1157.9, 1132.7, 1091.9, 1023.9, 913.6, 854.1, 802.4, 743.2, 690.0, 648.2, 552.0, 461.3.$

Curing of AVA acetal 12 with 50 (P7):

54.0 mg of **12** was mixed with 20.7 mg of **50** and 3.30 mg DMPA. The curing was carried out according to the general procedure described above.

DSC: $T_g = -13\text{ }^\circ\text{C}$

TGA: $T_{d5\%} = 171\text{ }^\circ\text{C}$

IR (ATR platinum diamond): $\nu / \text{cm}^{-1} = 3518.7, 2930.7, 2868.9, 1663.0, 1591.7, 1511.4, 1463.4, 1419.1, 1386.2, 1326.4, 1260.8, 1230.9, 1158.3, 1134.9, 1093.3, 1024.6, 912.3, 854.6, 802.8, 741.4, 690.0, 647.6, 551.7.$

Thiol-ene curing of AVA Biginelli 14 with 50 (P8):

50.6 mg of **14** was mixed with 16.3 mg of **50** and 2.60 mg DMPA. The curing was carried out according to the general procedure described above.

DSC: $T_g = 37\text{ }^\circ\text{C}$

TGA: $T_{d5\%} = 182\text{ }^\circ\text{C}$

IR (ATR platinum diamond): $\nu / \text{cm}^{-1} = 3230.2, 3090.6, 2932.1, 1695.5, 1639.7, 1592.3, 1510.9, 1451.2, 1420.7, 1380.6, 1255.7, 1216.4, 1160.7, 1136.7, 1075.9, 1020.0, 994.7, 924.6, 853.3, 800.3, 757.1, 681.4, 553.0, 463.2.$

Thiol-ene curing of allyl eugenol 7 with 50 (P9):

52.6 mg of **7** was mixed with 40.9 mg of **50** and 6.60 mg DMPA. The curing was carried out according to the general procedure described above.

DSC: $T_g = -5\text{ }^\circ\text{C}$

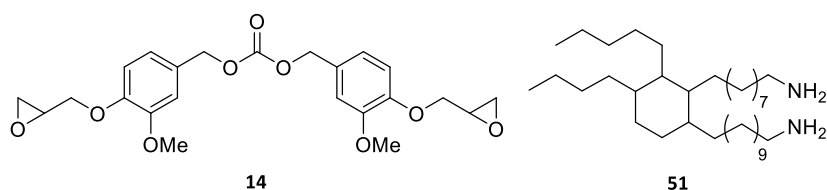
TGA: $T_{d5\%} = 226\text{ }^\circ\text{C}$

IR (ATR platinum diamond): $\nu / \text{cm}^{-1} = 2927.2, 2867.8, 1719.7, 1661.8, 1589.3, 1511.1, 1449.9, 1417.5, 1381.5, 1259.8, 1229.5, 1138.9, 1028.3, 912.0, 850.0, 801.7, 773.3, 689.5, 647.7, 556.1, 461.4.$

Stress-strain measurements: Young's modulus: $0.850 \pm 0.0730\text{ MPa}$, elongation at break: $44.2 \pm 7.21\%$, ultimate tensile strength: $0.361 \pm 0.08153\text{ MPa}$.

6.3.4 Experimental Procedures for Chapter 4.4

First curing test GVA carbonate **16** with Priamine® **51**:



100 mg (224 μmol , 1.00 eq) GVA carbonate **16** was mixed with 60.9 mg (112 μmol , 0.50 eq) Priamine® **51** in a silicon mold. The resin was cured at 130 °C for 1 h and 230 °C for 1 h.

DSC: $T_g = 30$ °C (DSC system A)

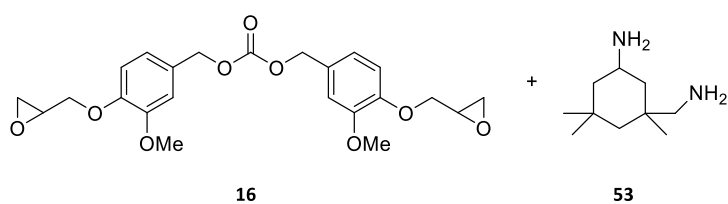
TGA: $T_{d\ 5\%} = 329$ °C

DMA: $E' = 0.787$ GPa, $T_g = 34$ °C

General procedure for the synthesis of epoxy resins

For the curing of epoxy resins, the respective amount of bisepoxide and hardener were mixed in a silicon mold with dimensions of 5 mm×23 mm×5 mm (The ratio of epoxide to amine groups was 2:1 in all samples). Solid samples were heated to melting temperatures with a heatgun to enable mixing. The sample was then cured in a vacuum oven at the respective lower temperature for 2 h. Vacuum was applied 5 min after insertion for 30 min. Then, the sample was post-cured at the respective higher temperature for another 2 h. DSC analyses were carried out using DSC system A.

Curing of GVA carbonate with IPDA P12:



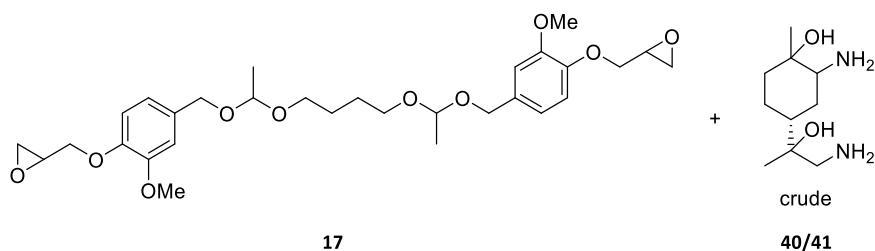
207 mg of **16** (4.48 mmol epoxy/g) were mixed with 39.5 mg of **53** (23.5 mmol amine eq/g). The curing was carried out by heating to 100 °C for 0.5 h, to 110 °C for 0.5 h, to 120 °C for 1 h and to 160 °C for 2.5 h. Vacuum was drawn at 160 °C for 50 min.

DSC: $T_g = 58\text{ °C}$

TGA: $T_{d\ 5\%} = 274\text{ °C}$

DMA: $E' = 1.26\text{ GPa}$, $T_g = 57\text{ °C}$

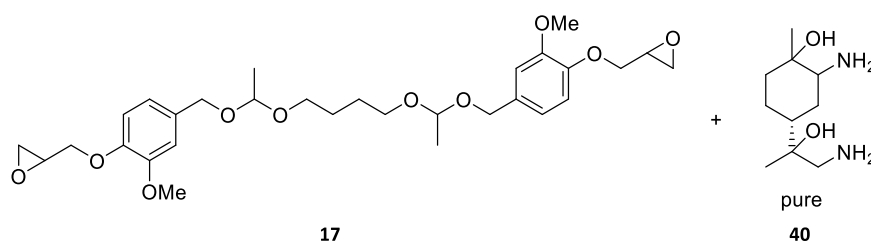
Curing of GVA bisacetal with crude limonene bis-amino alcohol P13:



244 mg of **17** (3.56 mmol epoxy/g) were mixed with 56.0 mg of **40/41** (15.5 mmol amine eq/g). The curing was carried out according to the general procedure described above at 80 °C and 180 °C.

DSC: $T_g = 11\text{ °C}$

TGA: $T_{d\ 5\%} = 261\text{ °C}$

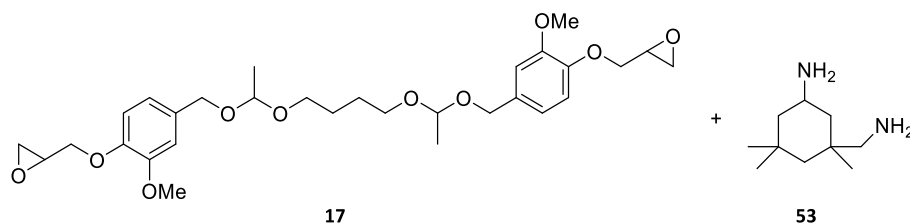
Curing of GVA bisacetal with pure limonene bis-amino alcohol P14:

285 mg of **17** (3.56 mmol epoxy/g) were mixed with 51.2 mg of **40** (19.8 mmol amine eq/g). The curing was carried out according to the general procedure described above at 110 °C and 180 °C.

DSC: $T_g = 3\text{ °C}$

TGA: $T_{d5\%} = 250\text{ °C}$

DMA: $E' = 0.665\text{ GPa}$, $T_g = 14\text{ °C}$

Curing of GVA bisacetal with IPDA P15:

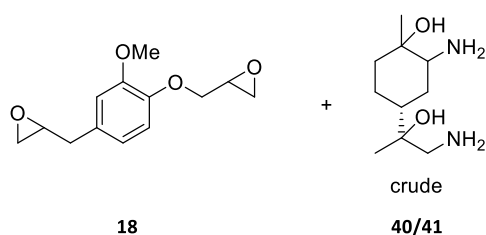
411 mg of **17** (3.56 mmol epoxy/g) were mixed with 62.2 mg of **53** (23.5 mmol amine eq/g). The curing was carried out according to the general procedure described above at 80 °C and 180 °C.

DSC: $T_g = 39\text{ °C}$

TGA: $T_{d5\%} = 235\text{ °C}$

DMA: $E' = 0.542\text{ GPa}$, $T_g = 36\text{ °C}$

Curing of epoxidized allyl eugenol with crude limonene bis-amino alcohol P16:

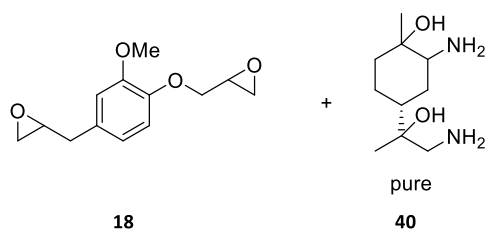


198 mg of **18** (8.47 mmol epoxy/g) were mixed with 108 mg of **40/41** (15.5 mmol amine eq/g). The curing was carried out by heating to 70 °C for 1.5 h. Vacuum was drawn 10 min after insertion for 30 min. Then, the sample was heated to 160 °C for 2 h.

DSC: $T_g = 52\text{ °C}$

TGA: $T_{d\ 5\%} = 282\text{ °C}$

Curing of epoxidized allyl eugenol with pure limonene bis-amino alcohol P17:

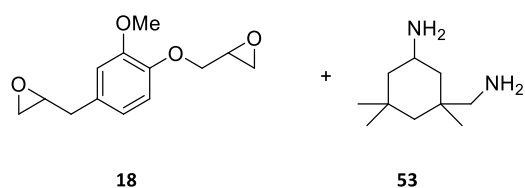


204 mg of **18** (8.47 mmol epoxy/g) were mixed with 87.2 mg of **40** (19.8 mmol amine eq/g). The curing was carried out according to the general procedure described above at 70 °C and 160 °C.

DSC: $T_g = 91\text{ °C}$

TGA: $T_{d\ 5\%} = 293\text{ °C}$

DMA: $E' = 1.86\text{ GPa}$, $T_g = 88\text{ °C}$

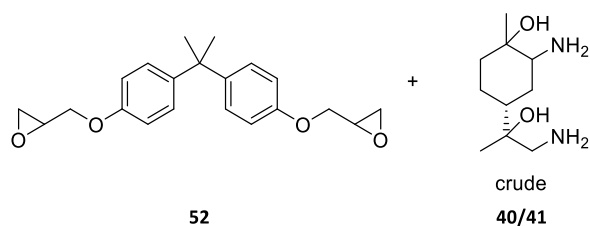
Curing of epoxidized allyl eugenol with IPDA P18:

219 mg of **18** (8.47 mmol epoxy/g) were mixed with 78.9 mg of **53** (23.5 mmol amine eq/g). The curing was carried out according to the general procedure described above at 80 °C and 180 °C.

DSC: $T_g = 122$ °C

TGA: $T_{d5\%} = 331$ °C

DMA: $E' = 1.62$ GPa, $T_g = 122$ °C

Curing of DGEBA with crude limonene bis-amino alcohol P19:

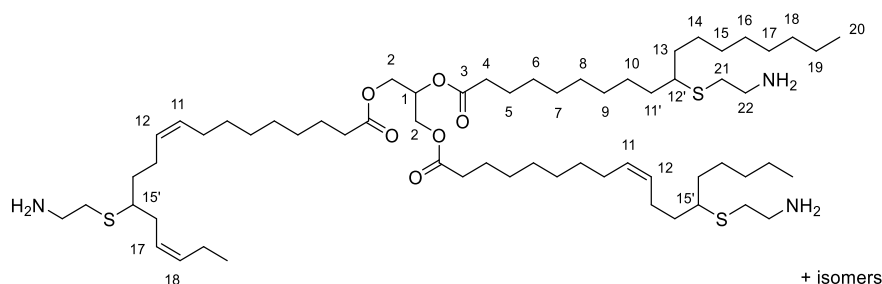
307 mg of **52** (5.88 mmol epoxy/g) were mixed with 116 mg of **40/41** (15.5 mmol amine eq/g). The curing was carried out according to the general procedure described above at 85 °C and 175 °C.

DSC: $T_g = 89$ °C

TGA: $T_{d5\%} = 278$ °C

6.3.5 Additional procedures

Triamine *via* thiol-ene with cysteamine hydrochloride from linseed oil* 54



The synthesis was carried out following a literature known procedure.^[315]

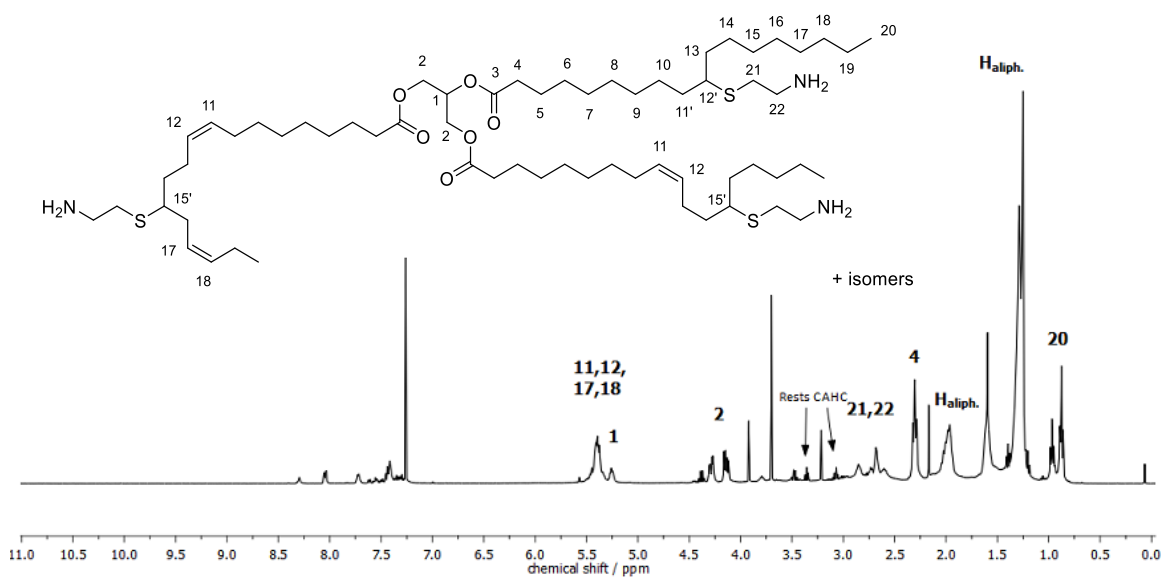
In a round bottom quartz crystal flask, 2.00 g (2.27 mmol, 1.00 eq) linseed oil were mixed with 1.03 g (9.07 mmol, 4.00 eq) cysteamine hydrochloride. The solid was dissolved in 4.50 mL ethanol and 10.5 mL 1,4-dioxane with gentle heating. To the stirring mixture, 349 mg (1.36 mmol, 0.60 eq) DMPA were added. The reaction was carried out at room temperature under UV irradiation with two handheld UV lamps for 53 h. The solvent was removed under reduced pressure and the residue redissolved in 20.0 mL chloroform. To remove unreacted cysteamine hydrochloride, the solution was washed with sodium carbonate solution and water and stored in the freezer for CAHC crystallization. After filtration of the solid parts, the washing and crystallization procedure was repeated until no more CAHC crystallized. The organic phase was dried and the solvent was removed under reduced pressure. The product was obtained as brown oil.

Yield: 1.06 g (due to the mixture of different isomers, no exact yield could be determined)

¹H-NMR (400 MHz, CDCl₃) δ / ppm = 5.50–5.32 (m, 6H, H11+H12+H17+H18), 5.29-5.23 (m, 1H, H1), 4.31-4.12 (m, 4H, H2), 2.97–2.48 (m, 11H, H21+H22), 2.30 (t, *J* = 7.5 Hz, 6H, H4), 2.06-1.86 (m, 11H, H_{aliph.}), 1.76-1.13 (m, 52H, H_{aliph.}), 1.08-0.81 (m, 9H, H20).

IR (ATR platinum diamond): ν / cm⁻¹ = 2924.4, 2851.6, 1738.0, 1449.9, 1367.7, 1305.5, 1276.4, 1241.5, 1161.7, 1101.0, 1049.4, 1044.8, 967.8, 710.7.

* This reaction was performed by Alina Wagner in the scope of her Bachelor thesis “Synthese bio-basierter Polyamine für Polymeranwendungen” under my co-supervision.



7

Appendix

7.1 Abbreviations

2-MeTHF	2-Methyl tetrahydrofuran
3Å-MS	3 Ångström molecular sieve
9-BBN	9-Borabicyclo[3.3.1]nonane
Å	Ångström
ADMET	Acyclic diene metathesis
AES-ICP	Atomic emission spectroscopy with inductively coupled plasma
AIBN	2,2'-Azobis(2-methylpropionitrile)
ATR	Attenuated total reflection
AVA	Allyl vanillyl alcohol
Boc	<i>tert</i> -butyloxycarbonyl
BPA	Bisphenol A
BPF	4,4'-methylenediphenol
BPS	Bis(4-hydroxyphenyl) sulfone
bpy	2,2'-Bipyridine
CAHC	Cysteamine hydrochloride
CALB	<i>Candida Antarctica</i> lipase B
CAN	Covalent adaptable network
CH	Cyclohexane
CoA	Coenzyme A
COSY	Correlated spectroscopy
Đ	Dispersity
d	Doublet

DA	Diels-Alder
DCM	Dichloromethane
DETA	Diethylenetriamine
DGEBA	Diglycidylether of bisphenol A
DGEMHY	Diglycidyl ether of methoxy hydroquinone
DGEVA	Diglycidyl ether of vanillyl alcohol
DGEVAC	Diglycidyl ether of vanillic acid
DHC	Dihydrocarvone
DLS	Dynamic light scattering
DMA	Dynamic mechanical analysis
DMC	Dimethyl carbonate
DMDO	Dimethyl dioxirane
DMF	Dimethyl formamide
DMPA	2,2-Dimethoxy-2-phenylacetophenone
DMSO	Dimethyl sulfoxide
DSC	Differential scanning calorimetry
E'	Storage modulus
EATOS	Environmental assessment tool for organic chemistry
EI	Electron ionisation
EQ	Environmental quotient
eq	Equivalents
ESI	Electrospray ionisation
EtOAc	Ethyl acetate
FAB	Fast atom bombardment
GC	Gas chromatography
GC-MS	Gas chromatography- mass spectrometry
GVA	Glycidyl vanillyl alcohol
HFIP	Hexafluoroisopropanol
HG	Hoveyda-Grubbs
HMBC	Heteronuclear multiple bond correlation
HSQC	Heteronuclear single quantum coherence
IPDA	isophorone diamine
IR	Infrared
LA	Lewis acid
LCA	Life cycle assessment
m	Multiplet
<i>m</i> CPBA	<i>m</i> -chloroperbenzoic acid
M_n	Number average molecular weight
MOF	Metal-organic framework
MS	Mass spectrometry
Mt	Million metric tons
MTO	Methyltrioxorhenium
MVL	β -Methyl- δ -valerolactone
M_w	Weight average molecular weight
NIPU	Non-isocyanate-based polyurethanes

NMI	1-Methylimidazole
NMR	Nuclear magnetic resonance
PA	Polyamide
PBAT	Polybutylene adipate terephthalate
PBS	Polybutylene succinate
Pd/C	Palladium on activated charcoal
PE	Polyethylene
PEG	Polyethylene glycol
PET	Polyethylene terephthalate
PHA	Polyhydroxy alkanates
PLA	Poly(lactic acid)
PLLA	Poly(L-lactic acid)
PP	Polypropylene
ppm	Parts per million
PPNCl	Bis(triphenylphosphine)iminium chloride
PPTS	Pyridinium <i>p</i> -toluenesulfonate
<i>p</i> -TSA	<i>p</i> -Toluenesulfonic acid
PTT	Polytrimethylene terephthalate
PVP	Poly(vinyl pyrrolidone)
q	Quartet
R _f	Retardation factor
rt	Room temperature
s	Singlet
SEC	Size exclusion chromatography
t	Triplet
TBAB	Tetrabutyl ammonium bromide
TBAI	Tetrabutylammonium iodide
TBD	1,5,7-Triazabicyclo(4.4.0)dec-5-ene
T _d	Degradation temperature
TEM	Transmission electron microscopy
TEMPO	2,2,6,6-Tetramethylpiperidinyloxy
T _g	Glass transition temperature
TGA	Thermogravimetric analysis
TGEVAM	Triglycidylether of vanillylamine
THF	Tetrahydrofuran
TLC	Thin layer chromatography
UHP	Urea-hydrogen peroxide
UV	Ultraviolet

7.2 List of Figures

Figure 2.1 Environmental Indices applying EATOS introduced by Eissen and Metzger. ^[36]	9
Figure 2.2 Technical and biological circle according to the cradle-to-cradle model. ^[46]	10
Figure 2.3 Amount and type of renewable resources used in the German chemical industry in 2018. ^[47]	11
Figure 2.4 Relative time scales for production and degradation of polymers and an example for the drop-in strategy for the replacement of fossil-based polymers (adapted from ^[16]).	12
Figure 2.5 Most important renewable resources for polymer applications.....	13
Figure 2.6 Possibilities for the direct polymerization of lignin (adapted from ^[55]).	17
Figure 2.7 Products obtained from lignin depolymerization and following upgrading strategies (adapted from ^[56]).	20
Figure 2.8 Electrochemical polymerization of vanillin to polyvanillin. ^[90]	21
Figure 2.9 Poly(dihydroferulic acid) as PET alternative published by Miller <i>et al.</i> ^[95]	22
Figure 2.10 Synthesis of renewable copolymers derived from vanillin and fatty acid derivatives. ^[99]	23
Figure 2.11 (Meth)acrylates functionalized with vanillin or syringaldehyde for the synthesis of partially bio-based poly acrylate and poly(meth) acrylate polymers. ^[100]	24
Figure 2.12 Vinyl ester resin based on vanillin and glycerol dimethacrylate. ^[107]	25
Figure 2.13 Examples for terpenes sorted by the amount of isoprene units. ^[115]	27
Figure 2.14 Biosynthetic pathway for the intermediate geranyl pyrophosphate starting from acetyl-CoA. ^[115]	28
Figure 2.15 Transformation of geranyl pyrophosphate into different monoterpene structures. ^[14]	29
Figure 2.16 Chemical modification pathways for pinene (adopted from reference ^[24]).	30
Figure 2.17 Mechanism for the epoxidation of double bonds applying <i>m</i> CPBA. ^[119]	31
Figure 2.18 Catalyst-free epoxidation of limonene with Oxone [®] and acetone. ^[120]	32
Figure 2.19 Proposed reaction mechanism for the epoxidation employing CALB in dimethyl carbonate. ^[124]	33
Figure 2.20 Preparation of microencapsulated Lewis base adducts of MTO according to Saladino <i>et al.</i> ^[136]	35
Figure 2.21 Mechanism of the Meinwald rearrangement. ^[151]	36
Figure 2.22 Main products obtained in the thermal transformation of α -pinene oxide in supercritical solvents. ^[164]	37
Figure 2.23 Possible reaction products for the rearrangement of limonene oxide.	38
Figure 2.24 Functionalization of limonene with acrylic acid applying a hydroboration and esterification protocol. ^[164]	40
Figure 2.25 Alternating copolymerization of limonene oxide using a β -diiminate zinc acetate complex as catalyst. ^[183]	40
Figure 2.26 Tandem copolymerization of limonene oxide with camphoric acid resulting in alternating, bio-based polyesters. ^[192]	42

Figure 2.27 Limonene-based synthesis of AB-type hydroxy acids and subsequent polymerization; and alternative polyester synthesis <i>via</i> copolymerization of the diol intermediate with succinic acid. ^[193]	42
Figure 2.28 Monomers obtained from limonene by thiol-ene coupling reactions and subsequent polymerization to polyesters, polyamides, polyurethanes and polyether polysulfides. ^{[194][195][196]}	44
Figure 2.29 Synthesis of branched tri- and tetraenes obtained by thiol-ene reaction between limonene and tri- and tetrathiols. Polymers were obtained by subsequent thiol-ene reaction combining the formed monomers (gray arrows). ^[198]	46
Figure 2.30 Aminolysis of limonene dioxide for the preparation of bio-based curing agents as reported by Mülhaupt <i>et al.</i> ^[203]	48
Figure 2.31 Most common mechanisms for cross-linking of epoxy resins: primary amine curing (A), anhydride curing (B) and catalytic curing with tertiary amines (C). ^[207]	49
Figure 2.32 Synthesis of DGEBA from bisphenol A and epichlorohydrin. ^[207]	50
Figure 2.33 Chemical structures of bisphenol A and the natural estrogen 17 β -estradiol. ^[209]	50
Figure 2.34 Bio-based glycidyl ethers synthesized from vanillin and its derivatives. All monomers were polymerized with IPDA and the resulting polymer properties (T_g , E' and T_d) were compared to the DGEBA reference. ^{[214][215]}	52
Figure 2.35 Substrates used in the oxidative decarboxylation and subsequent glycidylation for the preparation of a lignin model mixture for epoxy resin synthesis. ^[216]	54
Figure 2.36 Structures of bio-based epoxy monomers obtained from divanillyl alcohol, reported by Cramail <i>et al.</i> ^[217]	55
Figure 2.37 Synthesis of bisguaiacol bisepoxide from vanillyl alcohol and guaiacol reported by Stanzione and co-workers. ^[218]	55
Figure 2.38 Synthesis of lignin-derived triphenolic structures with different numbers of methoxy groups for the synthesis of epoxy resins. ^[221]	56
Figure 2.39 Synthesis of a spiroacetal diglycidyl ether monomer from the reaction of vanillin with pentaerythritol and epichlorohydrin ^[223] (A) and vanillin coupled by aldol condensation ^[224] (B).....	57
Figure 2.40 Synthesis of bisepoxide monomers by allylation and subsequent epoxidation reported by Aouf <i>et al.</i> ^[226]	58
Figure 2.41 Phenol-limonene addition product for epoxy resin synthesis reported in 1964. ^[230] ..	59
Figure 2.42 Structure of a terpene-maleic ester type epoxy monomer and a hydrophilic amine for the synthesis of waterborne thermoset nanocomposites with cellulose nanowhiskers. ^[234]	60
Figure 2.43 Synthesis of multi-functional epoxide monomers from limonene oxide <i>via</i> thiol-ene reaction (adapted from ^[235]).	60
Figure 2.44 Terpene-based curing agents: 1,8-diamino- <i>p</i> -menthane (A), limonene dithioether of cysteamine (B), cyclic anhydride from alloocimene and maleic anhydride (C), cyclic anhydride from myrcene and maleic anhydride (D) and cyclic anhydride from α -terpinene and maleic anhydride (E).	61
Figure 2.45 Plastic post-consumer waste treatment in 2016 in Europe (EU28+NO/CH) and Germany. ^[244]	63
Figure 2.46 Strategies for the implementation of recyclability in thermosetting polymers (adapted from ^[247]).	65

Figure 2.47 Cross-linking of bio-based β -methyl- δ -valerolactone (MVL) by tandem copolymerization/cross-linking with a bis(six-membered cyclic carbonate) and cross-linking of linear poly(MVL) with a free-radical generator. Thermal depolymerization was carried out using $\text{Sn}(\text{oct})_2$ and pentaerythritol ethoxylate at 150 °C. ^[249]	66
Figure 2.48 Synthesis of a poly(hexahydrotriazine) network from 4,4'-oxydianiline and paraformaldehyde. ^[251]	67
Figure 2.49 Synthesis of recyclable, bio-based polyester from isosorbide, succinic anhydride and glycerol. ^[252]	67
Figure 2.50 Schematic illustration of covalent adaptable networks (CANs): a) dissociative and b) associative CANs (black: binding, blue: non-binding). ^[248]	69
Figure 2.51 Structures of tung oil and 1,1'-(methylenedi-4,1-phenylene)bismaleimide (BMI) used for the synthesis of Diels-Alder-based CANs as reported by Shibata et al. ^[256]	70
Figure 2.52 Synthesis of isosorbide-based epoxy resin bearing disulfide bonds for thermal reprocessability through disulfide exchange reaction. ^[259]	70
Figure 2.53 Synthesis of a vanillin-based triepoxy monomer. Curing was performed using a cyclic anhydride and $\text{Zn}(\text{acac})_2$ as catalyst to yield high T_g vitrimers. ^[263]	71
Figure 2.54 Possible reactions in imine vitrimers: a) Imine formation and hydrolysis, b) transamination between an imine and a free amine group, c) imine metathesis between two imine groups. ^[248]	73
Figure 2.55 Fully bio-based polyimine vitrimer from 2,5-furandicarboxaldehyde and fatty acid-based di- and triamines. ^[270]	73
Figure 2.56 Vanillin-based polyimine vitrimers: synthesis of a dialdehyde through coupling at the phenol group and subsequent cross-linking with polyamines (A), ^[271] synthesis of imine-containing bisphenol for cross-linking with DGEBA (B). ^[272]	74
Figure 4.1 Synthesis of allyl methyl carbonate 3 and subsequent allylation of vanillyl alcohol, eugenol and vanillin catalyzed by palladium nanoparticles.....	81
Figure 4.2 ¹ H-NMR spectra of allyl vanillyl alcohol 5 (a), allyl eugenol 7 (b) and allyl vanillin 9 (c) in DMSO-d ₆	82
Figure 4.3 Coupling of AVA 5 to symmetric bis-allyl ether monomers 10-12.....	83
Figure 4.4 Formation of an ether side product from AVA 5 catalyzed by <i>p</i> -TSA.....	84
Figure 4.5 Proposed reaction sequence for the formation of mono-acetal 12 from AVA 5 and 1,4-butanediol divinyl ether.	85
Figure 4.6 ¹ H-NMR spectra of coupled bis-allyl ether monomers: carbonate 10 (a), bisacetal 11 (b) and monoacetal 12 (c) in DMSO-d ₆	86
Figure 4.7 Synthesis of bis-allyl ether 14 <i>via</i> Biginelli reaction between allyl vanillin 9, AVA acetoacetate 13 and urea in DMSO-d ₆	87
Figure 4.8 Coupling strategy for the formation of diglycidyl ether of vanillyl alcohol 16 and 17 as sustainable alternative to DGEBA.	88
Figure 4.9 Epoxidation of AVA Carbonate 10 to bisepoxide 14 using peracetic acid solution.	88
Figure 4.10 Epoxidation of AVA 5 to GVA 15 applying ammonium bicarbonate and hydrogen peroxide.....	89
Figure 4.11 (a) GC-MS chromatogram after the epoxidation of AVA 5 (dashed line) applying hydrogen peroxide and ammonium bicarbonate after 17 h reaction time, (b) ¹ H-NMR spectrum of isolated GVA 15 in DMSO-d ₆	90
Figure 4.12 Coupling of GVA 15 to GVA carbonate 16 and GVA bisacetal 17.	91

Figure 4.13 ^1H -NMR spectra of glycidyl ether monomers: carbonate 16 (a), bisacetal 17 (b) and epoxidized allyl eugenol 18 (c) in DMSO-d_6 .	92
Figure 4.14 Epoxidation of allylated eugenol 7 applying ammonium bicarbonate and hydrogen peroxide to form epoxidized allyl eugenol 18.	92
Figure 4.15 Two strategies for the synthesis of a dihydrocarvone-derived diamine: (a) Four-step synthesis <i>via</i> acetoxylation, saponification, isomerization and reductive amination, (b) Three-step synthesis <i>via</i> epoxidation, rearrangement and reductive amination.	94
Figure 4.16 Epoxidation of (+)-dihydrocarvone 19 to epoxide 20 and epoxy lactone 21 using several epoxidation procedures.	95
Figure 4.17 Epoxidation of (<i>R</i>)-(-)-carvone 22 to carvone-8,9-oxide 23 or carvone-1,2-oxide 24.	97
Figure 4.18 Epoxidation of γ -terpinene 25 to γ -terpinene dioxide 26.	98
Figure 4.19 Rearrangement of (+)-limonene oxide 27 to dihydrocarvone 19 as model reaction to determine the best catalytic conditions applying a deconvolution approach.	101
Figure 4.20 Effect of different solvents (at 40 °C) (a) and temperatures (in THF) (b) on the rearrangement of (+)-limonene oxide 27 to dihydrocarvone 19 in the presence of the catalyst mixture (1 mol% each).	102
Figure 4.21 Yield of dihydrocarvone 19 obtained from the deconvolution of different catalyst combinations (a) and final deconvolution step with $\text{BF}_3\cdot\text{Et}_2\text{O}$ and $\text{Bi}(\text{OTf})_3$ (b).	103
Figure 4.22 ^1H - and ^{13}C -NMR spectra of carvone-derived aldehyde 28 in CDCl_3 .	105
Figure 4.23 ^1H - and ^{13}C -NMR spectra of (+)-dihydrocarvone-based biscarbonyl 30 in CDCl_3 .	106
Figure 4.24 ^1H and ^{13}C spectra of γ -terpinene-derived biscarbonyl 32.	107
Figure 4.25 Rearrangement of limonene dioxide 33 to aldehyde 30: Test of different catalysts (a) and solvents with $\text{In}(\text{OTf})_3$ and $\text{Bi}(\text{OTf})_3$ (b).	108
Figure 4.26 Reaction conditions for the reductive amination of dihydrocarvone aldehyde 30 (a) and carvone aldehyde 28 (b).	110
Figure 4.27 GC-MS chromatogram of the reductive amination of carvone-based aldehyde 28: (a) starting material, (b) reaction applying Pd/C and ammonium formate after 22 h, (c) reaction applying Rh/ Al_2O_3 , ammonia and hydrogen after 1 h reaction time.	111
Figure 4.28 Reaction conditions for the reductive amination of thymoquinone 37.	112
Figure 4.29 GC-MS chromatogram of the reductive amination of thymoquinone 37 shown in Figure 4.28: (a) starting material, (b) reaction applying Raney-Ni, NH_4OAc , NH_4Cl and H_2 (30 bar) after 24 h, (c) reaction applying Rh/ Al_2O_3 , ammonia and hydrogen (20 bar) after 42 h reaction time, (d) products after washing, (e) product mixture after the addition of isobutyraldehyde.	113
Figure 4.30 Reaction conditions for the aminolysis of limonene dioxide using ammonia (adapted from ^[203]).	115
Figure 4.31 GC chromatograms of the aminolysis of limonene dioxide 34 before and after column chromatography: (a) crude product mixture, (b) fraction 1, (c) fraction 2, (d) fraction 3.	115
Figure 4.32 ^{13}C -NMR spectra of the aminolysis of limonene dioxide after column chromatography: (a) fraction 1, (b) fraction 2, (c) fraction 3.	117
Figure 4.33 Benzylation of limonene dioxide-derived aminoalcohols as tool to confirm the structural assignment derived from NMR spectra.	117

Figure 4.34 Epoxidation of 1,4-cyclohexadiene 44 applying Oxone®, sodium bicarbonate and acetone and subsequent aminolysis with methanolic ammonia solution to the two regioisomeric diamines 46 and 47.....	119
Figure 4.35 ¹³ C-NMR spectra of the aminolysis of the two 1,4-cyclohexane dioxide diastereoisomers: (a) product of the <i>trans</i> -isomer, (b) product of the <i>cis</i> -isomer...	119
Figure 4.36 Synthesis of linear polymers from AVA carbonate 10 <i>via</i> ADMET and thiol-ene polymerization with the limonene-based dithiol 48.	121
Figure 4.37 HFIP-SEC traces for the thiol-ene polymerization of AVA carbonate 10 and limonene-based dithiol 48 (a) (SEC system C), ¹ H-NMR spectrum of P2 with 1.07 eq dithiol 48 (b).	122
Figure 4.38 HFIP-SEC traces for the thiol-ene polymerization of AVA carbonate 10 with limonene dithiol 48 (P2), 1,6-hexanedithiol (P3) and of allyl eugenol 7 with limonene dithiol (P4) (SEC system C).	123
Figure 4.39 Synthesis of myrcene-based trithiol 50 in a two-step procedure applying thioacetic acid followed by saponification of the resulting ester groups using TBD in methanol.	124
Figure 4.40 GC-MS chromatograms for the synthesis of myrcene-based trithiol 50: (a) starting material myrcene, (b) reaction mixture after reaction with thioacetic acid for 23 h, (c) crude product after thioester hydrolysis, (d) fraction 1, (e) fraction 2 and (f) fraction 3 after column chromatography.	124
Figure 4.41 Structures of dienes used for the formation of thiol-ene films with myrcene-based trithiol 50.	125
Figure 4.42 DSC graphs indicating the glass transition temperatures for the polymers P5-P9 (a), photo of polymer film P5 (b) (DSC system A).	127
Figure 4.43 TGA analyses of the obtained thiol-ene films and the respective degradation onset temperature at a weight loss of 5%.	128
Figure 4.44 IR spectra of the thiol-ene films P5-P9.	129
Figure 4.45 Stress-strain measurements of thiol-ene films P5 and P9: Combined measurements of the carbonate film P5 (a), combined measurements of the allyl eugenol film P9 (b).	130
Figure 4.46 Comparison of stress-strain measurements of polymer films P5 and P9.....	131
Figure 4.47 ¹ H-NMR spectra of AVA carbonate 10 before (a) and after the reactivity test (b) with octylamine (entry 5 in Table 4.8).....	134
Figure 4.48 DSC curing of GVA carbonate 16 with the fatty acid-based Priamine® hardener (DSC system A).	136
Figure 4.49 Thermomechanical analysis after curing GVA carbonate 16 with Priamine®: Onset degradation temperature ($T_{d5\%}$) obtained by TGA (a), storage modulus E' and T_g obtained by DMA analysis (b).....	137
Figure 4.50 Monomers tested in the epoxy resin curing study: bisepoxides 16, 17, 18 and commercial DGEBA 52 (left), crude limonene bis-amino alcohol 40/41, pure limonene bis-amino alcohol 40 and commercial IPDA 53 (right).	138
Figure 4.51 Thermomechanical properties of the samples cured with pure limonene bis-amino alcohol 40: DSC traces (a) and storage moduli obtained by DMA (b).	140
Figure 4.52 Thermomechanical properties of the monomers cured with IPDA 53: DSC traces (a) and storage moduli obtained by DMA (b).	141

Figure 4.53 TGA traces for the synthesized epoxy resins: samples cured with crude limonene bis-amino alcohol 40/41 (a), samples cured with pure limonene bis-amino alcohol 40 (b) and samples cured with IPDA 53 (c).	142
Figure 4.54 Degradation of AVA carbonate 10 to AVA 5 to establish degradation conditions....	144
Figure 4.55 Degradation test of AVA carbonate 10 in water at 150 °C: GC-MS chromatogram after 3 h and the corresponding GC-MS mass spectrum (a), chromatogram and mass spectrum of the AVA 5 reference (b).	145
Figure 4.56 Establishment of degradation conditions for AVA carbonate 10: test of different reaction conditions (a), monitoring of the degradation <i>via</i> SEC applying the DMF/HCl system (b) (SEC system B).	146
Figure 4.57 Degradation of acetal monomers 11 and 12 to AVA 5 using the established degradation conditions for the DMF/HCl system.	147
Figure 4.58 Degradation of AVA bisacetal 11 (a) and AVA acetal 12 (b) applying the established degradation conditions (DMF 0.2M, HCl _{conc.} 0.5M, 100 °C, 24 h) (SEC system B).	148
Figure 4.59 Degradation of polymer film P5 applying the established degradation conditions (DMF, HCl _{conc.} , 100 °C).....	148
Figure 4.60 ESI-MS spectrum of degraded polymer film P5 (negative mode) and proposed structures for the most intense peak signals.....	149
Figure 4.61 Main degradation product of polymer film P5: calculated isotopic pattern (left), measured isotopic pattern (right).....	150
Figure 5.1 General scheme for the formation of imine vitrimer networks from biscarbonyl 30 (top) and representative structure of the amine 54 obtained from linseed oil <i>via</i> thiol-ene reaction applying cysteamine hydrochloride (bottom).	154
Figure 5.2 DSC curing measurement of biscarbonyl 30 with amine 54 (bold line) and the DSC analysis of the cured sample (dashed lines) (DSC system B).	155

7.3 List of Tables

Table 2.1 The 12 Principles of Green Chemistry. ^[28]	5
Table 2.2: E factors in the chemical industry. ^[34]	8
Table 2.3 Lignin content and composition of the main lignocellulosic sources. ^[1]	15
Table 2.4 Material properties obtained by the polymerization of limonene-based monomers shown in Figure 2.28.	45
Table 4.1 Summarized results for the epoxidation of (+)-dihydrocarvone 19 to dihydrocarvone oxide 20 or epoxy lactone 21.	96
Table 4.2 Summarized results for the epoxidation of (<i>R</i>)-(-)-carvone 22 to carvone-8,9-oxide 23 or carvone-1,2-oxide 24.	97
Table 4.3 Summarized results for the epoxidation of γ -terpinene 25 to γ -terpinene dioxide 26.	99
Table 4.4 Epoxidation of selected terpenes to mono- and bisepoxides and subsequent rearrangement to biscarbonyl compounds.	104
Table 4.5 Results for the benzylation of limonene-dioxide-derived aminoalcohols.	118
Table 4.6 Summarized results for the thiol-ene film formation of dienes 10-12, 14 and 7 with myrcene-based trithiol 50.	126

Table 4.7 Mechanical properties of polymer films P5 and P9 obtained from stress-strain measurements.....	130
Table 4.8 Reactivity test of the carbonate linker monomers 10 and 16 with varying amounts of octylamine.	134
Table 4.9 Results for the epoxy resin study using the monomers depicted in Figure 4.50.	139

7.4 Publications

- [2] Löser P.S., Rauthe P., Meier M.A.R., Llevot A., *Sustainable catalytic rearrangement of terpene-derived epoxides: towards bio-based biscarbonyl monomers*, *Phil. Trans. R. Soc. A* **2020**, 378: 20190267.
- [1] G. Klein, A. Llevot, P. S. Löser, B. Bitterer, J. Helfferich, W. Wenzel, C. Barner-Kowollik, M. A. R. Meier, *On the macrocyclization selectivity of meta-substituted diamines and dialdehydes: towards macrocycles with tunable functional peripheries*, *J Incl Phenom Macrocycl Chem* **2019**, 95, 119-134.

7.5 Conference Contributions

- [6] ‘*Synthesis of cleavable bio-based monomers: Towards recyclable thermosets*’, Poster at the 4th Conference on Green and Sustainable Chemistry of the European Chemical Society, September 22nd – 25th, 2019, Tarragona, Spain (**poster prize**).
- [5] ‘*Synthesis of cleavable bio-based monomers: Towards recyclable thermosets*’, Oral presentation at the 7th International Conference on Biobased and Biodegradable Polymers, June 17th – 19th, 2019, Stockholm, Sweden.
- [4] ‘*Sustainable synthesis of biobased recyclable thermosets*’, Poster at the 10th Workshop on Fats and Oils as Renewable Feedstock for the Chemical Industry, March 17th – 19th, 2019, Karlsruhe, Germany (**poster prize**).
- [3] ‘*Sustainable synthesis of biobased recyclable thermosets*’, Poster at the Annual meeting of the GDCh-division Sustainable Chemistry, September 17th – 19th, 2018, Aachen, Germany.
- [2] ‘*Sustainable synthesis of biobased recyclable thermosets*’, Poster at the Bordeaux Polymer Conference, May 28th - 31th, 2018, Bordeaux, France.
- [1] ‘*Sustainable synthesis of biobased recyclable thermosets*’, Poster at the 3rd Green & Sustainable Chemistry Conference, May 13th – 16th, 2018, Berlin, Germany.

8

Bibliography

- [1] P. Azadi, O. R. Inderwildi, R. Farnood, D. A. King, *Renewable and Sustainable Energy Reviews* **2013**, *21*, 506.
- [2] P. Marion, B. Bernela, A. Piccirilli, B. Estrine, N. Patouillard, J. Guilbot, F. Jérôme, *Green Chem* **2017**, *19*, 4973.
- [3] P. B. Weisz, *Physics Today* **2004**, *57*, 47.
- [4] G. H. Brundtland, *Our common future*, Oxford Univ. Press, Oxford, **1987**.
- [5] retrieved 20.05.2020, "Transforming our world_ The 2030 Agenda for Sustainable Development", can be found under <https://sustainabledevelopment.un.org/content/documents/21252030%20Agenda%20for%20Sustainable%20Development%20web.pdf>.
- [6] R. A. Sheldon, *Green Chem* **2017**, *19*, 18.
- [7] retrieved 26.03.2020, "Plastics - the facts 2019", can be found under https://www.plasticseurope.org/application/files/9715/7129/9584/FINAL_web_version_Plastics_the_facts2019_14102019.pdf.
- [8] C. Williams, M. Hillmyer, *Polymer Reviews* **2008**, *48*, 1.
- [9] J. Hopewell, R. Dvorak, E. Kosior, *Phil. Trans. R. Soc. B* **2009**, *364*, 2115.
- [10] retrieved 20.05.2020, "The New Plastics Economy: Rethinking the Future of Plastics", can be found under https://www.ellenmacarthurfoundation.org/assets/downloads/EllenMacArthurFoundation_TheNewPlasticsEconomy_Pages.pdf.
- [11] I. T. Horvath, P. T. Anastas, *Chem. Rev.* **2007**, *107*, 2169.

- [12] Y. Zhu, C. Romain, C. K. Williams, *Nature* **2016**, *540*, 354.
- [13] A. Llevot, P.-K. Dannecker, M. von Czapiewski, L. C. Over, Z. Söyler, M. A. R. Meier, *Chem. Eur. J.* **2016**, *22*, 11510.
- [14] A. Gandini, T. M. Lacerda, *Progress in Polymer Science* **2015**, *48*, 1.
- [15] R. Mülhaupt, *Macromol. Chem. Phys.* **2013**, *214*, 159.
- [16] D. K. Schneiderman, M. A. Hillmyer, *Macromolecules* **2017**, *50*, 3733.
- [17] J. H. Clark in *RSC green chemistry, no. 46* (Eds.: H. F. Sneddon, J. Clark, L. Summerton, L. C. Jones), Royal Society of Chemistry, Cambridge, **2016**, pp. 1–11.
- [18] P. Anastas, N. Eghbali, *Chem. Soc. Rev.* **2010**, *39*, 301.
- [19] J. H. Clark, *Green Chem* **2006**, *8*, 17.
- [20] R. A. Sheldon, *Pure Appl. Chem.* **2000**, *72*, 1233.
- [21] C. J. Clarke, W.-C. Tu, O. Levers, A. Bröhl, J. P. Hallett, *Chem. Rev.* **2018**, *118*, 747.
- [22] M. S. Holzwarth, B. Plietker, *ChemCatChem* **2013**, *5*, 1650.
- [23] R. A. Sheldon, J. M. Woodley, *Chem. Rev.* **2018**, *118*, 801.
- [24] A. Corma, S. Iborra, A. Velty, *Chem. Rev.* **2007**, *107*, 2411.
- [25] P. T. Anastas, M. M. Kirchhoff, *Acc. Chem. Res.* **2002**, *35*, 686.
- [26] retrieved 23.03.2020, can be found under <https://www.rsc.org/journals-books-databases/about-journals/green-chemistry/>.
- [27] K. Kümmeler, *Angewandte Chemie (International ed. in English)* **2017**, *56*, 16420.
- [28] P. T. Anastas, J. C. Warner, *Green chemistry. Theory and practice*, Oxford Univ. Press, Oxford, **2000**.
- [29] H. C. Erythropel, J. B. Zimmerman, T. M. de Winter, L. Petitjean, F. Melnikov, C. H. Lam, A. W. Lounsbury, K. E. Mellor, N. Z. Janković, Q. Tu et al., *Green Chem* **2018**, *20*, 1929.
- [30] G. P. Taber, D. M. Pfisterer, J. C. Colberg, *Org. Process Res. Dev.* **2004**, *8*, 385.
- [31] retrieved 22.03.2020, "Presidential Green Chemistry Challenge: 2002 Greener Synthetic Pathways Award", can be found under <https://www.epa.gov/greenchemistry/presidential-green-chemistry-challenge-2002-greener-synthetic-pathways-award>.
- [32] J. F. Jenck, F. Agterberg, M. J. Droescher, *Green Chem* **2004**, *6*, 544.
- [33] B. M. Trost, *Science* **1991**, *34*, 1471.
- [34] R. A. Sheldon, *Chem. Commun.* **2008**, 3352.
- [35] R. A. Sheldon, *ACS Sustainable Chem. Eng.* **2018**, *6*, 32.
- [36] M. Eissen, J. O. Metzger, *Chem. Eur. J.* **2002**, *8*, 3580.

- [37] Linda M. Tufvesson, Pär Tufvesson, John M. Woodley, Pål Börjesson, *Int J Life Cycle Assess* **2013**, *18*, 431.
- [38] D. J. C. Constable, A. D. Curzons, V. L. Cunningham, *Green Chem* **2002**, *4*, 521.
- [39] R. E. Horne, T. Grant, K. Verghese, *Life Cycle Assessment: Principles, Practice and Prospects*, CSIRO PUBLISHING, Collingwood, **2009**.
- [40] D. Kralisch, D. Ott, D. Gericke, *Green Chem* **2015**, *17*, 123.
- [41] Alan D. Curzons, Concepción Jiménez-González, Ailsa L. Duncan, David J. C. Constable, Virginia L. Cunningham, *Int J Life Cycle Assess* **2007**, *12*, 272.
- [42] Peter Saling, Andreas Kicherer, Brigitte Dittrich-Krämer, Rolf Wittlinger, Winfried Zombik, Isabell Schmidt, Wolfgang Schrott, Silke Schmidt, *Int J LCA* **2002**, *7*, 203.
- [43] P. T. Anastas in *ACS Symposium Series* (Eds.: P. T. Anastas, C. A. Farris), American Chemical Society, Washington, DC, **1994**, pp. 2–22.
- [44] C. A. Bakker, R. Wever, C. Teoh, S. de Clercq, *International Journal of Sustainable Engineering* **2010**, *3*, 2.
- [45] W. McDonough, M. Braungart, *Cradle to cradle. Remaking the way we make things*, North Point Press, New York, **2002**.
- [46] A. Bjørn, M. Z. Hauschild, *Journal of Industrial Ecology* **2013**, *17*, 321.
- [47] retrieved 26.03.2020, Fachagentur Nachwachsende Rohstoffe e.V., "Anbau und Verwendung nachwachsender Rohstoffe in Deutschland", can be found under <http://www.fnr-server.de/ftp/pdf/berichte/22004416.pdf>.
- [48] Y. Xia, R. C. Larock, *Green Chem* **2010**, *12*, 1893.
- [49] E. B. retrieved 27.03.2020, "Bioplastics facts and figures", can be found under https://docs.european-bioplastics.org/publications/EUBP_Facts_and_figures.pdf.
- [50] J. Zakzeski, P. C. A. Bruijninx, A. L. Jongerius, B. M. Weckhuysen, *Chem. Rev.* **2010**, *110*, 3552.
- [51] C. O. Tuck, E. Pérez, I. T. Horváth, R. A. Sheldon, M. Poliakoff, *Science (New York, N.Y.)* **2012**, *337*, 695.
- [52] A. Duval, M. Lawoko, *Reactive and Functional Polymers* **2014**, *85*, 78.
- [53] W.-J. Liu, H. Jiang, H.-Q. Yu, *Green Chem* **2015**, *17*, 4888.
- [54] D. Stewart, *Industrial Crops and Products* **2008**, *27*, 202.
- [55] B. M. Upton, A. M. Kasko, *Chem. Rev.* **2016**, *116*, 2275.
- [56] W. Schutyser, T. Renders, S. van den Bosch, S.-F. Koelewijn, G. T. Beckham, B. F. Sels, *Chem. Soc. Rev.* **2018**, *47*, 852.
- [57] F. S. Chakar, A. J. Ragauskas, *Industrial Crops and Products* **2004**, *20*, 131.

- [58] L. C. Over, M. A. R. Meier, *Green Chem* **2016**, *18*, 197.
- [59] M. Ionescu, *Chemistry and technology of polyols for polyurethanes*, Rapra Technology Ltd, Shawbury, U.K, **2005**.
- [60] P. Furtwengler, L. Avérous, *Polym. Chem.* **2018**, *9*, 4258.
- [61] N. Mahmood, Z. Yuan, J. Schmidt, C. Xu, *Renewable and Sustainable Energy Reviews* **2016**, *60*, 317.
- [62] C. Bonini, M. D'Auria, L. Emanuele, R. Ferri, R. Pucciariello, A. R. Sabia, *J. Appl. Polym. Sci.* **2005**, *98*, 1451.
- [63] D.V. Evtuguin, J.P. Andreolety, A. Gandini, *Eur. Polym. J.* **1998**, *34*, 1163.
- [64] M. N. Vanderlaan, R. W. Thring, *Biomass and Bioenergy* **1998**, *14*, 525.
- [65] Xuejun Pan, Jack N Saddler, *Biotechnol Biofuels* **2013**, *6*, 1.
- [66] Z.-X. Guo, A. Gandini, F. Pla, *Polym. Int.* **1992**, *27*, 17.
- [67] G. Sivasankarapillai, A. G. McDonald, *Biomass and Bioenergy* **2011**, *35*, 919.
- [68] G. Vázquez, G. Antorrena, J. González, J. Mayor, *Bioresource technology* **1995**, *51*, 187.
- [69] S. Sarkar, B. Adhikari, *Journal of Adhesion Science and Technology* **2000**, *14*, 1179.
- [70] C. G. da Silva, S. Grelier, F. Pichavant, E. Frollini, A. Castellan, *Industrial Crops and Products* **2013**, *42*, 87.
- [71] G.-H. Delmas, B. Benjelloun-Mlayah, Y. Le Bigot, M. Delmas, *J. Appl. Polym. Sci.* **2013**, *127*, 1863.
- [72] J. Wang, D. Banu, D. Feldman, *Journal of Adhesion Science and Technology* **1992**, *6*, 587.
- [73] H. Sadeghifar, C. Cui, D. S. Argyropoulos, *Ind. Eng. Chem. Res.* **2012**, *51*, 16713.
- [74] S. Sen, S. Patil, D. S. Argyropoulos, *Green Chem* **2015**, *17*, 1077.
- [75] I. Kühnel, J. Podschun, B. Saake, R. Lehnen, *Holzforschung* **2015**, *69*, 531.
- [76] O. Gordobil, I. Egüés, J. Labidi, *Reactive and Functional Polymers* **2016**, *104*, 45.
- [77] S. Laurichesse, C. Huillet, L. Avérous, *Green Chem.* **2014**, *16*, 3958.
- [78] H. Chung, N. R. Washburn, *ACS applied materials & interfaces* **2012**, *4*, 2840.
- [79] A. Llevot, B. Monney, A. Sehlinger, S. Behrens, M. A. R. Meier, *Chem. Commun.* **2017**, *53*, 5175.
- [80] L. C. Over, M. Hergert, M. A. R. Meier, *Macromol. Chem. Phys.* **2017**, *218*, 1700177.
- [81] H. Luo, M. M. Abu-Omar in *Encyclopedia of Sustainable Technologies* (Ed.: M. Abraham), Elsevier Science, Saint Louis, **2017**, pp. 573–585.
- [82] M. P. Pandey, C. S. Kim, *Chem. Eng. Technol.* **2011**, *34*, 29.

- [83] M. Fache, B. Boutevin, S. Caillol, *ACS Sustainable Chem. Eng.* **2016**, *4*, 35.
- [84] M. B. Hocking, *J. Chem. Educ.* **1997**, *74*, 1055.
- [85] L. T. Sandborn, S. J. Richter, H. G. Clemens, Process of Making Vanillin, US Patent Nr. 2,057,117, **1936**.
- [86] H. Hibbert, G. H. Tomlinson, Manufacture of vanillin from waste sulphite pulp liquor, US Patent Nr. 2,069,185, **1937**.
- [87] E. B. d. Silva, M. Zabkova, J. D. Araújo, C. A. Cateto, M. F. Barreiro, M. N. Belgacem, A. E. Rodrigues, *Chemical Engineering Research and Design* **2009**, *87*, 1276.
- [88] A. Llevot, E. Grau, S. Carlotti, S. Grelier, H. Cramail, *Macromol. Rapid Commun.* **2016**, *37*, 9.
- [89] F. H. Isikgor, C. R. Becer, *Polym. Chem.* **2015**, *6*, 4497.
- [90] A. S. Amarasekara, B. Wiredu, A. Razzaq, *Green Chem* **2012**, *14*, 2395.
- [91] A. S. Amarasekara, A. Razzaq, *ISRN Polymer Science* **2012**, *2012*, 1.
- [92] L. H. Bock, J. K. Anderson, *J. Polym. Sci.* **1955**, *17*, 553.
- [93] C. Pang, J. Zhang, Q. Zhang, G. Wu, Y. Wang, J. Ma, *Polym. Chem.* **2015**, *6*, 797.
- [94] C. Pang, J. Zhang, G. Wu, Y. Wang, H. Gao, J. Ma, *Polym. Chem.* **2014**, *5*, 2843.
- [95] L. Mialon, A. G. Pemba, S. A. Miller, *Green Chem* **2010**, *12*, 1704.
- [96] L. Mialon, R. Vanderhenst, A. G. Pemba, S. A. Miller, *Macromol. Rapid Commun.* **2011**, *32*, 1386.
- [97] A. Llevot, E. Grau, S. Carlotti, S. Grelier, H. Cramail, *Polym. Chem.* **2015**, *6*, 6058.
- [98] A. Llevot, E. Grau, S. Carlotti, S. Grelier, H. Cramail, *Polym. Chem.* **2015**, *6*, 7693.
- [99] M. Firdaus, M. A.R. Meier, *European Polymer Journal* **2013**, *49*, 156.
- [100] J. Zhou, H. Zhang, J. Deng, Y. Wu, *Macromol. Chem. Phys.* **2016**, *217*, 2402.
- [101] B. G. Harvey, A. J. Guenther, H. A. Meylemans, S. R. L. Haines, K. R. Lamison, T. J. Groshens, L. R. Cambrea, M. C. Davis, W. W. Lai, *Green Chem* **2015**, *17*, 1249.
- [102] Yu. N. Sazanov, I. V. Podeshvo, G. M. Mikhailov, G. N. Fedorova, M. Ya. Goikhman, M. F. Lebedeva, V. V. Kudryavtsev, *Russian Journal of Applied Chemistry* **2002**, *75*, 777.
- [103] Ananda S. Amarasekara, Muhammad A. Hasan, *Polym. Sci. Ser. B* **2016**, *58*, 307.
- [104] A. G. Pemba, M. Rostagno, T. A. Lee, S. A. Miller, *Polym. Chem.* **2014**, *5*, 3214.
- [105] C. Zhang, S. A. Madbouly, M. R. Kessler, *Macromol. Chem. Phys.* **2015**, *216*, 1816.
- [106] C. Zhang, M. Yan, E. W. Cochran, M. R. Kessler, *Materials Today Communications* **2015**, *5*, 18.

- [107] J. F. Stanzione III, J. M. Sadler, J. J. La Scala, K. H. Reno, R. P. Wool, *Green Chem* **2012**, *14*, 2346.
- [108] A. W. Bassett, A. E. Honnig, C. M. Breyta, I. C. Dunn, J. J. La Scala, J. F. Stanzione, *ACS Sustainable Chem. Eng.* **2020**, *8*, 5626.
- [109] E. Renbutsu, S. Okabe, Y. Omura, F. Nakatsubo, S. Minami, H. Saimoto, Y. Shigemasa, *Carbohydrate Polymers* **2007**, *69*, 697.
- [110] N. K. Sini, J. Bijwe, I. K. Varma, *Polymer Degradation and Stability* **2014**, *109*, 270.
- [111] E. A. Hoff, G. X. de Hoe, C. M. Mulvaney, M. A. Hillmyer, C. A. Alabi, *J. Am. Chem. Soc.* **2020**, *142*, 6729.
- [112] G. Foyer, B.-H. Chanfi, B. Boutevin, S. Caillol, G. David, *European Polymer Journal* **2016**, *74*, 296.
- [113] S.-H. Li, S.-K. Gao, S.-X. Liu, Y.-N. Guo, *Crystal Growth & Design* **2010**, *10*, 495.
- [114] W. Schwab, C. Fuchs, F.-C. Huang, *Eur. J. Lipid Sci. Technol.* **2013**, *115*, 3.
- [115] E. Breitmaier, *Terpene. Aromen, Düfte, Pharmaka, Pheromone*, Wiley-VCH, Weinheim, **2005**.
- [116] José Luiz F. Monteiro, Cláudia O. Veloso, *Topics in Catalysis* **2004**, *27*, 169.
- [117] Denicourt-Nowicki, Rauchdi, Ali, Roucoux, *Catalysts* **2019**, *9*, 893.
- [118] S. A. Hauser, M. Cokoja, F. E. Kühn, *Catal. Sci. Technol.* **2013**, *3*, 552.
- [119] K. K. W. Mak, Y. M. Lai, Y.-H. Siu, *J. Chem. Educ.* **2006**, *83*, 1058.
- [120] L. Charbonneau, X. Foster, D. Zhao, S. Kaliaguine, *ACS Sustainable Chem. Eng.* **2018**, *6*, 5115.
- [121] H. Hussain, I. R. Green, I. Ahmed, *Chem. Rev.* **2013**, *113*, 3329.
- [122] G. Fioroni, F. Fringuelli, F. Pizzo, L. Vaccaro, *Green Chem.* **2003**, *5*, 425.
- [123] E. G. Ankudey, H. F. Olivo, T. L. Peebles, *Green Chem* **2006**, *8*, 923.
- [124] M. Rüschen Klaas, S. Warwel, *Org. Lett.* **1999**, *1*, 1025.
- [125] A. A. Tziolla, E. Kalogeris, A. Enotiadis, A. A. Taha, D. Gournis, H. Stamatis, *Materials Science and Engineering: B* **2009**, *165*, 173.
- [126] S. Sakaguchi, Y. Nishiyama, Y. Ishii, *J. Org. Chem.* **1996**, *61*, 5307.
- [127] A. Mouret, L. Leclercq, A. Mühlbauer, V. Nardello-Rataj, *Green Chem* **2014**, *16*, 269.
- [128] W. B. Cunningham, J. D. Tibbetts, M. Hutchby, K. A. Maltby, M. G. Davidson, U. Hintermair, P. Plucinski, S. D. Bull, *Green Chem* **2020**, *22*, 513.
- [129] J. Zhang, Q. Zhou, X.-H. Jiang, A.-K. Du, T. Zhao, J. van Kasteren, Y.-Z. Wang, *Polymer Degradation and Stability* **2010**, *95*, 1077.

- [130] G. Grigoropoulou, J. H. Clark, *Tetrahedron Letters* **2006**, *47*, 4461.
- [131] A. L.P. de Villa, D. E. de Vos, C. C. de Montes, P. A. Jacobs, *Tetrahedron Letters* **1998**, *39*, 8521.
- [132] H. Rudler, J. Ribeiro Gregorio, B. Denise, J.-M. Brégeault, A. Deloffre, *Journal of Molecular Catalysis A: Chemical* **1998**, *133*, 255.
- [133] T. Michel, D. Betz, M. Cokoja, V. Sieber, F. E. Kühn, *Journal of Molecular Catalysis A: Chemical* **2011**, *340*, 9.
- [134] T. Michel, M. Cokoja, V. Sieber, F. E. Kühn, *Journal of Molecular Catalysis A: Chemical* **2012**, *358*, 159.
- [135] S. Yamazaki, *Organic & biomolecular chemistry* **2010**, *8*, 2377.
- [136] R. Saladino, A. Andreoni, V. Neri, C. Crestini, *Tetrahedron* **2005**, *61*, 1069.
- [137] Y. S. Raupp, C. Yildiz, W. Kleist, M. A.R. Meier, *Applied Catalysis A: General* **2017**, *546*, 1.
- [138] L. D. Dias, R. M. B. Carrilho, C. A. Henriques, G. Piccirillo, A. Fernandes, L. M. Rossi, M. Filipa Ribeiro, M. J. F. Calvete, M. M. Pereira, *J. Porphyrins Phthalocyanines* **2018**, *22*, 331.
- [139] C. Bihanic, S. Diliberto, F. Pelissier, E. Petit, C. Boulanger, C. Grison, *ACS Sustainable Chem. Eng.* **2020**, *8*, 4044.
- [140] D. Mandelli, M. C.A. van Vliet, R. A. Sheldon, U. Schuchardt, *Applied Catalysis A: General* **2001**, *219*, 209.
- [141] M. C. A. van Vliet, D. Mandelli, I. W. C. E. Arends, U. Schuchardt, R. A. Sheldon, *Green Chem.* **2001**, *3*, 243.
- [142] A. J. Bonon, Y. N. Kozlov, J. O. Bahú, R. M. Filho, D. Mandelli, G. B. Shul'pin, *Journal of Catalysis* **2014**, *319*, 71.
- [143] R. Dileep, B. J. Rudresha, *RSC Adv.* **2015**, *5*, 65870.
- [144] Y. Qi, Y. Luan, J. Yu, X. Peng, G. Wang, *Chem. Eur. J.* **2015**, *21*, 1589.
- [145] M. Guidotti, L. Conti, A. Fusi, N. Ravasio, R. Psaro, *Journal of Molecular Catalysis A: Chemical* **2002**, *182-183*, 151.
- [146] P. A. Robles-Dutenhefner, B. B.N.S. Brandão, L. F. de Sousa, E. V. Gusevskaya, *Applied Catalysis A: General* **2011**, *399*, 172.
- [147] D. Mandelli, Y. N. Kozlov, C. A.R. da Silva, W. A. Carvalho, P. P. Pescarmona, D. d. A. Cella, P. T. de Paiva, G. B. Shul'pin, *Journal of Molecular Catalysis A: Chemical* **2016**, *422*, 216.
- [148] R. W. Saalfrank, S. Reihls, M. Hug, *Tetrahedron Letters* **1993**, *34*, 6033.
- [149] a) A. S. Rao, S. K. Paknikar, J. G. Kirtane, *Tetrahedron* **1983**, *39*, 2323; b) R. E. Parker, N. S. Isaacs, *Chem. Rev.* **1959**, *59*, 737; c) G. G. Kolomeyer, J. S. Oylo, WO 03/004448 A1, **2002**; d) B. J. Kane, G. P. Sanders, J. W. Snow, M. B. Erman, WO 02/090261 A3, **2002**.

- [150] J. Meinwald, S. S. Labana, M. S. Chadha, *J. Am. Chem. Soc.* **1963**, *85*, 582.
- [151] B. C. Ranu, U. Jana, *J. Org. Chem.* **1998**, *63*, 8212.
- [152] K. Arata, K. Tanabe, *Catal. Rev.-Sci. Eng.* **1983**, *25*, 365.
- [153] I. C. Nigam, L. Levi, *Can. J. Chem.* **1968**, *46*, 1944.
- [154] N. Ravasio, F. Zaccheria, M. Guidotti, R. Psaro, *Topics in Catalysis* **2004**, *27*, 157.
- [155] T. E. Davies, S. A. Kondrat, E. Nowicka, J. L. Kean, C. M. Harris, J. M. Socci, D. C. Apperley, S. H. Taylor, A. E. Graham, *Applied Catalysis A: General* **2015**, *493*, 17.
- [156] R.A. Sheldon, J.A. Elings, S.K. Lee, H.E.B. Lempers, R.S. Downing, *Journal of Molecular Catalysis A: Chemical* **1998**, *134*, 129.
- [157] L. A. Rios, B. A. Llano, W. F. Hoelderich, *Applied Catalysis A: General* **2012**, *445-446*, 346.
- [158] a) I. Karamé, M.L. Tommasino, M. Lemaire, *Tetrahedron Letters* **2003**, *44*, 7687; b) S. Kulasegaram, R. J. Kulawiec, *J. Org. Chem.* **1997**, *62*, 6547.
- [159] K. Suda, T. Kikkawa, S.-I. Nakajima, T. Takanami, *J. Am. Chem. Soc.* **2004**, *126*, 9554.
- [160] Y. Tian, E. Jürgens, D. Kunz, *Chem. Commun.* **2018**, *54*, 11340.
- [161] R. R. Shaikh, R. A. Khan, A. Alsalme, *J. Ind. Eng. Chem.* **2018**, *64*, 446.
- [162] J. B. Lewis, G. W. Hedrick, *J. Org. Chem.* **1965**, *30*, 4271.
- [163] M. W.C. Robinson, K. S. Pillinger, I. Mabbett, D. A. Timms, A. E. Graham, *Tetrahedron* **2010**, *66*, 8377.
- [164] V. I. Anikeev, I. V. Il'ina, K. P. Volcho, A. Yermakova, N. F. Salakhutdinov, *The Journal of Supercritical Fluids* **2010**, *52*, 71.
- [165] A. M. Anderson, J. M. Blazek, P. Garg, B. J. Payne, R. S. Mohan, *Tetrahedron Letters* **2000**, *41*, 1527.
- [166] R. L. Settine, G. L. Parks, G. L. K. Hunter, *J. Org. Chem.* **1964**, *29*, 616.
- [167] A. Procopio, R. Dalpozzo, A. de Nino, M. Nardi, G. Sindona, A. Tagarelli, *Synlett* **2004**, *14*, 2633.
- [168] R. Sudha, K. Malola Narasimhan, V. Geetha Saraswathy, S. Sankararaman, *J. Org. Chem.* **1996**, *61*, 1877.
- [169] V. V. Costa, K. A. da Silva Rocha, I. V. Kozhevnikov, E. F. Kozhevnikova, E. V. Gusevskaya, *Catal. Sci. Technol.* **2013**, *3*, 244.
- [170] R. K. Henderson, C. Jiménez-González, D. J. C. Constable, S. R. Alston, G. G. A. Inglis, G. Fisher, J. Sherwood, S. P. Binks, A. D. Curzons, *Green Chem.* **2011**, *13*, 854.
- [171] M. R. Thomsett, T. E. Storr, O. R. Monaghan, R. A. Stockman, S. M. Howdle, *Green Materials* **2016**, *4*, 115.

- [172] P. A. Wilbon, F. Chu, C. Tang, *Macromol. Rapid Commun.* **2013**, *34*, 8.
- [173] M. Winnacker, B. Rieger, *ChemSusChem* **2015**, *8*, 2455.
- [174] W. J. Roberts, A. R. Day, *J. Am. Chem. Soc.* **1950**, *72*, 1226.
- [175] M. Modena, R. B. Bates, C. S. Marvel, *J. Polym. Sci. A Gen. Pap.* **1965**, *3*, 949.
- [176] F. J. B. Brum, F. N. Laux, M. M. C. Forte, *Designed Monomers and Polymers* **2013**, *16*, 291.
- [177] S. Sharma, A. K. Srivastava, *Journal of Macromolecular Science, Part A* **2003**, *40*, 593.
- [178] S. Sharma, A. K. Srivastava, *European Polymer Journal* **2004**, *40*, 2235.
- [179] S. Sharma, A. K. Srivastava, *Designed Monomers and Polymers* **2006**, *9*, 503.
- [180] K. Satoh, M. Matsuda, K. Nagai, M. Kamigaito, *J. Am. Chem. Soc.* **2010**, *132*, 10003.
- [181] M. Matsuda, K. Satoh, M. Kamigaito, *Macromolecules* **2013**, *46*, 5473.
- [182] M. F. Sainz, J. A. Souto, D. Regentova, M. K. G. Johansson, S. T. Timhagen, D. J. Irvine, P. Buijsen, C. E. Koning, R. A. Stockman, S. M. Howdle, *Polym. Chem.* **2016**, *7*, 2882.
- [183] C. M. Byrne, S. D. Allen, E. B. Lobkovsky, G. W. Coates, *J. Am. Chem. Soc.* **2004**, *126*, 11404.
- [184] M. Reiter, S. Vagin, A. Kronast, C. Jandl, B. Rieger, *Chem. Sci.* **2017**, *8*, 1876.
- [185] O. Hauenstein, M. Reiter, S. Agarwal, B. Rieger, A. Greiner, *Green Chem* **2016**, *18*, 760.
- [186] L. Peña Carrodegua, J. González-Fabra, F. Castro-Gómez, C. Bo, A. W. Kleij, *Chem. Eur. J.* **2015**, *21*, 6115.
- [187] N. Kindermann, À. Cristòfol, A. W. Kleij, *ACS Catal.* **2017**, *7*, 3860.
- [188] O. Hauenstein, S. Agarwal, A. Greiner, *Nat Commun* **2016**, *7*, 1.
- [189] R. C. Jeske, A. M. DiCiccio, G. W. Coates, *J. Am. Chem. Soc.* **2007**, *129*, 11330.
- [190] E. H. Nejad, A. Paoniasari, C. G. W. van Melis, C. E. Koning, R. Duchateau, *Macromolecules* **2013**, *46*, 631.
- [191] L. Peña Carrodegua, C. Martín, A. W. Kleij, *Macromolecules* **2017**, *50*, 5337.
- [192] C. Robert, F. d. Montigny, C. M. Thomas, *Nat Commun* **2011**, *2*, 1.
- [193] M. R. Thomsett, J. C. Moore, A. Buchard, R. A. Stockman, S. M. Howdle, *Green Chem.* **2019**, *21*, 149.
- [194] M. Firdaus, M. A. R. Meier, *Green Chem.* **2013**, *15*, 370.
- [195] M. Firdaus, M. A. R. Meier, U. Biermann, J. O. Metzger, *Eur. J. Lipid Sci. Technol.* **2014**, *116*, 31.
- [196] M. Firdaus, L. Montero de Espinosa, M. A. R. Meier, *Macromolecules* **2011**, *44*, 7253.

- [197] L. Breloy, C. A. Ouarabi, A. Brosseau, P. Dubot, V. Brezova, S. Abbad Andaloussi, J.-P. Malval, D.-L. Versace, *ACS Sustainable Chem. Eng.* **2019**, *7*, 19591.
- [198] M. Claudino, J.-M. Mathevet, M. Jonsson, M. Johansson, *Polym. Chem.* **2014**, *5*, 3245.
- [199] K. Hearon, L. D. Nash, J. N. Rodriguez, A. T. Lonnecker, J. E. Raymond, T. S. Wilson, K. L. Wooley, D. J. Maitland, *Adv. Mater.* **2014**, *26*, 1552.
- [200] C. Li, M. Johansson, R. J. Sablong, C. E. Koning, *European Polymer Journal* **2017**, *96*, 337.
- [201] M. Bähr, A. Bitto, R. Mülhaupt, *Green Chem* **2012**, *14*, 1447.
- [202] V. Schimpf, B. S. Ritter, P. Weis, K. Parison, R. Mülhaupt, *Macromolecules* **2017**, *50*, 944.
- [203] H. Blattmann, R. Mülhaupt, *Green Chem* **2016**, *18*, 2406.
- [204] R. Auvergne, S. Caillol, G. David, B. Boutevin, J.-P. Pascault, *Chem. Rev.* **2014**, *114*, 1082.
- [205] J.-M. Raquez, M. Deléglise, M.-F. Lacrampe, P. Krawczak, *Progress in Polymer Science* **2010**, *35*, 487.
- [206] F.-L. Jin, X. Li, S.-J. Park, *Journal of Industrial and Engineering Chemistry* **2015**, *29*, 1.
- [207] S. Koltzenburg, M. Maskos, O. Nuyken, *Polymer Chemistry*, Springer Verlag, Berlin, Heidelberg, **2017**.
- [208] L. N. Vandenberg, R. Hauser, M. Marcus, N. Olea, W. V. Welshons, *Reprod. Toxicol.* **2007**, *24*, 139.
- [209] F. Ng, G. Couture, C. Philippe, B. Boutevin, S. Caillol, *Molecules* **2017**, *22*, 149.
- [210] M. Galià, L. M. de Espinosa, J. C. Ronda, G. Lligadas, V. Cádiz, *Eur. J. Lipid Sci. Technol.* **2010**, *112*, 87.
- [211] A. Llevot, *J Am Oil Chem Soc* **2017**, *94*, 169.
- [212] S. Kumar, S. K. Samal, S. Mohanty, S. K. Nayak, *Polymer-Plastics Technology and Engineering* **2017**, *57*, 133.
- [213] E. A. Baroncini, S. Kumar Yadav, G. R. Palmese, J. F. Stanzione, *J. Appl. Polym. Sci.* **2016**, *133*, 1473.
- [214] M. Fache, R. Auvergne, B. Boutevin, S. Caillol, *European Polymer Journal* **2015**, *67*, 527.
- [215] M. Fache, C. Montéréal, B. Boutevin, S. Caillol, *European Polymer Journal* **2015**, *73*, 344.
- [216] M. Fache, B. Boutevin, S. Caillol, *Green Chem* **2016**, *18*, 712.
- [217] E. Savonnet, E. Grau, S. Grelier, B. Defoort, H. Cramail, *ACS Sustainable Chem. Eng.* **2018**, *6*, 11008.
- [218] E. D. Hernandez, A. W. Bassett, J. M. Sadler, J. J. La Scala, J. F. Stanzione III, *ACS Sustainable Chem. Eng.* **2016**, *4*, 4328.

- [219] J. R. Mauck, S. K. Yadav, J. M. Sadler, J. J. La Scala, G. R. Palmese, K. M. Schmalbach, J. F. Stanzione III, *Macromol. Chem. Phys.* **2017**, *218*, 1700013.
- [220] K. H. Nicastro, C. J. Kloxin, T. H. Epps III, *ACS Sustainable Chem. Eng.* **2018**, *6*, 14812.
- [221] S. Zhao, X. Huang, A. J. Whelton, M. M. Abu-Omar, *ACS Sustainable Chem. Eng.* **2018**, *6*, 7600.
- [222] T. Koike, *Polym Eng Sci* **2012**, *52*, 701.
- [223] S. Ma, J. Wei, Z. Jia, T. Yu, W. Yuan, Q. Li, S. Wang, S. You, R. Liu, J. Zhu, *J. Mater. Chem. A* **2019**, *7*, 1233.
- [224] M. Shibata, T. Ohkita, *European Polymer Journal* **2017**, *92*, 165.
- [225] G. M. Lari, G. Pastore, C. Mondelli, J. Pérez-Ramírez, *Green Chem* **2018**, *20*, 148.
- [226] C. Aouf, J. Lecomte, P. Villeneuve, E. Dubreucq, H. Fulcrand, *Green Chem* **2012**, *14*, 2328.
- [227] L. Gu, G. Chen, Y. Yao, *Polymer Degradation and Stability* **2014**, *108*, 68.
- [228] S. Wang, S. Ma, C. Xu, Y. Liu, J. Dai, Z. Wang, X. Liu, J. Chen, X. Shen, J. Wei et al., *Macromolecules* **2017**, *50*, 1892.
- [229] X. Xu, S. Wang, S. Ma, W. Yuan, Q. Li, J. Feng, J. Zhu, *Polym Adv Technol* **2019**, *30*, 264.
- [230] R. F. Sellers, N. J. Somerset, Epoxy Resins from Polyhydric Phenol-Terpene Addition Products, US Patent Nr. 3,378,525, **1968**.
- [231] K. Xu, M. Chen, K. Zhang, J. Hu, *Polymer* **2004**, *45*, 1133.
- [232] G.-M. Wu, Z.-W. Kong, H. Huang, J. Chen, F.-X. Chu, *J. Appl. Polym. Sci.* **2009**, *113*, 2894.
- [233] G.-M. Wu, Z.-W. Kong, J. Chen, S.-p. Huo, G.-f. Liu, *Progress in Organic Coatings* **2014**, *77*, 315.
- [234] G.-M. Wu, Di Liu, G.-f. Liu, J. Chen, S.-p. Huo, Z.-W. Kong, *Carbohydrate Polymers* **2015**, *127*, 229.
- [235] H. Morinaga, M. Sakamoto, *Tetrahedron Letters* **2017**, *58*, 2438.
- [236] G. Couture, L. Granado, F. Fanget, B. Boutevin, S. Caillol, *Molecules* **2018**, *23*, 2739.
- [237] C. H. Mckeever, R. N. Washburne, Process for the preparation of menthane diamine, US Patent Nr. 2,955,138, **1960**.
- [238] T. Donnellan, D. Roylance, *Polym. Eng. Sci.* **1982**, *22*, 821.
- [239] J. E. Milks, J. E. Lancaster, *J. Org. Chem.* **1965**, *30*, 888.
- [240] T. Takahashi, K.-i. Hirayama, N. Teramoto, M. Shibata, *J. Appl. Polym. Sci.* **2008**, *108*, 1596.
- [241] X. Yang, C. Wang, S. Li, K. Huang, M. Li, W. Mao, S. Cao, J. Xia, *RSC Adv.* **2017**, *7*, 238.
- [242] R. Chang, J. Qin, J. Gao, *J Polym Res* **2014**, *21*, 19.

- [243] M. Hong, E. Y.-X. Chen, *Green Chem* **2017**, *19*, 3692.
- [244] retrieved 19.04.2020, "Plastics - the facts 2018", can be found under https://www.plasticseurope.org/application/files/6315/4510/9658/Plastics_the_facts_2018_AF_web.pdf.
- [245] S. Lambert, M. Wagner, *Chem. Soc. Rev.* **2017**, *46*, 6855.
- [246] T. E. Long, *Science* **2014**, *344*, 706.
- [247] D. J. Fortman, J. P. Brutman, G. X. de Hoe, R. L. Snyder, W. R. Dichtel, M. A. Hillmyer, *ACS Sustainable Chem. Eng.* **2018**, *6*, 11145.
- [248] W. Denissen, J. M. Winne, F. E. Du Prez, *Chem. Sci.* **2016**, *7*, 30.
- [249] J. P. Brutman, G. X. de Hoe, D. K. Schneiderman, T. N. Le, M. A. Hillmyer, *Ind. Eng. Chem. Res.* **2016**, *55*, 11097.
- [250] D. K. Schneiderman, M. E. Vanderlaan, A. M. Mannion, T. R. Panthani, D. C. Batiste, J. Z. Wang, F. S. Bates, C. W. Macosko, M. A. Hillmyer, *ACS Macro Lett.* **2016**, *5*, 515.
- [251] J. M. Garcia, G. O. Jones, K. Virwani, B. D. McCloskey, D. J. Boday, G. M. ter Huurne, H. W. Horn, D. J. Coady, A. M. Bintaleb, A. M. S. Alabulrahman et al., *Science* **2014**, *344*, 732.
- [252] P. A. Wilbon, J. L. Swartz, N. R. Meltzer, J. P. Brutman, M. A. Hillmyer, J. E. Wissinger, *ACS Sustainable Chem. Eng.* **2017**, *5*, 9185.
- [253] X. Zhao, X.-L. Wang, F. Tian, W.-L. An, S. Xu, Y.-Z. Wang, *Green Chem.* **2019**, *9*, 667.
- [254] A. Gandini, *Progress in Polymer Science* **2013**, *38*, 1.
- [255] Y. Zhang, A. A. Broekhuis, F. Picchioni, *Macromolecules* **2009**, *42*, 1906.
- [256] M. Shibata, N. Teramoto, Y. Nakamura, *J. Appl. Polym. Sci.* **2011**, *119*, 896.
- [257] M. Shibata, E. Miyazawa, *Polym. Bull.* **2017**, *74*, 1949.
- [258] A. Duval, G. Couture, S. Caillol, L. Avérous, *ACS Sustainable Chem. Eng.* **2017**, *5*, 1199.
- [259] Z. Ma, Y. Wang, J. Zhu, J. Yu, Z. Hu, *J. Polym. Sci. A Polym. Chem.* **2017**, *55*, 1790.
- [260] D. Montarnal, M. Capelot, F. Tournilhac, L. Leibler, *Science* **2011**, *334*, 965.
- [261] A. Demongeot, S. J. Mougner, S. Okada, C. Soulié-Ziakovic, F. Tournilhac, *Polym. Chem.* **2016**, *7*, 4486.
- [262] T. Liu, C. Hao, L. Wang, Y. Li, W. Liu, J. Xin, J. Zhang, *Macromolecules* **2017**, *50*, 8588.
- [263] T. Liu, C. Hao, S. Zhang, X. Yang, L. Wang, J. Han, Y. Li, J. Xin, J. Zhang, *Macromolecules* **2018**, *51*, 5577.
- [264] C. Hao, T. Liu, S. Zhang, L. Brown, R. Li, J. Xin, T. Zhong, L. Jiang, J. Zhang, *ChemSusChem* **2019**, *12*, 1049.
- [265] S. Zhang, T. Liu, C. Hao, L. Wang, J. Han, H. Liu, J. Zhang, *Green Chem.* **2018**, *20*, 2995.

- [266] J. P. Brutman, P. A. Delgado, M. A. Hillmyer, *ACS Macro Lett.* **2014**, *3*, 607.
- [267] F. I. Altuna, V. Pettarin, R. J. J. Williams, *Green Chem* **2013**, *15*, 3360.
- [268] P. Taynton, K. Yu, R. K. Shoemaker, Y. Jin, H. J. Qi, W. Zhang, *Adv. Mater.* **2014**, *26*, 3938.
- [269] A. Chao, I. Negulescu, D. Zhang, *Macromolecules* **2016**, *49*, 6277.
- [270] S. Dhers, G. Vantomme, L. Avérous, *Green Chem.* **2019**, *21*, 1596.
- [271] H. Geng, Y. Wang, Q. Yu, S. Gu, Y. Zhou, W. Xu, X. Zhang, D. Ye, *ACS Sustainable Chem. Eng.* **2018**, *6*, 15463.
- [272] V.-D. Mai, S.-R. Shin, D.-S. Lee, I. Kang, *Polymers* **2019**, *11*, 293.
- [273] Q. Yu, X. Peng, Y. Wang, H. Geng, A. Xu, X. Zhang, W. Xu, D. Ye, *European Polymer Journal* **2019**, *117*, 55.
- [274] R. Mo, L. Song, J. Hu, X. Sheng, X. Zhang, *Polym. Chem.* **2020**, *114*, 1082.
- [275] S. Wang, S. Ma, Q. Li, X. Xu, B. Wang, W. Yuan, S. Zhou, S. You, J. Zhu, *Green Chem* **2019**, *21*, 1484.
- [276] S. Wang, S. Ma, Q. Li, W. Yuan, B. Wang, J. Zhu, *Macromolecules* **2018**, *51*, 8001.
- [277] H Surya Prakash Rao, S P Senthilkumar, *J Chem Sci* **2001**, *113*, 191.
- [278] B. Liu, S. Thayumanavan, *J. Am. Chem. Soc.* **2017**, *139*, 2306.
- [279] A. M. Jazani, J. K. Oh, *Macromolecules* **2017**, *50*, 9427.
- [280] E. J. Kepola, C. S. Patrickios, *Macromol. Chem. Phys.* **2017**, *23*, 1700404.
- [281] M. J. Heffernan, N. Murthy, *Bioconjugate chemistry* **2005**, *16*, 1340.
- [282] J. Li, X. Zhang, M. Zhao, L. Wu, K. Luo, Y. Pu, B. He, *Biomacromolecules* **2018**, *19*, 3140.
- [283] H. Yao, D. E. Richardson, *J. Am. Chem. Soc.* **2000**, *122*, 3220.
- [284] J. Qin, H. Liu, P. Zhang, M. Wolcott, J. Zhang, *Polym. Int.* **2014**, *63*, 760.
- [285] V. Froidevaux, C. Negrell, S. Caillol, J.-P. Pascault, B. Boutevin, *Chem. Rev.* **2016**, *116*, 14181.
- [286] Y. Liu, K. Zhou, M. Lu, L. Wang, Z. Wei, X. Li, *Ind. Eng. Chem. Res.* **2015**, *54*, 9124.
- [287] M. von Czapiewski, K. Gugau, L. Todorovic, M. A.R. Meier, *European Polymer Journal* **2016**, *83*, 359.
- [288] Over, L. C., 'Sustainable Derivatization of Lignin and Subsequent Synthesis of Cross-Linked Polymers', *Dissertation*, Karlsruher Institut für Technologie, Karlsruhe, **2017**.
- [289] E. Kaczmarczyk, E. Milchert, E. Janus, *Chem. Eng. Technol.* **2009**, *32*, 881.
- [290] J. R. Lowe, W. B. Tolman, M. A. Hillmyer, *Biomacromolecules* **2009**, *10*, 2003.
- [291] E. Wolf, E. Richmond, J. Moran, *Chem. Sci.* **2015**, *6*, 2501.

- [292] J. A. R. Salvador, S. M. Silvestre, R. M. A. Pinto, *Molecules* **2011**, *16*, 2884.
- [293] K. A. Bhatia, K. J. Eash, N. M. Leonard, M. C. Oswald, R. S. Mohan, *Tetrahedron Letters* **2001**, *42*, 8129.
- [294] W. Engel, *Journal of agricultural and food chemistry* **2001**, *49*, 4069.
- [295] S. A. Torosyan, F. A. Gimalova, R. F. Valeev, M. S. Miftakhov, *Russ J Org Chem* **2011**, *47*, 682.
- [296] R. D. Stolow, P. M. McDonagh, M. M. Bonaventura, *J. Am. Chem. Soc.* **1964**, *86*, 2165.
- [297] R. D. Stolow, K. Sachdev, *J. Org. Chem.* **1971**, *36*, 960.
- [298] V. Pace, P. Hoyos, L. Castoldi, P. Domínguez de María, A. R. Alcántara, *ChemSusChem* **2012**, *5*, 1369.
- [299] V. Antonucci, J. Coleman, J. B. Ferry, N. Johnson, M. Mathe, J. P. Scott, J. Xu, *Org. Process Res. Dev.* **2011**, *15*, 939.
- [300] M. von Czapiewski, M. A. R. Meier, *Eur. J. Lipid Sci. Technol.* **2018**, *120*, 1700350.
- [301] V. Berdini, M. C. Cesta, R. Curti, G. D'Anniballe, N. Di Bello, G. Nano, L. Nicolini, A. Topai, M. Allegretti, *Tetrahedron* **2002**, *58*, 5669.
- [302] M. Chatterjee, T. Ishizaka, H. Kawanami, *Green Chem.* **2016**, *18*, 487.
- [303] T. Günay, Y. Çimen, R. B. Karabacak, H. Türk, *Catal Lett* **2016**, *146*, 2306.
- [304] M. Milos, *Applied Catalysis A: General* **2001**, *216*, 157.
- [305] E. R. Dockal, Q. B. Cass, T. J. Brocksom, U. Brocksom, A. G. Corrêa, *Synthetic Communications* **1985**, *15*, 1033.
- [306] S. Oelmann, M. A. R. Meier, *Macromol. Chem. Phys.* **2015**, *216*, 1972.
- [307] T. W. Craig, G. R. Harvey, G. A. Berchtold, *J. Org. Chem.* **1967**, *32*, 3743.
- [308] G. Kavadias, R. Droghini, *Can. J. Chem.* **1979**, *57*, 1870.
- [309] P. Saint-louis-Augustin, G. Fremy, B. Monguillon, L. Corbel, Method for preparing polythiols via radical sulfhydrylation of polyenes, US Patent Nr. US 2020/0010412 A1, **2020**.
- [310] C.-T. Chen, Y.-D. Lin, C.-Y. Liu, *Tetrahedron* **2009**, *65*, 10470.
- [311] B. C. Ranu, A. Das, S. Samanta, *Synlett* **2002**, *2002*, 727.
- [312] Y. Tian, Q. Wang, J. Cheng, J. Zhang, *Green Chem* **2020**, *7*, 257.
- [313] G. Yang, S. L. Kristufek, L. A. Link, K. L. Wooley, M. L. Robertson, *Macromolecules* **2016**, *49*, 7737.
- [314] T. Yoshimura, T. Shimasaki, N. Teramoto, M. Shibata, *European Polymer Journal* **2015**, *67*, 397.

- [315] M. Stemmelen, F. Pessel, V. Lapinte, S. Caillol, J.-P. Habas, J.-J. Robin, *Journal of Polymer Science Part A: Polymer Chemistry* **2011**, *49*, 2434.
- [316] J. S. Witzeman, W. D. Nottingham, *J. Org. Chem.* **1991**, *56*, 1713.
- [317] A. C. Boukis, B. Monney, M. A. R. Meier, *Beilstein J. Org. Chem.* **2017**, *13*, 54.